UNIVERSIDAD DE SEVILLA

Departamento de Matemática Aplicada II

Sistemas diferenciales lineales a trozos: ciclos límite y análisis de bifurcaciones.

Piecewise linear differential systems: limit cycles and analysis of bifurcations.

Elísabet Vela Felardo

Tesis doctoral

Sistemas diferenciales lineales a trozos: ciclos límite y análisis de bifurcaciones.

Piecewise linear differential systems: limit cycles and analysis of bifurcations.

Memoria presentada por Elísabet Vela Felardo para optar al grado de Doctora en Matemáticas por la Universidad de Sevilla

V^{o} B^{o} de los Directores:

Fdo. Dr. Enrique Ponce Núñez
Catedrático de Universidad
Dpto. Matemática Aplicada II
Universidad de Sevilla

Fdo. Dr. Fco. Javier Ros Padilla
Profesor Titular de Universidad
Dpto. Matemática Aplicada II
Universidad de Sevilla

Sevilla, mayo de 2013.

A Jesús.
A mis padres y hermanas.
A mis abuelos.

Agradecimientos

Son muchas las personas que me han ayudado durante estos años en los que he estado realizando mi tesis, así que quiero dejar reflejado aquí mi más sincero agradecimiento a todas ellas.

Quiero empezar dándoles las gracias a mis dos directores, Enrique Ponce y Javier Ros, ellos han hecho posible este trabajo. No sólo quiero agradecerles el haberme sumergido en el mundo de los Sistemas Dinámicos, sino también su apoyo, paciencia y optimismo. Gracias por vuestro tiempo y esfuerzo.

Por extensión, me gustaría agradecer también el apoyo mostrado por los compañeros de mi grupo de Sistemas Dinámicos, en especial a Francisco Torres, por sus consejos y ánimos, a Fernando Fernández, por su sinceridad y amistad, y por supuesto a Emilio Freire, por su genial sencillez.

También quiero agradecerles a todos los miembros del departamento de Matemática Aplicada II la buena acogida que me dieron desde el primer día, y en concreto a aquellos con los que he compartido docencia y que me han hecho el trabajo mucho más cómodo.

A Eli, Inés y Soledad, por su ayuda y amistad. A Eva y Mónica, por hacerme el camino más llevadero, gracias por esas risas en el despacho, así todo ha sido más fácil. A Alicia, mi amiga, por muchas cosas, pero sobre todo por creer en mí.

Agradezco al profesor Mario di Bernardo el haberme dado la oportunidad de trabajar con él en Bristol, a Mike Jeffrey su recibimiento, y a mis compañeros de despacho allí su ayuda, tan necesaria estando lejos de casa.

Por supuesto doy las gracias a mi familia, a la que le debo todo lo que soy. Tengo mucho que agradecerles, pero sobre todo a mis padres su apoyo incondicional, a mis hermanas su complicidad, y a Jesús su comprensión y generosidad. Tampoco quiero olvidarme de mis abuelos, gracias.

Me gustaría además darles las gracias a todos esos amigos que me han apoyado durante estos años. No voy a nombrarlos porque son muchos, pero no quiero dejar pasar la oportunidad de agradecerles el ánimo que me han brindado.

En definitiva, gracias a todos los que han aportado aunque sólo sea un granito de arena para hacer que esto haya sido posible.

Contents

1 Introduction **1**
- 1.1 Motivation and objectives . . . 3
- 1.2 Main contributions . . . 4
- 1.3 Outline of this thesis . . . 6

2 Canonical forms and analysis of periodic orbits **9**
- 2.1 A unified Liénard form for 2Z/3Z planar systems . . . 10
- 2.2 Canonical forms for Luré systems in higher dimension . . . 16
- 2.3 Some generic results about equilibria . . . 23
  - 2.3.1 Observable 2CPWL$_n$ systems . . . 23
  - 2.3.2 Observable S3CPWL$_n$ systems . . . 25
- 2.4 Analysis of periodic orbits through their closing equations . . . 26
  - 2.4.1 Closing equations for 2CPWL$_n$ . . . 27
  - 2.4.2 Closing equations for S3CPWL$_n$ . . . 29
- 2.5 Poincaré maps of CPWL$_n$ systems . . . 32
  - 2.5.1 Poincaré maps in 2CPWL$_n$ . . . 32
  - 2.5.2 Poincaré maps in S3CPWL$_n$ . . . 34

3 Planar PWL dynamical systems **39**
- 3.1 Analysis of 2CPWL$_2$ systems . . . 39
  - 3.1.1 Preliminary results on equilibria . . . 41
  - 3.1.2 Preliminary results on limit cycles . . . 44
  - 3.1.3 The Massera's method for uniqueness of limit cycles . . . 46
  - 3.1.4 Boundary equilibrium bifurcations (BEB's) . . . 55
- 3.2 3CPWL$_2$ systems with one equilibrium . . . 61
  - 3.2.1 Application to Wien bridge oscillators . . . 75

3.2.2 Algebraically Computable PWL Nodal Oscillators . . . 81
3.2.3 Application to a PWL Van der Pol oscillator 96
3.3 A limit cycle bifurcation in 2DPWL$_2$ systems 99
3.3.1 Discontinuous models of Wien bridge oscillators 115

4 Three-dimensional PWL dynamical systems 121
4.1 A short review of the PWL analogous of Hopf bifurcation . . . 122
4.2 The PWL analogous of Hopf-pitchfork bifurcation 125
4.3 A Hopf-pitchfork degeneration 155
4.4 Examples for PWL Hopf-pitchfork 160
4.4.1 Realization in a generalized Chua's circuit 160
4.4.2 Realization in a extended BPV oscillator 166

5 Conclusions 173

CHAPTER 1

Introduction

The class of piecewise-linear differential systems (PWL systems, for short) is an important class of nonlinear dynamical systems in a twofold sense. First, they naturally appear in realistic nonlinear engineering models, as certain devices are accurately modeled by piecewise linear vector fields, see [18]. In fact, this kind of models are frequent in applications from electronic engineering and nonlinear control systems, where piecewise linear models cannot be considered as idealized ones; they are used in mathematical biology as well, see [16, 84, 85, 86], where they constitute approximate models. Therefore, they constitute a significant subclass of piecewise-smooth dynamical systems.

Second, since non-smooth piecewise linear characteristics can be considered as the uniform limit of smooth nonlinearities, the global dynamics of smooth models has been sometimes approximated by piecewise linear models and viceversa, as done in [57, 87], obtaining a good qualitative agreement between the two modelling approaches. Note that, in practice, nonlinear characteristics use to have a saturated part, which is difficult to be approximated by polynomial models. Therefore, this possibility of what we could call 'global linearization' by linear pieces emphasizes even more the importance of PWL systems, frequently being the most natural extensions to linear systems in order to capture nonlinear phenomena.

In fact, it is a widely extended feeling among researchers in the field that the richness of dynamical behavior found in piecewise linear systems

covers almost all the instances of dynamics found in general smooth nonlinear systems: limit cycles, homoclinic and heteroclinic orbits, strange attractors...

The consideration of this class as an alternative to smooth nonlinear systems is gaining popularity due to the fact that one can write in closed form the solutions when they are restricted to a region of the phase space where the system becomes linear. Nevertheless, the analysis of the corresponding dynamics is far from being trivial since one must match the different solutions in every linear zone and such matching typically requires the explicit knowing of flight times, what is true only by exception. On the other hand, standard families of PWL systems have a non-small number of parameters, so that the complete analysis of possible dynamical behaviors uses to be a formidable task. In this sense, the disposal of good canonical forms is a preliminary aim of great relevance, as it will be patent throughout the thesis.

As far as we know, the pioneering investigation of piecewise-linear systems in a rigorous way is due to Andronov and coworkers [2]. Their book "Theory of Oscillations" remains nowadays an obligated reference, still being a source of ideas. Precisely, from the reading of such book there arose the inspiration for the first works of our group about PWL systems, see [23] and [26] . The analysis of piecewise-linear systems also received some growing attention after the work on PWL chaotic systems [64] and references therein.

This thesis in PWL system dynamics can be seen as a further step in a series by other members of our Dynamical Systems group in the Applied Mathematics department of University of Sevilla: after the seed laid in by Francisco Rodrigo's thesis (1997), co-directed by professors Emilio Freire and Francisco Torres, mainly devoted to planar PWL systems (see [80]), some years later Victoriano Carmona (2002) and Javier Ros (2003) finished their respective Ph. D. dissertations, where some problems in three dimensional systems were also addressed, see [5, 81]. Since two more theses have been recently presented by menbers of our group, namely by Elisabeth García Medina (2011) and by Soledad Fernández García (2012) (see [32, 22]), this work constitutes so the sixth ring of an enthusiastic 'research' chain, always nourished by the tireless impulse and generous suggestions coming from our highly regarded professor Emilio Freire.

1.1 Motivation and objectives

As it has been emphasized in previous works, the lack of differentiability of PWL systems precludes the standard application of the powerful results coming from the modern geometric theory of dynamical systems and bifurcations of differentiable dynamics to be found in so celebrated books as [36] or [52]. Simple tasks, as it would be for instance the determination of the topological type of an equilibrium point, surprisingly become sometimes intricate problems, see [11]. This fact makes the endeavor of building a general theory for PWL systems to be a impressively large puzzle, as you must proceed via a case-study approach, trying not to neglect any particular case. It is precisely in this context of contributing to fill in the remaining empty shelves of the PWL general theory where we encounter the motivation and targets of our work.

Nowadays, the family of planar, continuous PWL systems (CPWL_2, for short) seems to be well understood, at least for some frequent subfamilies, as are the systems with only two zones ($\mathrm{2CPWL}_2$ systems) or with three zones but having symmetry with respect to the origin ($\mathrm{S3CPWL}_2$ systems). Other problems however, as the determination of the maximum number of limit cycles in planar, simplest discontinuous PWL systems with only two zones ($\mathrm{2DPWL}_2$, for short) still are the subject of intensive, contemporary research.

However, some results for general $\mathrm{2CPWL}_2$ systems were obtained as the consequence of the cumbersome consideration of all the possible cases, one-by-one, through the detailed study of properties of different half-return maps. A paradigmatic case of this, related to the uniqueness of limit cycles, is the so called Lum-Chua conjecture. In a memorandum by Robert Lum and Leon O. Chua, see [63], never published as a paper, there appeared the following conjecture:

> **Conjecture 0.1**. A continuous piecewise linear vector field with one boundary has at most one limit cycle. The limit cycle, if it exists, is either attracting or repelling.

The Lum-Chua conjecture was shown true after the long study made in [23]. A natural question arises: is there a shorter way to arrive at the same conclusion? As an specific objective, thanks to some recent results that take

advantage of Massera's geometric method, we wanted to give an answer to this question.

In the case of $3CPWL_2$ systems, the situation is acceptable regarding the subfamily of vector fields with symmetry respect to the origin, to be denoted $S3CPWL_2$ systems, for short. Here, there are obligated references, as the Ph. D. dissertation of Francisco Rodrigo, see [80], which among other papers leaded to [24], and the thorough study made in the Ph. D. dissertation of A. Teruel, see [83], following a different approach. In fact, we know that such a tesis is the germ of an incoming book to be published in next August. In this specific PWL family we incidentally contribute by studying the possible existence of algebraically computable nodal oscillators.

However, for quasi-symmetric $3CPWL_2$ vector fields (translated of symmetric ones) or general non-symmetric systems, there are few results available related to the existence and uniqueness of limit cycles, a situation we want to improve in this work, by resorting again to the quoted Massera's geometric method and showing also some outstanding applications.

Much has been done in $CPWL_3$ systems, both in $2CPWL_3$ and $S3CPWL_3$ systems in the last decade, thanks to the aforementioned theses by V. Carmona and J. Ros first, see [5, 81], and by E. García Medina and S. Fernández García later, see [32, 22], leading to a variety of papers. Without entering into the intricate world of chaotic dynamics, but looking for new ways to move ahead towards the chaotic frontier, we want to study partial unfoldings of the analogous to Hopf-pitchfork bifurcations in PWL systems. A particular objective here is to determine how many limit cycles can bifurcate from such a critical situation, where three eigenvalues (a zero and a imaginary pair of the linear piece containing the involved equilibrium point) are simultaneously located at the imaginary axis of complex plane.

1.2 Main contributions

The scientific contributions of this thesis appear distributed mainly within chapters 3 and 4, since previous chapters are devoted to introduce notation, a review of the terminology and standard techniques to be later needed. As usual, the development of new results during the preparation of this work has been the subject of scientific publications, some of them already appeared but some other still in press. Thus, we can summarize a significant part of our new results in the following four publications.

(1) Algebraically computable piecewise linear nodal oscillators. Applied Mathematics and Computation. See [74].

(2) Unfolding the fold-Hopf bifurcation in piecewise linear continuous differential systems with symmetry. Physica D: Nonlinear Phenomena. See [77].

(3) A Hopf-zero degenerated case in symmetric piecewise linear systems, to appear in the Springer book *Dynamical systems: 100 years after Poincaré*. See [75].

(4) The focus-center-limit cycle bifurcation in discontinuous planar piecewise linear systems without sliding, to appear in the Springer book *Dynamical systems: 100 years after Poincaré*. See [76].

Other included achievements deserve to be send for publication and therefore we plan to do it in a near future.

For the sake of concision, we want to specifically mention the main mathematical contributions included in our thesis.

- A new approach, following Massera's method, to get a concise proof for the Lum-Chua Conjecture in planar PWL systems with two zones (2CPWL_2).
- Characterization for a variety of boundary equilibrium bifurcations (BEB's, for short) in 2CPWL_2 systems.
- Alternative proofs of existence and uniqueness results for limit cycles in an important family of planar PWL systems with three zones (3CPWL_2).
- Characterization for a variety of boundary equilibrium bifurcations (BEB's, for short) in 3CPWL_2 systems, detecting some situations with two nested limit cycles surrounding the only equilibrium point.
- Analysis of the focus-center-limit cycle bifurcation in discontinuous planar PWL systems without sliding set.
- A thorough analysis of electronic Wien bridge oscillators, characterizing qualitatively (and quantitatively in some cases) the oscillatory behaviour and determining the parameter regions for oscillations.

- Analysis of a new family of algebraically computable nodal oscillators, including real examples of members of the family.

- Analysis of some specific unfolding for the Hopf-zero or Hopf-pitchfork bifurcation and its main degenerations in symmetric PWL systems in 3D (S3CPWL$_3$), with the detection of the simultaneous bifurcation of three limit cycles.

- Study of some real electronic devices where the Hopf-zero bifurcation appears.

1.3 Outline of this thesis

After this introduction, in Chapter 2 we review some terminology and results related to canonical forms in the study of PWL systems along with certain techniques that are useful for the bifurcation analysis of their periodic orbits. First, we develop a unified 2Z/3Z Liénard canonical form without assuming the system in Luré form to facilitate the subsequent study on existence and uniqueness of limit cycles. Next, we work in arbitrary dimension to review general results even we later deal only with systems in dimension 2 and 3. The included material is not entirely new but it is needed to make this work as much self-contained as possible.

Next, Chapter 3 is completely devoted to planar PWL systems. Some boundary equilibrium bifurcations (BEB, for short) are characterized, putting emphasis in the ones capable of giving rise to limit cycles. We exploit and extend some recent results achieved in [59], which allows us to pave the way for a shorter proof of Lum-Chua conjecture. After other general results for existence and uniqueness of limit cycles in 3CPWL$_2$ systems, we show some applications of the theory in nonlinear electronics. In a different direction of research, it is introduced a new family of algebraically computable piecewise linear nodal oscillators and shown some real electronic devices that belong to the family. The outstanding feature of this family makes it an exceptional benchmark for testing approximate methods of analysis of oscillators. Finally, we include our only contribution in the exciting world of discontinuous PWL systems: the analysis of the focus-center-limit cycle bifurcation in planar PWL systems with two zones and without a proper sliding set, which naturally includes the continuous case.

Chapter 4 represents our particular incursion in PWL systems in dimension 3, namely in S3CPWL$_3$ ones, notwithstanding some results are also interesting for 2CPWL$_3$ vector fields. Pursuing the aim of fill in the pending gaps in the catalog of possible bifurcations, we study some unfoldings of the analogous to Hopf-pitchfork bifurcations in PWL systems. Our theorems predict the simultaneous bifurcation of 3 limit cycles but we also formulate a natural, strongly numerically based conjecture on the simultaneous bifurcation of 5 limit cycles.

Finally, in Chapter 5 some conclusions and recommendations for future work are offered for consideration of interested readers.

CHAPTER 2

Canonical forms and analysis of periodic orbits

In this chapter we review some terminology and results related to canonical forms in the study of PWL systems an certain techniques that are useful for the bifurcation analysis of their periodic orbits. As main references for the material here included, we must quote [8] and chapters 2 and 3 of [81].

Attempting to do a systematic study of piecewise linear systems, some canonical forms are tackled with in several works, see [41, 42, 43, 46, 55, 56] and [66]. On the other hand, most of nonlinear models needed in practice do not require such rather general canonical forms, since they can be adequately modeled with only two or three linear regions separated by parallel boundaries hyperplanes, see [34]. Moreover, for elementary models, the number of state variables is typically two or three.

As the second main ingredient of this chapter, we introduce some techniques for the study of limit cycle bifurcations in PWL systems. Such problem is, after the analysis of equilibrium solutions of a differential system, one of the most important issues in the qualitative analysis of dynamical systems. Several tools from bifurcation theory are available in the case of smooth systems in order to guarantee the bifurcation and existence of limit cycles, see [33, 36, 52]. The situation is not so good in the case of piecewise smooth systems, see [18], so that new results concerning this class of

differential non-smooth systems are needed.

By considering for instance the situation associated to the classical Hopf bifurcation for smooth systems, in [26] authors obtained bifurcation results for limit cycles in planar non-smooth systems, see also [50]. For discontinuous cases, we refer to [15, 19, 51, 91]. Later, several results were extended to 3D continuous piecewise linear systems, see [7] and [27]. Other results for these systems appeared in [9, 10, 11, 50, 73]. More recently, as mentioned in the introduction, another bifurcation problems related with limit cycles have been addressed in [74] and [77], to be later reported.

We start by considering the case of planar systems, where it is not difficult to deal simultaneously with the two zone and three zone cases, under general mild assumptions. For higher dimension however, we prefer to study separately such two basic situations and to start from the so called Luré form, that is, the case of vector fields obtained by adding a linear term with a nonlinear one; this nonlinear term is just the result of multiplying a constant vector by one piecewise scalar nonlinearity.

2.1 A unified Liénard form for 2Z/3Z planar systems

As mentioned before, in most interesting applications, continuous piecewise linear differential systems only have two or three different linearity regions separated by one straight line or two parallel straight lines, respectively, see [8]. Therefore, and trying to minimize efforts, we adopt a general point of view by assuming that we have three linearity zones, so that our results for such cases can be translated to the two-zone case by extending the central vector field to one of the external zones.

For such three-zone systems we assume without loss of generality that the lines separating the regions are $x = -1$ and $x = 1$. Typically, it is rather usual for these systems to exhibit only one anti-saddle singular point, that is, one equilibrium point of focus or node type. Such a point is normally supposed to be in the central linearity region when the system has three linear zones, to be denoted in the sequel as L (left), C (central), and R (right). We use these three letters to denote the zone by using them as subscripts or superscripts, whatever be more convenient in each case. If the system has only two zones, we assume for instance that the left and the central zones

have equal parameters and so they are in fact only one. Thus we have a system defined as follows

$$\begin{aligned}
\begin{pmatrix} \dot{x} \\ \dot{y} \end{pmatrix} &= A_L \begin{pmatrix} x \\ y \end{pmatrix} + \mathbf{b}_L, \quad \text{if } x < -1, \\
\begin{pmatrix} \dot{x} \\ \dot{y} \end{pmatrix} &= A_C \begin{pmatrix} x \\ y \end{pmatrix} + \mathbf{b}_C, \quad \text{if } |x| \leq 1, \\
\begin{pmatrix} \dot{x} \\ \dot{y} \end{pmatrix} &= A_R \begin{pmatrix} x \\ y \end{pmatrix} + \mathbf{b}_R, \quad \text{if } x > 1,
\end{aligned} \tag{2.1}$$

requiring that the full vector field be continuous. This condition leads to impose

$$\begin{aligned}
A_L \begin{pmatrix} -1 \\ y \end{pmatrix} + \mathbf{b}_L &= A_C \begin{pmatrix} -1 \\ y \end{pmatrix} + \mathbf{b}_C, \\
A_R \begin{pmatrix} 1 \\ y \end{pmatrix} + \mathbf{b}_R &= A_C \begin{pmatrix} 1 \\ y \end{pmatrix} + \mathbf{b}_C,
\end{aligned} \tag{2.2}$$

for all $y \in \mathbb{R}$. Obviously, taking $y = 0$, we deduce

$$\begin{array}{l} a_{11}^L - b_1^L = a_{11}^C - b_1^C, \\ a_{21}^L - b_2^L = a_{21}^C - b_2^C, \end{array} \quad \text{and} \quad \begin{array}{l} a_{11}^R + b_1^R = a_{11}^C + b_1^C, \\ a_{21}^R + b_2^R = a_{21}^C + b_2^C, \end{array}$$

and canceling these terms in (2.2) we have the condition

$$A_L \begin{pmatrix} 0 \\ y \end{pmatrix} = A_C \begin{pmatrix} 0 \\ y \end{pmatrix} = A_R \begin{pmatrix} 0 \\ y \end{pmatrix} \text{for all } y \neq 0, \tag{2.3}$$

which implies that the last columns of A_L, A_C and A_R must be equal. This elementary reasoning makes only 10 the number of parameters needed to define this family, instead of the 18 matrix entries initially assumed.

Thus, from (2.3) we can write

$$\begin{aligned}
A_L &= \begin{pmatrix} a_{11}^L & a_{12} \\ a_{21}^L & a_{22} \end{pmatrix}, \quad A_C = \begin{pmatrix} a_{11}^C & a_{12} \\ a_{21}^C & a_{22} \end{pmatrix}, \quad A_R = \begin{pmatrix} a_{11}^R & a_{12} \\ a_{21}^R & a_{22} \end{pmatrix}, \\
\mathbf{b}_L &= \begin{pmatrix} b_1 + a_{11}^L - a_{11}^C \\ b_2 + a_{21}^L - a_{21}^C \end{pmatrix}, \quad \mathbf{b}_C = \begin{pmatrix} b_1 \\ b_2 \end{pmatrix}, \quad \mathbf{b}_R = \begin{pmatrix} b_1 - a_{11}^R + a_{11}^C \\ b_2 - a_{21}^R + a_{21}^C \end{pmatrix},
\end{aligned} \tag{2.4}$$

but anyway, there are still a large number of parameters to consider all possible cases.

We emphasize that the phase plane is divided into three zones with different linear dynamics: namely the central band or zone C, given by the set

$$\mathcal{S}_0 = \{(x, y) \in \mathbb{R}^2 : -1 < x < 1\},$$

and the external zones L and R, to be denoted also as

$$\mathcal{S}_+ = \{(x, y) \in \mathbb{R}^2 : x > 1\}, \quad \mathcal{S}_- = \{(x, y) \in \mathbb{R}^2 : x < -1\},$$

separated by the two straight lines

$$\Sigma_1 = \{(x, y) \in \mathbb{R}^2 : x = 1\}, \quad \Sigma_{-1} = \{(x, y) \in \mathbb{R}^2 : x = -1\}.$$

Notice that the vector field of the family of system (2.1)-(2.4) is of class $\mathcal{C}^1$ in each linear region, but it is only of class $\mathcal{C}^0$ on $\mathbb{R}^2$. Nevertheless, they satisfy a Lipschitz condition on the whole $\mathbb{R}^2$. Thus, the classical theorems on existence, uniqueness and continuity of solutions with respect to initial conditions and parameters apply to these systems. Their solution curves are in general $\mathcal{C}^1$, but not $\mathcal{C}^2$.

The following result can be proved easily; its proof is included in order that the theoretical development be as self-contained as possible.

In what follows, when we discuss about periodic solutions, we discard the trivial case of constant solutions, that is, equilibrium points.

Lemma 2.1 *If system* (2.1)-(2.4) *has periodic solutions, then* $a_{12} \neq 0$.

Proof If we assume $a_{12} = 0$, then the dynamics in x would be decoupled from the dynamic in y, since we would have

$$\dot{x} = a_{11}^{\{L,C,R\}} x + b_1^{\{L,C,R\}},$$

that does not depend on y. Obviously this autonomous, one-dimensional equation cannot have non-constant periodic solutions. Hence, as any periodic solution of the complete system gives rise to a periodic function $x(t)$, the proof is completed. ■

Next, we see that the previous necessary condition for existence of periodic orbits is also a sufficient condition to achieve a celebrated canonical form.

Proposition 2.1 (Liénard form) *The condition $a_{12} \neq 0$ is sufficient to write system* (2.1)-(2.4) *in Liénard form*

$$\begin{array}{rcl} \dot{x} & = & F(x) - y, \\ \dot{y} & = & g(x) - \delta, \end{array} \tag{2.5}$$

where

$$F(x) = \begin{cases} t_L(x+1) - t_C & \text{if } x < -1, \\ t_C x & \text{if } |x| \leq 1, \\ t_R(x-1) + t_C & \text{if } x > 1, \end{cases} \tag{2.6}$$

and

$$g(x) = \begin{cases} d_L(x+1) - d_C & \text{if } x < -1, \\ d_C x & \text{if } |x| \leq 1, \\ d_R(x-1) + d_C & \text{if } x > 1. \end{cases} \tag{2.7}$$

Proof First, we make the change of variables $X = x$, $Y = a_{22}x - a_{12}y$, to obtain

$$\begin{aligned} \dot{X} &= a_{11}^{\{L,C,R\}} X + a_{12} y + b_1^{\{L,C,R\}} = \left(a_{11}^{\{L,C,R\}} + a_{22}\right) X - Y + b_1^{\{L,C,R\}} = \\ &= t_{\{L,C,R\}} X - Y + b_1^{\{L,C,R\}}, \\ \dot{Y} &= a_{22}\left(a_{11}^{\{L,C,R\}} X + a_{12} y + b_1^{\{L,C,R\}}\right) - a_{12}\left(a_{21}^{\{L,C,R\}} X + a_{22} y + b_2^{\{L,C,R\}}\right) = \\ &= d_{\{L,C,R\}} X + a_{22} b_1^{\{L,C,R\}} - a_{12} b_2^{\{L,C,R\}}, \end{aligned}$$

where we introduce the traces

$$t_{\{L,C,R\}} = a_{11}^{\{L,C,R\}} + a_{22}$$

in each zone, and the respective determinants

$$d_{\{L,C,R\}} = a_{11}^{\{L,C,R\}} a_{22} - a_{21}^{\{L,C,R\}} a_{12}.$$

Now, a translation in the second variable $y = Y - b_1 = Y - b_1^C$, leads to the required canonical form, since from (2.4) we have

$$b_1^{\{L,R\}} - b_1^C = \pm(t_{\{L,R\}} - t_C)$$

and

$$d_{\{L,R\}} - \delta = \pm(d_{\{L,R\}} - d_C)$$

where

$$\delta = a_{12}b_2^C - a_{22}b_1^C.$$

■

The above canonical form will be profusely used along the whole work. We note that without other additional assumptions this form is not a Luré form, having two different nonlinearities.

Remark 2.1 *The above formulation includes as particular cases the following ones. If $t_C = t_L$ and $d_C = d_L$ then we have a system with only two different linearity zones, thoroughly analyzed in [23]. If $t_R = t_L$, $d_R = d_L$ and $\delta = 0$, then we have a symmetric system with three different linearity zones, first considered in [62] and thoroughly analyzed in [24]. The case $t_R = t_L$, $d_R = d_L$ and $\delta \neq 0$ has been considered in [58]. Some relevant applications of this last situation have appeared in [16].*

As mentioned before, we assume for the equilibrium point to be an anti-saddle in the band $-1 < x < 1$. This requires for the determinant in the central region to be positive, that is, $d_C > 0$, and also $-d_C < \delta < d_C$. The uniqueness of this equilibrium point also requires $d_L, d_R \geq 0$. Thus, the only equilibrium point is located at the line $x = \bar{x} = \delta/d_C \in (-1, 1)$.

The different traces t_L, t_C, t_R could be arbitrary, but we know from the Bendixson theorem, see for instance Theorem 7.10 in [21], that they cannot have the same sign for the existence of limit cycles. In fact, if we suppose the existence of a simple invariant close curve Γ and define $\mathrm{int}_L(\Gamma) = \mathrm{int}(\Gamma) \bigcap \mathcal{S}_L$, $\mathrm{int}_C(\Gamma) = \mathrm{int}(\Gamma) \bigcap \mathcal{S}_C$, and $\mathrm{int}_R(\Gamma) = \mathrm{int}(\Gamma) \bigcap \mathcal{S}_R$, the following result can be stated. For a proof, it suffices to use Green's formula, see for instance Proposition 3 in [62].

Proposition 2.2 *If system* (2.5)-(2.7) *has a simple invariant closed curve* Γ*, then*

$$\iint_{\mathrm{int}_L(\Gamma)} t_L dxdy + \iint_{\mathrm{int}_C(\Gamma)} t_C dxdy + \iint_{\mathrm{int}_R(\Gamma)} t_R dxdy = t_L S_L + t_C S_C + t_R S_R = 0,$$

where

$$\begin{aligned} S_L &= \mathrm{area}\left(\mathrm{int}_L(\Gamma)\right), \\ S_C &= \mathrm{area}\left(\mathrm{int}_C(\Gamma)\right), \\ S_R &= \mathrm{area}\left(\mathrm{int}_R(\Gamma)\right). \end{aligned}$$

Our next result is just a preparation lemma, putting the equilibrium point at the origin (we speak of *unbiased* form), reducing by one the number of parameters (unitary central determinant) and obtaining an equivalent expression for system (2.5)-(2.7) to be used later. The location of the equilibrium point at the origin will be a crucial fact for the analysis of Chapter 3.

Note that if we make in system (2.5) the change $X = -x, Y = -y$ (we will give a more detailed explanation about this, later), we get the system

$$\begin{array}{rcl} \dot{X} & = & \widehat{F}(X) - Y, \\ \dot{Y} & = & \widehat{g}(X) + \delta, \end{array} \tag{2.8}$$

where the new functions $\widehat{F}$ and $\widehat{g}$ are obtained from that given in (2.6)-(2.7) by interchanging the subscripts L and R, so that, the sign of δ is not relevant.

Lemma 2.2 (Unbiased normalized Liénard form)
System (2.5)-(2.7) *with* $-d_C < \delta < d_C$ *is topologically equivalent to the system*

$$\begin{array}{rcl} \dot{x} & = & F_n(x) - y, \\ \dot{y} & = & g_n(x), \end{array} \tag{2.9}$$

where

$$F_n(x) = \begin{cases} a_R(x - x_R) + a_C x_R & \text{if } x > x_R, \\ a_C x & \text{if } x_L \leq x \leq x_R, \\ a_L(x - x_L) + a_C x_L & \text{if } x < x_L, \end{cases} \tag{2.10}$$

and

$$g_n(x) = \begin{cases} b_R(x - x_R) + x_R & \text{if } x > x_R, \\ x & \text{if } x_L \leq x \leq x_R, \\ b_L(x - x_L) + x_L & \text{if } x < x_L, \end{cases} \tag{2.11}$$

with $x_L = -1 - \bar{x}$, $x_R = 1 - \bar{x}$, *for* $-1 < \bar{x} = \delta/d_C < 1$, *and the new piecewise slopes satisfy* $a_Z\sqrt{d_C} = t_Z, b_Z d_C = d_Z$, *for each* $Z \in \{L, C, R\}$.

Proof First, we put the equilibrium point at the origin by the translation $\tilde{x} = x - \bar{x}$, $\tilde{y} = y - t_C\bar{x}$. This makes that the new vertical lines separating the zones are $\tilde{x} = x_L$ and $\tilde{x} = x_R$ and the δ-term in the second equation disappears. Next, we make the change of variables and time defined by $X = \tilde{x}$, $\omega Y = \tilde{y}$, and $\tau = \omega t$, with $\omega^2 = d_C$. We obtain

$$\frac{dX}{d\tau} = \frac{F(X + \bar{x})}{\omega} - Y, \quad \frac{dY}{d\tau} = \frac{g(X + \bar{x})}{\omega^2},$$

so that the conclusion follows from the two obvious equalities $F(X+\bar{x}) = \omega F_n(X)$ and $g(X+\bar{x}) = \omega^2 g_n(X)$. ■

We finish this section with a remark that will be later useful to split the analysis of planar systems with three zones into two different subcases with only two zones.

Remark 2.2 *System* (2.9)-(2.11) *is invariant under the transformation*

$$(x, y, t, a_C, a_L, a_R, b_L, b_R, x_L, x_R) \to (-x, -y, t, a_C, a_R, a_L, b_R, b_L, -x_R, -x_L).$$

2.2 Observable 2CPWL$_n$ and S3CPWL$_n$ Luré systems

As a natural previous step to facilitate their mathematical analysis, we review here the more important canonical forms for n-dimensional piecewise-linear models from our point of view, starting for a general formulation but having in mind the case of Luré systems, that is, those with basically one nonlinearity given by a scalar piecewise-linear function with up to three linear pieces. The two-zone case is obviously included by assuming that two of the three pieces glue not only continuously but also with continuous derivative.

To begin with, we formally introduce a rather general family of systems as our starting point in looking for canonical forms.

Definition 2.1 *A differential equation*

$$\dot{\mathbf{x}} = F(\mathbf{x})$$

with $\mathbf{x} = (x_1, x_2, \dots x_n)^T$ *is said to be a 3PWL$_n$ system if there exist three vectors* B_0, B_1, B_2 *and one vector* $\mathbf{v} \neq \mathbf{0}$ *in* $\mathbb{R}^n$, *two scalars* $\delta_1 < \delta_2$ *and three matrices* A_0, A_1, A_2 *in* $\mathcal{M}_n(\mathbb{R})$ *so that*

$$\dot{\mathbf{x}} = F(\mathbf{x}) = \begin{cases} A_0\mathbf{x} + B_0, & \text{if } \mathbf{v}^T\mathbf{x} < \delta_1, \\ A_1\mathbf{x} + B_1, & \text{if } \delta_1 \leq \mathbf{v}^T\mathbf{x} \leq \delta_2, \\ A_2\mathbf{x} + B_2, & \text{if } \delta_2 < \mathbf{v}^T\mathbf{x}. \end{cases} \tag{2.12}$$

If F *is continuous, we have a 3CPWL$_n$ system, that is, for all* $\mathbf{x}$ *such that* $\mathbf{v}^T\mathbf{x} = \delta_i$,

$$A_i\mathbf{x} + B_i = A_{i-1}\mathbf{x} + B_{i-1}, i = 1, 2.$$

If F *is discontinuous, we have a 3DPWL$_n$ system.*

A relevant subclass of 3PWL$_n$ systems can also be distinguished, namely the case when the linear part of the outer regions coincide.

Definition 2.2 *A 3PWL$_n$ system with $A_0 = A_2$ is called a quasi-symmetrical 3PWL$_n$ system.*

Of course, in the case of continuous systems, if the linear part of two adjacent regions are equal, then the continuity assumption enforces that the corresponding nonhomogeneous terms B_i are also equal, so that the hyperplane involved should be a false boundary, since it really does not separate different zones. In this case, we say that the system is a 2CPWL$_n$ system.

It is important to remark that the hyperplanes $\mathbf{v}^T\mathbf{x} = \delta_i$, $i = 1, 2$, can be transformed, by means of a linear change of variables, into the hyperplanes $x_1 = \pm 1$, i.e., without loss of generality, one can assume in what follows that $\mathbf{v} = \mathbf{e}_1$, $\delta_1 = -1$ and $\delta_2 = 1$ in (2.12). We rewrite so system (2.12) as

$$\dot{\mathbf{x}} = F(\mathbf{x}) = \begin{cases} A_0\mathbf{x} + B_0, & \text{if } \mathbf{e}_1^T\mathbf{x} < -1, \\ A_1\mathbf{x} + B_1, & \text{if } -1 \leq \mathbf{e}_1^T\mathbf{x} \leq 1, \\ A_2\mathbf{x} + B_2, & \text{if } 1 < \mathbf{e}_1^T\mathbf{x}. \end{cases} \tag{2.13}$$

In applications, there is frequently just one basic nonlinearity appearing in the different components of the vector field. This is the case of the so-called Luré systems in control theory. A sufficient condition to have a Luré system is given in the following result, which is a slightly improved version of another appeared in [8].

Lemma 2.3 *The matrices A_i, $i = 0, 1, 2$, in system* (2.13) *share the last $n-1$ columns. Furthermore, if we assume that there exists a linear dependence between the first columns of matrices $A_1 - A_0$ and $A_2 - A_1$, then system* (2.13) *can be written in Lur form, that is, in the form*

$$\dot{\mathbf{x}} = A\mathbf{x} + B\,\mathrm{pwl}(\mathbf{e}_1^T\mathbf{x}) + C, \tag{2.14}$$

where $\mathbf{x} = (x_1, x_2, \ldots x_n)^T$, $A \in \mathcal{M}_n(\mathbb{R})$, $B, C \in \mathbb{R}^n$, and pwl(.) *is a piecewise-linear function. In particular, the following statements are true.*

(a) *If either $A_0 = A_1$ or $A_1 = A_2$ then the function* pwl *can be taken equal to the function*

$$\mathrm{ramp}(v) = \begin{cases} 0, & \text{if } v \leq 0, \\ v, & \text{if } v > 0. \end{cases} \tag{2.15}$$

(b) *If $A_0 = A_2$, then the condition on linear dependence between the first columns of matrices $A_1 - A_0$ and $A_2 - A_1$ is automatically fulfilled, and the function* pwl *can be taken equal to the function*

$$\mathrm{sat}(v) = \begin{cases} v, & \text{if } |v| < 1, \\ \mathrm{sgn}(v), & \text{if } |v| \geq 1. \end{cases} \tag{2.16}$$

Proof We start like in the previous section by noting that the continuity of the vector field assures that

$$\begin{array}{ll} A_0(-\mathbf{e}_1 + \mu\mathbf{e}_k) + B_0 & = A_1(-\mathbf{e}_1 + \mu\mathbf{e}_k) + B_1, \\ A_1(\mathbf{e}_1 + \mu\mathbf{e}_k) + B_1 & = A_1(\mathbf{e}_1 + \mu\mathbf{e}_k) + B_2, \end{array} \tag{2.17}$$

for all $\mu \in \mathbb{R}$ and $2 \leq k \leq n$. Thus, taking $\mu = 0$, we deduce

$$\begin{array}{ll} B_1 & = B_0 + (A_1 - A_0)\mathbf{e}_1, \\ B_2 & = B_1 - (A_2 - A_1)\mathbf{e}_1, \end{array}$$

and then from (2.17) we have for $2 \leq k \leq n$ the equalities

$$A_0\mathbf{e}_k = A_1\mathbf{e}_k = A_2\mathbf{e}_k.$$

Thus, the three matrices have in common the last $n-1$ columns.

As a consequence, we see that

$$\begin{array}{ll} A_1 & = A_0 + (A_1 - A_0)\mathbf{e}_1\mathbf{e}_1^T, \\ A_2 & = A_1 + (A_2 - A_1)\mathbf{e}_1\mathbf{e}_1^T, \end{array}$$

and then, by substituting $\mathbf{e}_1^T\mathbf{x} = x_1$, we conclude that

$$\begin{array}{ll} A_1\mathbf{x} + B_1 & = A_0\mathbf{x} + (A_1 - A_0)\mathbf{e}_1 x_1 + (A_1 - A_0)\mathbf{e}_1 + B_0 = \\ & = A_0\mathbf{x} + (A_1 - A_0)\mathbf{e}_1(x_1 + 1) + B_0, \end{array}$$

and similarly,

$$\begin{array}{ll} A_2\mathbf{x} + B_2 & = A_0\mathbf{x} + (A_1 - A_0)\mathbf{e}_1 x_1 + (A_2 - A_1)\mathbf{e}_1 x_1 - \\ & -(A_2 - A_1)\mathbf{e}_1 + (A_1 - A_0)\mathbf{e}_1 + B_0 =, \\ & = A_0\mathbf{x} + (A_1 - A_0)\mathbf{e}_1(x_1 + 1) + (A_2 - A_1)\mathbf{e}_1(x_1 - 1) + B_0. \end{array}$$

Introducing now the 'ramp' function

$$\varphi_\delta(x) = \begin{cases} 0, & x < \delta, \\ x - \delta, & x \geq \delta, \end{cases}$$

we get for the system the compact form

$$\dot{\mathbf{x}} = A_0\mathbf{x} + (A_1 - A_0)\mathbf{e}_1\varphi_{-1}(x_1) + (A_2 - A_1)\mathbf{e}_1\varphi_1(x_1) + B_0. \tag{2.18}$$

Under the hypothesis concerning the existence of a vanishing non-trivial linear combination of the first columns of matrices $A_1 - A_0$ and $A_2 - A_1$, namely

$$\mu_1(A_1 - A_0)\mathbf{e}_1 + \mu_2(A_2 - A_1)\mathbf{e}_1 = 0,$$

there exist a vector B and constants b_1, b_2, such that

$$(A_1 - A_0)\mathbf{e}_1 = b_1 B, \quad (A_2 - A_1)\mathbf{e}_1 = b_2 B,$$

and then (2.18) becomes

$$\dot{\mathbf{x}} = A_0\mathbf{x} + B[b_1\varphi_{-1}(x_1) + b_2\varphi_1(x_1)] + B_0.$$

Hence, system (2.14) comes from the identification $A = A_0$, $C = B_0$, and

$$\mathrm{pwl}(x) = b_1\varphi_{-1}(x) + b_2\varphi_1(x).$$

Once arrived at (2.14), the particular case of statement (a) is a direct consequence after observing that at least one of the b_i must vanish and doing next an adequate translation in the variable x_1 to get as the only nonlinearity $\varphi_0(x)$. The case of statement (b) comes from the fact that then $\mu_1 = -\mu_2 = 1$, we also have trivially $b_1 = -b_2 = 1$ and we take advantage of the equality

$$\mathrm{sat}(x) = -1 + \varphi_{-1}(x) - \varphi_1(x),$$

that is (2.18) simplifies to

$$\begin{aligned}\dot{\mathbf{x}} &= A_0\mathbf{x} + (A_1 - A_0)\mathbf{e}_1[\varphi_{-1}(x_1) - \mathbf{e}_1\varphi_1(x_1)] + B_0 = \\ &= A_0\mathbf{x} + (A_1 - A_0)\mathbf{e}_1[-1 + \varphi_{-1}(x_1) - \mathbf{e}_1\varphi_1(x_1)] + B_0 + (A_1 - A_0)\mathbf{e}_1.\end{aligned}$$

It suffices now to identify $A = A_0$, $B = (A_1 - A_0)\mathbf{e}_1$, and $C = B_0 + (A_1 - A_0)\mathbf{e}_1$. ■

Of course, the configuration obtained from statement (a) of Lemma 2.3 is in fact a 2CPWL$_n$ system. In the case of statement (b) of Lemma 2.3, one gets in (2.14) the vector field as the sum of the function

$$H(\mathbf{x}) = A\mathbf{x} + B\,\mathrm{sat}(\mathbf{e}_1^T\mathbf{x})$$

plus a vector C, where the symmetry relation $H(\mathbf{x}) = H(-\mathbf{x}) = \mathbf{0}$ holds for all $\mathbf{x}$, leading to a quasi-symmetrical (just symmetrical, when $C = 0$) 3CPWL$_n$ system.

A key observation is that systems (2.14) for $C = 0$ are particular instances of the control systems

$$\left\{ \begin{array}{ll} \dot{\mathbf{x}} = & A\mathbf{x} + Bu, \\ y = & \mathbf{e}_1^T\mathbf{x}, \end{array} \right. \tag{2.19}$$

where $u = \mathrm{pwl}(y)$ is the *input* or control signal and y is the *output*. Then, some concepts of classical linear time invariant control systems are useful in obtaining reduced canonical forms for CPWL$_n$ systems with parallel boundaries. We recall them following [1] and [3].

Proposition 2.3 *System* (2.19) *is observable if and only if the observability matrix*

$$\mathcal{O} = \left(\mathbf{e}_1 \,|\, A^T\mathbf{e}_1 \,|\, (A^T)^2\mathbf{e}_1 \,|\, \cdots \,|\, (A^T)^{n-1}\mathbf{e}_1\right)^T$$

has rank n.

As is well known, the rank of observability matrix is invariant under linear changes of variables. Now, we give a canonical form for observable systems (2.19), which is slightly different from that of [3] but totally equivalent.

Proposition 2.4 *If system* (2.19) *is observable then it can be transformed by a linear change of variables into the canonical form*

$$\left\{ \begin{array}{ll} \dot{\mathbf{x}} = & M\mathbf{x} + Nu, \\ y = & \mathbf{e}_1^T\mathbf{x}, \end{array} \right. \tag{2.20}$$

where $N \in \mathbb{R}^n$, *and*

$$M = \left(\begin{array}{c|c} d_1 & \\ \vdots & -I_{n-1} \\ d_{n-1} & \\ \hline d_n & \mathbf{0} \end{array} \right).$$

Proof To begin with, let us assume for the matrix A in (2.19) that its characteristic polynomial is

$$p_A(\lambda) = (-1)^n\lambda^n + (-1)^{n-1}d_1\lambda^{n-1} + (-1)^{n-2}d_2\lambda^{n-2} + \cdots + (-1)d_{n-1}\lambda + d_n.$$

By the observability assumption, there exists a unique vector $\mathbf{z} \in \mathbb{R}^n$ such that

$$\mathbf{z}^T \left(\left(-A^T\right)^{n-1} \mathbf{e}_1 \,|\, \left(-A^T\right)^{n-2} \mathbf{e}_1 \,|\, \cdots \,|\, -A^T\mathbf{e}_1 \,|\, \mathbf{e}_1 \right) = \mathbf{e}_1^T. \tag{2.21}$$

Now, the following column-partitioned matrix is regular,

$$P = \left((-A)^{n-1}\mathbf{z} \,|\, (-A)^{n-2}\mathbf{z} \,|\, \cdots \,|\, -A\mathbf{z} \,|\, \mathbf{z} \right)$$

and we will use this matrix for the change of variables $\mathbf{x} = P\tilde{\mathbf{x}}$ in (2.19). First we see that our choice of $\mathbf{z}$ produces

$$y = \mathbf{e}_1^T\mathbf{x} = \mathbf{e}_1^T P\tilde{\mathbf{x}} = \tilde{\mathbf{x}}^T P^T\mathbf{e}_1 = \tilde{\mathbf{x}}^T\mathbf{e}_1 = \mathbf{e}_1^T\tilde{\mathbf{x}},$$

where we have used that condition (2.21) is equivalent, by transposition, to $P^T\mathbf{e}_1 = \mathbf{e}_1$. Now, we note that by Cayley-Hamilton theorem,

$$-(-1)^n A^n = (-1)^{n-1} d_1 A^{n-1} + (-1)^{n-2} d_2 A^{n-2} + \cdots + (-1) d_{n-1} A + d_n I,$$

so that

$$-(-A)^n = d_1(-A)^{n-1} + d_2(-A)^{n-2} + \cdots + d_{n-1}(-A) + d_n I,$$

and therefore

$$AP = \left(-(-A)^n\mathbf{z} \,|\, -(-A)^{n-1}\mathbf{z} \,|\, \cdots \,|\, -(-A)^2\mathbf{z} \,|\, -(-A)\mathbf{z} \right),$$

that is

$$AP = P \left(\begin{array}{c|c} d_1 & \\ \vdots & -I_{n-1} \\ d_{n-1} & \\ \hline d_n & \mathbf{0} \end{array} \right).$$

Hence, after substituting the change in (2.19), we see that $M = P^{-1}AP$, $N = P^{-1}B$, and we have discarded the tildes in achieving (2.20). ■

Remark 2.3 *From the proof of Proposition 2.2 it follows that* $\mathbf{e}_1^T P = \mathbf{e}_1^T$ *and so, the linear change does not modify the first state variable.*

Now, we resort to the control system properties previously established in order to obtain canonical forms for 2CPWL$_n$ and symmetrical 3CPWL$_n$ systems, also trying to deduce dynamical consequences in some cases. Due to the connection between (2.14) and (2.19), it is natural to state the following definition.

Definition 2.3 *The CPWL$_n$ system* (2.14) *is said to be observable if the control system* (2.19) *is observable.*

Under the assumption of observability, one can obtain a canonical form with both a simpler leading matrix and a simpler last constant vector. The next result constitutes a generalization of what have been made for particular systems, see for instance the elementary canonical models in [78] and [79].

Proposition 2.5 ***(Generalized Liénard's Form):*** *If system* (2.14) *is observable then it can be transformed by a linear change of variables into the canonical form*

$$\dot{\mathbf{x}} = M\mathbf{x} + N\,\mathrm{pwl}(x_1) + a\mathbf{e}_n, \tag{2.22}$$

where $a \in \mathbb{R}$, $N \in \mathbb{R}^n$, *and*

$$M = \begin{pmatrix} d_1 & -1 & 0 & \cdots & 0 \\ d_2 & 0 & -1 & \cdots & 0 \\ \vdots & \vdots & \vdots & \ddots & \vdots \\ d_{n-1} & 0 & 0 & \cdots & -1 \\ d_n & 0 & 0 & \cdots & 0 \end{pmatrix}.$$

Moreover, if $C = 0$ *in* (2.14), *then* $a = 0$.

Proof From hypothesis we can apply Proposition 2.4. The change of variables used there, given by the matrix P, transforms (2.22) into

$$\dot{\mathbf{x}} = M_L\mathbf{x} + N\,\mathrm{pwl}(x_1) + \tilde{N},$$

where M_L is as indicated above, and $\widetilde{N} = P^{-1}C$. Now, to obtain (2.22) it suffices to do a translation in the variables $x_2, \ldots, x_n$ to annihilate the first $n-1$ components of vector $\widetilde{N}$, namely

$$\mathbf{x} \to \mathbf{x} + \left(\begin{array}{c|c} \mathbf{0} & 0 \\ \hline I_{n-1} & \mathbf{0} \end{array}\right) \tilde{N}$$

and then $a = \mathbf{e}_n^T\tilde{N}$. ■

In the case of 2CPWL$_n$ systems, (2.22) can be written as follows

$$\dot{\mathbf{x}} = \begin{cases} M_L\mathbf{x} + a\mathbf{e}_n, & \text{if } x_1 < 0, \\ M_R\mathbf{x} + a\mathbf{e}_n, & \text{if } x_1 \geq 0, \end{cases} \tag{2.23}$$

where $M_L = M$, $M_R = M + N\mathbf{e}_1^T$ and both matrices only differ in their first columns.

2.3 Some generic results about equilibria

The knowledge of the structure of equilibria is an obligated previous step for the subsequent analysis of periodic orbits; equilibria and periodic orbits together, they provide a skeleton of the dynamical system, giving us important information. Next in Section 2.3.1, we review some dynamical properties of observable 2CPWL$_n$ systems (2.14) dealing with (2.23), where the number and location of equilibrium points can be easily deduced. After that, the analysis of equilibria in observable symmetric 3CPWL$_n$ systems is tackled in Section 2.3.2.

2.3.1 Observable 2CPWL$_n$ systems

If system (2.23) has an equilibrium point at the hyperplane $x_1 = 0$, where the system is not differentiable, we cannot determine its topological type by linearization and some counter-intuitive phenomena can appear, see [11]. However, equilibria at the hyperplane $x_1 = 0$ only can be located at the origin, as we state below.

Proposition 2.6 *If system* (2.23) *has one equilibrium with* $x_1 = 0$*, then such equilibrium is at the origin and* $a = 0$*.*

Proof If $x_1 = 0$, from the ith equation of (2.23) we have $x_{i+1} = 0$ for $1 \leq i \leq n-1$, and from the nth equation we get $a = 0$. ■

Corollary 2.1 *Equilibria of* (2.23) *different to the origin are not in the hyperplane* $x_1 = 0$*, so that corresponding linearizations are enough to analyze their topological type.*

Next result deals with the absence of equilibria, emphasizing that in such a case we cannot have periodic orbits.

Proposition 2.7 *If a 2CPWL$_n$ system* (2.14) *is observable and it has no equilibrium points, then it has no periodic orbits.*

Proof By Proposition 2.5, system (2.14) can be transformed in (2.23). Denoting $d_n^{\{L,R\}} = \mathbf{e}_n^T M_{\{L,R\}} \mathbf{e}_1$, we must have, by the absence of equilibria,

$a \cdot d_n^R > 0$ and $a \cdot d_n^L < 0$ and so

$$a\dot{x}_n = a(d_n^{\{L,R\}} x_1 + a) = \begin{cases} a \cdot d_n^L x_1 + a^2 > 0, & \text{if } x_1 < 0, \\ a \cdot d_n^R x_1 + a^2 > 0, & \text{if } x_1 \geq 0. \end{cases}$$

Then, the variable x_n is strictly monotone, and therefore neither (2.23) nor (2.14) can have periodic orbits. ■

Starting from system (2.23), we can write the system as follows,

$$\dot{\mathbf{x}} = M_L \mathbf{x} + N \operatorname{ramp}(x_1) + a\mathbf{e}_n, \tag{2.24}$$

where

$$N = (M_R - M_L)\mathbf{e}_1$$

and

$$M_{\{L,R\}} = \begin{pmatrix} d_1^{\{L,R\}} & -1 & 0 & \cdots & 0 \\ d_2^{\{L,R\}} & 0 & -1 & \cdots & 0 \\ \vdots & \vdots & \vdots & \ddots & \vdots \\ d_{n-1}^{\{L,R\}} & 0 & 0 & \cdots & -1 \\ d_n^{\{L,R\}} & 0 & 0 & \cdots & 0 \end{pmatrix}.$$

We study briefly the possible equilibria configurations for such 2CPWL$_n$ systems.

Proposition 2.8 *For system* (2.24) *the following statements holds.*

(a) *If $d_n^L d_n^R > 0$, then the system has one equilibrium point for all values of a.*

(b) *If $d_n^L d_n^R < 0$, then the system can have none, one or two equilibrium points depending on the sign of a.*

(c) *If $d_n^L = 0$ or $d_n^R = 0$, then degenerate situations appear for $a = 0$; leading to a half straight line of equilibrium points. For $a \neq 0$, there can be one or none equilibrium points.*

Proof All the assertions come from the analysis of last components of the vector field, namely by considering the equations $d_n^L x_1 + a = 0$, $d_n^R x_1 + a = 0$, and studying the sign of products $d_n^{\{L,R\}} a$. ■

2.3.2 Observable S3CPWL$_n$ systems

If we consider now an observable symmetric 3CPWL$_n$ system, we can write it in Liénard form, see Proposition 2.19, as follows,

$$\dot{\mathbf{x}} = M\mathbf{x} + N\,\mathrm{sat}(x_1),$$

where

$$M = \begin{pmatrix} d_1 & -1 & 0 & \cdots & 0 \\ d_2 & 0 & -1 & \cdots & 0 \\ \vdots & \vdots & \vdots & \ddots & \vdots \\ d_{n-1} & 0 & 0 & \cdots & -1 \\ d_n & 0 & 0 & \cdots & 0 \end{pmatrix}.$$

Thus, we can write

$$\dot{\mathbf{x}} = \begin{cases} M\mathbf{x} - N, & \text{if } x_1 < -1, \\ (M + N\mathbf{e}_1^T)\mathbf{x}, & \text{if } |x_1| \leq 1, \\ M\mathbf{x} + N, & \text{if } x_1 > 1. \end{cases}$$

If we define $D_i = N_i + d_i$, we can express N as

$$N = \begin{pmatrix} D_1 - d_1 \\ D_2 - d_2 \\ \vdots \\ D_n - d_n \end{pmatrix}.$$

Then, we can write the above system as follows

$$\dot{\mathbf{x}} = \begin{cases} M_E\mathbf{x} - N, & \text{if } x_1 < -1, \\ M_C\mathbf{x}, & \text{if } |x_1| \leq 1, \\ M_E\mathbf{x} + N, & \text{if } x_1 > 1, \end{cases} \tag{2.25}$$

where $M_E = M$,

$$M_C = \begin{pmatrix} D_1 & -1 & 0 & \cdots & 0 \\ D_2 & 0 & -1 & \cdots & 0 \\ \vdots & \vdots & \vdots & \ddots & \vdots \\ D_{n-1} & 0 & 0 & \cdots & -1 \\ D_n & 0 & 0 & \cdots & 0 \end{pmatrix}$$

and the subscript E means external zones, while the subscript C stands for central zone. For the above system, we have the following result, whose proof appears in [81], showing that these systems can undergo a degenerate pitchfork bifurcation at the origin.

Proposition 2.9 *For system* (2.25) *the following statements holds.*

(a) *If $D_n \neq 0$, and $d_n D_n \geq 0$, then the origin is the only equilibrium point.*

(b) *If $d_n D_n < 0$, then the system has three equilibrium points, the origin, the point*

$$\bar{\mathbf{x}}_L = \frac{1}{d_n} \begin{pmatrix} D_n - d_n \\ D_n d_1 - d_n D_1 \\ \vdots \\ D_n d_{n-1} - d_n D_{n-1} \end{pmatrix},$$

in the left zone, and its symmetric $\bar{\mathbf{x}}_R = -\bar{\mathbf{x}}_L$ in the right zone.

(c) *If $D_n = 0$, then the segment points $\bar{\mathbf{x}}_C(\mu) = \mu(1, D_1, D_2, \ldots, D_{n-1})^T$ with $|\mu| \leq 1$ are equilibrium points of system* (2.25) *and we have the following cases.*

(i) *If $d_n = 0$, the points of the ray*

$$\bar{\mathbf{x}}_L(\mu) = \mu \begin{pmatrix} 1 \\ d_1 \\ d_2 \\ \vdots \\ d_{n-1} \end{pmatrix} + \frac{\mu}{|\mu|} \begin{pmatrix} 0 \\ D_1 - d_1 \\ D_2 - d_2 \\ \vdots \\ D_{n-1} - d_{n-1} \end{pmatrix},$$

for all μ with $|\mu| > 1$, are also equilibrium points of the system.

(ii) *If $d_n \neq 0$, the system has no equilibrium points in the outer zones.*

2.4 Analysis of periodic orbits through their closing equations

With the name *closing equations method*, we mean a method for determining periodic orbits in piecewise linear dynamical systems, to be used in the

analysis of 2CPWL$_n$ and S3CPWL$_n$ along the manuscript. The main idea of the method is to integrate the corresponding system in each linear zone and obtain a system of equations, called closing equations, whose solutions correspond to the periodic orbits of the initial dynamical system. This idea already appears for the first time in [2], and revisited later by other authors, see [48] and [69]. In [49], appropriate series expansions were used in the closing equations to approximate the amplitude and period of periodic orbits of piecewise linear systems successfully.

In the Section 2.4.1 we explain the approach of the method of closing equations for 2CPWL$_n$, while in the Section 2.4.2 we apply the method to symmetric 3CPWL$_n$.

2.4.1 Closing equations for 2CPWL$_n$

Let us consider the method for 2CPWL$_n$ systems and denote by Σ_0 the hiperplane $x_1 = 0$. Our interest is to analyze the properties of periodic orbits that use both zones of $\mathbb{R}^n$; on the contrary there should be periodic orbits totally contained in one of the half-spaces $x_1 > 0$ or $x_1 < 0$, thereby being purely linear periodic orbits belonging to a linear center. Assume the existence of one periodic orbit intersecting Σ_0 at the two points

$$\hat{\mathbf{x}}^0 = \begin{pmatrix} 0 \\ \hat{x}_2^0 \\ \hat{x}_3^0 \\ \vdots \\ \hat{x}_n^0 \end{pmatrix}, \ \hat{\mathbf{x}}^1 = \begin{pmatrix} 0 \\ \hat{x}_2^1 \\ \hat{x}_3^1 \\ \vdots \\ \hat{x}_n^1 \end{pmatrix}.$$

See figure 2.1. We write the flight time in the left zone ($x_1 < 0$) as τ_L, being τ_R the corresponding flight time in the right zone ($x_1 > 0$).

Assume that the point $\hat{\mathbf{x}}_0$ is mapped into $\hat{\mathbf{x}}_1$ by the flow on the left zone. Since system (2.23) is linear in each zone, we can write the solution starting at $\hat{\mathbf{x}}_0$ as

$$\mathbf{x}(\tau) = e^{M_L \tau} \hat{\mathbf{x}}_0 + \int_0^\tau e^{M_L(\tau - s)} a \mathbf{e}_n ds.$$

Consequently, we must have

$$\hat{\mathbf{x}}_1 = e^{M_L \tau_L} \hat{\mathbf{x}}_0 + \int_0^{\tau_L} e^{M_L(\tau_L - s)} a \mathbf{e}_n ds. \tag{2.26}$$

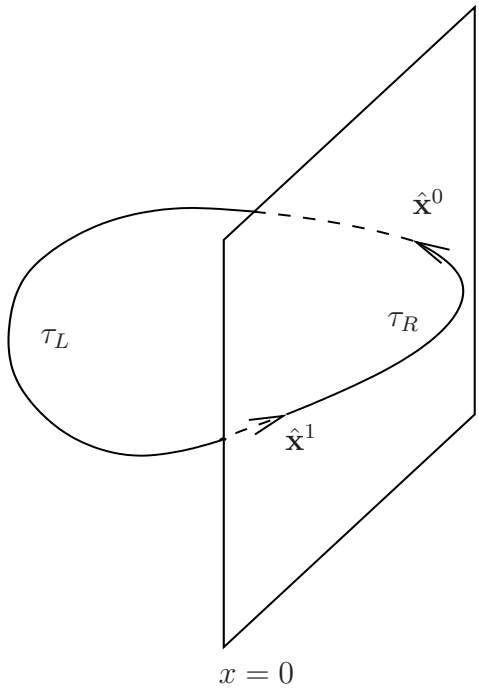

Figure 2.1: Bizonal periodic orbit of system (2.23) and the relevant points necessary to build the closing equations.

Doing the same procedure in the right zone, we conclude that

$$\hat{\mathbf{x}}_0 = e^{M_R \tau_R} \hat{\mathbf{x}}_1 + \int_0^{\tau_R} e^{M_R(\tau_R - s)} a \mathbf{e}_n ds. \tag{2.27}$$

Note that (2.26) and (2.27) form a nonlinear system with $2n$ equations and $2n$ unknowns. From these unknowns, $(2n-2)$ correspond to the Σ_0-coordinates of the periodic orbit intersections and the other two are the flight times τ_L, τ_R. For the analysis of the closing equations, typically we start from a known solution coming from a degenerate situation, see Chapter 4.

We summarize the above ideas in the following result.

Proposition 2.10 *Assume that the system* (2.23) *has a bizonal periodic orbit that transversely intersecting the hyperplane* Σ_0 *in the points* $\hat{\mathbf{x}}^0$ *and* $\hat{\mathbf{x}}^1$ *respectively, with flight times* $\hat{\tau}_L > 0$ *and* $\hat{\tau}_R > 0$ *in the zones* L *and* R*. Then, the values* $\hat{\tau}_L$, $\hat{\tau}_R$, $\hat{\mathbf{x}}^0$ *and* $\hat{\mathbf{x}}^1$ *satisfy closing equations* (2.26) *and* (2.27)*.*

Alternatively, whenever the system $M_{\{L,R\}}\mathbf{x} + a\mathbf{e}_n = 0$ is compatible and $\overline{\mathbf{x}}_{\{L,R\}}$ is a equilibrium solution, we can transform system (2.23) by a translation in a homogeneous one to solve it, and next undo the translation. Thus, the solution can be written

$$\mathbf{x}(\tau) = \bar{\mathbf{x}}_{\{L,R\}} + e^{M_{\{L,R\}}\tau}\left(\hat{\mathbf{x}}(0) - \bar{\mathbf{x}}_{\{L,R\}}\right).$$

Thus, in this cases, the expression (2.26) can be replaced by

$$\hat{\mathbf{x}}_1 = \bar{\mathbf{x}}_L + e^{M_L\tau_L}\left(\hat{\mathbf{x}}_0 - \bar{\mathbf{x}}_L\right),$$

while the equality (2.27) can be replaced by

$$\hat{\mathbf{x}}_0 = \bar{\mathbf{x}}_R + e^{M_R\tau_R}\left(\hat{\mathbf{x}}_1 - \bar{\mathbf{x}}_R\right).$$

2.4.2 Closing equations for S3CPWL$_n$

System (2.25) can have different kinds of periodic orbits, regarding their intersections of these orbits with separating hyperplanes. First, there could be periodic orbits completely contained in each linearity zone, but then, due to the linear dynamics of the system in each zone, these orbits can only occur as members of a linear center, which leads to a simple, almost trivial case.

More interestingly, there can appear periodic orbits that intersect at only one of the hyperplanes Σ_1 or Σ_{-1}. We call them bizonal periodic orbits. Each of these orbits has its corresponding symmetrical due to the symmetry of the system, and so they come in pairs. We consider only such bizonal orbits when they have just two intersection points with one of the hyperplanes. These bizonal periodic orbits in S3CPWL$_n$ can be analyzed using a similar approach of the Section 2.4.1.

Finally, there could exist orbits transversely intersecting the two hyperplanes Σ_1 and Σ_{-1}. These orbits use the three zones and are called tri-zonal periodic orbits; they can be symmetrical with respect to the origin or not. Even the method is also applicable to such last case, it will not be the studied in this thesis, due to the higher number of unknowns to consider. We will limit our attention to tri-zonal symmetric periodic orbits with two intersection points in each hyperplane, and here we are going to explain the closing equations method only for such closed orbits.

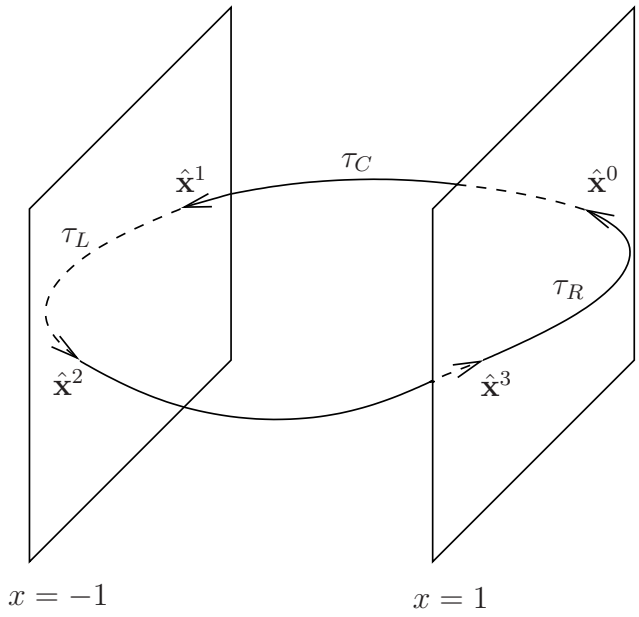

Figure 2.2: Symmetric tri-zonal periodic orbit of system (2.25) and the relevant points necessary to build the closing equations.

We assume the existence of one of these orbits. Their intersections with Σ_1 are $\hat{\mathbf{x}}^0$, $\hat{\mathbf{x}}^3$, and their intersections with Σ_{-1} are $\hat{\mathbf{x}}^2$, $\hat{\mathbf{x}}^1$, where

$$\hat{\mathbf{x}}^0 = \begin{pmatrix} 1 \\ \hat{x}_2^0 \\ \hat{x}_3^0 \\ \vdots \\ \hat{x}_n^0 \end{pmatrix}, \hat{\mathbf{x}}^1 = \begin{pmatrix} -1 \\ \hat{x}_2^1 \\ \hat{x}_3^1 \\ \vdots \\ \hat{x}_n^1 \end{pmatrix}, \hat{\mathbf{x}}^2 = \begin{pmatrix} -1 \\ \hat{x}_2^2 \\ \hat{x}_3^2 \\ \vdots \\ \hat{x}_n^2 \end{pmatrix}, \hat{\mathbf{x}}^3 = \begin{pmatrix} 1 \\ \hat{x}_2^3 \\ \hat{x}_3^3 \\ \vdots \\ \hat{x}_n^3 \end{pmatrix},$$

see Figure 2.2. The symmetry of the periodic orbit of the system (2.25) implies $\hat{\mathbf{x}}^2 = -\hat{\mathbf{x}}^0$ and $\hat{\mathbf{x}}^3 = -\hat{\mathbf{x}}^1$, then the study of the trajectory between $\hat{\mathbf{x}}^0$ and $\hat{\mathbf{x}}^2$ is sufficient to completely determine the orbit.

We define the flight time τ_C of the central zone C, as the time taken by an orbit of (2.25) to move from $\hat{\mathbf{x}}^0$ to $\hat{\mathbf{x}}^1$. Similarly, we denote the flight time of the zone L with τ_L, which is the time taken by the trajectory to move from $\hat{\mathbf{x}}^1$ to $\hat{\mathbf{x}}^2$.

Since system (2.25) is linear in each zone, we can write explicitly their solutions as follows. In the central zone C, we have $\dot{\mathbf{x}} = M_C\mathbf{x}$, with the

initial condition

$$\mathbf{x}(0) = \mathbf{x}^0 = \left(1, x_2^0, x_3^0, \ldots, x_n^0\right)^T,$$

so that the corresponding solution of (2.25) in the zone C is

$$\mathbf{x}(\tau) = e^{M_C \tau_C} \mathbf{x}^0.$$

Now, let $\mathbf{x}^1 \in \Sigma_{-1}$, the point of the trajectory where $\tau = \tau_C$, thus satisfies

$$e^{M_C \tau_C} \mathbf{x}^0 - \mathbf{x}^1 = \mathbf{0}, \tag{2.28}$$

and this equation is the first closing equation of system (2.25).

In the left zone L, the system is not homogeneous, and taking as initial condition $\mathbf{x}(0) = \mathbf{x}^1 = (-1, x_2^1, x_3^1, \ldots, x_n^1)^T$, we obtain that the solution is

$$\mathbf{x}(\tau) = e^{M_E \tau} \mathbf{x}^1 + \int_0^\tau e^{M_E(\tau - s)}(-N) ds.$$

If we denote $\mathbf{x}^2 \in \Sigma_{-1}$ the point the trajectory reaches for $\tau = \tau_L$, we have

$$e^{M_E \tau_L} \mathbf{x}^1 + \int_0^{\tau_L} e^{M_E(\tau_L - s)}(-N) ds - \mathbf{x}^2 = \mathbf{0}. \tag{2.29}$$

Due to the symmetry of the periodic orbit, we have $\mathbf{x}^2 = -\mathbf{x}^0$ and equation (2.29) becomes

$$e^{M_E \tau_L} \mathbf{x}^1 + \int_0^{\tau_L} e^{M_E(\tau_L - s)}(-N) ds + \mathbf{x}^0 = \mathbf{0}. \tag{2.30}$$

Equation (2.30) is the second closing equation of system (2.25). Equations (2.28) and (2.30) form a nonlinear system with $2n$ equations and $2n$ unknowns, τ_L, τ_C, x_2^0, x_3^0, ..., x_n^0, x_2^1, x_3^1, ..., x_n^1.

The following result summarizes the above ideas.

Proposition 2.11 *Assume that the system* (2.25) *has a tri-zonal symmetric periodic orbit that transversely intersecting the hyperplanes* Σ_1 *and* Σ_{-1} *in the points* $\hat{\mathbf{x}}^0$ *and* $\hat{\mathbf{x}}^1$ *respectively, with flight times* $\hat{\tau}_L > 0$ *and* $\hat{\tau}_C > 0$ *in the zones* L *and* C*. Then, the values* $\hat{\tau}_L$, $\hat{\tau}_C$, $\hat{\mathbf{x}}^0$ *and* $\hat{\mathbf{x}}^1$ *satisfy closing equations* (2.28) *and* (2.30)*.*

2.5 Poincaré maps of CPWL$_n$ systems

In this section we remind basic ideas about Poincaré maps and some specific related results of 2CPWL$_n$ and S3CPWL$_n$ systems, that we apply to the analysis of several bifurcation problems in chapters 3 and 4 of this document.

2.5.1 Poincaré maps in 2CPWL$_n$

We begin by considering a bizonal periodic orbit Γ_{2Z} of system (2.23), intersecting transversally Σ_0 hyperplane at points $\hat{\mathbf{x}}^0$ and $\hat{\mathbf{x}}^1$.

The transversality condition of Γ_{2Z} with respect to Σ_0 at $\hat{\mathbf{x}}^0$ can be written as

$$\langle \mathbf{e}_1^T, M_L \hat{\mathbf{x}}^0 \rangle = -\hat{x}_2^0 \neq 0.$$

Denote by Φ_{2Z} the vector field of system (2.23) and assume $\Phi_{2Z}(\tau_0, \hat{\mathbf{x}}^0) = \hat{\mathbf{x}}^1$ for $\tau_0 > 0$.

Under the previous transversality hypothesis, we can assure the existence of an open neighborhood of $\hat{\mathbf{x}}^0$ named U_0, another neighborhood U_1 of $\hat{\mathbf{x}}^1$, and an application $\tau_L : U_0 \longrightarrow \mathbb{R}$ such that $\tau_L(\hat{\mathbf{x}}^0) = \tau_0$, $\Phi_{2Z}(\tau_L(\mathbf{x}^0), \mathbf{x}^0) \in U_1 \cap \Sigma_0$ for all $\mathbf{x}^0 \in U_0 \cap \Sigma_0$.

We denote by Π_L the Poincaré map in the zone L associated to the periodic orbit Γ_{2Z}, that is,

$$\begin{array}{rccc} \Pi_L : & U_0 \cap \Sigma_0 & \longrightarrow & U_1 \cap \Sigma_0 \\ & \mathbf{x}^0 & \longmapsto & \Phi_{2Z}(\tau_L(\mathbf{x}^0), \mathbf{x}^0). \end{array}$$

Analogously, in the zone R, we can assure the existence of an open neighborhood of $\hat{\mathbf{x}}^1$ named V_0, an open neighborhood V_1 of $\hat{\mathbf{x}}^2$ and an application $\tau_R : V_0 \longrightarrow \mathbb{R}$ such that $\tau_R(\hat{\mathbf{x}}^1) = \tau_1$, $\Phi_{2Z}(\tau_R(\mathbf{x}^1), \mathbf{x}^1) \in V_1 \cap \Sigma_0$ for all $\mathbf{x}^1 \in V_0 \cap \Sigma_0$.

We denote by Π_R the Poincaré map in the zone R associated to the periodic orbit Γ_{2Z}, that is

$$\begin{array}{rccc} \Pi_R : & V_0 \cap \Sigma_0 & \longrightarrow & V_1 \cap \Sigma_0 \\ & \mathbf{x}^1 & \longmapsto & \Phi_{2Z}(\tau_R(\mathbf{x}^1), \mathbf{x}^1). \end{array}$$

Each point $\mathbf{x}^0$ in Σ_0 has a unique $\mathbf{p}_0 \in \mathbb{R}^{n-1}$ associated. In the same way, $\mathbf{x}^1$ in Σ_0 has associated a unique $\mathbf{p}_1 \in \mathbb{R}^{n-1}$. The points $\mathbf{p}_0$ and $\mathbf{p}_1$ are called reduced coordinates of $\mathbf{x}^0$ and $\mathbf{x}^1$ respectively, and verify

$$\mathbf{x}^0 = \begin{pmatrix} 0 \\ \mathbf{p}_0 \end{pmatrix}, \mathbf{x}^1 = \begin{pmatrix} 0 \\ \mathbf{p}_1 \end{pmatrix} \in \Sigma_0.$$

Suppose that $\mathbf{x}^0$ and $\mathbf{x}^1$ are in Σ_0, so that $\mathbf{x}^1 = \Pi_L(\mathbf{x}^0)$, and $\mathbf{p}_0$ and $\mathbf{p}_1$ are the reduced coordinates of $\mathbf{x}^0$ and $\mathbf{x}^1$ respectively, then we can define the function π_L that provides the reduced coordinates of the Poincaré map Π_L associated with Γ_{2Z} in the zone L, as follows

$$\begin{array}{rccl} \pi_L: & \mathbb{P}_{n-1}(U_0 \cap \Sigma_0) & \longrightarrow & \mathbb{P}_{n-1}(U_1 \cap \Sigma_0) \\ & \mathbf{p}_0 & \longmapsto & \pi_L(\mathbf{p}_0) = \mathbf{p}_1, \end{array}$$

where $\mathbb{P}_{n-1}$ represents the canonical projection associated with the $n-1$ last coordinates. We define the flight time $\bar{\tau}_L$ in the zone L as $\bar{\tau}_L(\mathbf{p}_0) = \tau_L(\mathbf{x}^0)$.

Suppose $\mathbf{x}^1, \mathbf{x}^2 \in \Sigma_0$, so that $\mathbf{x}^2 = \Pi_R(\mathbf{x}^1)$, and $\mathbf{p}_1, \mathbf{p}_2$ are the reduced coordinates of $\mathbf{x}^1$ and $\mathbf{x}^2$ respectively. We define the function π_R that gives the reduced coordinates of the Poincaré map Π_R associated with Γ_{2Z} in the zone R, as

$$\begin{array}{rccl} \pi_R: & \mathbb{P}_{n-1}(V_0 \cap \Sigma_0) & \longrightarrow & \mathbb{P}_{n-1}(V_1 \cap \Sigma_0) \\ & \mathbf{p}_1 & \longmapsto & \pi_R(\mathbf{p}_1) = \mathbf{p}_2, \end{array}$$

and we define the flight time $\bar{\tau}_R$ in the zone R as $\bar{\tau}_R(\mathbf{p}_1) = \tau_R(\mathbf{x}^1)$.

Under the above conditions and choosing V_0 such that $U_1 \subset V_0$, we define the complete Poincaré map Π as follows

$$\begin{array}{rccl} \Pi: & U_0 \cap \Sigma_0 & \longrightarrow & V_1 \cap \Sigma_0 \\ & \mathbf{x}^0 & \longmapsto & \Pi(\mathbf{x}^0) = (\Pi_R \circ \Pi_L)(\mathbf{x}^0). \end{array}$$

It is easy to see that $\Pi(\mathbf{x}^0) = \Phi_{2Z}(\tau_L(\mathbf{x}^0) + \tau_R(\Pi_L(\mathbf{x}^0)), \mathbf{x}^0)$.

Also, we define the function that gives the reduced coordinates of the complete Poincaré map π as

$$\begin{array}{rccl} \pi: & \mathbb{P}_{n-1}(U_0 \cap \Sigma_0) & \longrightarrow & \mathbb{P}_{n-1}(V_1 \cap \Sigma_0) \\ & \mathbf{p}_0 & \longmapsto & \pi(\mathbf{p}_0) = (\pi_R \circ \pi_L)(\mathbf{p}_0) = \mathbf{x}^2. \end{array}$$

The following proposition, see Proposition 3 of [7] for the proof, is useful to study the stability of periodic orbits in 2CPWL$_n$ systems.

Proposition 2.12 *Let Γ_{2Z} be a bizonal periodic orbit of system (2.23), transversely intersecting boundary Σ_0 at the points $\hat{\mathbf{x}}^0$ and $\hat{\mathbf{x}}^1$, and let $\hat{\mathbf{p}}^0$, $\hat{\mathbf{p}}^1$ in $\mathbb{R}^{n-1}$ be theirs respective reduced coordinates. Denote by $\hat{\tau}_L > 0$ and $\hat{\tau}_R > 0$ the flight times of Γ_{2Z} in the zone L and R respectively. If we define the matrices Q_L and Q_R as*

$$Q_L = \begin{pmatrix} 1 & \nabla\bar{\tau}_L(\hat{\mathbf{p}}_1) \\ \mathbf{0} & D\pi_L(\hat{\mathbf{p}}_1) \end{pmatrix}, Q_R = \begin{pmatrix} 1 & \nabla\bar{\tau}_R(\hat{\mathbf{p}}_0) \\ \mathbf{0} & D\pi_R(\hat{\mathbf{p}}_0) \end{pmatrix},$$

then the product of matrices $e^{M_L\hat{\tau}_L}e^{M_R\hat{\tau}_R}$ *is similar to the matrix*

$$Q_LQ_R = \begin{pmatrix} 1 & \nabla\bar{\tau}_L + \nabla\bar{\tau}_R D\pi_L \\ \mathbf{0} & D\pi \end{pmatrix}_{\Gamma_{2Z}}.$$

The following corollary relates the characteristic multipliers of periodic orbits in 2CPWL$_n$ with the product of matrices of the previous lemma.

Corollary 2.2 *Under the conditions of Proposition 2.12, an eigenvalue of*

$$e^{M_L\hat{\tau}_L}e^{M_R\hat{\tau}_R}$$

is 1 *and the other* $n-1$ *eigenvalues are the characteristic multipliers of a periodic orbit* Γ_{2Z} *of system* (2.23)*.*

2.5.2 Poincaré maps in S3CPWL$_n$

Let Γ_{3Z} be a tri-zonal periodic orbit of system (2.25) symmetric respect to the origin, intersecting transversally Σ_1 hyperplane at points $\hat{\mathbf{x}}^0$ and $\hat{\mathbf{x}}^3$, and Σ_{-1} in $\hat{\mathbf{x}}^1$ and $\hat{\mathbf{x}}^2$.

The transversality condition of Γ_{3Z} with respect to Σ_1 at $\hat{\mathbf{x}}^0$ can be written as

$$\langle \mathbf{e}_1^T, M_C\hat{\mathbf{x}}^0\rangle = D_1 - \hat{x}_2^0 \neq 0.$$

Similarly for Σ_{-1}, we have

$$\langle \mathbf{e}_1^T, M_C\hat{\mathbf{x}}^1\rangle = -D_1 - \hat{x}_2^1 \neq 0.$$

We denote by Φ_{3Z} the vector field of system (2.25) and assume $\Phi_{3Z}(\tau_0, \hat{\mathbf{x}}^0) = \hat{\mathbf{x}}^1$ for $\tau_0 > 0$.

Under the previous transversality hypothesis, we can assure the existence of an open neighborhood U_0 of $\hat{\mathbf{x}}^0$, another neighborhood U_1 of $\hat{\mathbf{x}}^1$, and an application $\tau_C : U_0 \longrightarrow \mathbb{R}$ such that $\tau_C(\hat{\mathbf{x}}^0) = \tau_0$, $\Phi_{3Z}(\tau_C(\mathbf{x}^0), \mathbf{x}^0) \in U_1 \cap \Sigma_{-1}$ for all $\mathbf{x}^0 \in U_0 \cap \Sigma_1$.

We denote by Π_C the Poincaré map in the zone C associated to the periodic orbit Γ_{3Z}, that is,

$$\begin{array}{rccc} \Pi_C : & U_0 \cap \Sigma_1 & \longrightarrow & U_1 \cap \Sigma_{-1} \\ & \mathbf{x}^0 & \longmapsto & \Phi_{3Z}(\tau_C(\mathbf{x}^0), \mathbf{x}^0). \end{array}$$

Analogously in the zone L, if we assure the existence of an open neighborhood V_0 of $\hat{\mathbf{x}}^1$, an open neighborhood V_1 of $\hat{\mathbf{x}}^2$, and an application $\tau_L : V_0 \longrightarrow \mathbb{R}$ such that $\tau_L(\hat{\mathbf{x}}^1) = \tau_1$, $\Phi_{3Z}(\tau_L(\mathbf{x}^1), \mathbf{x}^1) \in V_1 \cap \Sigma_{-1}$ for all $\mathbf{x}^1 \in V_0 \cap \Sigma_{-1}$.

We denote by Π_L the Poincaré map in the zone L associated to the periodic orbit Γ_{3Z}, that is

$$\begin{array}{rccl} \Pi_L : & V_0 \cap \Sigma_{-1} & \longrightarrow & V_1 \cap \Sigma_{-1} \\ & \mathbf{x}^1 & \longmapsto & \Phi_{3Z}(\tau_L(\mathbf{x}^1), \mathbf{x}^1). \end{array}$$

Associated with every point $\mathbf{x}^0 \in \Sigma_1$ and $\mathbf{x}^1 \in \Sigma_{-1}$, unique $\mathbf{p}_0, \mathbf{p}_1 \in \mathbb{R}^{n-1}$ points exist. They are called reduced coordinates of $\mathbf{x}^0$ and $\mathbf{x}^1$ respectively, and verify

$$\mathbf{x}^0 = \begin{pmatrix} 1 \\ \mathbf{p}_0 \end{pmatrix} \in \Sigma_1, \; \mathbf{x}^1 = \begin{pmatrix} -1 \\ \mathbf{p}_1 \end{pmatrix} \in \Sigma_{-1}.$$

Suppose $\mathbf{x}^0 \in \Sigma_1$ and $\mathbf{x}^1 \in \Sigma_{-1}$, so that $\mathbf{x}^1 = \Pi_C(\mathbf{x}^0)$, and $\mathbf{p}_0$ and $\mathbf{p}_1$ are the reduced coordinates of $\mathbf{x}^0$ and $\mathbf{x}^1$ respectively, then we can define the function π_C which gives reduced coordinates of the Poincaré map Π_C associated with Γ_{3Z} in the central zone C, as follows

$$\begin{array}{rccl} \pi_C : & \mathbb{P}_{n-1}(U_0 \cap \Sigma_1) & \longrightarrow & \mathbb{P}_{n-1}(U_1 \cap \Sigma_{-1}) \\ & \mathbf{p}_0 & \longmapsto & \pi_C(\mathbf{p}_0) = \mathbf{p}_1, \end{array}$$

where $\mathbb{P}_{n-1}$ represents the canonical projection associated with the $n-1$ last coordinates. We define the flight time $\bar{\tau}_C$ in the zone C as $\bar{\tau}_C(\mathbf{p}_0) = \tau_C(\mathbf{x}^0)$.

Suppose $\mathbf{x}^1, \mathbf{x}^2 \in \Sigma_{-1}$, so that $\mathbf{x}^2 = \Pi_L(\mathbf{x}^1)$, and $\mathbf{p}_1, \mathbf{p}_2$ are the reduced coordinates of $\mathbf{x}^1$ and $\mathbf{x}^2$ respectively, then we define the function π_L which gives the reduced coordinates of the Poincaré map Π_L associated with Γ_{3Z} in the left zone L, as

$$\begin{array}{rccl} \pi_L : & \mathbb{P}_{n-1}(V_0 \cap \Sigma_{-1}) & \longrightarrow & \mathbb{P}_{n-1}(V_1 \cap \Sigma_{-1}) \\ & \mathbf{p}_1 & \longmapsto & \pi_L(\mathbf{p}_1) = \mathbf{p}_2, \end{array}$$

and we define the flight time $\bar{\tau}_L$ in the zone L as $\bar{\tau}_L(\mathbf{p}_1) = \tau_L(\mathbf{x}^1)$.

Under the above conditions and choosing V_0 such that $U_1 \subset V_0$, we define the Poincaré semi-map Π_1 as follows

$$\begin{array}{rccl} \Pi_1 : & U_0 \cap \Sigma_1 & \longrightarrow & V_1 \cap \Sigma_{-1} \\ & \mathbf{x}^0 & \longmapsto & \Pi_1(\mathbf{x}^0) = (\Pi_L \circ \Pi_C)(\mathbf{x}^0). \end{array}$$

It is easy to see that $\Pi_1(\mathbf{x}^0) = \Phi_{3Z}(\tau_C(\mathbf{x}^0) + \tau_L(\Pi_C(\mathbf{x}^0)), \mathbf{x}^0)$.

Also, we define the function that gives the reduced coordinates of the Poincaré semi-map π_1 as

$$\begin{array}{rccl} \pi_1: & \mathbb{P}_{n-1}(U_0 \cap \Sigma_1) & \longrightarrow & \mathbb{P}_{n-1}(V_1 \cap \Sigma_{-1}) \\ & \mathbf{p}_0 & \longmapsto & \pi_1(\mathbf{p}_0) = (\pi_L \circ \pi_C)(\mathbf{p}_0). \end{array}$$

We define the full Poincaré map as follows

$$\begin{array}{rccl} \Pi: & U_0 \cap \Sigma_1 & \longrightarrow & \Sigma_1 \\ & \mathbf{x}^0 & \longmapsto & \Pi(\mathbf{x}^0) = \mathbf{x}^3, \end{array}$$

providing the transformed of a point $\mathbf{x}^0 \in \Sigma_1$ through the flow of the system vector field in other point $\mathbf{x}^3 \in \Sigma_1$.

Due to the symmetry of the system, the equality

$$\mathbf{x}^3 = -\Pi_1(-\mathbf{x}^2) = -\Pi_1(-\Pi_1(\mathbf{x}^0))$$

holds and then $\Pi = (-\Pi_1) \circ (-\Pi_1)$. We can define the function π which gives the reduced coordinates of the Poincaré complete map Π as

$$\begin{array}{rccl} \pi: & \mathbb{P}_{n-1}(U_0 \cap \Sigma_1) & \longrightarrow & \mathbb{R}_{n-1} \\ & \mathbf{p}_0 & \longmapsto & \pi(\mathbf{p}_0) = (-\pi_1) \circ (-\pi_1)(\mathbf{p}_0). \end{array}$$

The following proposition will be used to determine the stability of periodic orbits in S3CPWL$_n$ in Chapter 4, see [27] for the proof.

Proposition 2.13 *Let Γ_{3Z} be a tri-zonal symmetrical periodic orbit of system (2.25), transversely intersecting boundaries Σ_1 at the points $\hat{\mathbf{x}}^0$ and $\hat{\mathbf{x}}^3$, and Σ_{-1} at the points $\hat{\mathbf{x}}^1$ and $\hat{\mathbf{x}}^2$, and let $\hat{\mathbf{p}}^0$, $\hat{\mathbf{p}}^3$, $\hat{\mathbf{p}}^1$, $\hat{\mathbf{p}}^2 \in \mathbb{R}^{n-1}$ be theirs respective reduced coordinates. Denote by $\hat{\tau}_L > 0$ and $\hat{\tau}_C > 0$ the flight times of Γ_{3Z} in the external and central zones respectively. If we define the matrices Q_L and Q_C*

$$Q_L = \begin{pmatrix} 1 & \nabla\bar{\tau}_L(\hat{\mathbf{p}}_1) \\ \mathbf{0} & D\pi_L(\hat{\mathbf{p}}_1) \end{pmatrix}, \; Q_C = \begin{pmatrix} -1 & \nabla\bar{\tau}_C(\hat{\mathbf{p}}_0) \\ \mathbf{0} & D\pi_C(\hat{\mathbf{p}}_0) \end{pmatrix},$$

then the product of matrices $e^{M_L\hat{\tau}_L}e^{M_C\hat{\tau}_C}$ is similar to the matrix

$$Q_LQ_C = \begin{pmatrix} -1 & \nabla\bar{\tau}_C + \nabla\bar{\tau}_L D\pi_C \\ \mathbf{0} & D\pi_1 \end{pmatrix}_{\Gamma_{3Z}}.$$

The following corollary relates the characteristic multipliers of periodic orbits in S3CPWL$_n$ with the product of matrices of the previous lemma.

Corollary 2.3 *Under the conditions of Proposition 2.13, an eigenvalue of*

$$e^{M_L\hat{\tau}_L}e^{M_C\hat{\tau}_C}$$

is -1 *and the squares of the other* $n-1$ *eigenvalues are the characteristic multipliers of the periodic orbit* Γ_{3Z} *of system* (2.25).

Once reviewed all these auxiliary results, we can pass to the main part of our thesis, that is, to the analysis of limit cycles and bifurcations in specific families of 2PWL and 3PWL differential systems.

CHAPTER 3

Some contributions to planar dynamical systems

In this chapter we pay attention to planar piecewise linear systems, including some new results, but also reviewing others already known. Most of the new material reported can be also found in [59, 76, 74]; some extensions of these recent results are also included. In particular, we give a shorter, alternative approach to the study done in [23] in order to show the Lum-Chua Conjecture, and new results on existence of limit cycles in 3CPWL_2 without symmetry.

3.1 Analysis of 2CPWL_2 systems

When dealing with planar piecewise linear systems with only two zones, which we assume to be observable, according to Remark 2.1, we consider that $t_C = t_L$ and $d_C = d_L$. Then, the Liénard canonical form (2.5)-(2.7) becomes

$$\begin{array}{rcl} \dot{x} & = & F(x) - y, \\ \dot{y} & = & g(x) - \delta, \end{array} \tag{3.1}$$

where

$$F(x) = \begin{cases} t_L x & \text{if } x < 1, \\ t_R(x-1) + t_L & \text{if } x \geq 1, \end{cases} \tag{3.2}$$

and

$$g(x) = \begin{cases} d_L x & \text{if } x < 1, \\ d_R(x-1) + d_L & \text{if } x \geq 1. \end{cases} \tag{3.3}$$

Sometimes it is more convenient to displace the boundary $x = 1$ to $x = 0$. If we make $X = x - 1$, $Y = y - t_L$, $a = \delta - d_L$ we obtain the alternative canonical form

$$\begin{array}{rcl} \dot{X} & = & \widetilde{F}(X) - Y, \\ \dot{Y} & = & \widetilde{g}(X) - a, \end{array} \tag{3.4}$$

where

$$\widetilde{F}(X) = \begin{cases} t_L X & \text{if } X < 0, \\ t_R X & \text{if } X \geq 0, \end{cases} \tag{3.5}$$

and

$$\widetilde{g}(X) = \begin{cases} d_L X & \text{if } X < 0, \\ d_R X & \text{if } X \geq 0. \end{cases} \tag{3.6}$$

Remark 3.1 *In system* (3.4)-(3.6)*, only the sign of* a *is relevant. In fact, when* $a \neq 0$*, the system can be rewritten with* $a = 1$ *by changing* $x = aX$*,* $y = aY$*. However, we will not do it in order to capture possible bifurcations in* $a = 0$*.*

Remark 3.2 *In what follows we use* (x, y) *for coordinates for both canonical forms, independently on whether we choose the boundary at* $x = 1$ *or at* $x = 0$*.*

Remark 3.3 *If we denote by* s *the time variable of system* (3.4)-(3.6)*, this canonical form is invariant under the following transformations:*

Π_1			Π_2			Π_3		
s	$\longrightarrow$	$-s$	s	$\longrightarrow$	$-s$	s	$\longrightarrow$	s
x	$\longrightarrow$	$-x$	x	$\longrightarrow$	x	x	$\longrightarrow$	$-x$
y	$\longrightarrow$	y	y	$\longrightarrow$	$-y$	y	$\longrightarrow$	$-y$
t_L	$\longrightarrow$	$-t_R$	t_L	$\longrightarrow$	$-t_L$	t_L	$\longrightarrow$	t_R
t_R	$\longrightarrow$	$-t_L$	t_R	$\longrightarrow$	$-t_R$	t_R	$\longrightarrow$	t_L
a	$\longrightarrow$	$-a$	a	$\longrightarrow$	a	a	$\longrightarrow$	$-a$
d_L	$\longrightarrow$	d_R	d_L	$\longrightarrow$	d_L	d_L	$\longrightarrow$	d_R
d_R	$\longrightarrow$	d_L	d_R	$\longrightarrow$	d_R	d_R	$\longrightarrow$	d_L

(3.7)

Note that as the result of transformation Π_1*, we obtain the symmetrical version of the system with respect to the Y-axis along with a reversal of time*

to maintain the rotation sense of orbits around the origin. Similarly, the transformation Π_2 *returns the symmetrical version of the system with respect to the X-axis, while* $\Pi_3 = \Pi_1 \circ \Pi_2 = \Pi_2 \circ \Pi_1$ *gets the mirror image of the system respect to the origin of coordinates.*

3.1.1 Preliminary results on equilibria

We easily see that in canonical form (3.4), the parameter a controls the number and position of the equilibrium points. In fact, we have the following general results regarding equilibria of system (3.4)-(3.6). The proof is direct and is omitted.

Proposition 3.1 *For system* (3.4)-(3.6) *we have the following*

- **(a)** *If* $a = 0$ *and* $d_L d_R \neq 0$*, then the origin is the single equilibrium point.*
- **(b)** *If* $a = 0$ *and* $d_L = 0$ *(resp.* $d_R = 0$*), then the system has infinite equilibrium points constituting the ray given by equation* $y = t_L x$*, with* $x \leq 0$ *(resp.* $y = t_R x$*,* $x > 0$*).*
- **(c)** *If* $a \neq 0$*, then the following cases arise.*
  - **(c1)** *If* $d_L d_R > 0$*, then the system has a single equilibrium point.*
  - **(c2)** *If* $d_L d_R < 0$*, and* $a d_L < 0$ *(or equivalently,* $a d_R > 0$*), then the system has two equilibrium points, a saddle point and another anti-saddle point (node or focus).*
  - **(c3)** *If* $d_L d_R < 0$*, and* $a d_L > 0$ *(equiv.* $a d_R < 0$*), then the system has no equilibrium points.*
  - **(c4)** *If* $d_L = 0$ *(resp.* $d_R = 0$*), then the system has no equilibrium points with* $x \leq 0$ *(resp.* $x \geq 0$*). Furthermore, if* $d_R > 0$ *and* $a > 0$ *(resp.* $d_L > 0$ *and* $a < 0$*) then the system has a single equilibrium point.*

In view of Proposition 3.1, considering other parameters fixed, we can deduce the existence of bifurcations of equilibria when the parameter a passes through the critical value $a = 0$, that is, when a changes its sign. Moreover, in an analogous way to boundary equilibrium bifurcations in discontinuous Filippov systems, see for example [20], the phenomena of persistence or creation-annihilation of equilibria can appear, as we see below.

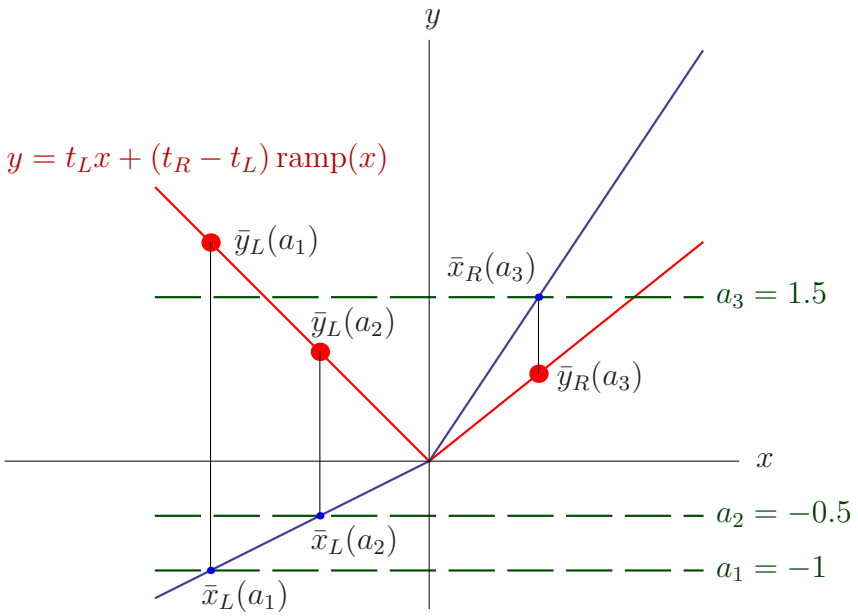

Figure 3.1: Boundary equilibrium bifurcation in system (3.4)-(3.6) for $d_L > 0$, $d_R > 0$, $t_L < 0$, $t_R > 0$, with persistence of the equilibrium point under variation of parameter a. The vertical nulcline $y = F(x)$ appears in red, and the graph of $y = g(x)$ is drawn in blue.

Without trying to cover all possible cases we consider as a first typical case the configuration

$$d_L > 0, \quad d_R > 0, \quad t_L < 0, \quad t_R > 0.$$

Then for $a \neq 0$, we are in the situation of paragraph (c1) of the Proposition 3.1 and furthermore the coordinates x of the equilibria governing the dynamics of each zone are

$$\bar{x}_L(a) = \frac{a}{d_L}, \; \bar{x}_R(a) = \frac{a}{d_R}$$

that is, both coordinates have the same sign. This tells us that one equilibrium is virtual and other is real. In particular, if $a < 0$ the equilibrium $\bar{\mathbf{x}}_L$ is real and $\bar{\mathbf{x}}_R$ is virtual, while for $a > 0$ the equilibrium $\bar{\mathbf{x}}_L$ is virtual and $\bar{\mathbf{x}}_R$ is real. For $a = 0$ we have, by the statement (a) of the same proposition, one equilibrium at the origin, which requires a particular analysis in order

to determine its topological type. Summarizing, when both determinants are positive the sign change of the parameter a leads to the persistence of a single equilibrium, but with possible topological change. This situation can be visualized in the Figure 3.1. Moreover, as it will be seen, under certain assumptions, this transition entails the appearance of a limit cycle, surrounding the equilibrium point. Let us consider now the situation

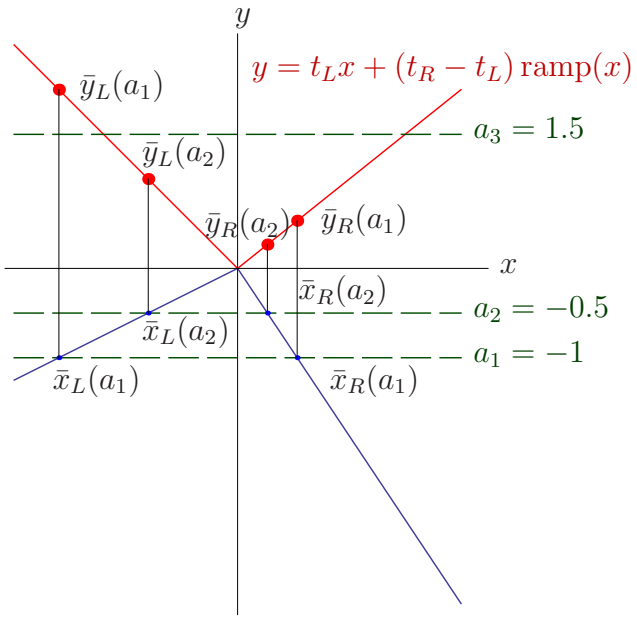

Figure 3.2: Boundary equilibrium bifurcation in system (3.4)-(3.6) for $d_L > 0$, $d_R < 0$, $t_L < 0$, $t_R > 0$, with creation-annihilation of two equilibrium points under variation of parameter a.

$$d_L > 0, \quad d_R < 0, \quad t_L < 0, \quad t_R > 0.$$

For $a \neq 0$, we are in the situation of statements (c2) and (c3) of Proposition 3.1, depending on the sign of a. That is, if $a < 0$, then statement (c2) assumptions are fulfilled, and the system has two equilibrium points, one saddle point and another anti-saddle one (focus or node). Regarding Figure 3.2 which shows an example of the situation at hand, we observe that for $a = -1$, we have an anti-saddle in $(\bar{x}_L(a_1), \bar{y}_L(a_1))$, and a saddle point in $(\bar{x}_R(a_1), \bar{y}_R(a_1))$. Analogously, if $a = -0.5$, we have an anti-saddle point in

$(\bar{x}_L(a_2), \bar{y}_L(a_2))$ and a saddle point in $(\bar{x}_R(a_2), \bar{y}_R(a_2))$. It is clearly observed that when a approaches the zero value taking negative values, equilibrium points are coming closer to the origin of coordinates. However, when $a > 0$, we have in the situation of statement (c3), which says us that the system has no equilibrium points. For $a = 0$, as in the previous case, by statement (a), we have one equilibrium point in the origin. In short, the sign change of the parameter a leads to the creation-annihilation of two equilibria.

If we now analyze the situation with

$$d_L < 0, \quad d_R > 0, \quad t_L < 0, \quad t_R > 0,$$

a phenomenon contrary to the previous situation happens. That is, for $a < 0$ there not exist equilibria, for $a = 0$ we have an equilibrium point in the origin, and for $a > 0$ we have two equilibrium points, one saddle point and another anti-saddle one. So, by changing the sign of the parameter a, a different creation-annihilation situation of new equilibrium points occurs. In Figure 3.3 an example of this situation can be observed.

Remark 3.4 *It should be emphasized that the possibility of having a saddle-focus bifurcation appears, which can never occur in planar smooth systems.*

3.1.2 Preliminary results on limit cycles

We include here for sake of completeness some results already appeared in [23].

Proposition 3.2 *System* (3.4)-(3.6) *has only one equilibrium inside each periodic orbit and it is a topological center or a topological focus.*

Proof As it is well known [37], any periodic orbit in a planar continuous vector field must contain at least an equilibrium point inside.

If we assume that system (3.4)-(3.6) has periodic orbits, then some equilibrium points must appear. In fact, the system may have one or two equilibria (this case only if $d_L d_R < 0$). In the case of two equilibria, one is a saddle and the other should be an anti-saddle. Clearly, a saddle or a node cannot be in the interior of the periodic orbit, because the existence of such equilibria involves invariant straight lines precluding any periodic orbit. The conclusion follows. ■

From Proposition 2.2 we also have the following result.

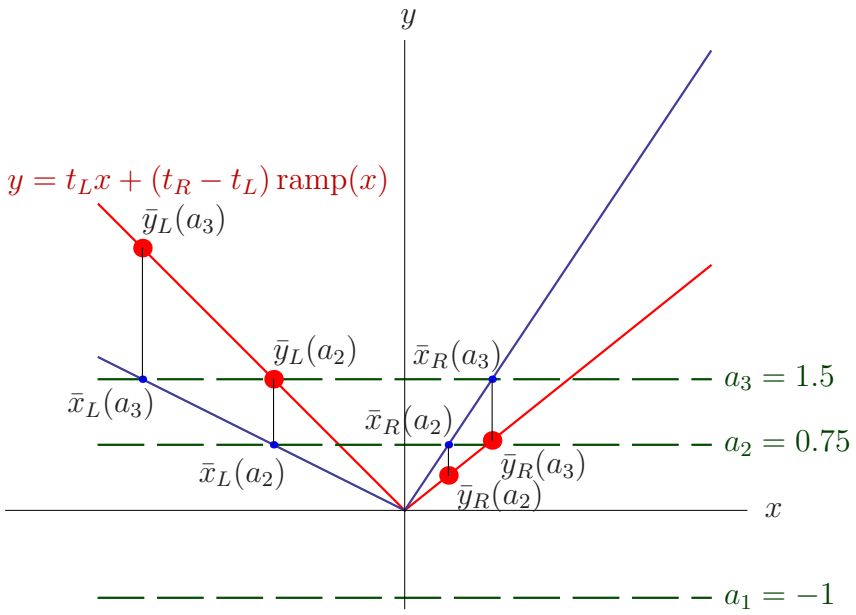

Figure 3.3: Boundary equilibrium bifurcation in system (3.4)-(3.6) for $d_L < 0$, $d_R > 0$, $t_L < 0$, $t_R > 0$, with creation-annihilation of two equilibrium points. Here the two equilibria exist for $a > 0$.

Proposition 3.3 *If Γ is a limit cycle or a homoclinic orbit of the system* (3.4)-(3.6) *then the intersection of Γ with the two zones is not empty, and $t_L t_R < 0$ or $t_L = t_R = 0$. Furthermore, when Γ is a limit cycle then $t_L t_R < 0$.*

Proof System (3.4)-(3.6) is linear within each zone, and since linear systems have neither limit cycles nor homoclinic orbits, the curve Γ lives in the two zones.

If $t_L t_R > 0$, we know from Proposition 2.2 that system (3.4)-(3.6) cannot have periodic orbits or homoclinic orbits, so we have $t_L t_R \leq 0$.

Finally, if Γ is a limit cycle with $t_L t_R = 0$, by Proposition 2.2, we must have $t_L = t_R = 0$, which leads to a conservative system that cannot have limit cycles, getting a contradiction. The proposition follows. ■

These preliminary results help to understand the hypotheses that becomes natural in order to look for results concerning the existence and uniqueness of limit cycles, as we are going to see in next sections.

3.1.3 The Massera's method for uniqueness of limit cycles

We review in this section, following [59], a geometrical argument which is usually known as Massera's method; it will allow us, after adequate adaptations, to show the uniqueness of limit cycles in the CPWL differential systems considered in this chapter, when they satisfy certain hypotheses. Uniqueness results for limit cycles are typically rather involved; see [89, 90], for a review on the subject. Here we reformulate in a specific way the simple and elegant idea proposed by J.L. Massera in his brief note extending a previous result of G. Sansone, see [65] and the recent study on the legacy of the latter author in [82].

First, we recall some notions and introduce some definitions. A *period annulus* is a region in the plane completely filled by non-isolated periodic orbits. Following [82], we say that a vector field has the *radial angular monotonicity* property (RAM property, for short) when the vector field rotates monotonically along rays as the radius increases. For instance, if along any ray starting from the origin the angle of the vector field measured with respect the positive direction of the x-axis does not decrease as one moves far from the origin on the ray, then the vector field is radially angular monotonically increasing on rays and we say that it has the *RAM increasing* property. For a closed orbit surrounding the origin, we say that it is *star-like with respect to the origin* when any segment joining the origin and a point of the closed orbit has no other points in common with the closed orbit, and consequently such segments are in the interior of the closed orbit. The following result can be stated.

Lemma 3.1 (Massera's method) *Consider a Liénard system with a continuous vector field given by* $\dot{x} = F(x) - y$, $\dot{y} = g(x)$, *and assume that* $xg(x) > 0$ *for* $x \neq 0$, *and that* $F(0) = 0$, *so that the only equilibrium point is at the origin. Assume that the system has the RAM increasing property and that period annuli are not possible. If the system has a closed orbit then it is star-like with respect to the origin and it is a limit cycle which is unique and stable.*

Proof First, we show that if the system has a closed orbit then it is star-like with respect to the origin. Obviously, since the vector field is continuous the periodic orbit must surround the origin, see Theorem 3.1 in [37]. Suppose

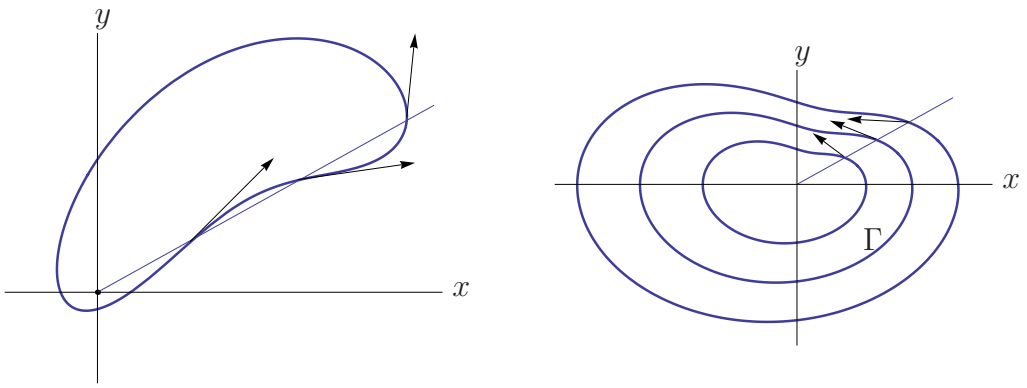

Figure 3.4: (Left) Closed orbits that are not star-like with respect to the origin cannot appear in systems with the RAM increasing property. (Right) If Γ is a star-like closed orbit, one can build a geodesic system of closed curves by homothetical transformations. Then, the RAM increasing property assures the stability of the closed orbit Γ and hence its uniqueness.

that such an orbit is not star-like with respect to the origin. Then there must be a ray that starting from the origin intersects the closed orbit in more than one point; in fact such a ray can be chosen such that it will have at least three points in common with the closed orbit, see Figure 3.4 (left). It is easy to conclude that, going far away from the origin on this ray, the angle of the vector field measured with respect to the positive direction of the x-axis cannot be monotone, that is, it first decreases to increase later or vice versa. This is not compatible with the RAM increasing property, getting the desired contradiction.

We now assume that there exists a closed orbit Γ that surrounds the origin, which must be star-like with respect to it by the above argument, see Figure 3.4 (right). Then, using Γ as a starting point, one can build a geodesic system of closed curves by homothetical transformations, foliating the entire plane by the curves $k\Gamma$ for all $k > 0$. Consider now a half-ray starting from the origin and take into account the RAM increasing property. Of course the vector field is tangent to Γ at the point where the half-ray intersects Γ, see Figure 3.4 (right). Now the RAM increasing property assures that in the points where the half-ray intersects the closed curves of the geodesic system near Γ the vector field points in such a direction that it is guaranteed the stability of the periodic orbit, even in the case the periodic orbit considered is not isolated. Since we exclude the possibility of any period annulus and

there cannot be consecutive nested stable periodic orbits, if there exists such an orbit then it must be isolated and stable, that is, it should be the unique stable limit cycle. The conclusion follows. ■

In order to be able of applying the Massera's method to 2CPWL_2 systems, we must investigate whether these systems have the RAM property. We recall that, from Lemma 2.1 and Proposition 2.1, we can start from the unbiased normalized Liénard form given in Lemma 2.2, that is from (2.9)-(2.11) (neglecting the left zone and extending the central zone to the left, that is, assuming $a_L = a_C$ and taking $b_L = 1$). Furthermore, it is not restrictive to assume there $a_C > 0$, $a_R < 0$ and $x_R > 0$. Thus, we now extend a result recently appeared in [59], by including the case when there exists a second equilibrium of saddle type.

Proposition 3.4 *Consider the two-zone continuous piecewise linear differential system*

$$\begin{array}{rl} \dot{x} = & F(x) - y, \\ \dot{y} = & g(x), \end{array} \tag{3.8}$$

where

$$g(x) = \begin{cases} x & \text{if } x < x_R, \\ b_R(x - x_R) + x_R & \text{if } x \geq x_R, \end{cases} \tag{3.9}$$

and

$$F(x) = \begin{cases} a_C x & \text{if } x < x_R, \\ a_R(x - x_R) + a_C x_R & \text{if } x \geq x_R, \end{cases} \tag{3.10}$$

with $a_C > 0$, $a_R < 0$, $b_R \geq 0$ and $x_R > 0$. Then the following statements hold.

(a) *If $b_R = 1$ then the system has the RAM increasing property.*

(b) *If $0 \leq b_R \neq 1$ then the system can be transformed in an equivalent system with the RAM increasing property.*

(c) *If we consider the case $b_R < 0$, keeping the remaining hypotheses, then the system has, apart from the equilibrium point at the origin, a saddle equilibrium point at $(\bar{x}_{RS}, \bar{y}_{RS})$, where*

$$\bar{x}_{RS} = x_R \left(1 - \frac{1}{b_R}\right) > x_R, \quad \bar{y}_{RS} = x_R \left(a_C - \frac{a_R}{b_R}\right).$$

Nevertheless, the restriction of the system to the open half-plane $x < \bar{x}_{RS}$ can still be transformed in an equivalent system having the RAM increasing property.

Proof To show the RAM increasing property we will compute the slope of the vector field along half-rays of the form $y = \lambda x$. In the following computations there naturally appears the expression $F(x) - \lambda x$ in some denominators; obviously, we can disregard the points of vertical slope in which such an expression vanishes.

If $b_R = 1$ then $g(x) = x$ for all $x \in \mathbb{R}$. In this case, the slope of the vector field along the half-rays $y = \lambda x$ is given by

$$m_\lambda(x) = \left.\frac{dy}{dx}\right|_{y=\lambda x} = \frac{x}{F(x) - \lambda x},$$

which is constant for $x \leq x_R$. For $x > x_R$, it has the derivative

$$\frac{dm_\lambda(x)}{dx} = \frac{F(x) - \lambda x - x(a_R - \lambda)}{[F(x) - \lambda x]^2} = \frac{x_R(a_C - a_R)}{[F(x) - \lambda x]^2},$$

which is always positive. The RAM increasing property is concluded for this simple case and statement (a) is shown.

Assume now that we are under hypotheses of statement (b). If $0 \leq b_R \neq 1$, the numerator in the computation of the derivative of $m_\lambda(x)$ turns out to be dependent on λ and the sign of the numerator could change. However, we can transform the system by introducing a new first variable $u = u(x)$ so that the new second equation become $\dot{y} = u$ for all u. For that, it suffices to write $u = \operatorname{sgn}(x)\sqrt{2G(x)}$, where $G(x) = \int_0^x g(s)ds$, so that $G(x) > 0$ for all $x \neq 0$. Note that $u = x$ if $x \leq x_R$ and then the slope of the vector field in this case is not altered. Now, we study its slope for $u > x_R$. Clearly, from $u^2(x) = 2G(x)$ we have $u(x)u'(x) = g(x)$ for all x, and so

$$\frac{du}{dx} = \frac{g(x)}{u}. \tag{3.11}$$

Therefore

$$\frac{du}{dt} = \frac{du}{dx}\frac{dx}{dt} = \frac{g(x)}{u}\left[F(x) - y\right],$$

and in the new variables the system is equivalent to the equation

$$\frac{dy}{du} = \frac{dy/dt}{du/dt} = \frac{u}{F(x(u)) - y},$$

that is, to the system $\dot{u} = F(x(u)) - y$, $\dot{y} = u$. As in the previous case $g(x) = x$, and we can write

$$m_\lambda(u) = \left.\frac{dy}{du}\right|_{y=\lambda u} = \frac{u}{F(x(u)) - \lambda u},$$

and consequently

$$\frac{dm_\lambda(u)}{du} = \frac{F(x(u)) - \lambda u - u\,[F'(x(u))x'(u) - \lambda]}{[F(x(u)) - \lambda u]^2} = \frac{F(x(u)) - a_R u\,x'(u)}{[F(x(u)) - \lambda u]^2},$$

finally arriving at

$$\frac{dm_\lambda(u)}{du} = \frac{x_R(a_C - a_R) + a_R[x(u) - u\,x'(u)]}{[F(x(u)) - \lambda u]^2}. \tag{3.12}$$

We will study the sign of $x(u) - u\,x'(u)$ for $x > x_R$. From (3.11) and the equality $u^2 = 2G(x) = b_R(x - x_R)^2 + 2x_R x - x_R^2$ for $x > x_R$, we have

$$x(u) - u\,x'(u) = \frac{xg(x) - u^2}{g(x)} =$$

$$= \frac{x[b_R(x - x_R) + x_R] - [b_R(x - x_R)^2 + 2x_R x - x_R^2]}{g(x)},$$

and after obvious simplifications, we get

$$x(u) - u\,x'(u) = \frac{(b_R - 1)x_R(x - x_R)}{g(x)}. \tag{3.13}$$

Now, if $b_R \leq 1$ the above expression is non-positive for $x > x_R$, and then the expression in (3.12) is obviously positive. The RAM increasing property follows.

Still being under the hypotheses of statement (b), the remaining case $b_R > 1$ can be also managed by noticing that, when $x > x_R$, we have

$$0 < \frac{(b_R - 1)x_R(x - x_R)}{g(x)} = \frac{(b_R - 1)x_R(x - x_R)}{b_R(x - x_R) + x_R} < \frac{(b_R - 1)x_R}{b_R},$$

so that

$$x_R(a_C - a_R) + a_R[x(u) - u\,x'(u)] >$$

$$> x_R(a_C - a_R) + a_R\frac{(b_R - 1)x_R}{b_R} =$$

$$= x_R\left(a_C - \frac{a_R}{b_R}\right) > 0,$$

and since (3.12) is again positive, the conclusion follows.

Finally, assume we are under the hypotheses of statement (c). Clearly, we see that $g(\bar{x}_{RS}) = 0$ and the existence of the saddle point is obvious. Note that the previous transformation $u = \text{sgn}(x)\sqrt{2G(x)}$, is still valid for $x > 0$ as long as $g'(x) > 0$, that is, when $x < \bar{x}_{RS}$. For points in such a half-plane, we can repeat the computations to get (3.13) (clearly non-positive) and to conclude that (3.12) is obviously positive. The proof is complete. ■

From the above result it should be noticed that some systems originally not having the RAM increasing property can be transformed in equivalent systems satisfying such a property. Possible periodic orbits can be deformed in shape by the transformation given in the above proof, but stability and uniqueness results for periodic orbits can be translated between such equivalent systems.

More precisely, the following remark can be stated.

Remark 3.5 *From Lemma 3.1, we can conclude for the systems* (3.8)-(3.10) *with two linearity zones, under hypotheses of Proposition 3.4, that if there is a closed orbit then it surrounds the origin and it is a limit cycle which is unique and stable.*

It should be noticed that every 2CPWL$_2$ system susceptible of having limit cycles, that is, isolated periodic orbits, must have a focus and possibly another equilibrium, which from Proposition 3.1.c2 must be a saddle. Once translated the focus to the origin and using the change of variables given in the proof of Lemma 2.2, the system can be recast, by means of the transformations given in Remark 3.3 if needed, in the form of system (3.8)-(3.10). As a consequence, by resorting to Lemma 3.1, we obtain in a very elegant way a new shortcut to achieve the following result.

Corollary 3.1 *Every 2CPWL$_2$ system has at most one limit cycle. In such a case, the limit cycle is stable or unstable but not semistable. In other words, the Lum-Chua conjecture is true.*

Endowed with these uniqueness results, we analyze the problem of existence of limit cycles. In fact, we can now state an important result which includes a necessary and sufficient condition for limit cycles in 2CPWL$_2$ systems.

Theorem 3.1 *Consider the differential system*

$$\begin{array}{rcl} \dot{x} & = & F(x) - y, \\ \dot{y} & = & g(x) - \delta, \end{array} \tag{3.14}$$

where

$$F(x) = \begin{cases} t_L x & \text{if } x < 1, \\ t_R(x-1) + t_L & \text{if } x \geq 1, \end{cases} \tag{3.15}$$

and

$$g(x) = \begin{cases} d_L x & \text{if } x < 1, \\ d_R(x-1) + d_L & \text{if } x \geq 1. \end{cases} \tag{3.16}$$

with only one equilibrium point in the left zone, i.e. $\delta < d_L$, and $d_L > 0$, $d_R \geq 0$ so that $\bar{x} = \delta/d_L < 1$. Assume also that the left trace satisfy $t_L > 0$, while the right trace is negative, that is $t_R < 0$. Then the following statements hold.

(a) *A necessary condition for the existence of periodic orbits is that the equilibrium point be a topological focus, that is $t_L^2 - 4d_L < 0$.*

(b) *If $t_L^2 - 4d_L < 0$ then the system has periodic orbits if and only if the following condition holds*

$$\frac{t_L}{\sqrt{d_L}} + \frac{t_R}{\sqrt{d_R}} < 0. \tag{3.17}$$

In such case, the equilibrium point is surrounded by a limit cycle which is unique and stable.

Proof The equilibrium point cannot be a node since its invariant manifolds are straight lines that should extend to infinity, precluding so the existence of periodic orbits. Thus, the equilibrium point must be a focus and statement (a) follows.

From Lemma 2.2 we can pass to the corresponding system in the form (2.9)-(2.11), now with $d_L = d_C$, $a_L = a_C = t_L/\sqrt{d_L}$, $a_R = t_R/\sqrt{d_L}$, $b_L = 1$, $b_R = d_R/d_L$. We study now the existence of periodic orbits for such equivalent system, which has the advantage of having the equilibrium at the origin. To do this, we consider the right half-return map P_R defined in the whole negative y-axis, by taking the orbit starting at the point $(0, -y)$, with $y > 0$, and coming back to the positive y-axis at the point $(0, P_R(y))$. Similarly,

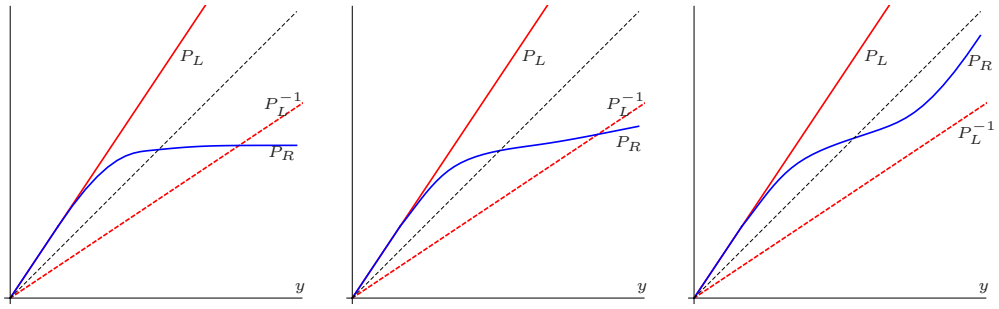

Figure 3.5: Scheme of the different possibilities for the proof of Theorem 3.1. If the left dynamics is a stable node the graph of P_R is bounded (left panel), and we have a limit cycle. This is not the case for left stable focus dynamics, and we can have intersection (central panel) or not (right panel) depending on the asymptotic slope of P_R. The graph of P_L^{-1} is the symmetrical of P_L with respect to the diagonal of the first quadrant.

we introduce a left half-return map P_L as follows. The orbits starting at the point $(0, y)$, with $y > 0$, enter the half-plane $x < 0$ and go around the origin in a counterclockwise path, coming back to the y-axis at the point $(0, -P_L(y))$, where $P_L(y)) > 0$.

The unstable focus condition in the left zone is equivalent to

$$0 < \frac{t_L}{\sqrt{d_L}} = a_L < 2,$$

and now the system becomes purely linear for $x < x_R = 1 - \bar{x}$ with the unstable focus at the origin. Then it is easy to check, see for instance [30], that the left half-return map P_L is a linear function given by $P_L(y) = e^{\pi\gamma_L} y$ where

$$\gamma_L = \frac{a_L}{\sqrt{4 - a_L^2}} = \frac{t_L/\sqrt{d_L}}{\sqrt{4 - t_L^2/d_L}} > 0.$$

Regarding the right left-return map P_R, we know that its graph coincides for small values of y with the graph of P_L (while the orbits do not enter the zone $x > x_R$ they only use the left focus dynamics), but it is no longer linear since for greater values of y the orbits use the right dynamics. We distinguish two possible cases.

If the dynamics on the right zone is of node type, then we know that P_R is bounded by the invariant manifolds of the virtual node, so that its graph has a horizontal asymptote. The existence of periodic orbits is clearly equivalent

to the existence of a positive value y such that $P_R(y) = P_L^{-1}(y) = e^{-\pi\gamma_L}y$. Since the graph of $P_L^{-1}(y)$ is linear with positive slope but less than 1, and the graph of P_R is bounded, the intersection is assured and we have one periodic orbit. Note that in this case we have in terms of original parameters

$$\frac{t_R}{\sqrt{d_R}} \leq -2,$$

so that the condition (3.17) in the theorem always holds.

If the dynamics on the right zone is of focus type and we define

$$\gamma_R = \frac{a_R}{\sqrt{4b_R - a_R^2}} = \frac{t_R}{\sqrt{4d_R - t_R^2}} < 0,$$

it is easy to deduce that

$$\lim_{y\to\infty} \frac{P_R(y)}{e^{\pi\gamma_R}y} = 1,$$

so that

$$\lim_{y\to\infty} \frac{P_R(y)}{y} = e^{\pi\gamma_R},$$

which means that the effect of the band $0 < x < x_R$, which also uses the left focus dynamics, is negligible when $y \to \infty$.

Therefore the slope of the graph of P_R tends to $e^{\pi\gamma_R}$ as $y \to \infty$, and now we can assure the existence of intersection between the graphs of $P_R(y)$ and $P_L^{-1}(y)$ if

$$e^{-\pi\gamma_L} > e^{\pi\gamma_R} \Leftrightarrow e^{\pi(\gamma_L+\gamma_R)} < 1 \Leftrightarrow \gamma_L + \gamma_R < 0.$$

This last condition reads, in terms of the original parameters, as

$$\gamma_L + \gamma_R = \frac{t_L}{\sqrt{4d_L - t_L^2}} + \frac{t_R}{\sqrt{4d_R - t_R^2}} < 0.$$

We claim that such sufficient condition for existence of periodic orbits is equivalent to

$$\frac{t_L}{\sqrt{d_L}} + \frac{t_R}{\sqrt{d_R}} < 0,$$

as stated in the theorem. To show this claim, take the auxiliary function

$$h(\xi) = \frac{\xi}{\sqrt{4 - \xi^2}},$$

which is odd and monotone increasing in $(-2, 2)$. Defining

$$\xi_L = \frac{t_L}{\sqrt{d_L}}, \quad \xi_R = \frac{t_R}{\sqrt{d_R}},$$

since $-2 < \xi_R < 0 < \xi_L < 2$, we have

$$\xi_L + \xi_R < 0 \Leftrightarrow \xi_L < -\xi_R \Leftrightarrow h(\xi_L) < h(-\xi_R) = -h(\xi_R) \Leftrightarrow h(\xi_L) + h(\xi_R) < 0,$$

and the claim follows.

When the sufficient condition for existence of periodic orbits (3.17) holds, the uniqueness of periodic orbits and its stability come directly from Remark 3.5 and the conclusion follows. To see that such condition is also necessary, suppose that there are periodic orbits and the condition does not hold. Then eventually the slope of P_R is greater that the one of P_L^{-1}, so that as both graphs intersect, they must do it in two or more points. Thus, we get a contradiction with the uniqueness and stability predicted by Remark 3.5, and condition (3.17) is also a necessary condition. ■

The statements of Theorem 3.1 are not new, see [29]. In the quoted paper such a theorem appeared but only indicating how several existing results could be concatenated to get it, really without an explicit proof. It can also be considered as a byproduct of the case-by-case study made in [23]. The proof given here is somehow shorter and more direct than the one recently appeared in [59].

3.1.4 Boundary equilibrium bifurcations (BEB's)

We revisit in this section the possible bifurcations in systems with two zones when we move the parameter a, see Section 3.1.1, but now taking into account the above results on existence and uniqueness of limit cycles. Thus, we come back to the situation of system (3.4)-(3.6), which is rewritten here for sake of convenience, namely

$$\begin{array}{rcl} \dot{x} & = & F(x) - y, \\ \dot{y} & = & g(x) - a, \end{array} \tag{3.18}$$

where

$$F(x) = \begin{cases} t_L x & \text{if } x < 0, \\ t_R x & \text{if } x \geq 0, \end{cases} \tag{3.19}$$

and

$$g(x) = \begin{cases} d_L x & \text{if } x < 0, \\ d_R x & \text{if } x \geq 0. \end{cases} \tag{3.20}$$

Let us consider for instance the case of persistence of one equilibrium of anti-saddle type, that is, $d_L > 0$ and $d_R > 0$, with a change of stability associated to the change of sign of a, that is for $t_L t_R < 0$, see Figure 3.1. A direct consequence of our analysis is the following result, corresponding to some representative cases; other analogous results could be easily written in the same spirit.

Proposition 3.5 *Consider system* (3.18)-(3.20) *with* $d_L > 0$, $d_R > 0$, $t_L < 0$ *and* $t_R > 0$. *Selecting* a *as the bifurcation parameter, the following statements hold. When there exists a limit cycle, its size grows linearly with* $|a|$.

(a) (Supercritical node-focus transition with one limit cycle)
If $t_L^2 - 4d_L \geq 0$ *and* $t_R^2 - 4d_R < 0$ *then for* $a < 0$ *the equilibrium point is a global attractive node while for* $a > 0$ *the equilibrium becomes an unstable focus surrounded by one stable limit cycle. For* $a = 0$ *the equilibrium point is a global attractive node-focus.*

(b) (Subcritical node-focus transition with one limit cycle)
If $t_L^2 - 4d_L < 0$ *and* $t_R^2 - 4d_R \geq 0$ *then for* $a < 0$ *the equilibrium point is a stable focus surrounded by one ustable limit cycle, while for* $a > 0$ *the equilibrium becomes an unstable node, which is the* α*-limit set for the whole plane. For* $a = 0$ *the equilibrium point is a repulsive node-focus.*

(c) (Supercritical focus-focus transition with one limit cycle)
If $t_L^2 - 4d_L < 0$, $t_R^2 - 4d_R < 0$ *and furthermore*

$$\frac{t_L}{\sqrt{d_L}} + \frac{t_R}{\sqrt{d_R}} < 0, \tag{3.21}$$

then for $a \leq 0$ *the equilibrium point is a global attractive focus while for* $a > 0$ *the equilibrium becomes an unstable focus surrounded by one stable limit cycle.*

(d) (Subcritical focus-focus transition with one limit cycle)
If $t_L^2 - 4d_L < 0$, $t_R^2 - 4d_R < 0$ *and furthermore*

$$\frac{t_L}{\sqrt{d_L}} + \frac{t_R}{\sqrt{d_R}} > 0, \tag{3.22}$$

then for $a < 0$ *the equilibrium point is an attractive focus surrounded by one unstable limit cycle while for* $a \geq 0$ *the equilibrium becomes an unstable focus, which is the* α*-limit set for the whole plane.*

(e) (Degenerate focus-focus transition or 'center' BEB)
If $t_L^2 - 4d_L < 0$, $t_R^2 - 4d_R < 0$ *and furthermore*

$$\frac{t_L}{\sqrt{d_L}} + \frac{t_R}{\sqrt{d_R}} = 0, \tag{3.23}$$

then for $a < 0$ *the equilibrium point is a global attractive focus, a global center for* $a = 0$*, and an unstable focus for* $a > 0$*; in this last case, the point is the* α*-limit set for the whole plane.*

Proof The assertions about stability of the equilibrium point are a direct consequence of the comments given in Section 3.1.1. Therefore, we restrict our attention to the existence of limit cycles. The linear growth of the limit cycle with the bifurcation parameter a comes easily reasoning as in Remark 3.1.

The appearance of the limit cycle in the situation of statement (a) can be deduced from Theorem 3.1 (b), taking into account that here we have the focus for $a > 0$, that is, in the right zone. Effectively, from our hypotheses, we see that

$$\frac{t_L}{\sqrt{d_L}} \leq -2, \quad 0 < \frac{t_R}{\sqrt{d_R}} < 2,$$

so that the condition (3.17) holds and we are done. Roughly speaking, we can say that the left stable node dynamics always wins to the unstable focus one, bounding the stable limit cycle. Statement (b) is its dual result, which can be deduced by using the transformation Π_1 in Remark 3.3.

The statement (c) also comes from Theorem 3.1 (b), while statement (d) is the corresponding dual result, which can be deduced by using the transformation Π_1 in Remark 3.3.

Statement (e) corresponds to the case when, following the ideas appearing in the proof of Theorem 3.1, the graphs of P_R and P_L^{-1} become asymptotically parallel. For $a < 0$ it is easy to see that, since the slope of P_R is decreasing, there are no intersections between the quoted graphs. For $a = 0$ both graphs are straight lines and coincident and therefore we have a center. For $a > 0$ we have the dual case of $a < 0$ and we are done. ■

We illustrate the node-focus transition of the above proposition in Figure 3.6. We notice that the above bifurcation at $a = 0$, where the equilibrium point changes its stability and one stable limit cycle emerges, can be named Hopf-like bifurcation (due to its similarities with the smooth Hopf bifurcation) as done in [29]. However, we prefer to speak of boundary equilibrium

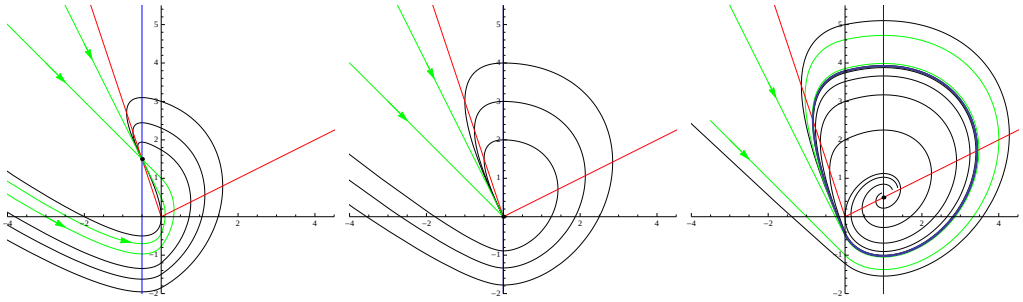

Figure 3.6: Persistence of the equilibrium point plus a limit cycle bifurcation in the transition node-focus of Proposition 3.5(a). Chosen values are $t_L = -3$, $d_L = 2$, $t_R = 0.5$, $d_R = 1$ and $a = -1$ (left panel), $a = 0$ (central), $a = 1$ (right).

bifurcation (sometimes named BEB, for short) to emphasize that the bifurcation is associated to the transition of the equilibrium point through the boundary, a typical phenomenon in more general piecewise-smooth systems, see [20].

As mentioned before, it is clear that, by changing the hypotheses related to the traces, other similar results can be stated with one unstable limit cycle existing for $a < 0$, for instance. Our intention is not to write all the possible cases but just to show a few significant ones.

Another different, interesting situation appears when the determinants have different sign. Thus we can write the following result, which emphasizes the possibility of having a saddle-focus bifurcation, see Figure 3.3, something not possible in smooth systems. As indicated in the statement (b), three different situations can appear for the saddle-focus bifurcation.

Proposition 3.6 (Saddle-focus bifurcation) *For system* (3.18)-(3.20) *with* $d_L < 0$, $d_R > 0$, $t_L < 0$ *and* $0 < t_R < 2\sqrt{d_R}$, *the following statements hold.*

(a) *The system has no equilibria for* $a < 0$ *while for* $a > 0$ *there are two equilibria: a saddle point in the left zone and an unstable focus in the right zone. For* $a = 0$ *the origin is a saddle-focus point.*

(b) *Depending on the parameter values the bifurcating focus appears surrounded by one stable limit cycle, by a homoclinic loop, or by nothing.*

(c) *In particular, once fixed d_L, d_R and t_L according to the hypotheses, there exist a critical value $t_R^{HC} > 0$ that discriminates the three possible situations. Namely, if $0 < t_R < t_R^{HC}$ then the stable limit cycle appears, while when $t_R > t_R^{HC}$ no limit cycle appears. The homoclinic loop exists exactly for $t_R = t_R^{HC}$. In the three cases, the phase planes for different values of $a > 0$ are homothetic.*

Proof Again, statement (a) is a direct consequence of the comments given in Section 3.1.1.

To show statements (b) and (c), we first observe that the unstable right focus could be surrounded by one stable limit cycle (the uniqueness coming from Corollary 3.1) or by a homoclinic loop, but not for both (on the contrary, through an adequate perturbation we should have two limit cycles, getting a contradiction with the uniqueness property). Now, using the homothety that comes from the reasoning done in Remark 3.1, we can assume $a = 1$ to study the different possibilities for the configuration in the phase plane when $a > 0$.

Taking so $a = 1$ and without going into detail, the linear invariant manifolds of the left saddle at $(1/d_L, t_L/d_L)$ intersect the y-axis in two points, namely $(-y_1, 0)$ with $y_1 > 0$ (the unstable manifold) and $(y_2, 0)$ with $y_2 > 0$ (the stable manifold). Now, it suffices to study the orbit starting at $(-y_1, 0)$, which entering the right zone, surrounds counter-clockwise the unstable focus at $(1/d_R, t_R/d_R)$ and eventually intersects again the y-axis in a point $(y_3, 0)$, with $y_3 > 0$.

Easy computations show that if we assume for the saddle the eigenvalues configuration $-\lambda_2 < 0 < \lambda_1$, we have

$$y_1 = \frac{1}{\lambda_2} < \frac{1}{\lambda_1} = y_2,$$

since $t_L = \lambda_1 - \lambda_2 < 0$ implies $\lambda_1 < \lambda_2$.

When $y_3 < y_2$ it is easy to conclude the existence of a positive invariant set and consequently the existence of a ω-limit set within it, which cannot be the unstable focus and so we must have one limit cycle. If $y_3 = y_2$ then we have the situation giving rise to the homoclinic loop, while if $y_3 > y_2$ then the orbit cannot returns and escapes to infinity. This last case is clearly not compatible with a stable limit cycle in between. Thus, by considering the continuous dependence of solutions with respect to parameters, that the system has a tangency to the y-axis at the origin and that the expansion of

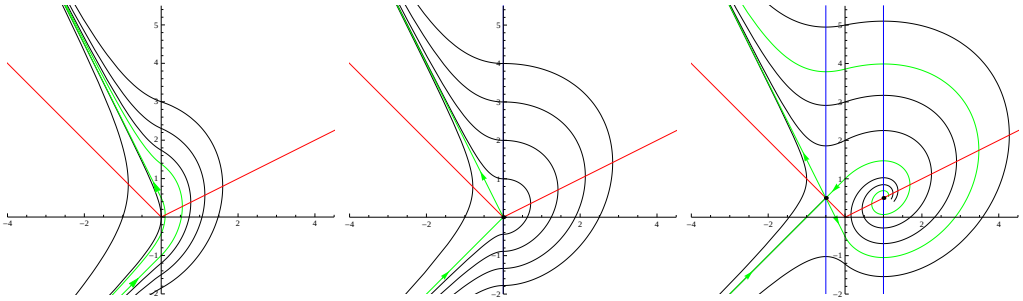

Figure 3.7: Creation of two equilibrium points, a saddle and a focus without limit cycle bifurcation. Chosen values are $t_L = -1$, $d_L = -2$, $t_R = 0.5$, $d_R = 1$ and $a = -1$ (left panel), $a = 0$ (central), $a = 1$ (right).

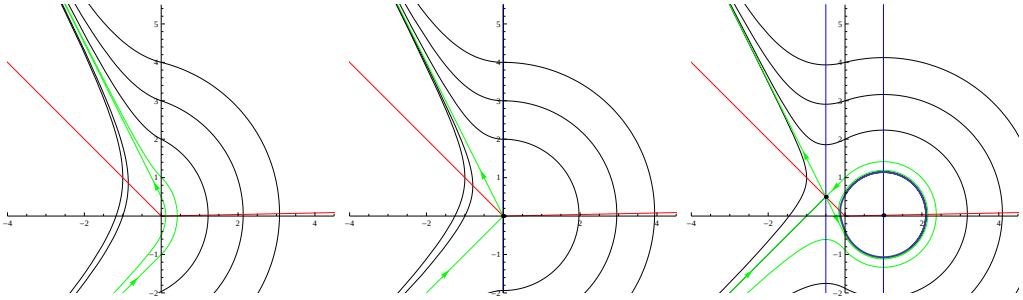

Figure 3.8: Creation of two equilibrium points, a saddle and a focus with limit cycle bifurcation. Chosen values are $t_L = -1$, $d_L = -2$, $t_R = 0.02$, $d_R = 1$ and $a = -1$ (left panel), $a = 0$ (central), $a = 1$ (right).

the focus is controlled by the parameter t_R, then we have that for sufficiently small $t_R > 0$ we have at the first case, that is $y_3 < y_2$. The other situations can be achieved by incrementing the parameter t_R, since for t_R tending to $2\sqrt{d_R}$ the expansion of the focus tends to infinity. ■

In next figures we illustrate the different possibilities by considering the two generic cases: saddle-focus bifurcation with a single focus or with the focus surrounded by a limit cycle. Thus, in Figure 3.7 we are in the case without limit cycle; after a significative reduction in the value of t_R, we see in Figure 3.8 the case of the simultaneous appearance of a stable limit cycle. Of course, there exist also the dual case corresponding to the appearance of an unstable limit cycle surrounding a stable focus, which can be easily deduced from Proposition 3.6 by taking the dual of the considered case.

These boundary equilibrium bifurcations are building blocks for other

possible situations appearing in systems with a greater number of zones; for instance, in the case of 3CPWL$_2$ systems is not difficult to reproduce all the above cases. Furthermore, as we see below, these systems with three zones can undergo unexpected bifurcations associated to boundary equilibrium bifurcations, namely explosive limit cycle bifurcations associated to node-node transitions, which from the point of view of 2CPWL$_2$ systems are not interesting at all, because they cannot have periodic orbit.

3.2 3CPWL$_2$ systems with one equilibrium

Here we come back to the systems with three linearity zones given in (2.5)-(2.7), assuming that the anti-saddle equilibrium is in the central zone and adopt for them the normalized form given in (2.9)-(2.11), that is, with the equilibrium at the origin, unitary central determinant and displaced boundaries. We rewrite them here for the sake of convenience, namely

$$\begin{array}{rcl} \dot{x} & = & F_n(x) - y, \\ \dot{y} & = & g_n(x), \end{array} \tag{3.24}$$

where

$$F_n(x) = \begin{cases} a_R(x - x_R) + a_C x_R & \text{if } x > x_R, \\ a_C x & \text{if } x_L \leq x \leq x_R, \\ a_L(x - x_L) + a_C x_L & \text{if } x < x_L, \end{cases} \tag{3.25}$$

and

$$g_n(x) = \begin{cases} b_R(x - x_R) + x_R & \text{if } x > x_R, \\ x & \text{if } x_L \leq x \leq x_R, \\ b_L(x - x_L) + x_L & \text{if } x < x_L, \end{cases} \tag{3.26}$$

with $x_L < 0 < x_R$.

To study the existence of limit cycles, we start by studying, in the general context of Liénard systems, the qualitative properties of the right half-return map P_R defined in the whole negative y-axis, by taking the orbit starting at the point $(0, -y)$, with $y > 0$, and coming back to the positive y-axis at the point $(0, P_R(y))$. The following lemma, proved here for the sake of completeness, is a modification of a classical result, see for instance [62] or the proof of Theorem 11.4 given in [40]. It assures, under certain hypotheses, the existence of such a map for all $y > 0$ and gives information about its asymptotic behavior as $y \to \infty$.

Lemma 3.2 *Consider a Liénard system with a continuous vector field given by* $\dot{x} = F(x) - y$, $\dot{y} = g(x)$. *Assume that* $F(x)$ *is positive and increasing for small positive values of* x, *it has a positive zero only at* $x = x_1 > 0$, *and it is decreasing to* $-\infty$ *as* $x \to \infty$ *monotonically for* $x > x_1$. *Assuming also that* $g(0) = 0$, *and* $g(x) > 0$ *for all* $x > 0$, *the following statements hold.*

The orbits starting at the point $(0, -y)$, *with* $y > 0$, *enter the half-plane* $x > 0$ *and go around the origin in a counterclockwise path, coming back to the* y*-axis at the point* $(0, P_R(y))$, *with* $P_R(y) > 0$. *The difference* $P_R(y) - y$ *is positive for small values of* y, *but eventually becomes negative, tending to* $-\infty$ *as* $y \to \infty$.

Proof Clearly, the unique equilibrium of the system in the half-plane $x \geq 0$ is the origin. From the hypotheses, any orbit starting at the point $(0, -y)$, with $y > 0$, enters the half-plane $x > 0$ with null slope, to have positive slope while $y < F(x)$. The slope of the orbit becomes infinite when $y = F(x)$ and eventually becomes negative, finally arriving again to the y-axis with zero slope, at the point $(0, P_R(y))$ after making a half turn around the origin. We study how much changes along such a half-turn the function

$$V(x, y) = G(x) + \frac{y^2}{2}$$

where

$$G(x) = \int_0^x g(u)du.$$

Note that $\dot{V}(x, y) = g(x)[F(x) - y] + y\, g(x) = F(x)\, g(x)$ and that $G(0) = 0$. Assume three nested arcs ACB, $A'C'B'$ and $A''C''B''$, see Figure 3.9, corresponding to orbits of the system. Suppose that the first orbit ACB is contained in the strip $0 < x < x_1$, where $F(x) > 0$ and $dy > 0$. Thus $F(x)dy > 0$ along such arc, and consequently

$$V(B) - V(A) = \int_A^B dV = \int_{y_A}^{y_B} F(x)dy > 0.$$

Therefore, since $2(V(B) - V(A)) = y_B^2 - y_A^2$, we have

$$y_B - |y_A| = P_R(|y_A|) - |y_A| > 0.$$

Consider now the arcs of orbits $A'C'B'$ and $A''C''B''$ not completely contained in the strip $0 < x < x_1$, see Fig. 3.9. Considering the parts of the arcs in

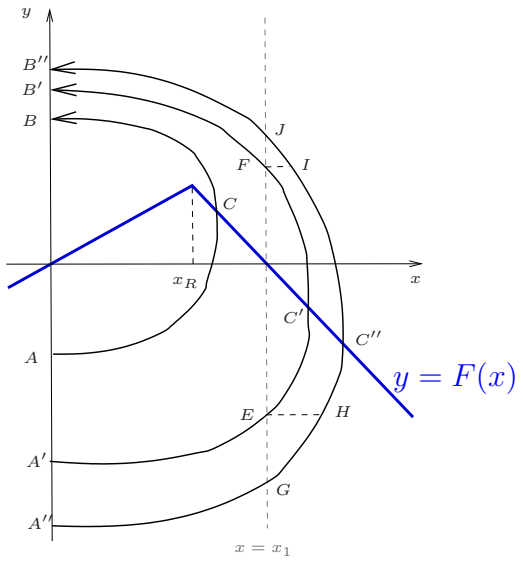

Figure 3.9: Three typical orbits of a Liénard system with a continuous piecewise linear function $F(x)$ satisfying hypotheses of Lemma 3.2.

such a strip where $F(x) > 0$, and since $F(x) - y$ along the arc $A''G$ is greater than along the arc $A'E$, where G and E are the points of the arcs which $x = x_1$, we have

$$\begin{aligned} V(G) - V(A'') &= \int_{A''}^{G} dV = \int_{A''}^{G} \frac{F(x)g(x)}{F(x) - y} dx < \\ &< \int_{A'}^{E} \frac{F(x)g(x)}{F(x) - y} dx = \int_{A'}^{E} dV = V(E) - V(A'). \end{aligned} \tag{3.27}$$

Let H and I the points where the parallel lines to the x-axis passing through E and F intersect the arc $A''C''B''$. Since $F(x) < 0$ along the arc GH and $dy > 0$ for $x > 0$, we obtain

$$V(H) - V(G) = \int_{G}^{H} dV = \int_{GH} F(x)dy < 0. \tag{3.28}$$

Now, since $F(x)$ along the arc HI is negative and exceeds in absolute value

$F(x)$ along the arc EF for the same value of y, it follows that

$$\begin{aligned} V(I) - V(H) &= \int_H^I dV = \int_{HI} F(x)dy < \\ &< \int_{EF} F(x)dy = \int_E^F dV = V(F) - V(E). \end{aligned} \tag{3.29}$$

Along the arc IJ, as in the study made along the arc GH, it holds that

$$V(J) - V(I) < 0 \tag{3.30}$$

As in (3.27), we obtain

$$V(B'') - V(J) < V(B') - V(F) \tag{3.31}$$

Adding inequalities (3.27)-(3.31), we obtain

$$V(B'') - V(A'') < V(B') - V(A'),$$

that is, $y_{B''}^2 - y_{A''}^2 < y_{B'}^2 - y_{A'}^2$, or equivalently,

$$P_R(|y_{A''}|) - |y_{A''}| < P_R(|y_{A'}|) - |y_{A'}|.$$

We conclude that for the orbits starting at $(0, -y)$ and crossing the graph $y = F(x)$ for $x > x_1$ the difference $P_R(y) - y$ is monotonically decreasing. It remains to show that it tends to $-\infty$ when $y \to \infty$. Of course, if $P_R(y)$ turns to be bounded then the conclusion is trivial. In any case, it suffices to observe that from the first part of (3.27) we have that $V(G) - V(A'') > 0$ but decreasing to 0 as the point C'' goes far from the origin; the same is true for $V(B'') - V(J)$. However the contribution of the difference $V(J) - V(G)$ is negative and unbounded as the point C'' goes far from the origin. The conclusion follows. ■

As is well known, under hypotheses of Lemma 3.2, it is easy to show the existence and uniqueness of limit cycles for Liénard vector fields that are symmetric with respect to the origin, since then it suffices to look for possible zeros of $P_R(y) - y$. As we see below, the situation is more involved when there are no symmetries.

Coming back to our 3CPWL$_2$ systems, we can easily extend Lemma 3.2, as follows. For the right part, that is for P_R the lemma applies directly. By using Remark 2.2, see Figure 3.10, we can conclude the same for the left part, an so the following result is straightforward.

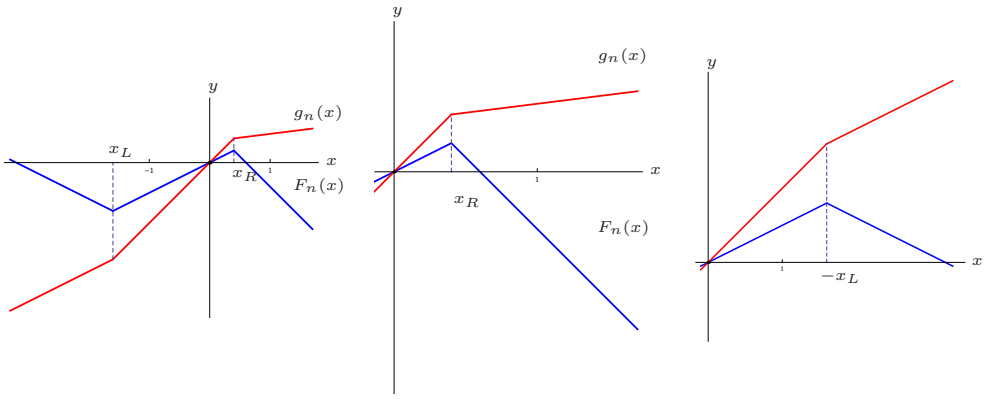

Figure 3.10: The splitting of the system into its right and left part, using Remark 2.2 for the latter, allows to apply twice Lemma 3.2, obtaining Lemma 3.3.

Lemma 3.3 *Consider systems with three linearity zones given in* (3.24)-(3.26) *with* $x_L < 0 < x_R$ *and satisfying the conditions* $a_L, a_R < 0$, $a_C > 0$ *and* $b_L, b_R \geq 0$. *The following statements hold.*

(a) *The orbits starting at the point* $(0, -y)$, *with* $y > 0$, *enter the half-plane* $x > 0$ *and go around the origin in a counterclockwise path, coming back to the* y*-axis at the point* $(0, P_R(y))$, *with* $P_R(y) > 0$. *The difference* $P_R(y) - y$ *is positive for small values of* y, *but eventually becomes negative, tending to* $-\infty$ *as* $y \to \infty$.

(b) *The orbits starting at the point* $(0, y)$, *with* $y > 0$, *enter the half-plane* $x < 0$ *and go around the origin in a counterclockwise path, coming back to the* y*-axis at the point* $(0, -P_L(y))$, *with* $P_L(y) > 0$. *The difference* $P_L(y) - y$ *is positive for small values of* y, *but eventually becomes negative, tending to* $-\infty$ *as* $y \to \infty$.

We could try to study the graphical intersections of P_R and P_L^{-1} under the hypotheses of Lemma 3.3 but it is not easy to deduce any direct conclusions. We proceed as follows. Clearly, the existence of periodic orbits is equivalent to the existence of two positive values y_L and y_R such that the orbit starting at $(0, -y_R)$ enters the half-plane $x > 0$ and goes around the origin in a counterclockwise path, coming back to the y-axis at the point $(0, P_R(y)) = (0, y_L)$, while the orbit starting at $(0, y_L)$ enters the half-plane $x < 0$ and goes around the origin in a counterclockwise path, coming back to the y-axis

at the point $(0, -P_L(y)) = (0, -y_R)$. In other words, we need

$$\begin{aligned} P_R(y_R) &= y_L, \\ y_R &= P_L(y_L). \end{aligned}$$

Adding and subtracting the above equations we get an equivalent system of sufficient and necessary conditions for existence of periodic orbits, namely

$$\begin{aligned} P_R(y_R) + y_R &= P_L(y_L) + y_L, \\ P_R(y_R) - y_R &= -\left[P_L(y_L) - y_L\right]. \end{aligned} \tag{3.32}$$

Since by standard results on uniqueness of solutions we know that P_R and P_L are monotone increasing functions, see Proposition 1.21 in [21], we can define two new functions as follows.

Definition 3.1 (A smart parameterization of half-return maps) *For each $Z \in \{L, R\}$, take instead of $y > 0$ a new variable $Y = P_Z(y) + y > 0$ and define $\widehat{P}_Z(Y) = P_Z(y) - y$.*

Denoting with I_f the identity function, we see that these new functions represent a different parameterization of the graphs of $P_R - I_f$ and $P_L - I_f$ and have, under hypotheses of Lemma 3.3, the same qualitative behavior, that is, both are positive for sufficiently small $Y > 0$ and eventually become negative, tending to $-\infty$ as $Y \to \infty$. Furthermore, the conditions (3.32) for existence of periodic orbits translate now to

$$\begin{aligned} Y_R &= Y_L, \\ \widehat{P}_R(Y_R) &= -\widehat{P}_L(Y_L), \end{aligned}$$

that is, to the existence of a value $Y > 0$ being solution of the single equation $\widehat{P}_R(Y) = -\widehat{P}_L(Y)$, that is of

$$\widehat{P}_R(Y) + \widehat{P}_L(Y) = 0. \tag{3.33}$$

We note that the left hand side of above equation is positive for sufficiently small $Y > 0$ and eventually becomes negative for sufficiently big Y. It suffices now to apply the intermediate value theorem for continuous functions to conclude the existence of at least a solution, and so the existence of a periodic orbit for the system. We summarize this conclusion in the following result.

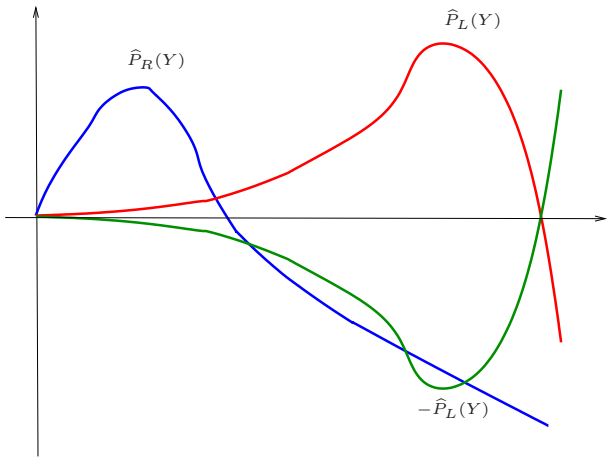

Figure 3.11: The qualitative behavior of half-Poincaré maps assures always a solution of (3.33) but could give rise to more than one periodic orbit: we see three intersection points between the graphs of $\widehat{P}_R(Y)$ and $-\widehat{P}_L(Y)$.

Corollary 3.2 *Systems with three linearity zones given in* (3.24)-(3.26) *with* $x_L < 0 < x_R$ *and satisfying the conditions* $a_L, a_R < 0$, $a_C > 0$ *and* $b_L, b_R \geq 0$ *always have at least one periodic orbit.*

Thus, it is immediate to conclude the existence of periodic orbits, but it is not guaranteed the uniqueness, see Figure 3.11. It is now very easy however to extend the uniqueness result for limit cycles of previous section, thanks again to Massera's method.

Proposition 3.7 *Systems* (3.24)-(3.26) *with* $x_L < 0 < x_R$ *and satisfying the conditions* $a_L, a_R < 0$, $a_C > 0$ *and* $b_L, b_R \geq 0$ *can be transformed in equivalent systems having the RAM increasing property in the whole plane. Consequently, if there is a closed orbit, then it surrounds the origin and it is a limit cycle which is unique and stable.*

Proof From Proposition 3.4 we can deduce that such systems can be transformed in equivalent systems having the RAM increasing property for all the rays contained in the half-plane $x \geq 0$. By using the symmetry given in Remark 2.2, and applying again Proposition 3.4, we can deduce that such systems can also be transformed in equivalent systems having the RAM increasing property for all the rays contained in the half-plane $x \leq 0$, and the

first assertion follows. Hence, the second assertion comes from Lemma 3.1 and the proposition follows. ■

Once having assured the uniqueness, we finally arrive to the first main result of this section. Note that we do not impose any strict symmetry, but only some symmetry in the signs of the traces (−,+,−) and determinants (+,+,+). We rewrite explicitly system (2.5)-(2.7) again for ease of reading.

Theorem 3.2 *Consider the differential system*

$$\begin{array}{rcl} \dot{x} & = & F(x) - y, \\ \dot{y} & = & g(x) - \delta, \end{array} \tag{3.34}$$

where

$$F(x) = \begin{cases} t_L(x+1) - t_C & \text{if } x < -1, \\ t_C x & \text{if } |x| \leq 1, \\ t_R(x-1) + t_C & \text{if } x > 1, \end{cases} \tag{3.35}$$

and

$$g(x) = \begin{cases} d_L(x+1) - d_C & \text{if } x < -1, \\ d_C x & \text{if } |x| \leq 1, \\ d_R(x-1) + d_C & \text{if } x > 1, \end{cases} \tag{3.36}$$

with only one equilibrium point in the central zone, i.e. $d_C > 0$, $-d_C < \delta < d_C$, *and* $d_L, d_R \geq 0$. *If the external traces satisfy* $t_L, t_R < 0$, *while the central trace is positive, that is* $t_C > 0$, *then the equilibrium point is surrounded by a limit cycle which is unique and stable.*

Proof From Lemma 2.2 we can pass to an equivalent system in the form (2.9)-(2.11), or equivalently to (3.24)-(3.26). The existence of limit cycles comes from Corollary 3.2 and its uniqueness and stability from Proposition 3.7. The conclusion follows. ■

Of course, by using the opposite sign distribution for the traces, we could state a similar theorem on existence and uniqueness of an unstable limit cycle.

We finish this section with other main results, gaining under strengthened hypotheses interesting information on the limit cycle predicted by Theorem 3.2 and showing that these systems with only one equilibrium can have two limit cycles. In fact, we try to answer a natural question: what happens with the limit cycle when we move δ out of the interval $[-d_C, d_C]$?

In the following proofs, we use the fact that under our hypotheses the system is dissipative in the sense that all the solutions are bounded. In fact,

by an adequate application of the ideas needed to prove Dragilev's theorem, see [89, 90], it can be shown that these systems possess a family of nested compact positive invariant sets for the flow, covering the whole phase plane, as follows.

Proposition 3.8 *Consider the differential system* (3.34)-(3.36) *with only one equilibrium point in the central zone, i.e.* $d_C > 0$, $-d_C < \delta < d_C$, *and* $d_L, d_R \geq 0$. *If the external traces satisfy* $t_L, t_R < 0$ *then there exist a compact positive invariant set containing the origin, so that orbits enter the set and no orbit escapes from it.*

Proof We start by obtaining the unbiased form of the system, by translating the equilibrium point to the origin. In doing so, we get the classical requirement $xg(x) > 0$ for all $x \neq 0$. Then, from the hypothesis $t_L, t_R < 0$, there exist a constant $M > 0$ and other two constants $K_R < K_L$, such that

$$F(x) \geq K_L \text{ for } x < -M, \text{ and } F(x) \leq K_R \text{ for } x > M,$$

see Figure 3.12.

As a second step in building a compact positive invariant set, it is clear that we can choose a sufficiently big value of y, namely $y_{LB} > 0$ such that (i) $y_{LB} > K_L$, (ii) $-y_{LB} < K_R$, and (iii) for the orbits starting at the points belonging to the two pieces of the band $-M < x < M$ with $y > y_{LB}$ and $y < -y_{LB}$ the inequality

$$\frac{dx}{dy} = \frac{g(x)}{F(x) - y} > s_N = \frac{K_R - K_L}{2M} \tag{3.37}$$

be satisfied, where it can be also assumed that $F(x) - y < 0$ for $y > y_{LB}$, and $F(x) - y > 0$ for $y < -y_{LB}$. Note that, since the right hand side is negative, the inequality is trivially true for instance when $-M \leq x \leq 0$ and $y > F(x)$, for then $g(x) \leq 0$ and the left hand side is positive. If we consider the case $0 \leq x \leq M$ and $y > F(x)$ then $g(x) \leq 0$ and the left hand side is negative; to fulfill the inequality we now must take y big enough, so that its absolute value be less than the absolute value of the negative right hand side. A similar argument can be done for the band $-M < x < M$ and $y < F(x)$, so that the choice of y_{LB} with the above requirements is always possible.

We next consider the definite positive function $G(x)$ with $G(0) = 0$ and $G'(x) = g(x)$ for all x. This function allows to build a family of ovals of

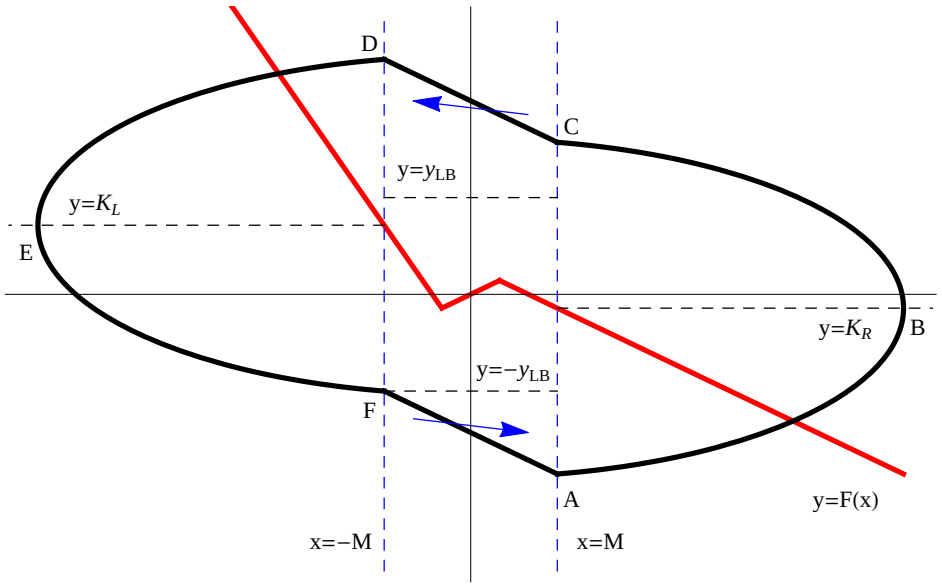

Figure 3.12: The polygonal ABCDEFA defines a compact positive invariant set for system (3.34)-(3.36) under the conditions of Proposition 3.8.

variable size $r > 0$, surrounding a point of the form $(0, K)$, namely $\Gamma_K(x, y) = r$, with

$$\Gamma_K(x, y) = \frac{(y - K)^2}{2} + G(x).$$

Observe that at the points of these ovals the derivative of r along the orbits (sometimes called orbital derivative) is

$$\begin{aligned} \frac{dr}{d\tau} &= \frac{d}{d\tau}\Gamma_K(x, y) = \frac{d}{dx}\Gamma_K(x, y)\dot{x} + \frac{d}{dy}\Gamma_K(x, y)\dot{y} = \\ &= (y - K)g(x) + g(x)(F(x) - y) = g(x)(F(x) - K), \end{aligned} \tag{3.38}$$

and therefore the orbits enter in (or escape from) the oval depending of the sign of the above expression.

After computing the quantity

$$H = \max\left\{\frac{(-y_{LB} - K_L)^2}{2}, \frac{(y_{LB} - K_R)^2}{2}\right\},$$

we choose the arc ABC with $x \geq M$ of the oval $\Gamma_{K_R}(x,y) = H + G(M)$, and the arc DEF with $x \leq -M$ of the oval $\Gamma_{K_L}(x,y) = H + G(-M)$, and close the circuit by considering the straight line segments CD and FA, see again Figure 3.12. We easily deduce that for the coordinates of the point A, namely (x_A, y_A), we have $x_A = M$ and

$$y_A = K_R - \sqrt{2H} = K_R - (y_{LB} + K_L) < -y_{LB}$$

when $\sqrt{2H} = y_{LB} + K_L$, while

$$y_A = K_R - \sqrt{2H} < K_R - (y_{LB} + K_L) < -y_{LB}$$

when $\sqrt{2H} = y_{LB} - K_R > y_{LB} + K_L$, so that in both cases we obtain $y_A < -y_{LB}$. For the coordinates of the point C, namely (x_C, y_C), we have $x_C = M$ and

$$y_C = K_R + \sqrt{2H} \geq K_R + y_{LB} - K_R = y_{LB}.$$

Similarly,for the coordinates of the point D, namely (x_D, y_D), we have $x_D = -M$ and

$$y_D = K_L + \sqrt{2H} \geq K_L + y_{LB} - K_R > y_{LB},$$

while for the coordinates of the point C, namely (x_F, y_F), we have $x_F = -M$ and

$$y_F = K_L - \sqrt{2H} = K_L - (y_{LB} + K_L) = -y_{LB}.$$

if $\sqrt{2H} = y_{LB} + K_L$, while

$$y_F = K_L - \sqrt{2H} = K_L - (y_{LB} - K_R) < K_L - (y_{LB} + K_L) = -y_{LB}.$$

when $\sqrt{2H} = y_{LB} - K_R > y_{LB} + K_L$.

At the two arcs ABC and DEF, from (3.38), we can guarantee that the orbits cross the arcs entering to the region bounded by the closed curve. The slopes of the segments CD and FA are

$$\frac{y_C - y_D}{2M} = \frac{K_R - K_L}{2M}, \quad \frac{y_A - y_F}{2M} = \frac{K_R - K_L}{2M},$$

that is, equal to s_N in both cases, and from the condition (3.37) we also conclude that the orbits cross these segments in such a way that they enter the closed curve, see the arrows drawn in Figure 3.12. The proposition follows.

■

Note that the compact set build in the proof of 3.8 is also called a trapping region and that we do not require any condition for t_C. The procedure can be clearly extended to the case $\delta \notin (-d_C, d_C)$ but then, we must impose $d_L, d_R > 0$ in order to maintain the uniqueness of the equilibrium and the condition $xg(x) > 0$ for all $x \neq 0$ in the associated unbiased system. As we can repeat the algorithm by increasing the value of M, we can define an increasing family of nested compact positive invariant sets, covering the whole phase plane, so that all the orbits eventually are trapped into the intersection of all the members of the family, that is, the first one. Thus, the system is dissipative in the sense that all the orbits are bounded forward in time.

To organize all the consequences of our previous analysis, we consider separately the cases of central node dynamics and central focus dynamics. We emphasize the situations leading to two limit cycles.

Theorem 3.3 (Central node dynamics) *Consider system* (3.34)-(3.36) *under the hypotheses of Theorem 3.2 but assuming* $d_L, d_R > 0$ *and central node dynamics, that is,* $t_C^2 - 4d_C \geq 0$. *The following statements hold.*

(a) *The stable limit cycle has always points in the three linearity zones.*

(b) *Assuming that the right (left) dynamics is of node type, that is* $t_R^2 - 4d_R \geq 0$ $(t_L^2 - 4d_L \geq 0)$, *the stable limit cycle disappears for* $\delta > d_C$ $(\delta < -d_C)$.

In passing through the values $\delta = d_C$ $(\delta = -d_C)$ *we have an explosive appearance/disappearance of the stable limit cycle through a configuration determined by a bounded continuum of homoclinic connections to the equilibrium point, which is located at the corner* $(1, t_C)$ *(respectively, at* $(-1, -t_C)$*).*

(c) (A BEB adding a new limit cycle)
If the right (left) dynamics is of focus type, that is $t_R^2 - 4d_R < 0$ $(t_L^2 - 4d_L < 0)$, *then there exists* $\epsilon > 0$ *such that for* $\delta_C < \delta < \delta_C + \epsilon$ *(respectively,* $-\delta_C - \epsilon < \delta < -\delta_C$*) there exists a stable focus surrounded by two limit cycles, the smaller unstable and the bigger stable. The smaller cycle is born through a BEB bifurcation at* $\delta = \delta_C$ $(\delta = -\delta_C)$, *where the equilibrium at the corner is a repulsive node-focus while the big limit cycle persists.*

Proof Statement (a) comes from the fact that the limit cycle predicted by Theorem 3.2 must surround the segments corresponding to the linear portions of the invariant manifolds of the node.

We only consider the assertions related to the right corner. To show first assertion of statement (b), recalling the arguments about the linear invariant manifolds of nodes used in the proof of Proposition 3.2, when $\delta > d_C$ we conclude that there cannot be periodic orbits.

The explosive transition of second assertion of statement (b) comes directly from statement (a). The bounded continuum of homoclinic connections to the equilibrium point when it is located at a corner of the vertical nullcline can be deduced from the node-node configuration (central unstable, external stable) and the dissipative character of the system.

Regarding statement (c), for $\delta = d_C$ we have a two-zone BEB corresponding to the transition unstable-node $\rightarrow$ stable-focus. Swapping the two zones involved in the transition of Proposition 3.5(b), we conclude that we must have an unstable limit cycle surrounding the focus as long as this new, initially small cycle only uses such two zones. Recall that the size of this cycle depends linearly on the difference $\delta - d_C > 0$. Again using the dissipative character of the system, we must have a bigger stable limit cycle surrounding the unstable one whenever the latter exists; the same must occur for the repulsive equilibrium at the corner for the transition value of δ. Statement (c) is shown. ■

Statement (b) of Theorem 3.3 generalizes a recent result appeared in [17]. Regarding statement (c) we conjecture that for some δ sufficiently big in absolute value both limit cycles collapse to disappear.

We finally analyze the case of central focus dynamics.

Theorem 3.4 (Central focus dynamics) *Consider system* (3.34)-(3.36) *under the hypotheses of Theorem 3.2 but assuming* $d_L, d_R > 0$ *and central focus dynamics, that is,* $t_C^2 - 4d_C < 0$. *The following statements hold.*

- **(a)** *If the right (left) dynamics is of node type, that is* $t_R^2 - 4d_R \geq 0$ ($t_L^2 - 4d_L \geq 0$), *then the stable limit cycle disappears for* $\delta > d_C$ ($\delta < -d_C$) *in a focus-node BEB, so that the size of the limit cycle eventually decreases linearly to zero.*

- **(b)** *If the right (left) dynamics is also of focus type, that is* $t_R^2 - 4d_R < 0$ ($t_L^2 - 4d_L < 0$), *then three cases arise.*

(b1) *If we also have the condition*

$$\frac{t_C}{\sqrt{d_C}} + \frac{t_R}{\sqrt{d_R}} < 0 \quad \left(\frac{t_L}{\sqrt{d_L}} + \frac{t_C}{\sqrt{d_C}} < 0 \right),$$

the stable limit cycle disappears for $\delta = d_C$ ($\delta = -d_C$) in a focus-focus BEB, so that the size of the limit cycle eventually decreases linearly to zero.

(b2) *If we also have the condition*

$$\frac{t_C}{\sqrt{d_C}} + \frac{t_R}{\sqrt{d_R}} = 0 \quad \left(\frac{t_L}{\sqrt{d_L}} + \frac{t_C}{\sqrt{d_C}} = 0 \right),$$

the stable limit cycle disappears for $\delta = d_C$ ($\delta = -d_C$) in a 'center' BEB, so that the size of the limit cycle decreases abruptly to zero for $\delta > d_C$ ($\delta < -d_C$).

(b3) (A BEB adding a new limit cycle)
If we also have the condition

$$\frac{t_C}{\sqrt{d_C}} + \frac{t_R}{\sqrt{d_R}} > 0 \quad \left(\frac{t_L}{\sqrt{d_L}} + \frac{t_C}{\sqrt{d_C}} > 0 \right),$$

then there exists $\epsilon > 0$ such that for $d_C < \delta < d_C + \epsilon$ (respectively, $-d_C - \epsilon < \delta < -d_C$) there exists a stable focus surrounded by two limit cycles, the smaller unstable and the bigger stable. The smaller cycle is born through a BEB bifurcation at $\delta = d_C$ ($\delta = -d_C$), where the equilibrium at the corner is an unstable focus while the big limit cycle persists.

Proof We only consider the assertions related to the right corner. In the situation of statement (a), we have for $\delta = d_C$ a focus-node BEB, and we know that for small $d_C - \delta > 0$ the equilibrium is surrounded by one stable limit cycle that only uses the zones C and R, whose size decreases linearly as long as the equilibrium in the central zone approaches the right corner. From Theorem 3.2, this limit cycle is the unique cycle.

Regarding statement (b), for $\delta = d_C$ we have a BEB corresponding to the transition unstable-focus $\rightarrow$ stable-focus. Swapping the two zones involved in the transition, in the case (b1) we are in the situation of Proposition 3.5(c), and we conclude that we must have a stable limit cycle surrounding the focus

and that for small $d_C - \delta > 0$ this cycle only uses such the zones C and R. Recall that the size of this cycle depends linearly on the difference $d_C - \delta > 0$. From Theorem 3.2, this limit cycle is the unique cycle shrinking to a point when $\delta = d_C$

In the case (b2), for $\delta = d_C$ we have a two-zone center BEB, but here bounded by the closed orbit of the center that is tangent to the vertical $x = -1$. Such configuration is attractive and not compatible with another stable limit cycle surrounding it; we conclude that the stable limit cycle that exists for small $d_C - \delta > 0$ collides with the closed orbit bounding the center. For $\delta > d_C$ the center collapses to the stable focus and no periodic orbits remain.

The case (b3) is totally similar to the case (c) of Theorem 3.3, but now we must resort by swapping the two zones involved in the transition to the statement (d) of Proposition 3.5, where we have a subcritical focus-focus transition leading to a new, small unstable limit cycle for $\delta > d_C$ to be surrounded by another stable limit cycle. ■

3.2.1 Application to Wien bridge oscillators

One of the most common electronic oscillators, useful for a wide range of frequencies is the Wien bridge oscillator. Its name is due to the German physicist M. Wien who invented it in 1891. In 1939, Bill Hewlett and Dave Packard (HP founders) implemented it successfully, from the viewpoint of oscillation, and it was the first product marketed by the multinational HP, called HP200A. Originally, it is a system that has symmetry when its state variables change sign. Here, we consider a variant without symmetry by including an additional battery E_B, see Figure 3.13.

Applying the Kirchhoff's laws to the circuit that appears in Figure 3.13 we obtain the following equations

$$R_1 C_1 \dot{V}_{C_1} = -V_{C_1} - V_{C_2} + V_0, \qquad C_1 \dot{V}_{C_1} - C_2 \dot{V}_{C_2} = \frac{V_{C_2} - E_B}{R_2} \tag{3.39}$$

where the variables V_{C_1} and V_{C_2} are the voltages on the capacitors C_1 y C_2, whilst $V_0 = f(V_{C_2})$ is the output voltage of the operational amplifier and $\dot{V}$ denotes the derivative with respect to the time variable τ.

Several proposals for modeling non-linearity of the operational amplifier

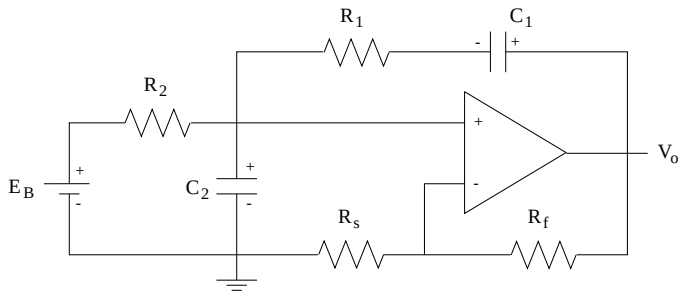

Figure 3.13: Diagram of the Wien Bridge asymmetrical electronic circuit.

have been formulated. In [67] authors consider the differentiable function

$$V_0 = f\left(V_{C_2}\right) = \frac{2E}{\pi}\arctan\left(\frac{\pi\alpha}{2E}V_{C_2}\right),$$

where E is saturation voltage of the operational amplifier and

$$\alpha = 1 + \frac{R_f}{R_s}$$

is the circuit gain equivalent to the operational amplifier. As shown in [26] the piecewise model proposed by Kriegsmann in [49], based on the following formulation

$$V_0 = f\left(V_{C_2}\right) = \begin{cases} E\ \mathrm{sgn}\left(\alpha V_{C_2}\right), & \text{if } |\alpha V_{C_2}| > E, \\ \alpha V_{C_2}, & \text{if } |\alpha V_{C_2}| \leq E, \end{cases}$$

is a rather accurate model, to be adopted in the sequel, see Figure 3.14.

Using in (3.39) the dimensionless voltages

$$x = \alpha\frac{V_{C_2}}{E},\ y = \alpha\frac{V_{C_1}}{E},\ x_B = \alpha\frac{E_B}{E},$$

and taking into account that

$$f\left(V_{C_2}\right) = f\left(\frac{E}{\alpha}x\right) = E\,\mathrm{sat}(x),$$

we get the nonsymmetric 3CPWL$_2$ system

$$\dot{\mathbf{x}} = \begin{pmatrix} -\left(\dfrac{1}{R_1C_2} + \dfrac{1}{R_2C_2}\right) & -\dfrac{1}{R_1C_2} \\ \\ -\dfrac{1}{R_1C_1} & -\dfrac{1}{R_1C_1} \end{pmatrix}\mathbf{x} + \begin{pmatrix} \dfrac{\alpha\,\mathrm{sat}(x) + x_B}{R_1C_2} \\ \\ \dfrac{\alpha\,\mathrm{sat}(x)}{R_1C_1} \end{pmatrix}. \quad (3.40)$$

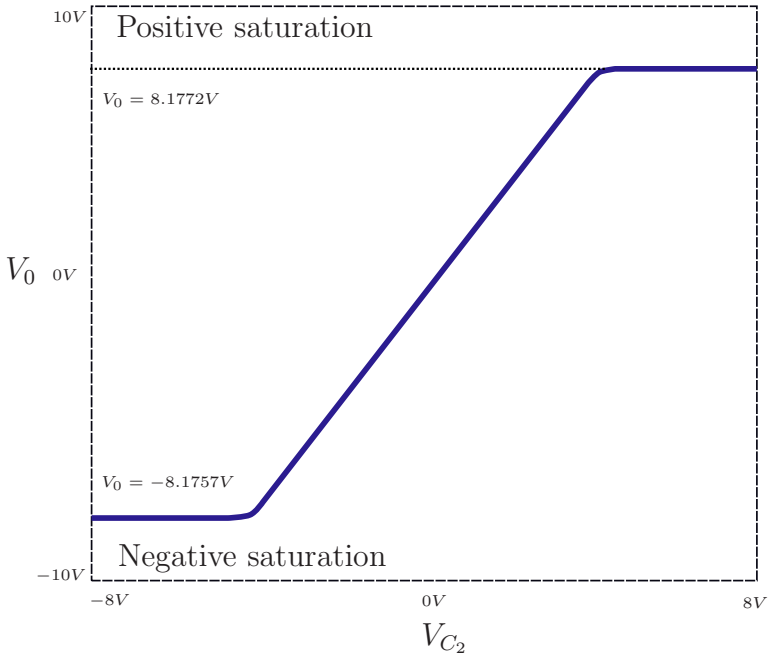

Figure 3.14: Output voltage V_0 versus input voltage V_{C_2} of LF411 operational amplifier.

Clearly, our system is observable since the entry a_{12} in the first matrix does not vanish. Changing now the variables by putting

$$X = x, \quad Y = \frac{y}{R_1C_2} - \frac{x}{R_1C_1} - \frac{x_B}{R_1C_2},$$

we transform (3.40) in the Liénard form

$$\begin{pmatrix} \dot{X} \\ \dot{Y} \end{pmatrix} = \begin{pmatrix} t & -1 \\ d & 0 \end{pmatrix} \begin{pmatrix} X \\ Y \end{pmatrix} + \begin{pmatrix} T-t \\ 0 \end{pmatrix} \mathrm{sat}(X) + \begin{pmatrix} 0 \\ -d \cdot x_B \end{pmatrix}, \quad (3.41)$$

where in terms of the notation of Theorem 3.2, we have

$$t_L = t_R = t = -\left(\frac{1}{R_1C_1} + \frac{1}{R_1C_2} + \frac{1}{R_2C_2}\right) < 0,$$

$$t_C = T = -\left(\frac{1}{R_1C_1} + \frac{1-\alpha}{R_1C_2} + \frac{1}{R_2C_2}\right) = t + \frac{\alpha}{R_1C_2},$$

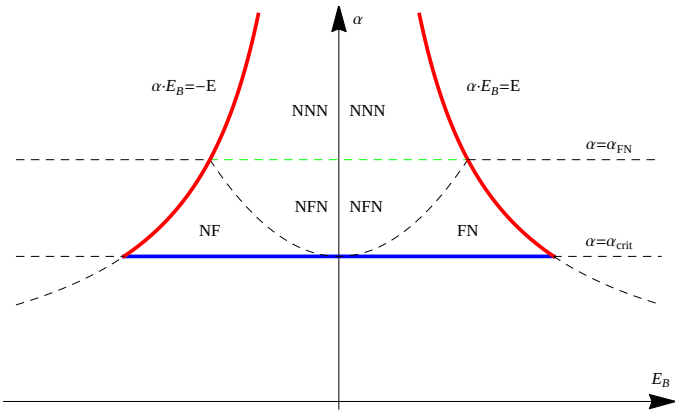

Figure 3.15: Bifurcation set of the Wien Bridge asymmetrical electronic circuit. The letters in different regions indicate the types of dynamics used by the limit cycle (N stands for node, F for focus). The curve where the oscillation passes from being bizonal to tri-zonal (or vice versa) is only sketched, and not really computed.

and

$$d_L = d_C = d_R = d = \frac{1}{R_1 R_2 C_1 C_2} > 0, \quad \delta = d \cdot x_B.$$

Note that to satisfy all the hypotheses of the theorem, we just need the condition $|x_B| < 1$, that is $|\alpha E_B| < E$, along with $T > 0$. This last condition is equivalent to $\alpha > \alpha_{\text{crit}}$, where the critical value of the operational amplifier gain is

$$\alpha_{\text{crit}} = 1 + \frac{C_2}{C_1} + \frac{R_1}{R_2}. \tag{3.42}$$

After this analysis, we can state the following result, which is a direct consequence of Theorem 3.2, see figure 3.15.

Proposition 3.9 *Consider the differential system* (3.41). *The following statements hold.*

(a) *If $E_B = 0$ and the operational amplifier gain satisfies*

$$\alpha > \alpha_{crit} = 1 + \frac{C_2}{C_1} + \frac{R_1}{R_2},$$

then the system exhibits a symmetric oscillation corresponding to a limit cycle surrounding the equilibrium at the origin. The limit cycle is unique and stable.

(b) *If $E_B \neq 0$ and $\alpha_{crit} < \alpha_{end}$, where*

$$\alpha_{end} = \frac{E}{|E_B|},$$

then we have oscillations whenever $\alpha_{crit} < \alpha < \alpha_{end}$. The oscillations are not symmetric and correspond to a limit cycle surrounding the biased equilibrium. The limit cycle is unique and stable.

We try now to apply Theorem 3.3. To do this, we study the kind of dynamics to be found in each linear region looking for a simpler form of the system. In fact, it is usual for the analysis of electronic models, and also very convenient, to scale the time by using a natural frequency of the circuit.

In an analogous way to what we made in Lemma 2.2, we use a normalized time $\tau_n = \omega\tau$ and scale again the second variable by writing $\omega y = Y$ to preserve the Liénard form, where $\omega^2 = d$. We obtain a system with unitary determinants in all the zones, namely

$$\begin{aligned} \frac{dx}{d\tau_n} &= \tilde{t}x + (\tilde{T} - \tilde{t})\,\mathrm{sat}(x) - y, \\ \frac{dy}{d\tau_n} &= x - x_B, \end{aligned} \tag{3.43}$$

where

$$\tilde{t} = -\sqrt{\frac{R_2C_1}{R_1C_2}}\alpha_{\mathrm{crit}}, \quad \tilde{T} = \sqrt{\frac{R_2C_1}{R_1C_2}}(\alpha - \alpha_{\mathrm{crit}}).$$

Thus, by introducing the auxiliary constants

$$\rho_R = \sqrt{\frac{R_1}{R_2}}, \quad \rho_C = \sqrt{\frac{C_2}{C_1}},$$

we see, recalling (3.42), that

$$|\tilde{t}| = \frac{1 + \rho_R^2 + \rho_C^2}{\rho_R\rho_C} = 2 + \frac{1 + \rho_R^2 + \rho_C^2 - 2\rho_R\rho_C}{\rho_R\rho_C} = 2 + \frac{1 + (\rho_R - \rho_C)^2}{\rho_R\rho_C} > 2,$$

so that, the dynamic in both external zones is of node type for all the choices of ρ_R and ρ_C. For $\alpha \approx \alpha_{\text{crit}}$, that is $\tilde{T} \approx 0$, we have that the central dynamics is of focus type. By imposing the condition $\tilde{T} \geq 2$, that is, for

$$\alpha \geq \alpha_{\text{crit}} + 2\rho_R\rho_C = 1 + \rho_R^2 + \rho_C^2 + 2\rho_R\rho_C = 1 + (\rho_R + \rho_C)^2$$

we also have a central node dynamics. Thus, the transition between the two regimes occurs for

$$\alpha_{FN} = 1 + \frac{C_2}{C_1} + \frac{R_1}{R_2} + 2\sqrt{\frac{R_2C_1}{R_1C_2}} = \alpha_{\text{crit}} + 2\sqrt{\frac{R_2C_1}{R_1C_2}}.$$

In typical designs, which use equal resistors and capacitors, that is $\rho_R = 1$, $\rho_C = 1$, we have $\alpha_{\text{crit}} = 3$ and $\alpha_{\text{FN}} = 5$, so that the oscillations with central focus dynamics appear for $3 < \alpha < 5$ being of node type for $\alpha \geq 5$.

We can now conclude our analysis by giving the consequences of theorems 3.3 and 3.4, see figure 3.15.

Proposition 3.10 *Consider the differential system* (3.41) *under the hypotheses* $E_B \neq 0$ *and* $\alpha_{crit} < \alpha_{end}$*, and assume a initial value of* α *satisfying* $\alpha_{crit} < \alpha < \alpha_{end}$*. The following statements hold.*

(a) *If the condition* $\alpha_{end} < \alpha_{FN}$ *holds, and we increase* α *to the value* $\alpha = \alpha_{end}$ *then the non-symmetric oscillation corresponding to a stable limit cycle decreases in a eventually linear process with constant period, up to become an equilibrium state with zero amplitude for* $\alpha > \alpha_{end}$*.*

(b) *If the condition* $\alpha_{end} > \alpha_{FN}$ *holds, then the non-symmetric oscillation corresponding to a stable limit cycle uses the three linear zones for* $\alpha_{FN} \leq \alpha < \alpha_{end}$*. If we increase* α *to the value* $\alpha = \alpha_{end}$ *then the non-symmetric oscillation corresponding to a stable limit cycle approaches a significant size with a period tending to infinity, to disappear for* $\alpha > \alpha_{end}$ *in an abrupt way, leading to an equilibrium state with zero amplitude.*

Proof Statement (a) corresponds to the case of central focus dynamics and external node dynamics, that is, to statement (a) of Theorem 3.4.

Statement (b) corresponds to the case of central node dynamics plus external node dynamics, that is, to statement (a) and (b) of Theorem 3.3. ■

Summarizing all our results, we obtain in Figure 3.15 an unbounded region in the parameter plane (E_B, α) where oscillations exist. The points of the horizontal segment $\alpha = \alpha_{crit}$ represent focus-center-limit cycle bifurcation points (see Section 3.3.1 later), while the two arcs of hyperbola lead to boundary equilibrium bifurcations, and in both cases the oscillation is created or annihilated but with different qualitative behavior (explosive or not).

3.2.2 Algebraically Computable PWL Nodal Oscillators

Here we study some symmetric piecewise linear oscillators whose involved linear parts are of node type. Typically, in explaining the origin of oscillations, it is required to have eigenvalues near the imaginary axis of the complex plane. As it has been shown above, this is not needed when dealing with piecewise linear systems. In fact, we introduce a family of PWL oscillators with all dynamics of node type, to be called nodal oscillators, having the outstanding characteristic of being algebraically determinable, that is, all the magnitudes related with the oscillation can be algebraically computed. The content of this section appeared very recently in [74].

We consider general planar piecewise linear systems with symmetry respect to the origin and three linearity regions separated by parallel straight lines, under the generic condition of observability. The key hypothesis to get an algebraically computable piecewise linear oscillation is to impose that the involved spectra have the same proportion between eigenvalues. Here, for sake of simplicity, we will choose the ratio $1 : 2$. Thus, as it will be seen, it is possible to convert the transcendental equations that characterize oscillations into algebraic equations.

Of course, from Bendixson-Dulac's Theorem, see also the previous section, we also need for periodic oscillations that the divergence of the vector field, which is the trace of the matrix ruling the dynamics in each linearity region, have no global constant sign; otherwise self-sustained oscillations are not possible. Thus, we assume that for the external zones we have a dissipative spectrum of the form $\{-\mu, -2\mu\}$, with $\mu > 0$, whilst in the central zone we have a region with the spectrum $\{\eta, 2\eta\}$, obeying the same proportion $1 : 2$. This idea has been also exploited in higher dimensions, by using the proportion $1 : 2 : 3$, see [60] and [61].

Our first result says that one needs only to study a one-parameter family to cope with all possible systems with the above characteristics.

Proposition 3.11 *Consider the family of piecewise linear differential systems*

$$\dot{\mathbf{x}} = A\mathbf{x} + \varphi(\mathbf{c}^T\mathbf{x})\mathbf{b}, \tag{3.44}$$

where $\mathbf{x} = (x, y)^T \in \mathbb{R}^2$, *A is a* 2×2 *matrix,* $\mathbf{b}$, $\mathbf{c} \in \mathbb{R}^2$ *and the nonlinearity* φ *is a symmetric piecewise linear continuous function*

$$\varphi(\sigma) = \begin{cases} m_a\sigma - (m_b - m_a)\,\delta, & \sigma < -\delta, \\ m_b\sigma, & |\sigma| \le \delta, \\ m_a\sigma + (m_b - m_a)\,\delta, & \sigma > \delta, \end{cases} \tag{3.45}$$

with $m_a \neq m_b$, $\delta > 0$, *see Figure 3.16. Assume that there exist* $\mu > 0$ *and* $\eta \in \mathbb{R}$, *such that the different linear parts satisfy*

$$\begin{array}{rcl} \mathrm{Spec}\left(A + m_a\mathbf{b}\,\mathbf{c}^T\right) & = & \{-\mu, -2\mu\}\,, \\ \mathrm{Spec}\left(A + m_b\mathbf{b}\,\mathbf{c}^T\right) & = & \{\eta, 2\eta\}\,, \end{array} \tag{3.46}$$

and that the system is observable, that is

$$\det\begin{pmatrix} \mathbf{c}^T \\ \mathbf{c}^T A \end{pmatrix} \neq 0.$$

Then the system (3.44) *is topologically equivalent to the Liénard system*

$$\begin{pmatrix} \dot{x} \\ \dot{y} \end{pmatrix} = \begin{pmatrix} -3 & -1 \\ 2 & 0 \end{pmatrix}\begin{pmatrix} x \\ y \end{pmatrix} + \begin{pmatrix} 3(\alpha+1) \\ 2(\alpha^2-1) \end{pmatrix}\mathrm{sat}(x), \tag{3.47}$$

where $\alpha = \dfrac{\eta}{\mu}$ *and* "sat" *stands for the normalized saturation function.*

Proof First, we will show that we can pass easily from the given piecewise linear characteristics to the normalized saturation. Effectively, by defining $\mathbf{x} = \delta\hat{\mathbf{x}}$, we have from the equality

$$\delta\dot{\hat{\mathbf{x}}} = A\delta\hat{\mathbf{x}} + \varphi(\delta\,\mathbf{c}^T\hat{\mathbf{x}})\mathbf{b},$$

by adding and substracting $m_a\mathbf{b}\mathbf{c}^T\hat{\mathbf{x}}$, that

$$\begin{array}{rcl} \dot{\hat{\mathbf{x}}} & = & \left(A + m_a\mathbf{b}\mathbf{c}^T\right)\hat{\mathbf{x}} + \dfrac{1}{\delta}\mathbf{b}\left(\varphi(\delta\mathbf{c}^T\hat{\mathbf{x}}) - m_a\delta\mathbf{c}^T\hat{\mathbf{x}}\right) = \\ & = & \left(A + m_a\mathbf{b}\mathbf{c}^T\right)\hat{\mathbf{x}} + \mathbf{b}\,(m_b - m_a)\,\mathrm{sat}\left(\mathbf{c}^T\hat{\mathbf{x}}\right). \end{array}$$

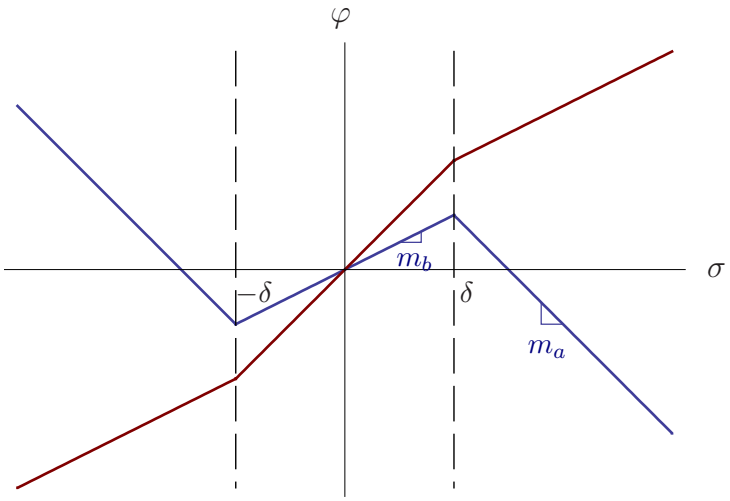

Figure 3.16: Two typical cases for the symmetric piecewise linear function φ; in one of them the slopes m_a and m_b are indicated.

Defining $A_a = A + m_a \mathbf{b}\mathbf{c}^T$, $A_b = A + m_b \mathbf{b}\mathbf{c}^T$ and $\hat{\mathbf{b}} = \mathbf{b}\,(m_b - m_a)$, the system becomes

$$\dot{\hat{\mathbf{x}}} = A_a \hat{\mathbf{x}} + \hat{\mathbf{b}}\,\mathrm{sat}\left(\mathbf{c}^T \hat{\mathbf{x}}\right).$$

Now, we do a new linear change of variables given by $\hat{\mathbf{x}} = M\tilde{\mathbf{x}}$, where

$$M = \left(\begin{array}{c|c} -A\mathbf{v} & \mathbf{v} \end{array}\right)$$

and the vector $\mathbf{v}$ is chosen such that $\mathbf{c}^T\mathbf{v} = 0$, and $\mathbf{c}^T A\mathbf{v} = -1$. This vector $\mathbf{v}$ is always uniquely determined due to the hypothesis of observability, and it is easy to show that

$$\begin{pmatrix} \mathbf{c}^T \\ \mathbf{c}^T A_a \end{pmatrix} \mathbf{v} = \begin{pmatrix} \mathbf{c}^T \\ \mathbf{c}^T A_b \end{pmatrix} \mathbf{v} = \begin{pmatrix} \mathbf{c}^T \\ \mathbf{c}^T A \end{pmatrix} \mathbf{v} = \begin{pmatrix} 0 \\ -1 \end{pmatrix}.$$

Now by using the Cayley-Hamilton Theorem, it can be concluded that

$$A_a M = \left(\begin{array}{c|c} -A_a^2\mathbf{v} & A_a\mathbf{v} \end{array}\right) = M \begin{pmatrix} \mathrm{trace}(A_a) & -1 \\ \det(A_a) & 0 \end{pmatrix} = M \begin{pmatrix} -3\mu & -1 \\ 2\mu^2 & 0 \end{pmatrix},$$

and analogously,

$$A_b M = M \begin{pmatrix} -3\eta & -1 \\ 2\eta^2 & 0 \end{pmatrix}.$$

Clearly, M is invertible. Effectively, otherwise $A\mathbf{v} = \lambda\mathbf{v}$, and $\mathbf{v}$ would be an A -eigenvector; then from $\mathbf{c}^T\mathbf{v} = 0$ we would obtain the contradiction $\mathbf{c}^T A\mathbf{v} = 0$. With the change given by the matrix M we get that $\mathbf{c}^T M = \mathbf{e}_1^T = (1, 0)$ arriving to the system

$$\dot{\tilde{\mathbf{x}}} = \bar{A}\tilde{\mathbf{x}} + \bar{\mathbf{b}}\,\mathrm{sat}(\tilde{x}),$$

where $\tilde{\mathbf{x}} = (\tilde{x}, \tilde{y})$ and

$$\bar{A} = M^{-1}A_a M = \begin{pmatrix} -3\mu & -1 \\ 2\mu^2 & 0 \end{pmatrix}, \quad \bar{\mathbf{b}} = M^{-1}\hat{\mathbf{b}}.$$

Note that for $|\tilde{x}| < 1$ the linear part of the system satisfy

$$\bar{A} + \bar{\mathbf{b}}\mathbf{e}^T = M^{-1}A_b M = \begin{pmatrix} 3\eta & -1 \\ 2\eta^2 & 0 \end{pmatrix}.$$

Thus, we conclude that

$$\bar{\mathbf{b}} = \begin{pmatrix} 3(\eta + \mu) \\ 2(\eta^2 - \mu^2) \end{pmatrix},$$

and that system (3.44) is topologically equivalent to the system

$$\begin{pmatrix} \dot{\tilde{x}} \\ \dot{\tilde{y}} \end{pmatrix} = \begin{pmatrix} -3\mu & -1 \\ 2\mu^2 & 0 \end{pmatrix} \begin{pmatrix} \tilde{x} \\ \tilde{y} \end{pmatrix} + \begin{pmatrix} 3(\eta + \mu) \\ 2(\eta^2 - \mu^2) \end{pmatrix} \mathrm{sat}(\tilde{x}). \tag{3.48}$$

Finally, to show the topological equivalence of above system with system (3.47) it suffices to rescale the variables and the time. Effectively if we denote by t the original time, we define a new time $\tau = \mu t$ and new variables (x, y) such that $(x, \mu y) = (\tilde{x}, \tilde{y})$, then we arrive at the system (3.47). The proposition follows. ■

From now on we focus our attention to the analysis of the dynamics of system (3.47), which permits to represent all the members of the original family (3.44). Recall the notation

$$\mathcal{S}_0 = \{(x, y) \in \mathbb{R}^2 : -1 < x < 1\}$$

for the zone C,

$$\mathcal{S}_+ = \{(x, y) \in \mathbb{R}^2 : x > 1\}, \quad \mathcal{S}_- = \{(x, y) \in \mathbb{R}^2 : x < -1\}$$

for the symmetrical external zones L and R, and separated by the two straight lines

$$\Sigma_1 = \{(x, y) \in \mathbb{R}^2 : x = 1\}, \quad \Sigma_{-1} = \{(x, y) \in \mathbb{R}^2 : x = -1\}$$

for the two separation straight lines. We also note that system (3.44) is a particular instance of single-input single-output Luré systems, formed by the *linear plant* $\dot{\mathbf{x}} = A\mathbf{x} + \mathbf{b}\xi$, subject to the nonlinear feedback $\xi = \varphi(\sigma)$, with $\sigma = \mathbf{c}^T\mathbf{x}$. In the case of system (3.47), we have

$$A = \begin{pmatrix} -3 & -1 \\ 2 & 0 \end{pmatrix}, \quad \mathbf{b} = \begin{pmatrix} 3(\alpha+1) \\ 2(\alpha^2-1) \end{pmatrix}, \quad \mathbf{c} = \begin{pmatrix} 1 \\ 0 \end{pmatrix},$$

and the nonlinearity φ is the normalized saturation, i.e., $\varphi(\sigma) = \text{sat}(\sigma)$. Note that system (3.47) is equivalent for $|x| < 1$ to the homogeneous system $\dot{\mathbf{x}} = B\mathbf{x}$, where

$$B = \begin{pmatrix} 3\alpha & -1 \\ 2\alpha^2 & 0 \end{pmatrix}, \tag{3.49}$$

with eigenvalues α and 2α. Thus the origin is an equilibrium which is a linear node for all $\alpha \neq 0$. On the other hand, the eigenvalues of A are -1 and -2, so that they are stepped in the same proportion $1 : 2$ as the eigenvalues of B, as a consequence of assumptions on the spectra of system (3.44). This fact will be crucial for determining algebraically the periodic orbits that appear for $\alpha > 0$, as it has been already mentioned.

Very few non-smooth oscillators can be analyzed in an exact way and typically one must resort to approximate or asymptotic methods, see [40]. Within a more general context, in [39] a piecewise quadratic oscillator was considered, getting information only for several values of the parameter. On the contrary, we will obtain here the exact magnitudes of the oscillation for all values of the bifurcation parameter. Thus, the family (3.47) is suitable for serving as a benchmark of different existing approximate methods for detecting periodic orbits by comparing their predictions with our exact results.

We must recall once more that the analytic determination of orbits in piecewise linear systems is by no means a trivial task: even each linear system can be easily integrated, one has to match different solutions of each linear piece, which requires the exact computation of flight times in each zone. In fact, we will not be able here to exactly compute all the orbits of system (3.47) but only its periodic orbits. Then, before tackling the main result of

this section, we present several auxiliary results that will be useful in the proof of the main result.

System (3.47), considered as a Liénard system, can be written in the form

$$\begin{aligned} \dot{x} &= F(x) - y, \\ \dot{y} &= g(x), \end{aligned} \tag{3.50}$$

where

$$\begin{aligned} F(x) &= -3x + 3(\alpha+1)\,\mathrm{sat}(x), \\ g(x) &= 2x + 2(\alpha^2-1)\,\mathrm{sat}(x). \end{aligned}$$

We start with the following auxiliary result.

Lemma 3.4 *Regarding the equilibrium points of differential system* (3.47)*, the following statements hold.*

(a) *For $\alpha < 0$ the origin is the only equilibrium point and it is a stable node, which becomes the global attractor for the system.*

(b) *For $\alpha = 0$ there exists a continuous of equilibrium points, namely all the points of the segment $\Sigma = \{(x,y) \in \mathbb{R}^2 : -1 \le x \le 1, y = 0\}$. This segment is then a global attractor for the system.*

(c) *For $\alpha > 0$ the only equilibrium point is the origin, which is an unstable node.*

Proof We will use the system written in its Liénard form (3.50). First we note that function g is always monotone increasing, independently on the value of parameter α, see Figure 3.17.

The equilibrium points are obviously given by the points in the set $\{(x,y) \in \mathbb{R}^2 : g(x) = 0, y = F(x)\}$. When $\alpha \neq 0$ the only equilibrium point is the origin. However, for $\alpha = 0$ we get the segment given in statement (b). Hence all the assertions about the existence of equilibrium points are shown. It remains to verify the stability properties of these points.

Regarding statement (a), we build the Lyapunov function

$$V(x,y) = \frac{y^2}{2} + G(x) \tag{3.51}$$

where

$$G(x) = \int_0^x g(s)ds = \begin{cases} x^2 + (1+2x)(1-\alpha^2), & \text{if } x < -1, \\ \alpha^2 x^2, & \text{if } -1 \le x \le 1, \\ x^2 + (1-2x)(1-\alpha^2), & \text{if } x > 1. \end{cases}$$

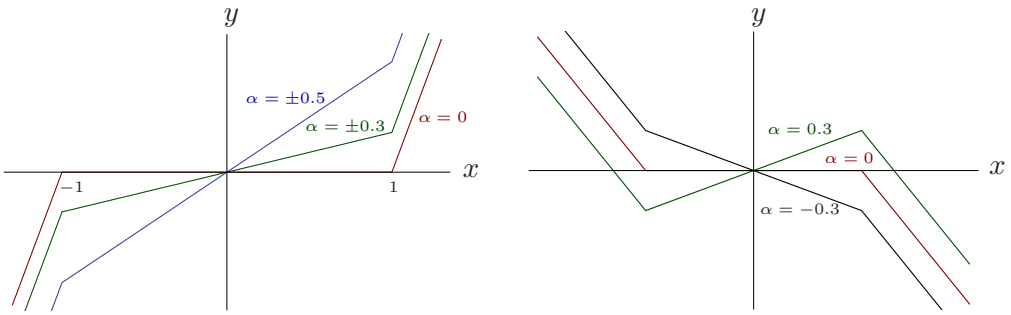

Figure 3.17: Graphs of $g(x)$ (left) and $F(x)$ (right) depending on the parameter α.

Then, the function $V(x, y)$ is continuously differentiable and satisfies $V(0, 0) = 0$, $V(x, y) > 0$ for all $(x, y) \neq (0, 0)$, it is radially unbounded and its orbital derivative is strictly negative, namely

$$\dot{V}(x, y) = V_x(x, y)\dot{x} + V_y(x, y)\dot{y} = g(x)(F(x) - y) + yg(x) = g(x)F(x) < 0,$$

for all $x \neq 0$. Then V is a global Lyapunov function for the origin and statement (a) follows, see for more details Theorem 4.2 of [47].

When $\alpha = 0$, the function $V(x, y)$ becomes degenerate along the segment of equilibrium. In fact, we see that

$$G(x) = \begin{cases} (x+1)^2, & \text{if } x < -1, \\ 0, & \text{if } -1 \leq x \leq 1, \\ (x-1)^2, & \text{if } x > 1. \end{cases}$$

Thus $\dot{V}(x, y) = 0$ in all the points of segment Σ. Nevertheless, we can apply the Invariance Principle of LaSalle, see Theorem 4.4 of [47], to obtain the assertion of statement (b).

Finally, the assertion on instability of the origin in the case $\alpha > 0$ follows directly from local linear analysis. ■

Now, we present an auxiliary result which is useful to justify the existence of periodic orbits. Although it is not strictly needed and its proof can be deduced from a similar result in [62], it is included as a beautiful alternative. In fact, since the matrix A has negative eigenvalues, we easily obtain the following result.

Lemma 3.5 *If* $\mathbf{x} = (x(t), y(t))$ *is a solution of system* (3.47) *then*

$$\mathbf{x}(t) = e^{At}\mathbf{x}(0) + \int_0^t e^{A(t-s)} b \,\mathrm{sat}(x(s)) ds. \tag{3.52}$$

As a consequence, the system is 'dissipative', in the sense that all the solutions forward in time are bounded.

Proof The equality (3.52) is standard, coming from the variation of constants formula. Now, as the eigenvalues of A are -1 and -2, there exists a constant L such that

$$\|e^{At}\| \leq Le^{-t}.$$

If we define another constant $K = \|b\|$ then $\|b\,\mathrm{sat}(x(t))\| \leq \|b\| = K$. Therefore from (3.52), we can write

$$\begin{aligned} \|\mathbf{x}(t)\| &\leq Le^{-t}(\|\mathbf{x}(0)\| + K\int_0^t e^s ds) = \\ &= Le^{-t}\left[\|\mathbf{x}(0)\| + K(e^t - 1)\right] = Le^{-t}(\|\mathbf{x}(0)\| - K) + LK, \end{aligned}$$

and the conclusion follows. ■

From (3.49) the origin is unstable for $\alpha > 0$ and by considering the boundedness of solutions coming from Lemma 3.5, we conclude that another attractive invariant set appears for such positive values of α. In fact, we know from Poincaré-Bendixson theorem that the ω-limit sets should be periodic orbits. The existence of periodic orbits is clearly guaranteed. To conclude the uniqueness of periodic orbits, we could apply the non-smooth version of Liénard's Theorem appearing in [74]. Clearly, it is more direct to resort to Theorem 3.2 for obtaining both existence and uniqueness of periodic orbits when $\alpha > 0$. The main result of this section is the following.

Theorem 3.5 *For the piecewise linear differential system* (3.47)*, the following statements hold.*

(a) *If* $\alpha < 0$ *then the origin is the only equilibrium point, in particular it is a stable node, being the global attractor for all the orbits of the system.*

(b) *For* $\alpha = 0$ *there exists a continuum of equilibrium points, namely all the points of the segment* $\Sigma = \{(x, y) \in \mathbb{R}^2 : -1 \leq x \leq 1, y = 0\}$*. This segment is the global attractor for the system. It is formed by unstable points, but the endpoints of the segment are the* ω*-limit set for* $\mathbb{R}^2 \setminus \Sigma$*.*

(c) *For $\alpha > 0$ the only equilibrium point is the origin, which is an unstable node. Furthermore there exists one periodic orbit which is a stable limit cycle, being symmetric with respect to the origin and the ω-limit set for all orbits except the origin.*

All the points of this limit cycle can be described in an algebraic way in terms of the parameter α. In particular, the limit cycle intersections $(1, y_0)$ and $(1, Y_0)$ with the line $x = 1$ can be algebraically determined as follows, see Figure 3.19. For each $\alpha > 0$ there exists only a value $v \in \left(\sqrt{2} - 1, 1\right)$ such that

$$\alpha = \alpha(v) = \frac{(1 + 2v - v^2)(v^2 + 2v - 1)}{(1 - v)^2(1 + 4v + v^2)}, \tag{3.53}$$

and

$$y_0 = -\frac{\alpha(1 - v + 2v^2)}{v(1 - v)}, \quad Y_0 = \frac{\alpha(2 - v + v^2)}{1 - v}. \tag{3.54}$$

Furthermore, the period of the limit cycle is

$$P = -2 \log \left(\frac{v^2 + 2v - 1}{1 + 2v - v^2} v^{\frac{\alpha+1}{\alpha}} \right), \tag{3.55}$$

and its characteristic multiplier ν satisfies

$$\nu = \left(\frac{v^2 + 2v - 1}{1 + 2v - v^2} \right)^6 < 1,$$

for all $v \in \left(\sqrt{2} - 1, 1\right)$.

Proof Statement (a) and the first part of statement (b) come from Lemma 3.4. The instability of the points belonging to the segment Σ is due to the horizontal flow, both from above and from below such segment. Thus, in any neighborhood of each equilibrium point there are points with $y > 0$, whose orbits go to the left tending to the point $(-1, 0)$, and points with $y < 0$, whose orbits go to the right tending to the point $(1, 0)$. These two endpoints are nodes from the outside (for $x < -1$ and $x > 1$, respectively) and have their stable linear invariant manifolds, which are half straight lines that eventually capture all the orbits.

The rest of the proof is devoted to show statement (c). Since the existence and uniqueness of the limit cycle is assured by Theorem 3.2, we describe now

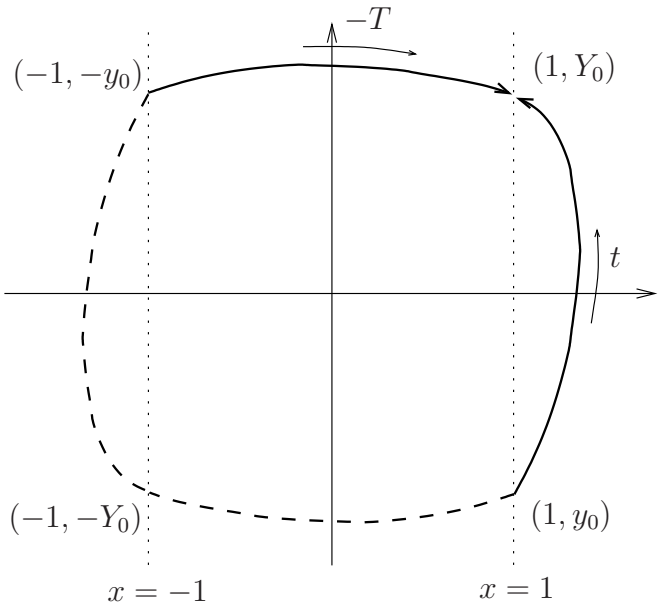

Figure 3.18: Sketch of the process to determine the periodic orbit, showing the intersection points with the lines $x = 1$ and $x = -1$.

in detail how to determine completely and algebraically the limit cycle in terms of the parameter α, using the closing equations method reviewed in Chapter 2. In fact, the computations that follow also lead to the existence and uniqueness of periodic orbits.

See Figure 3.18 for a geometrical sketch of the next computations. The solution $(x(t), y(t))$ of system (3.47) in the region $S_+ \cup \Sigma_1$ starting at the point $(1, y_0)$ when $t = 0$ is

$$\begin{pmatrix} x(t) \\ y(t) \end{pmatrix} = \begin{pmatrix} 1-\alpha^2 \\ 3\alpha(1+\alpha) \end{pmatrix} + e^{At}\left[\begin{pmatrix} 1 \\ y_0 \end{pmatrix} - \begin{pmatrix} 1-\alpha^2 \\ 3\alpha(1+\alpha) \end{pmatrix}\right], \qquad (3.56)$$

where

$$e^{At} = \begin{pmatrix} 2e^{-2t}-e^{-t} & e^{-2t}-e^{-t} \\ 2(e^{-t}-e^{-2t}) & 2e^{-t}-e^{-2t} \end{pmatrix} = u\begin{pmatrix} 2u-1 & u-1 \\ 2(1-u) & 2-u \end{pmatrix},$$

after introducing the auxiliary variable $u = e^{-t}$. Then (3.56) becomes

$$\begin{pmatrix} x(t) \\ y(t) \end{pmatrix} = \begin{pmatrix} 1-\alpha^2 \\ 3\alpha(1+\alpha) \end{pmatrix} + u \begin{pmatrix} 2u-1 & u-1 \\ 2(1-u) & 2-u \end{pmatrix} \begin{pmatrix} \alpha^2 \\ y_0 - 3\alpha(1+\alpha) \end{pmatrix}. \tag{3.57}$$

Of course, for all values of $t > 0$ we will have $0 < u < 1$.

Regarding the solution $(X(T), Y(T))$ of the system (3.47) in the region $\Sigma_{-1} \cup S_0 \cup \Sigma_1$ starting at the point $(1, Y_0)$ when $T = 0$, it satisfies

$$\begin{pmatrix} X(T) \\ Y(T) \end{pmatrix} = e^{BT} \begin{pmatrix} 1 \\ Y_0 \end{pmatrix}.$$

The way for computing the symmetric periodic orbits of system (3.47) by having two points in the line Σ_1 is as follows, see Figure 3.18. Assuming that there exists one of these periodic orbits, let $(1, y_0) \in \Sigma_1$ be the point where this periodic orbit enters into the zone $S_+ \cup \Sigma_1$ and let $(1, Y_0) \in \Sigma_1$ be the point where this periodic orbit exits such zone to enter S_0. Since this periodic orbit is symmetric it will enter into the zone $S_- \cup \Sigma_{-1}$ through the point $(-1, -y_0) \in \Sigma_{-1}$. Let t be the elapsed time for this periodic orbit going from the point $(1, y_0)$ to the point $(1, Y_0)$, and let T be the time needed for this periodic orbit to go from the point $(1, Y_0)$ to the point $(-1, -y_0)$. Then we have the *closing equations*

$$\begin{pmatrix} x(t) \\ y(t) \end{pmatrix} = \begin{pmatrix} 1 \\ Y_0 \end{pmatrix}, \quad \begin{pmatrix} X(T) \\ Y(T) \end{pmatrix} = \begin{pmatrix} -1 \\ -y_0 \end{pmatrix}. \tag{3.58}$$

Equivalently, see again Figure 3.18, we can integrate backwards in time the solution from $(-1, -y_0)$ to $(1, Y_0)$ within S_0, by defining $(\bar{X}(T), \bar{Y}(T))^T = e^{-BT}(-1, -y_0)^T$. Then the exponential e^{-BT} is the matrix

$$e^{-BT} = \begin{pmatrix} 2e^{-2\alpha T} - e^{-\alpha T} & \frac{1}{\alpha}(e^{-2\alpha T} - e^{-\alpha T}) \\ 2\alpha(e^{-\alpha T} - e^{-2\alpha T}) & 2e^{-\alpha T} - e^{-2\alpha T} \end{pmatrix}.$$

Again, if we introduce the auxiliary variable $v = e^{-\alpha T}$ then we can write the above matrix exponential as a polynomial matrix, namely

$$\begin{pmatrix} \bar{X}(t) \\ \bar{Y}(t) \end{pmatrix} = e^{-BT} \begin{pmatrix} -1 \\ -y_0 \end{pmatrix} = \begin{pmatrix} 2v^2 - v & \frac{1}{\alpha}(v^2 - v) \\ 2\alpha(v - v^2) & 2v - v^2 \end{pmatrix} \begin{pmatrix} -1 \\ -y_0 \end{pmatrix}. \tag{3.59}$$

Then we must now have $(\bar{X}(T), \bar{Y}(T)) = (1, Y_0)$. Note that for $\alpha > 0$, we have $0 < v < 1$.

If we take $Y_0 = y(t)$, then the three unknowns (y_0, t, T) associated to this symmetric periodic orbit must satisfy the three equations

$$\begin{aligned} x(t) - 1 &= 0, \\ 1 - \bar{X}(T) &= 0, \\ y(t) - \bar{Y}(T) &= 0. \end{aligned}$$

It should be noticed how the use of variables $u = e^{-t}$ and $v = e^{-\alpha T}$ instead of t and T allows to write algebraic equations for the determination of periodic orbits. Effectively, from (3.57) and (3.59), and taking $\tilde{y}_0 = y_0 - 3\alpha$ to simplify the equations a bit, we obtain three conditions $\mathrm{eq}_i = 0$, $i = 1, 2, 3$, where

$$\begin{aligned} \mathrm{eq}_1 &= (1-u)^2\alpha^2 + u(1-u)\tilde{y}_0, \\ \mathrm{eq}_2 &= (1+2v-v^2)\alpha + (1-v)v\tilde{y}_0, \\ \mathrm{eq}_3 &= (3-4u+u^2)\alpha^2 + (3+4v-v^2)\alpha + (2u-u^2+2v-v^2)\tilde{y}_0. \end{aligned} \tag{3.60}$$

Since $\dot{x} = 3\alpha - y$ when $x = 1$, we must have $3\alpha - y_0 > 0$ or, equivalently, $\tilde{y}_0 = y_0 - 3\alpha < 0$. Note that to every symmetric periodic orbit having two points in the line Σ_1, we can associate one solution $(\tilde{y}_0, u, v)$ of equations (3.60) with $\tilde{y}_0 < 0$, $0 < u < 1$ and $0 < v < 1$. Reciprocally, it is clear that any solution satisfying these inequalities will correspond to a symmetric periodic orbit.

We can eliminate the factor $(1-u)$ in the expression of eq_1, so that we can solve the first two resulting equations and write

$$\tilde{y}_0 = -\frac{1-u}{u}\alpha^2 = -\frac{1+2v-v^2}{v(1-v)}\alpha.$$

This expression will have sense only if $\tilde{y}_0 < 0$. Then we must have $1+2v-v^2 > 0$, which is true for all $0 < v < 1$.

Finally, using the third equation we obtain the v-parametrizations

$$u = v\frac{v^2+2v-1}{1+2v-v^2}, \qquad \alpha = \frac{(1+2v-v^2)(v^2+2v-1)}{(1-v)^2(1+4v+v^2)}, \tag{3.61}$$

$$\tilde{y}_0 = -\frac{(1+2v-v^2)^2(v^2+2v-1)}{v(1-v)^3(1+4v+v^2)},$$

and note that $v^2+2v-1>0$ for positive values of v requires $v>\sqrt{2}-1$. Thus, the range of admissible values of v is shorter than expected. It is not difficult to show that the expression in (3.61) for α defines an invertible function of v in the interval $\left(\sqrt{2}-1,1\right)$ by computing its derivative. We omit these standard computations.

Retrieving y_0 by writing $y_0=\tilde{y}_0+3\alpha$, we obtain the expression given in (3.54). From the second coordinate of equality (3.59), we can also derive the expression for Y_0 by computing

$$Y_0=\bar{Y}(T)=2\alpha v(1-v)+y_0v(2-v)=\frac{[4v^2-(1-v^2)^2](2-v+v^2)}{(1-v)^3(1+4v+v^2)},$$

and so we have shown (3.53) and (3.54).

Furthermore, the period of limit cycle is given by

$$P=-2\log u-\frac{2}{\alpha}\log v,$$

which after substituting the expression for u in (3.61) leads to (3.55).

To study the stability of the limit cycle we will use a Poincaré map. Selecting as a transversal section the straight line Σ_1 and assuming that the periodic orbit passes though the point $(1,y_0)$, we can assure that there exists a neighborhood E in Σ_1 of the value y_0 so that for $(1,y)$ with $y\in E$, we can define the Poincaré return map Π, that relates the initial point $(1,y)$ with the return point of the orbit to Σ_1 after a complete turn around the origin, namely $(1,\Pi(y))$.

By the continuous dependence of solutions, it is clear that we can ensure $\Pi(y)\in E$ and $\Pi(y_0)=y_0$, i.e., Π has a fixed point corresponding to the periodic orbit. If this fixed point is attractive for Π, then the periodic orbit is stable. This condition is fulfilled if the characteristic multiplier ν satisfies

$$0<\nu=\frac{d\Pi}{dy}(y_0)<1.$$

Therefore, we need to calculate the value of ν. By the Implicit Function Theorem, using the vector field with $x>1$ we can affirm that for $y\neq 3\alpha$ there exist two functions $t(y)$ and $Y(y)$ such that

$$e^{At(y)}\left[\begin{pmatrix}1\\ y\end{pmatrix}-\begin{pmatrix}1-\alpha^2\\ 3\alpha(1+\alpha)\end{pmatrix}\right]=\begin{pmatrix}1\\ Y(y)\end{pmatrix}-\begin{pmatrix}1-\alpha^2\\ 3\alpha(1+\alpha)\end{pmatrix},$$

for all $y \in E$. In the same way, if starting from the point $(1, Y)$ we arrive following the orbit in the zone with $|x| < 1$ to the point $(-1, \tilde{Y})$, then two function $T(Y)$ and $h(Y)$ exist so that for a neighborhood E' of $Y_0 = Y(y_0)$ we can write

$$e^{BT(Y)} \begin{pmatrix} 1 \\ Y \end{pmatrix} = \begin{pmatrix} -1 \\ h(Y) \end{pmatrix},$$

where $\widetilde{Y} = h(Y)$. As the vector field is symmetrical, it is clear that in a complete return, we have $\Pi(y) = [-h \circ Y] \circ [-h \circ Y] = -h(Y(-h(Y(y))))$, and so, by using the chain rule and that $h \circ Y(y_0) = -y_0$, we assure that the characteristic multiplier ν satisfies

$$\nu = \frac{d\Pi}{dy}(y_0) = \left[\frac{d}{dy}(h \circ Y)(y_0)\right]^2. \tag{3.62}$$

Applying now Lemma 2.12, we conclude that the product of exponential matrices

$$e^{At(y_0)} e^{BT(Y_0)}$$

is similar to the matrix

$$\begin{pmatrix} -1 & \dfrac{dt}{dy} + \dfrac{dT}{dY}\dfrac{dY}{dy} \\ 0 & \dfrac{d}{dy}(h \circ Y)(y_0) \end{pmatrix}.$$

Thus, t is now direct to characterize the stability of the limit cycle. Effectively, as a consequence, we have

$$\frac{d}{dy}(h \circ Y)(y_0) = -\det\left[e^{At(y_0)} e^{BT(Y_0)}\right] = -\frac{u^3}{v^3}. \tag{3.63}$$

It is easy to see from (3.61) that

$$\frac{u}{v} = \frac{(v+1)^2 - 2}{(v+1)^2 - 2v^2} < 1.$$

From (3.62) and (3.63) we can assure that the characteristic multiplier ν of the periodic orbit is the one shown in the final statement of Theorem 3.5. The proof is complete. ■

Theorem 3.5 can be applied to predict accurately the oscillations of real nonlinear devices, see Section 3.2.3. It also shows a dramatic change in the qualitative behavior of system (3.47) when we vary the parameter α, passing through the critical value $\alpha = 0$. In fact, for $\alpha > 0$ we deduce that the limit cycle is born with infinite period from the segment of equilibrium points, see Fig. 3.19.

Although we have the exact value of the period, it can be useful to note that from $0 < \alpha \ll 1$ we can give an asymptotic estimate for it. Effectively, from (3.61) we have

$$\lim_{\alpha\to 0} \frac{u}{\alpha} = \lim_{v\to\sqrt{2}-1} \frac{u(v)}{\alpha(v)} = \lim_{v\to\sqrt{2}-1} \frac{v(1-v)^2(1+4v+v^2)}{(1+2v-v^2)^2} = \frac{2-\sqrt{2}}{4}.$$

Then, for $0 < \alpha \ll 1$ we have

$$e^{-t} = u \approx \frac{2-\sqrt{2}}{4}\alpha,$$

so that,

$$t \approx -\log\left(\frac{2-\sqrt{2}}{4}\alpha\right) = \log\frac{2\left(2+\sqrt{2}\right)}{\alpha}.$$

On the other hand, $\lim_{\alpha\to 0} v = \sqrt{2}-1$, so for $\alpha > 0$ small we can write

$$T = -\frac{1}{\alpha}\log v = \log v^{(-1/\alpha)} \approx \log\left(\frac{1}{\sqrt{2}-1}\right)^{1/\alpha}.$$

Thus,

$$P = 2(t+T) \approx 2\log\frac{2\left(2+\sqrt{2}\right)}{\alpha\left(\sqrt{2}-1\right)^{1/\alpha}},$$

and after some standard manipulations, we arrive at

$$P \approx 2\log\frac{\left(4+2\sqrt{2}\right)\left(1+\sqrt{2}\right)^{1/\alpha}}{\alpha}. \tag{3.64}$$

This asymptotic expression avoids to invert $\alpha(v)$ in computing the value of v to get the period for small values of α.

The bifurcation leading to the appearance of stable periodic orbits in Theorem 3.5 is very different from the standard bifurcations giving rise to

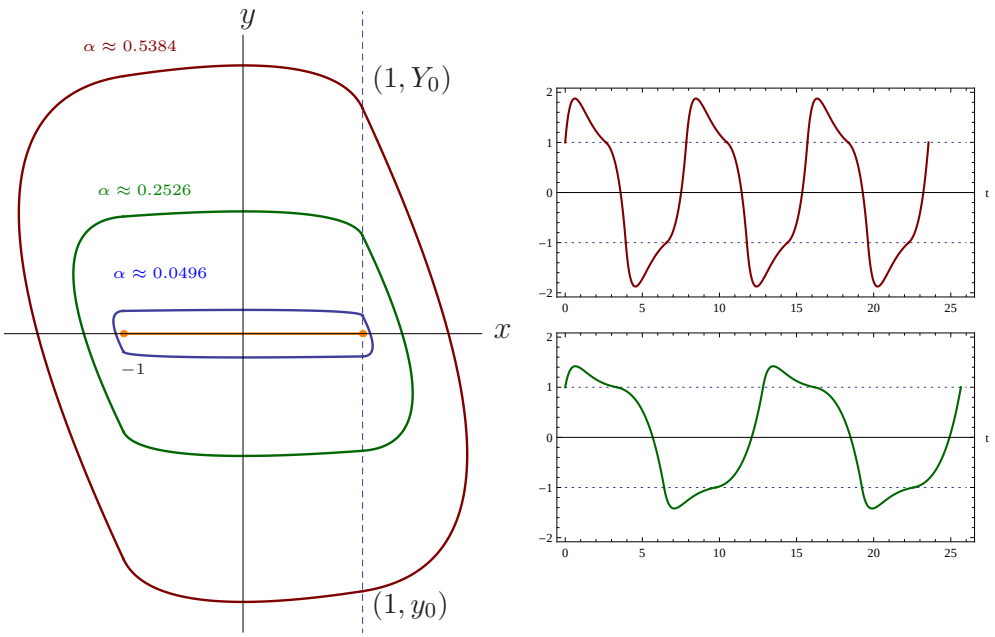

Figure 3.19: The segment of equilibrium points for $\alpha = 0$ and the limit cycle for several values of $\alpha > 0$ (left). The waveforms for $x(t)$ when $\alpha \approx 0.2526$ ($v = 0.46$, two cycles), and $\alpha \approx 0.5384$ ($v = 0.5$, three cycles) (right).

oscillations in smooth differential systems. For instance, in the case of supercritical Hopf bifurcations, one has that a stable focus becomes an unstable focus surrounded by a stable limit cycle. In the case of Theorem 3.5, however, the stable limit cycle that appear for $\alpha > 0$ always surrounds an unstable node. Thus, Theorem 3.5 describes completely, for the first time up to the best of our knowledge, a planar non-smooth bifurcation leading to a limit cycle without involving equilibria of focus type.

3.2.3 Application to a PWL Van der Pol oscillator

In this section, we show that system (3.47) is realized in a family of electronic circuits after certain adequate choice of parameters. We consider the electronic circuit proposed in [44], to simulate the FitzHugh-Nagumo equations, introduced as a simplification of the Hodgkin-Huxley model describing the neuronal electrical activity, see [38, 70]. More precisely, we will deal with the circuit shown in Figure 3.20, which is the symmetrical case of the circuit introduced by Keener, and was analyzed in [25]. In the quoted paper, it is

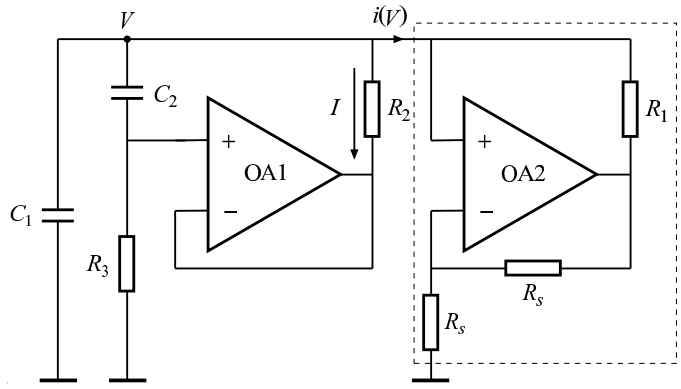

Figure 3.20: Circuit realization of a Van der Pol electronic oscillator, completely analyzed in [25].

also shown that the model is a piecewise linear version of the classical Van der Pol oscillator. The dynamical equations of the circuit are

$$\begin{aligned} C_1 R_3 \frac{dV}{dt} &= -V - (R_3 - R_2)\, I - i(V) R_3, \\ C_2 R_2 R_3 \frac{dI}{dt} &= V - R_2 I, \end{aligned} \tag{3.65}$$

where R_1, R_2, R_3, C_1 and C_2 stand for the resistors and capacitors values for the circuit. The current-voltage characteristics $i(V)$ of the biased operational amplifier OA2 is described very accurately by the piecewise linear function

$$i(V) = \frac{V}{R_1} - \frac{V_s}{R_1} \operatorname{sat}\left(\frac{2V}{V_s}\right),$$

where V_s is the saturation voltage of the operational amplifier, see Figure 3.21.

Doing in (3.65) the change of variables

$$\hat{x} = \frac{2}{V_s} V, \quad \hat{y} = \frac{2R_3}{V_s} I,$$

we obtain the system

$$\begin{aligned} C_1 R_3 \frac{d\hat{x}}{dt} &= -\left(1 + \frac{R_3}{R_1}\right) \hat{x} + \frac{R_2 - R_3}{R_3} \hat{y} + \frac{2R_3}{R_1} \operatorname{sat} \hat{x}, \\ C_2 R_2 \frac{d\hat{y}}{dt} &= \hat{x} - \frac{R_2}{R_3} \hat{y}, \end{aligned}$$

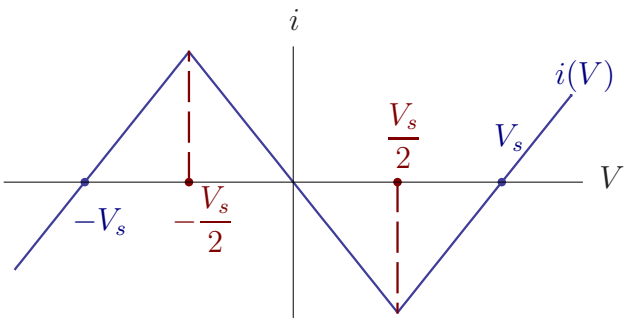

Figure 3.21: The current-voltage characteristics $i(V)$ of the biased OA2 is described accurately by a piecewise linear function.

and introducing the dimensionless time and parameters

$$\hat{t} = \frac{t}{C_1 R_3},\ \rho = \frac{C_1}{C_2},\ r_1 = \frac{R_3}{R_1},\ r_2 = \frac{R_3}{R_2}$$

we finally obtain the differential equations

$$\begin{aligned} \frac{d\hat{x}}{d\hat{t}} &= -(1+r_1)\,\hat{x} + \left(\frac{1}{r_2} - 1\right)\hat{y} + 2r_1\,\mathrm{sat}(\hat{x}), \\ \frac{d\hat{y}}{d\hat{t}} &= \rho\, r_2\,\hat{x} - \rho\,\hat{y}. \end{aligned} \tag{3.66}$$

System (3.66) is in the canonical form (3.44) with $\varphi(\sigma) = \mathrm{sat}(\sigma)$, that is $m_a = 0$, $m_b = 1$, $\delta = 1$, and

$$A = \begin{pmatrix} -1 - r_1 & \dfrac{1}{r_2} - 1 \\ \rho r_2 & -\rho \end{pmatrix}, \quad \mathbf{b} = \begin{pmatrix} 2r_1 \\ 0 \end{pmatrix}, \quad \mathbf{c}^T = (1, 0).$$

The observability condition becomes $r_2 \neq 1$, to be assumed in the sequel. In order to apply Proposition 3.11, we must also check the assumption on the spectra of matrices A and $B = A + \mathbf{b}\mathbf{c}^T$. Thus, in terms of the traces and determinants, we must have

$$\begin{aligned} -r_1 - \rho - 1 &= -3\mu, \\ \rho\,(r_1 + r_2) &= 2\mu^2, \\ r_1 - \rho - 1 &= 3\eta = 3\alpha\mu, \\ \rho\,(r_2 - r_1) &= 2\eta^2 = 2\alpha^2\mu^2, \end{aligned} \tag{3.67}$$

where we have substituted $\eta = \alpha\mu$. Solving (3.67) for r_1, r_2, ρ and μ, we obtain that whenever

$$r_1 = \frac{9}{5}\frac{\alpha+1}{1-\alpha},\ r_2 = \frac{9}{5}\frac{\alpha^2+1}{(1-\alpha)^2},\ \rho = \frac{4}{5},\ \mu = \frac{6}{5}\frac{1}{1-\alpha}, \tag{3.68}$$

and provided that $r_2 \neq 1$, i.e. $\alpha \notin \{-2, -\frac{1}{2}\}$, all the hypothesis of Proposition 3.11 are fulfilled. Of course, since r_1 and r_2 represent ratios of resistors, they must have positive values, what also requires $\alpha \in (-1, 1)$.

As explained in the proof of Proposition 3.11, with a new change of variables given by $(\tilde{x}, \tilde{y})^T = M(\hat{x}, \hat{y})^T$, where the matrix M satisfies

$$M = \begin{pmatrix} 1 & 0 \\ \dfrac{\rho r_2}{r_2 - 1} & \dfrac{r_2}{r_2 - 1} \end{pmatrix},$$

we can put the system in the form (3.48), provided that all the matrix entries satisfy (3.68). Finally, using a new time given by $\tau = \mu\hat{t}$ and the rescaling of variables $(x, \mu y) = (\tilde{x}, \tilde{y})$, we arrive at the system (3.47).

Summarising, if the adimensional parameters fulfill (3.68) and we select new time and variables given by

$$\tau = \frac{\mu t}{C_1 R_3},\quad x = \frac{2V}{V_s},\quad y = \frac{r_2}{\mu(r_2 - 1)}\left(\frac{8V}{5V_s} + \frac{2R_3 I}{V_s}\right),$$

then we pass for all $\alpha \in (-1, -\frac{1}{2}) \cup (-\frac{1}{2}, 1)$ from system (3.65) to system (3.47), according to Proposition 3.11. Note that to each dimensionless representative of the set of parameters r_1, r_2, ρ and μ satisfying (3.68) corresponds an infinite number of physical values for the circuit. Therefore, for such physical values the dynamics of the circuit and in particular the oscillations that appear for $0 < \alpha < 1$ are algebraically determined by Theorem 3.5.

3.3 A limit cycle bifurcation in 2DPWL$_2$ systems

In this section we enter for the only time within this thesis in the discontinuous world. The analysis of discontinuous piecewise-linear systems is an emergent field of research since most of modern devices are well-modelled by this class of systems, see [18]. Recently, in [30] it has been proposed a

canonical form for the case of planar discontinuous systems with two zones of linearity. In the quoted paper, there are shown some bifurcation results for the case when both linear dynamics are of focus type without visible tangencies, that is, there are no real equilibrium points in the interior of each half-plane.

Here, by resorting to the canonical form given in [30], we consider a different situation when we have an equilibrium point of focus type in the interior of a halfplane without fixing the dynamics in the other halfplane. Our target is to describe qualitatively and quantitatively the possible bifurcation of limit cycles through the change of stability of such an equilibrium point.

A similar bifurcation was studied in [26] for the continuous case, so that this work is a relevant generalization not only to the discontinuous case but also by including all the different generic cases in the complementary dynamics to the focus zone, that is, both saddle and anti-saddle cases.

To begin with, we assume without loss of generality that the linearity regions in the phase plane are the left and right half-planes,

$$S^- = \{(x, y) : x < 0\}, \quad S^+ = \{(x, y) : x > 0\},$$

separated by the straight line $\Sigma = \{(x, y) : x = 0\}$. The systems to be studied become

$$\dot{\mathbf{x}} = \mathbf{F}(\mathbf{x}) = \begin{cases} \mathbf{F}^+(\mathbf{x}) = \left(F_1^+(\mathbf{x}), F_2^+(\mathbf{x})\right)^T = A^+\mathbf{x} + \mathbf{b}^+, & \text{if } x \in S^+, \\ \mathbf{F}^-(\mathbf{x}) = \left(F_1^-(\mathbf{x}), F_2^-(\mathbf{x})\right)^T = A^-\mathbf{x} + \mathbf{b}^-, & \text{if } x \in S^- \cup \Sigma, \end{cases} \tag{3.69}$$

where $\mathbf{x} = (x, y)^T \in \mathbb{R}^2$, $A^+ = (a_{ij}^+)$ and $A^- = (a_{ij}^-)$ are 2×2 constant matrices and $\mathbf{b}^+ = (b_1^+, b_2^+)^T$, $\mathbf{b}^- = (b_1^-, b_2^-)^T$ are constant vectors of $\mathbb{R}^2$.

Under the generic condition $a_{12}^+ a_{12}^- > 0$, which means that orbits can cross the discontinuity line in opposite directions allowing the existence of period orbits, by using Proposition 3.1 of [30] the following canonical form is obtained

$$\begin{aligned} \dot{\mathbf{x}} &= \begin{pmatrix} T_- & -1 \\ D_- & 0 \end{pmatrix} \mathbf{x} - \begin{pmatrix} 0 \\ a_- \end{pmatrix} \text{ if } \mathbf{x} \in S^-, \\ \dot{\mathbf{x}} &= \begin{pmatrix} T_+ & -1 \\ D_+ & 0 \end{pmatrix} \mathbf{x} - \begin{pmatrix} -b \\ a_+ \end{pmatrix} \text{ if } \mathbf{x} \in S^+, \end{aligned} \tag{3.70}$$

where

$$a_- = a_{12}^- b_2^- - a_{22}^- b_1^-, \quad b = \frac{a_{12}^-}{a_{12}^+} b_1^+ - b_1^-, \quad a_+ = \frac{a_{12}^-}{a_{12}^+}(a_{12}^+ b_2^+ - a_{22}^+ b_1^+),$$

and $T_\pm = \mathrm{tr}(A^\pm)$, $D_\pm = \det(A^\pm)$ are the linear invariants of each zone.

The canonical form (3.70) has seven parameters; apart from the mentioned linear invariants, we find two parameter a_+ related to the position of equilibria and a parameter b which is responsible for the existence of a sliding set. In fact, there exists a sliding set which is a segment joining the origin and the point $(0, b)$, see [30] for more details. These two endpoints are tangency points, the origin for the left region and the point $(0, b)$ for the right one. Furthermore, the sliding set becomes attractive for $b < 0$ and repulsive for $b > 0$, shrinking to the origin when $b = 0$. By computing the sign of $\ddot{x}$ at the tangency points, we obtain

$$\ddot{x}|_{(x,y)=(0,0)} = a_-, \qquad \ddot{x}|_{(x,y)=(0,b)} = a_+,$$

so that the left (right) tangency is called visible for $a_- < 0$ ($a_+ > 0$), being invisible for $a_- > 0$ ($a_+ < 0$), see [30]. Thus the $a_\pm$ parameters are related to the visibility of the tangencies, and when they vanish we have boundary equilibrium points, see [53] and also [72].

Note that the possible equilibria (real or virtual) are located at the points $(a_-/D_-, a_-T_-/D_-)$ and $(a_+/D_+, b + (a_+T_+/D_+))$ where it is assumed $D_+D_- \neq 0$. Without of loss of generality, we assume that there exists an equilibrium of focus type in the left zone, that is

$$\frac{a_-}{D_-} < 0, \qquad T_-^2 - 4D_- < 0,$$

and this last inequality implies that $D_- > 0$ and so $a_- < 0$.

Our interest is to study what happens when the trace T_- passes through the critical value zero, that is when the focus passes from stable to unstable or viceversa. Note that for $T_- = 0$ we have a center configuration in the left half-plane which terminates in a visible tangency at the origin. To avoid other non-local phenomena it is then natural to impose that in the right zone we have also a tangency at the origin of invisible character, which amounts to require $b = 0$. In fact, we allow to move this parameter b in a neighborhood of zero, then we should have the possibility of new bifurcations, namely the collision of tangencies, which has been reported in [53]. Thus, our study can

be seen as a first step in the analysis of the codimension-two bifurcation that appears when the parameter b is allowed to be moved. Such codimension-two bifurcation should be the aim of future work, since it turns out to be a situation not well explained in the analysis done in [35].

Thus, we will not have a proper sliding set nor jumps in the right dynamics with respect to the critical center. Under these assumptions our first result is the following.

Proposition 3.12 *Under the hypotheses $T_-^2 - 4D_- < 0$, $a_- < 0$ (left focus dynamics with visible tangency at the origin) and assuming that in the right zone we have an invisible tangency at the origin ($b = 0$, $a_+ < 0$), system (3.70) is topologically equivalent to the system*

$$\begin{cases} \dot{x} = Tx - y \\ \dot{y} = Dx + a, \end{cases} \qquad \text{if } x > 0$$

$$\begin{cases} \dot{x} = 2\gamma x - y \\ \dot{y} = (1+\gamma^2)(x+1), \end{cases} \qquad \text{if } x \leq 0 \tag{3.71}$$

where $T = T_+$, $D = D_+$, $\alpha = \dfrac{T_-}{2}$, $\gamma = \dfrac{\alpha}{\omega}$, $\alpha = \dfrac{T_-}{2}$, and $\omega > 0$ is such that

$$\omega^2 = D_- - \frac{(T_-)^2}{4}, \quad \text{and } a = \frac{D_-}{\omega}\frac{a_+}{a_-} > 0.$$

Proof Clearly, the assumption on right tangency at the origin, that is $(T_+x - y + b) \mid_{(x,y)=(0,0)} = 0$ reduces to $b = 0$. Now the tangency will be invisible for $a_+ < 0$.

Under the hypotheses, if we define $\omega > 0$ such that $\omega^2 = D_- - (T_-^2/4)$ and $\alpha = T_-/2$, the eigenvalues of the linear part at S^- in (3.70) are $\alpha \pm i\omega$. We make first the change $X = \omega x$, $Y = y$, $\tau = \omega t$ for the variables in the half plane S^-, without altering variables and time in S^+. Note that we do not change the coordinate y, so that periodic orbits using both half planes are preserved. Then,

$$\begin{aligned} \frac{dX}{d\tau} &= \frac{1}{\omega}\frac{dX}{dt} = \frac{dx}{dt} = \frac{X}{\omega}T_- - Y, \\ \frac{dY}{d\tau} &= \frac{1}{\omega}\frac{dY}{dt} = \frac{1}{\omega}\frac{dy}{dt} = \frac{1}{\omega}\left(D_-\frac{X}{\omega} - a_-\right) = \frac{D_-}{\omega^2}X - \frac{a_-}{\omega}. \end{aligned}$$

Introducing the parameter $\gamma = \dfrac{\alpha}{\omega}$, we see that $\dfrac{T_-}{\omega} = 2\gamma$ and $\dfrac{D_-}{\omega^2} = \gamma^2 + 1$. Making a homothety of factor k to the whole plane and removing the factor k in the equations, we have for $x < 0$,

$$\begin{aligned} \frac{dx}{d\tau} &= k\frac{dX}{d\tau} = k\left(2\gamma\frac{x}{k} - \frac{y}{k}\right) = 2\gamma x - y, \\ \frac{dy}{d\tau} &= k\frac{dY}{d\tau} = k\left((\gamma^2+1)\frac{x}{k} - \frac{a_-}{\omega}\right) = (\gamma^2+1)x - k\frac{a_-}{\omega}. \end{aligned}$$

While for $x > 0$,

$$\begin{aligned} \dot{x} &= Tx - y, \\ \dot{y} &= Dx - ka_+. \end{aligned}$$

By imposing that $-k\dfrac{a_-}{\omega} = \gamma^2 + 1$, we get

$$k = -\frac{\gamma^2+1}{a_-}\omega > 0,$$

and the expressions given in the statement. ■

With this result, we manage to describe the left dynamics with only one parameter, needing other three parameters to deal with the right region. The following remark should be taken into account.

Remark 3.6 *System* (3.71) *generically represents a discontinuous vector field since for* $x = 0$ *we will have* $a \neq 1 + \gamma^2$. *The original system* (3.70) *is continuous only in the case* $a_+ = a_-$ *and* $b = 0$, *but even in such non-generic case, the new system provided by Proposition 3.12 will be discontinuous. Thus, the analysis of system* (3.71) *is useful also for some continuous cases that could be studied by other specific methods in a continuous vector field context. This fact will be illustrated later in Section 3.3.1.*

Regarding equilibrium points, in the zone with $x < 0$, there exists a focus at $(\bar{x}, \bar{y})^T = (-1, -2\gamma)^T$, to be stable for $\gamma < 0$ and unstable for $\gamma > 0$. When $\gamma = 0$, we have a linear center. In the zone with $x > 0$ since $a > 0$ there are no equilibrium points if $D = 0$, while the possible equilibrium point for $D \neq 0$ is located at $(-a/D, -aT/D)^T$.

We take γ in (3.71) as the bifurcation parameter, having its critical value at $\gamma = 0$, where the center configuration takes place, see Figure 3.22.

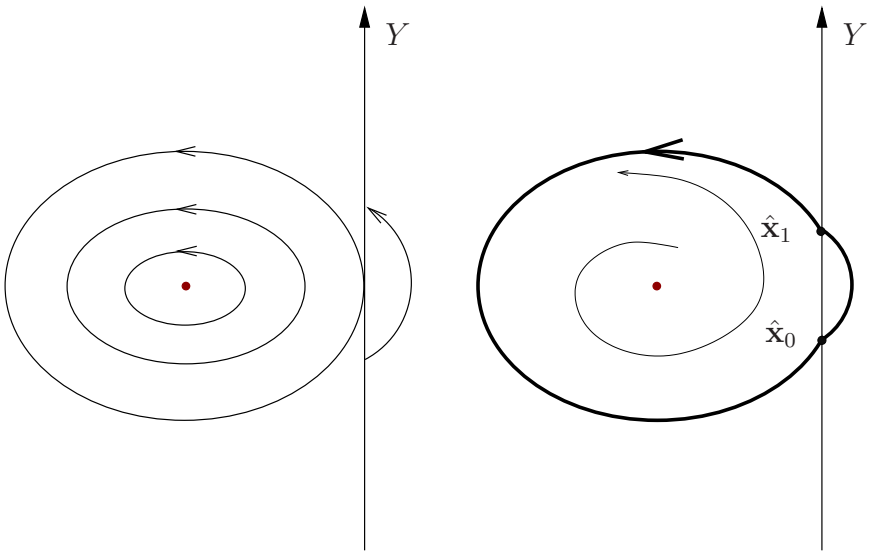

Figure 3.22: (Left) The critical situation for $\gamma = 0$. (Right) The bifurcating limit cycle for $\gamma T < 0$ and $|\gamma|$ small.

Before entering in the main results, we need first some technical results. The first one is a rather general result on local derivatives of half-return maps. Dealing with a discontinuous vector field, we cannot resort to Proposition 2.12 to determine the stability character of periodic orbits using the two zones. We acknowledge E. Freire and F. Torres for their permission to reproduce it, since it appears in [31], not yet published. At the end of the day, we will realize that the conclusion of Proposition 2.12 is still true, due to the fact that our discontinuity is not severe, affecting only to the second component of the vector field. Anyway, such possibility cannot a priori be considered without an additional justification.

Lemma 3.6 *Let us consider system* (3.69). *Assume that the orbit of vector field* F^+ *starting from an initial point* $\hat{\mathbf{x}}_0 = (0, \hat{y}_0)$ *lies in* S^+ *and eventually comes back to the discontinuity line, arriving transversally at the point* $\hat{\mathbf{x}}_1 = (0, \hat{y}_1)$ *which is its common point with the line* $x = 0$, *that is* $F_1^+(\hat{\mathbf{x}}_1) < 0$. *If we denote as* $\hat{\delta}^+(t) = (x(t, \hat{\mathbf{x}}_0), y(t, \hat{\mathbf{x}}_0))$ *the solution of* $\dot{\mathbf{x}} = F^+(x)$ *satisfying* $\hat{\delta}^+(0) = \hat{\mathbf{x}}_0$, *then a value* $\tau^+ > 0$ *exists such that* $x(t, \hat{\mathbf{x}}_0) > 0$ *for* $0 < t < \tau^+$ *and* $x(\tau^+, \hat{\mathbf{x}}_0) = 0$, $y(\tau^+, \hat{\mathbf{x}}_0) = \hat{y}_1$. *Then we can define a right Poincaré map* P_R *in a neighborhood of the point* $\hat{\mathbf{x}}_0$ *such that* $P_R(\hat{y}_0) = \hat{y}_1$ *and the first*

derivative of map P_R at $\hat{y}_0$ is given by

$$P_R'(\hat{y}_0) = \frac{F_1^+(\hat{\mathbf{x}}_0)}{F_1^+(\hat{\mathbf{x}}_1)} \exp\left(\int_0^{\tau^+} \operatorname{div}\left(F^+\right)\right).$$

Proof Let us consider the differential system $\dot{\mathbf{x}} = F^+(\mathbf{x})$ defined in $\mathbb{R}^2$, and let us denote as $\gamma^+(t) = (x(t, \mathbf{x}_0), y(t, \mathbf{x}_0))$, the solution satisfying $\gamma^+(0) = \mathbf{x}_0$ where $\mathbf{x}_0 = (x_0, y_0)$. Then we introduce the system of equations $\mathbf{Z}(t, \mathbf{x}_0, y_1) = \mathbf{0}$, where

$$\mathbf{Z}(t, \mathbf{x}_0, y_1) = \begin{pmatrix} x(t, \mathbf{x}_0) \\ y(t, \mathbf{x}_0) - y_1 \end{pmatrix}.$$

From our hypothesis we have $\mathbf{Z}(\tau^+, \hat{\mathbf{x}}_0, \hat{y}_1) = \mathbf{0}$ and $F_1^+(0, \hat{y}_1) \neq 0$. Then the Jacobian matrix

$$\frac{\partial(Z_1, Z_2)}{\partial(t, y_1)}(\tau^+, \hat{\mathbf{x}}_0, \hat{y}_1) = \begin{pmatrix} \dfrac{\partial x}{\partial t}(\tau^+, \hat{\mathbf{x}}_0, \hat{y}_1) & \dfrac{\partial x}{\partial y_1}(\tau^+, \hat{\mathbf{x}}_0, \hat{y}_1) \\ \dfrac{\partial y}{\partial t}(\tau^+, \hat{\mathbf{x}}_0, \hat{y}_1) & \dfrac{\partial y}{\partial y_1}(\tau^+, \hat{\mathbf{x}}_0, \hat{y}_1) \end{pmatrix} =$$

$$= \begin{pmatrix} F_1^+(0, \hat{y}_1) & 0 \\ F_2^+(0, \hat{y}_1) & -1 \end{pmatrix}$$

is nonsingular.

Then, we conclude from the implicit function theorem the existence of two functions $\varphi(\mathbf{x}_0)$, $\psi(\mathbf{x}_0)$ defined in a neighborhood of $\mathbf{x}_0$, such that

$$\begin{aligned} &x(\varphi(\mathbf{x}_0), \mathbf{x}_0) = 0, \\ &y(\varphi(\mathbf{x}_0), \mathbf{x}_0) - \psi(\mathbf{x}_0) = 0, \end{aligned} \tag{3.72}$$

with $\varphi(\mathbf{x}_0) = \tau^+$, $\psi(\mathbf{x}_0) = \hat{y}_1$.

Here, we define the right Poincaré map P_R in a neighborhood of the point $\mathbf{x}_0$ as $y_1 = P_R(y_0) = \psi(0, y_0)$, which verifies $\hat{y}_1 = P_R(\hat{y}_0) = \psi(\mathbf{x}_0)$.

To compute the first derivative of Poincaré map we will take derivatives with respect to (x_0, y_0) in equations (3.72) to get

$$\frac{\partial \mathbf{Z}}{\partial t}(\varphi(\mathbf{x}_0), \mathbf{x}_0, \psi(\mathbf{x}_0)) \cdot D_{\mathbf{x}}\varphi(\mathbf{x}_0) + B(\mathbf{x}_0) - \begin{pmatrix} \mathbf{0} \\ D_{\mathbf{x}}\psi(\mathbf{x}_0) \end{pmatrix} = \mathbf{0}, \tag{3.73}$$

where

$$\frac{\partial \mathbf{Z}}{\partial t}(\varphi(\mathbf{x}_0), \mathbf{x}_0, \psi(\mathbf{x}_0)) = \begin{pmatrix} \dfrac{\partial x}{\partial t}(\varphi(\mathbf{x}_0), \mathbf{x}_0) \\ \\ \dfrac{\partial y}{\partial t}(\varphi(\mathbf{x}_0), \mathbf{x}_0) \end{pmatrix} = F^+(\mathbf{x}_1)$$

and

$$B(\mathbf{x}_0) = D_{\mathbf{x}}\mathbf{Z}(\varphi(\mathbf{x}_0), \mathbf{x}_0, \psi(\mathbf{x}_0)) = \begin{pmatrix} \dfrac{\partial x}{\partial x_0}(\varphi(\mathbf{x}_0), \mathbf{x}_0) & \dfrac{\partial x}{\partial y_0}(\varphi(\mathbf{x}_0), \mathbf{x}_0) \\ \\ \dfrac{\partial y}{\partial x_0}(\varphi(\mathbf{x}_0), \mathbf{x}_0) & \dfrac{\partial y}{\partial y_0}(\varphi(\mathbf{x}_0), \mathbf{x}_0) \end{pmatrix}$$

satisfies the equality

$$B(\mathbf{x}_0)F^+(\mathbf{x}_0) = F^+(\mathbf{x}_1), \tag{3.74}$$

due to the elementary properties of variational equations.

By right-multiplying (3.73) by the vector $(0,1)^T$, we get

$$\varphi_y(\mathbf{x}_1)F^+(\mathbf{x}_0) + B(\mathbf{x}_0)\begin{pmatrix} 0 \\ 1 \end{pmatrix} - \begin{pmatrix} 0 \\ \psi_y(\mathbf{x}_0) \end{pmatrix} = \mathbf{0},$$

and so

$$B(\mathbf{x}_0)\begin{pmatrix} 0 \\ -1 \end{pmatrix} = \begin{pmatrix} F_1^+(\mathbf{x}_1)\varphi_y(\mathbf{x}_0) \\ F_2^+(\mathbf{x}_1)\varphi_y(\mathbf{x}_0) - \psi_y(\mathbf{x}_0) \end{pmatrix}. \tag{3.75}$$

Taking into account (3.74) and (3.75) we can write

$$\begin{pmatrix} F_1^+(\mathbf{x}_1) & 0 \\ F_2^+(\mathbf{x}_1) & -1 \end{pmatrix}\begin{pmatrix} 1 & \varphi_y(\mathbf{x}_0) \\ 0 & \psi_y(\mathbf{x}_0) \end{pmatrix} = B(\mathbf{x}_0)\begin{pmatrix} F_1^+(\mathbf{x}_0) & 0 \\ F_2^+(\mathbf{x}_0) & -1 \end{pmatrix}$$

and taking determinants we arrive at the relation

$$F_1^+(\mathbf{x}_1)\psi_y(\mathbf{x}_0) = F_1^+(\mathbf{x}_0)\exp\left(\int_0^{\varphi(\mathbf{x}_0)} \operatorname{div}(F^+)dt\right), \tag{3.76}$$

where we have used Liouville's formula in computing $\det B(\mathbf{x}_0)$. If we takes $\mathbf{x}_0 = \hat{\mathbf{x}}_0$ in (3.76), then $\mathbf{x}_1 = \hat{\mathbf{x}}_1 = (0, P_R(\hat{y}_0))$. Since $P_R'(\hat{y}_0) = \psi_y(\mathbf{x}_0)$, the proof is finished. ■

The second auxiliary result is given without proof; it appeared in [26].

Lemma 3.7 *Let $\eta = \xi^n \varrho(\xi)$ with n odd, where ϱ is a real analytic function in a neighborhood of the origin and such that $\varrho(0) \neq 0$. Then there exists a real analytic function χ in a neighborhood of the origin with $\chi(0) \neq 0$ such that $\xi = \eta^{1/n}\chi(\eta^{1/n})$.*

The first of our main results is the following.

Theorem 3.6 *Consider system* (3.71) *with $a > 0$ and under the assumption $T \neq 0$. The linear center configuration restricted to the zone $x \leq 0$, that exists for $\gamma = 0$ gives place to a unique periodic oscillation for $\gamma T < 0$ and $|\gamma|$ sufficiently small.*

More precisely, for $T < 0$ the limit cycle bifurcates for $\gamma > 0$ and it is stable, while for $T > 0$ the limit cycle bifurcates for $\gamma < 0$ and it is unstable. If we denote with $\hat{\mathbf{x}}_0 = (0, \hat{y}_0)^T$ a representative point of the bifurcating limit cycle, then the peak-to-peak amplitude A_{pp} in x, the period P of the periodic oscillation, the characteristic multiplier ρ of the periodic orbit and the coordinate $\hat{y}_0$ are analytic functions at 0 in the variable $\gamma^{1/3}$. Namely, we have

$$\begin{aligned}
A_{pp} = \;& 2 + \frac{(3\pi)^{2/3}}{2}\frac{1+a}{(T^2 a)^{1/3}}\gamma^{2/3} + \\
& + \frac{\pi^{4/3}}{40\cdot 3^{2/3}}\frac{(120a^2 + 75a^3 - 21D - 2T^2 + 4a(6D + 7T^2))}{a^{5/3}T^{4/3}}\gamma^{4/3} + O(\gamma^{5/3}),
\end{aligned}$$

$$\begin{aligned}
P = \;& 2\pi + 2(3\pi)^{1/3}\frac{a-1}{(a^2T)^{1/3}}\gamma^{1/3} - \frac{2\pi}{15}\frac{(15a^2 - 12D + T^2 - a(3D + T^2))}{a^2 T}\gamma + \\
& + \frac{4\pi^{1/3}}{3^{2/3}}\frac{a^{1/3}(a-1)}{T^{4/3}}\gamma^{4/3} + O(\gamma^{5/3}),
\end{aligned}$$

$$\begin{aligned}
\rho = \;& 1 - 2(3\pi)^{1/3}\left(\frac{T}{a}\right)^{2/3}\gamma^{1/3} + 2(3\pi)^{2/3}\left(\frac{T}{a}\right)^{4/3}\gamma^{2/3} + \\
& + \frac{2\pi}{15}\frac{15a^2 + 12D - 31T^2}{a^2}\gamma + \\
& + \frac{2\pi^{1/3}}{5\cdot 3^{2/3}}\frac{20a^3 - 30\pi a^2 T - 24\pi DT + 17\pi T^3}{a^{8/3}T^{1/3}}\gamma^{4/3} + O(\gamma^{5/3}),
\end{aligned}$$

and

$$\hat{y}_0 = \left(\frac{3\pi a}{T}\right)^{1/3}\gamma^{1/3} + \left(\frac{\pi^2 T}{3a}\right)^{1/3}\gamma^{2/3} + \frac{\pi\left(15a^2+3D+T^2\right)}{15aT}\gamma +$$

$$+\frac{\pi^{1/3}(30a^2(a+\pi T)-\pi T(3D+T^2))}{15(3^2a^5T^4)^{1/3}}\gamma^{4/3} + O(\gamma^{5/3}),$$

for $|\gamma|$ sufficiently small.

Proof If $\gamma = 0$, it is easy to see that system (3.71) has a linear center for $x \leq 0$, because the eigenvalues of the linearization matrix are $\pm i$.

For $\gamma \neq 0$ in the zone with $x \leq 0$, the linearization matrix has complex eigenvalues $\gamma \pm i$, that is, the equilibrium point at $(-1, -2\gamma)^T$ is a focus.

We want to analyze the possible bifurcation of a limit cycle from the linear center existing in the zone $x \leq 0$ for $\gamma = 0$. Obviously, it should be born from the most external periodic orbit of the center, that is tangent to the frontier $x = 0$ at the origin.

We assume the existence of a limit cycle living in the two zones of linearity, with intersections $\hat{\mathbf{x}}_0 = (0, \hat{y}_0)^T$ and $\hat{\mathbf{x}}_1 = (0, \hat{y}_1)^T$ with $x = 0$ as it is show in Figure 3.22.

Let consider an orbit of system (3.71) that starts from the point $\hat{\mathbf{x}}_0 = (0, \hat{y}_0)^T$ and it enters in the zone $x > 0$. The points of that orbit are given by the expression

$$\begin{pmatrix} x_R(\tau) \\ y_R(\tau) \end{pmatrix} = e^{A_R\tau}\left(\hat{\mathbf{x}}_0 - \mathbf{x}_{eq_R}\right) + \mathbf{x}_{eq_R},$$

where the subindices R stand for the right zone, that is, $x > 0$. Being

$$A_R = \begin{pmatrix} T & -1 \\ D & 0 \end{pmatrix}$$

the linearization matrix of the right zone and $\mathbf{x}_{eq_R} = (-a/D, -aT/D)^T$.

In the zone with $x < 0$, if we integrate backwards starting from point $\hat{\mathbf{x}}_0$ we obtain the orbit given by

$$\begin{pmatrix} x_{L_B}(\tau) \\ y_{L_B}(\tau) \end{pmatrix} = e^{-A_L\tau}\left(\hat{\mathbf{x}}_0 - \mathbf{x}_{eq_L}\right) + \mathbf{x}_{eq_L},$$

where the subindices L stand for the left zone, that is, $x \leq 0$. Being

$$A_L = \begin{pmatrix} 2\gamma & -1 \\ \gamma^2 + 1 & 0 \end{pmatrix}$$

the linearization matrix of the left zone and $\mathbf{x}_{eq_L} = (-1, -2\gamma)^T$.

The existence of the above mentioned limit cycle implies that exist two positive values τ_R and τ_L such that

$$\begin{pmatrix} x_R(\tau) \\ y_R(\tau) \end{pmatrix} = \hat{\mathbf{x}}_1 = \begin{pmatrix} 0 \\ \hat{y}_1 \end{pmatrix} = \begin{pmatrix} x_{L_B}(\tau) \\ y_{L_B}(\tau) \end{pmatrix}.$$

This expression is equivalent to the following system

$$\begin{cases} x_{L_B}(\tau_L) = 0, \\ x_R(\tau_R) = 0, \\ y_R(\tau_R) - y_{L_B}(\tau_L) = 0, \end{cases} \tag{3.77}$$

where $\hat{y}_1$ has been removed from the computation. System (3.77) has three unknowns: τ_L, τ_R, $\hat{y}_0$, the bifurcation parameter γ, and it is the closing equations system. The use of these equations goes back to Andronov and coworkers [2].

The sorted set formed by (3.77) will be denoted by

$$\mathbf{H}(\mathbf{z}) = \mathbf{0}, \tag{3.78}$$

where $\mathbf{z} = (\tau_L, \tau_R, \hat{y}_0, \gamma)$.

The outermost periodic orbit of the linear center that exist in zone $x \leq 0$ for $\gamma = 0$ must satisfy (3.78), with corresponding values $\tau_L = 2\pi$, $\tau_R = 0$, $\hat{y}_0 = 0$, $\gamma = 0$, that we write in the more compact form $\bar{\mathbf{z}} = (2\pi, 0, 0, 0)$.

Obviously, we are interested in a branch of solutions of (3.78) passing through $\bar{\mathbf{z}}$, and leading to positive values of τ_L and τ_R. It turns out that system (3.78) has a trivial branch of solutions that passes through $\bar{\mathbf{z}}$ and can be parameterized as $\mathbf{z}(\mu) = (2\pi, 0, \mu, 0)$ for every real μ. This trivial branch will be called the spurious branch because, for $\mu \neq 0$, these solutions do not correspond to periodic orbits of the system (3.78). The Jacobian matrix of $\mathbf{H}$ evaluated at $\bar{\mathbf{z}}$ is the following

$$\left.\frac{\partial \mathbf{H}}{\partial \mathbf{z}}\right|_{\mathbf{z}=\bar{\mathbf{z}}} = \begin{pmatrix} 0 & 0 & 0 & -2\pi \\ 0 & 0 & 0 & 0 \\ 1 & a & 0 & 0 \end{pmatrix},$$

and it has not full rank.

In order to apply the Implicit Function Theorem we must to remove this spurious branch. The second equation of (3.78), namely $H_2(\mathbf{z}) = 0$ is satisfied for every $\mathbf{z}$ with $\tau_R = 0$. The function $\widetilde{H}_2(\mathbf{z})$ such that $H_2(\mathbf{z}) = \tau_R \widetilde{H}_2(\mathbf{z})$ is an analytic function in a neighborhood of $\bar{\mathbf{z}}$. If we define the modified closing equations

$$\mathbf{G}(\mathbf{z}) = \mathbf{0}, \tag{3.79}$$

where $G_2 = \widetilde{H}_2$ and $G_i = H_i$ for $i \neq 2$, then the solution set of (3.79) in a neighborhood of $\bar{\mathbf{z}}$ is the solution set of (3.78) excepting the spurious branch solution.

The Jacobian matrix of system (3.79) is the following

$$J = \begin{pmatrix} 0 & 0 & 0 & -2\pi \\ 0 & -a/2 & -1 & 0 \\ 1 & a & 0 & 0 \end{pmatrix}.$$

If we remove the second column (corresponding to τ_R), the determinant of the resulting matrix is $-2\pi \neq 0$ and hence the matrix has full rank. From the Implicit Function Theorem for analytic functions (see [12]) we obtain that in a neighborhood of $\bar{\mathbf{z}}$ exist three unique analytic functions $\tau_L = \varphi_1(\tau_R)$, $\hat{y}_0 = \varphi_2(\tau_R)$ and $\gamma = \varphi_3(\tau_R)$, such that $\mathbf{H}(\varphi_1(\tau_R), \varphi_2(\tau_R), \varphi_3(\tau_R), \tau_R) = \mathbf{0}$. Thus, we can assume the existence of series expansions in τ_R, for the three functions. The procedure for the computation of these series is the following. First, we write series with undetermined coefficients for φ_1, φ_2 and φ_3, and second, we introduce these series in (3.78) and solve the system at order 1 in τ_R, obtaining the coefficients of φ_1, φ_2 and φ_3 of order 1. The computation is straight forward increasing the order of τ_R by one and solving a new linear system in each step. The results have been computed using for safety two different symbolic manipulators (Mathematica [88] and Maple [4]) and they are the following.

$$\begin{aligned}
\tau_L(\tau_R) = &\quad 2\pi - a\tau_R + \frac{a(a^2 - D)}{12}\tau_R^3 + O(\tau_R^5), \\
\hat{y}_0(\tau_R) = &\quad -\frac{a}{2}\tau_R + \frac{aT}{12}\tau_R^2 - \frac{aD}{24}\tau_R^3 + \frac{aT(7D - T^2)}{720}\tau_R^4 + O(\tau_R^5), \\
\gamma(\tau_R) = &\quad -\frac{a^2 T}{24\pi}\tau_R^3 + \frac{a^2 T(15a^2 - 12D + T^2)}{1440\pi}\tau_R^5 - \frac{a^5 T}{288\pi^2}\tau_R^6 + O(\tau_R^7).
\end{aligned} \tag{3.80}$$

Since $a > 0$, we can invert the series $\gamma(\tau_R)$ applying Lemma 3.7 taking $n = 3$, $\xi = \tau_R$ and $\eta = \gamma$, so that we obtain

$$\tau_R(\gamma) = -2\left(\frac{3\pi}{a^2T}\right)^{1/3}\gamma^{1/3} - \frac{2\pi(15a^2 - 12D + T^2)}{15a^2T}\gamma - \frac{4a\pi^{1/3}}{(9a^2T^4)^{1/3}}\gamma^{4/3} + O(\gamma^{5/3}). \tag{3.81}$$

Since τ_R provides the time spent by the orbit in the zone $x > 0$, this implies that τ_R must be positive for $|\gamma|$ sufficiently small, then γT must be negative. Replacing $\tau_R(\gamma)$ in (3.80) we obtain the expressions of $P = \tau_L(\gamma) + \tau_R(\gamma)$ and $y_0(\gamma)$ that appear in the statement of Theorem 3.6.

The peak-to-peak amplitude in x is measured as the maximum distance of x-coordinates between any two points of the periodic orbit. Let us denote by $\tau_{R_{max}}$ the time for which $x(\tau)$ reaches its maximum value $x(\tau_{R_{max}})$ in the zone with $x > 0$. In the same way, let us denote by $\tau_{L_{min}}$ the time for which $x(\tau)$ reaches its minimum value $x(\tau_{L_{min}})$ in the zone $x \leq 0$.

In a similar way to what happens for the variables τ_L, $\hat{y}_0$ and γ, the time $\tau_{R_{max}}$ has a series expansion with respect to the variable τ_R. The variable x reaches its maximum value for $\tau = \tau_{R_{max}}$, hence the following equality must hold

$$\dot{x} = Tx_R(\tau_{R_{max}}) - y_R(\tau_{R_{max}}) = 0, \tag{3.82}$$

where

$$\begin{pmatrix} x_R(\tau_{R_{max}}) \\ y_R(\tau_{R_{max}}) \end{pmatrix} = \mathbf{x}_{eq_R} + e^{A_R\tau_{R_{max}}(\tau_R)}\left[\begin{pmatrix} 0 \\ \hat{y}_0(\tau_R) \end{pmatrix} - \mathbf{x}_{eq_R}\right]. \tag{3.83}$$

From equalities (3.80), (3.82) and (3.83) it is easy to compute the series expansion for $\tau_{R_{max}}$, namely

$$\tau_{R_{max}} = \frac{\tau_R}{2} + \frac{T}{24}\tau_R^2 + \frac{2DT - T^3}{2880}\tau_R^4 + O(\tau_R^6). \tag{3.84}$$

Using (3.80) and (3.84) in (3.83) we obtain the following expansion

$$x_R(\tau_{R_{max}}) = \frac{a}{8}\tau_R^2 + \frac{a(15D - 2T^2)}{1152}\tau_R^4 + O(\tau_R^6). \tag{3.85}$$

The time $\tau_{L_{min}}$ has a series expansion with respect to the variable τ_R. The variable x reaches its minimum value for $\tau = \tau_{L_{min}}$, hence the following equality must hold

$$\dot{x} = 2\gamma x_{L_B}(\tau_{L_{min}}) - y_{L_B}(\tau_{L_{min}}) = 0 \tag{3.86}$$

where

$$\begin{pmatrix} x_{L_B}(\tau_{L_{min}}) \\ y_{L_B}(\tau_{L_{min}}) \end{pmatrix} = \mathbf{x}_{eq_L} + e^{-A_L \tau_{L_{min}}(\tau_R)} \left[\begin{pmatrix} 0 \\ \hat{y}_0(\tau_R) \end{pmatrix} - \mathbf{x}_{eq_L} \right]. \tag{3.87}$$

From equalities (3.80), (3.86) and (3.87) it is easy to compute the series expansion for $\tau_{L_{min}}$, namely

$$\tau_{L_{min}} = \pi - \frac{a}{2}\tau_R + \frac{aT}{12}\tau_R^2 + \frac{a(a^2-D)}{24}\tau_R^3 + \frac{aT(7D-T^2-15a^2)}{720}\tau_R^4 + O(\tau_R^5). \tag{3.88}$$

Using (3.80) and (3.88) in (3.87) we obtain

$$x_{L_B}(\tau_{L_{min}}) = -2 - \frac{a^2}{8}\tau_R^2 + \frac{a^2(9a^2-24D-4T^2)}{1152}\tau_R^4 + O(\tau_R^5). \tag{3.89}$$

Computing $A_{pp} = x_R(\tau_{R_{max}}) - x_{L_B}(\tau_{L_{min}})$ we obtain the expression that appears in Theorem 3.6.

In order to determine the stability of the limit cycle, first we apply Lemma 3.6 to system (3.71), obtaining

$$P_R'(\hat{y}_0) = \frac{-\hat{y}_0}{-\hat{y}_1} \exp\left(\int_0^{\tau_R} T d\tau \right) = \frac{\hat{y}_0}{\hat{y}_1} e^{T\tau_R}.$$

For the part of the limit cycle with $x \leq 0$ we can formulated a result analogous to Lemma 3.6 providing the derivative of the left Poincaré map

$$P_L'(\hat{y}_1) = \frac{F_1^-(\hat{\mathbf{x}}_1)}{F_1^-(\hat{\mathbf{x}}_0)} \exp\left(\int_0^{\tau^-} \operatorname{div}(F^-) \right) = \frac{-\hat{y}_1}{-\hat{y}_0} \exp\left(\int_0^{\tau_L} 2\gamma d\tau \right) = \frac{\hat{y}_1}{\hat{y}_0} e^{2\gamma\tau_L}.$$

Taking into account that we can write the complete Poincaré map as $P(\hat{y}_0) = P_L\left(P_R(\hat{y}_0)\right)$, we have

$$P'(\hat{y}_0) = P_L'\left(P_R(\hat{y}_0)\right) P_R'(\hat{y}_0) = P_L'(\hat{y}_1) P_R'(\hat{y}_0).$$

Therefore, the characteristic multiplier of the periodic orbit is the following $\rho = P'(\hat{y}_0) = e^{T\tau_R + 2\gamma\tau_L}$. Substituting the series $\tau_L(\tau_R)$ from (3.80) in the above expression of ρ, then using the series $\tau_R(\gamma)$ from (3.81) and finally, computing the series expansion of ρ with respect to γ, we obtain the expression given for ρ in Theorem 3.6. ■

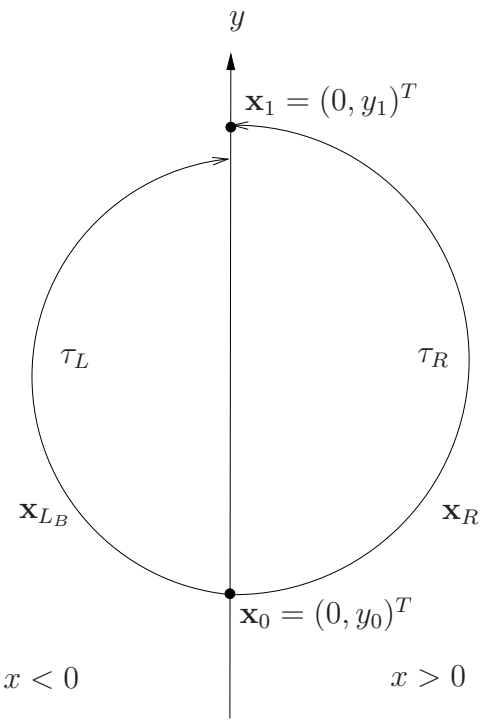

Figure 3.23: A typical orbit with the notation used in the proof of Theorem 3.6.

It should be noted that the sign of the parameter D is not relevant for the bifurcation. Thus, our result covers not only the focus-focus case but also the case of $D = 0$ (parabolic case) and the saddle case ($D < 0$). Of course, the uniqueness of the bifurcating limit cycle is referred to a neighborhood of the most external periodic orbit of the linear center existing for $\gamma = 0$, and so it is a local uniqueness. The case $T = 0$ is explicitly excluded from our result because then we should have a global center for the critical value $\gamma = 0$; the possible bifurcation of limit cycles for such non-generic case requires different techniques, as considered in [6].

Undoing the changes of variables introduced in the proof of Proposition 3.12, it is easy now to obtain a similar result for system (3.70) with $b = 0$ and under adequate hypotheses.

Theorem 3.7 *Consider system* (3.70) *under the hypotheses* $T_-^2 - 4D_- < 0$, $a_- < 0$, $a_+ < 0$, $T_+ \neq 0$ *and assuming that in the zone* $x > 0$ *we have an*

invisible tangency at the origin, that is $b = 0$. *The linear center configuration restricted to the zone* $x \leq 0$, *that exists for* $T_- = 0$ *gives place to a unique periodic oscillation for* $T_-T_+ < 0$ *and* $|T_-|$ *sufficiently small.*

More precisely, for $T_+ < 0$ *the limit cycle bifurcates for* $T_- > 0$ *and it is stable, while for* $T_+ > 0$ *the limit cycle bifurcates for* $T_- < 0$ *and it is unstable. If we denote by* $\hat{\mathbf{x}}_0 = (0, \hat{y}_0)^T$ *a representative point of the bifurcating limit cycle, the peak-to-peak amplitude* A_{pp} *in* x, *the period* P, *the characteristic multiplier* ρ *and* $\hat{y}_0$ *are analytic functions at* 0 *in the variable* $T_-^{1/3}$. *Namely, we have*

$$A_{pp} = -2\frac{a_-}{D_-} - \frac{1}{2}\left(\frac{3\pi}{2}\right)^{2/3}\frac{a_+ + a_-}{D_-}\left(\frac{a_-}{a_+}\right)^{1/3}\left(\frac{T_-}{T_+}\right)^{2/3} + O(T_-)^{4/3}, \quad (3.90)$$

$$\begin{aligned} P = \ & \frac{2\pi}{\sqrt{D_-}} - (12\pi)^{1/3}\frac{a_- - a_+}{a_-^{1/3}a_+^{2/3}\sqrt{D_-}}\left(\frac{T_-}{T_+}\right)^{1/3} + \\ & + \frac{\pi}{15}\frac{\left[15a_+^2D_- - 3D_+(4a_-^2 + a_-a_+) + T_+^2a_-(a_- - a_+)\right]}{a_+^2D_-^{3/2}}\frac{T_-}{T_+} + \\ & + O(T_-)^{4/3}, \end{aligned} \quad (3.91)$$

$$\begin{aligned} \rho = \ & 1 + \frac{(12\pi)^{1/3}}{\sqrt{D_-}}T_+\left(\frac{a_-}{a_+}\right)^{2/3}\left(-\frac{T_-}{T_+}\right)^{1/3} + (18\pi^2)^{1/3}\frac{T_+^2}{D_-}\left(\frac{a_-}{a_+}\right)^{4/3}\left(\frac{T_-}{T_+}\right)^{2/3} + \\ & + \frac{\pi}{15}\frac{45a_+^2 + a_-^2(12D_+ - 31T_+^2)}{a_+^2D_-^{3/2}}T_- + O(T_-)^{4/3}, \end{aligned}$$

and

$$\begin{aligned} \hat{y}_0 = \ & \left(\frac{3\pi}{2}\right)^{1/3}\frac{a_+^{1/3}a_-^{2/3}}{\sqrt{D_-}}\left(-\frac{T_-}{T_+}\right)^{1/3} - \left(\frac{\pi^2}{12}\right)^{1/3}\frac{a_-^{4/3}T_+}{a_+^{1/3}D_-}\left(\frac{T_-}{T_+}\right)^{2/3} - \\ & - \frac{\pi}{30}\frac{15a_+^2D_- + a_-^2(3D_+ + T_+^2)}{a_+D_-^{3/2}}\frac{T_-}{T_+} + O(T_-)^{4/3}, \end{aligned} \quad (3.92)$$

for $|T_-|$ *sufficiently small.*

Proof To prove this theorem it suffices to consider the statements in Theorem 3.6 for the system (3.71), to substitute the parameters T, a and γ by

their expressions provided in Proposition 3.12, and undo the changes that convert the system (3.70) in (3.71).

In particular, to get the new expression in the period P, we start from (3.81) and the first expression in (3.80). This last expression is rescaled by $1/\omega$ and added to (3.81), which after written in terms of the original parameters in (3.70) leads to the expression given in (3.91).

Similarly, to get the expression in (3.90) we must start from (3.85) and (3.89). This last expression should be affect by a factor $1/(\omega k)$ while (3.85) must be multiplied by $1/k$. After substituting in such expressions the value of τ_R given in (3.81), and resorting to the original parameters we arrive at (3.90).

To get the new expression for the characteristic multiplier, it suffices to use the original parameters, while to get the expression (3.92) we only must divide by k the expression for $\hat{y}_0$ in Theorem 3.6. ■

This theorem is an extension of the results obtained in [26], where only the continuous case with symmetry respect to the origin was analyzed. Note that, if we put in the above expressions $a^+ = a^-$ the focus-center-limit cycle bifurcation in the continuous case without symmetry is included. In other words, Theorem 3.7 covers the focus-center-limit cycle bifurcation for 2CPWL$_2$ systems. The expressions (3.90)-(3.92) have been computed with the help of a symbolic computation systems (Mathematica [88] and Maple [4]) and only the first coefficients of the series are explicitly shown. More terms can be computed with the same techniques, if required.

3.3.1 Discontinuous models of Wien bridge oscillators

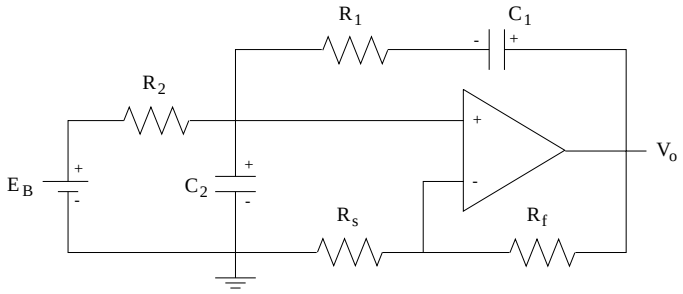

Figure 3.24: Diagram of the Wien Bridge asymmetrical electronic circuit.

We come back to the electronic circuit analyzed in Section 3.2.1, this time following the discontinuous formulation proposed in [49]. We start from the normalized differential system (3.43), which is here rewritten for convenience,

$$\begin{aligned} \frac{dx}{d\tau_n} &= \tilde{t}x + (\widetilde{T} - \tilde{t})\,\mathrm{sat}(x) - y, \\ \frac{dy}{d\tau_n} &= x - x_B, \end{aligned} \tag{3.93}$$

and we recall that we use the dimensionless voltages

$$x = \alpha\frac{V_{C_2}}{E},\ y = \alpha\frac{V_{C_1}}{E},\ x_B = \alpha\frac{E_B}{E},$$

and the parameters

$$\tilde{t} = -\sqrt{\frac{R_2C_1}{R_1C_2}}\alpha_{\mathrm{crit}}, \quad \widetilde{T} = \sqrt{\frac{R_2C_1}{R_1C_2}}(\alpha - \alpha_{\mathrm{crit}}),$$

and

$$\alpha = 1 + \frac{R_f}{R_s}, \quad \alpha_{\mathrm{crit}} = 1 + \frac{C_2}{C_1} + \frac{R_1}{R_2}.$$

We can now write a discontinuous, second order differential equation in x from (3.93) by taking time derivatives in the first equation and substituting the second one. This requires to accept the discontinuous pulse function

$$H(1-|x|) = \begin{cases} 0, & |x| > 1, \\ 1, & |x| < 1, \end{cases}$$

as the derivative of $\mathrm{sat}(x)$. Thus, we arrive at the equation

$$\ddot{x} - \tilde{t}\dot{x} - (\widetilde{T} - \tilde{t})H(1-|x|)\dot{x} + x - x_B = 0.$$

Now, following [49], we introduce two new parameters Γ, ε instead of traces, such that

$$\tilde{t} = 2\Gamma, \quad \varepsilon = -\frac{\widetilde{T}}{\tilde{t}} = \frac{\alpha}{\alpha_{\mathrm{crit}}} - 1,$$

so that the differential equation becomes

$$\ddot{x} - 2\Gamma\dot{x} + 2\Gamma(1+\varepsilon)H(1-|x|)\dot{x} + x - x_B = 0.$$

Working with the symmetric case, that is, for $x_B = 0$, an analysis of the bifurcation at $\varepsilon = 0$, that is $\alpha = \alpha_{\text{crit}}$, giving rise to the jump appearance of oscillations for $\varepsilon > 0$ can be found in [49]. Note that the same analysis can be done in a continuous context, see the analysis for the focus-center-limit cycle bifurcation done in [26], but we want to deal with these discontinuous models in order to show how our previous results apply.

Here, we will assume the more general situation $x_B \neq 0$, so that the nonlinear characteristic of the electronic device has some lack of symmetry as viewed from the equilibrium point, and we want to gain quantitative information about the focus-center-limit cycle bifurcation that occurs at $\varepsilon = 0$. To fix ideas, suppose

$$0 < x_B < 1.$$

Then, for $\varepsilon = 0$ we have a bounded center configuration, a period annulus in other words, which is tangent to the vertical line $x = 1$ and totally contained in the region $x > -1 + x_B > -1$; it is precisely the most external periodic orbit of the annulus where the non-symmetric limit cycle will bifurcate from. Thus, for small $\varepsilon > 0$ the resulting limit cycle only uses the zones C and R; therefore, in the bifurcation analysis we can discard the zone L. Thus we assume that the circuit model is given by

$$\begin{cases} \ddot{x} + 2\Gamma\dot{x} + x - x_B = 0, & x > 1, \\ \ddot{x} - 2\Gamma\varepsilon\dot{x} + x - x_B = 0, & x \leq 1. \end{cases}$$

To put the equilibrium at the origin keeping at the same time the discontinuity line at the unitary value of the variable, we adopt the change

$$v = \frac{x - x_B}{1 - x_B},$$

so that, after substituting and removing the scale factor $(1 - x_B)$, we arrive at the discontinuous differential equation

$$\begin{cases} \ddot{v} + 2\Gamma\dot{v} + v = 0, & v > 1, \\ \ddot{v} - 2\Gamma\varepsilon\dot{v} + v = 0, & v \leq 1. \end{cases}$$

Using now the notation $x = v - 1$, $y = \dot{v}$, the above equations can be written in the form

$$\begin{cases} \dot{x} = y \\ \dot{y} = -x - 2\Gamma y - 1, \end{cases} \quad \text{if } x > 0, \qquad \begin{cases} \dot{x} = y \\ \dot{y} = -x + 2\Gamma\varepsilon y - 1, \end{cases} \quad \text{if } x \leq 0. \tag{3.94}$$

System (3.94) is discontinuous but is in the formulation (1.1) given in [30], so that we can apply the Proposition 3.1 of that paper in order to put system (3.94) in Liénard form. The homeomorphism

$$\tilde{\mathbf{x}} = \begin{pmatrix} 1 & 0 \\ -2\Gamma & -1 \end{pmatrix} \mathbf{x}, \qquad \text{if } x > 0,$$

$$\tilde{\mathbf{x}} = \begin{pmatrix} 1 & 0 \\ 2\Gamma\varepsilon & -1 \end{pmatrix} \mathbf{x}, \qquad \text{if } x \leq 0,$$

transform system (3.94) in

$$\begin{cases} \dot{x} = -2\Gamma x - y \\ \dot{y} = x + 1, \end{cases} \quad \text{if } x > 0, \qquad \begin{cases} \dot{x} = 2\Gamma\varepsilon x - y \\ \dot{y} = x + 1, \end{cases} \quad \text{if } x < 0, \tag{3.95}$$

where the tildes have been dropped for the sake of simplicity. Although it is not really important for our purposes, note that, starting from a discontinuous system, we have at the end a continuous system, that is, we are in the case $a_+ = a_-$.

We could now apply Proposition 3.12 and next Theorem 3.6 to system (3.95). Clearly, it is more direct to resort to Theorem 3.7 by taking $T_+ = -2\Gamma$, $T_- = 2\Gamma\varepsilon$, $D_+ = D_- = 1$, $a_+ = a_- = -1$, concluding that the bifurcation takes place for $\varepsilon = 0$, the limit cycle exists for sufficiently small $\varepsilon > 0$ and it is stable.

Therefore, the peak-to-peak amplitude in x, the period and the characteristic multiplier of the limit cycle are

$$A_{pp} = \; 2 + \left(\frac{3\pi}{2}\right)^{2/3} \varepsilon^{2/3} - \frac{\pi^{4/3}(99 + 52\Gamma^2)}{40 \cdot 18^{1/3}} \varepsilon^{4/3} + O(\varepsilon^{5/3}),$$

$$P = \quad 2\pi + \frac{4(18\pi^5)^{1/3}}{5} \varepsilon^{5/3} + O(\varepsilon^2),$$

and

$$\rho = \; 1 - 2(12\pi)^{1/3}\Gamma\varepsilon^{1/3} + 4(18\pi^2)^{1/3}\Gamma^2\varepsilon^{2/3} + \frac{2\pi}{15}\Gamma(27 - 124\Gamma^2)\varepsilon +$$

$$+ \frac{4}{5}\left(\frac{4\pi}{9}\right)^{1/3} \Gamma(34\pi\Gamma^3 - 27\pi\Gamma - 5)\varepsilon^{4/3} + O(\varepsilon^{5/3}).$$

The order $\varepsilon^{5/3}$ term in the last expression of the period P was not explicitly given by Theorem 3.6; of course, it has been computed with the same procedure given in the proof of Theorem 3.6, increasing the number of terms in (3.80).

We finish this section (and the chapter) by remarking the importance of the study of the bi-parametric unfolding of this bifurcation when the parameter b is allowed to be moved from zero. We suspect the possible appearance of two limit cycles in certain cases; anyway, this is left as the subject for future work.

CHAPTER 4

Some contributions to the dynamics of three-dimensional systems

In this chapter, we focus our attention to S3CPWL$_3$ systems. We start by recalling the bifurcation results for this family when considering the analogous situation to the Hopf bifurcation in smooth systems, leading to a focus-center-limit cycle bifurcation in 3D. Afterwards, we advance in the analysis by studying a more complicated situation, as is the piecewise linear analogous of the Hopf-pitchfork bifurcation, which is the main subject of the chapter. In the last section, we consider some examples taken from nonlinear electronics where the previous theoretical analysis allows to obtain relevant practical consequences.

Along the chapter, we consider the following family of piecewise linear differential systems written in the Luré form,

$$\dot{\mathbf{x}} = \mathbf{F}(\mathbf{x}) = A_R\mathbf{x} + \mathbf{b}\,\mathrm{sat}(x), \tag{4.1}$$

where $\mathbf{x} = (x, y, z)^T \in \mathbb{R}^3$, the saturation function is given by

$$\mathrm{sat}(u) = \begin{cases} 1 & \text{if } u > 1, \\ u & \text{if } |u| \leq 1, \\ -1 & \text{if } u < -1, \end{cases}$$

the dot represents derivative with respect to the time τ,

$$A_R = \begin{pmatrix} t & -1 & 0 \\ m & 0 & -1 \\ d & 0 & 0 \end{pmatrix} \quad \text{and} \quad \mathbf{b} = \begin{pmatrix} T-t \\ M-m \\ D-d \end{pmatrix}, \tag{4.2}$$

where t, m, d, T, M and D are certain coefficients. System (4.1)-(4.2), as a menber of S3CPWL$_3$ family, has the following properties:

(a) It is symmetric with respect to the origin, i.e. $\mathbf{F}(\mathbf{x}) = -\mathbf{F}(-\mathbf{x})$.

(b) In the region with $|x| \leqslant 1$ it becomes the homogeneous system

$$\dot{\mathbf{x}}(\tau) = A_C\mathbf{x}(\tau) = \begin{pmatrix} T & -1 & 0 \\ M & 0 & -1 \\ D & 0 & 0 \end{pmatrix} \mathbf{x}(\tau). \tag{4.3}$$

(c) The coefficients t, m, d and T, M, D are the linear invariants (trace, sum of principal minors and determinant) of the matrices A_R and A_C, respectively.

Note that $A_C = A_R + \mathbf{b}\mathbf{e}_1^T$, where $\mathbf{e}_1 = (1,0,0)^T$, and that the considered family of systems is in the generalized Liénard form, see Chapter 2. Thus, under generic conditions for every system of the form (4.1) after some change of variables, we can get the matrices in the form given in (4.2) and (4.3).

In next section, we recall the known results about the PWL analogous of the Hopf bifurcation for these systems.

4.1 A short review of the PWL analogous of Hopf bifurcation

Regarding system (4.1), the transition of an eigenvalue pair of the matrix A_C through the imaginary axis of the complex plane constitutes an analogous situation to the smooth Hopf bifurcation. Here, at the critical value of parameters, the system has a linear center configuration, to be restricted to the zone C. If we choosing T as the bifurcation parameter, this happens for the critical value $T_c = D/M$ provided that $M > 0$. Then system (4.1) has a linear center in the zone C, see Fig. 4.1, that is, the matrix A_C has

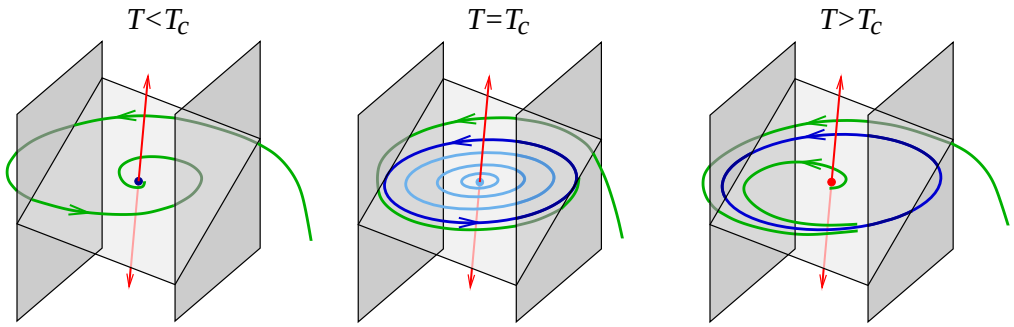

Figure 4.1: The focus-center-limit cycle bifurcation in the case $D > 0$, $\delta > 0$. The focal plane and the complementary one-dimensional invariant manifold at the origin are shown, along with the two parallel planes which separate the three linear regions. In the situation sketched, as deduced from Theorem 4.1, the bifurcating limit cycle is of saddle type.

a pair of pure imaginary eigenvalues. If we want to analyze whether a limit cycle bifurcates from this configuration as the bifurcation parameter T varies around the critical value T_c, the key result is the following, see [27] for the proof.

Theorem 4.1 *Considering system* (4.1) *with* $M > 0$, $T_c = D/M$ *and*

$$\delta = DM - Dm + dM - tM^2 \neq 0,$$

the following statements hold. For $T = T_c$ *the system undergoes a focus-center-limit cycle bifurcation, that is, from the lineal center configuration in the central zone, which exists for* $T = T_c$, *one limit cycle appears for* $\delta(T - T_c) > 0$ *and* $T - T_c$ *sufficiently small.*

The amplitude A *(measured as the maximum of* $|x_1|$*), the period* P_{er} *and the logarithms of characteristic multipliers* μ_r *and* μ_a *of the periodic orbit are analytic functions at* 0, *in the variable* $(T - T_c)^{1/3}$, *namely*

$$A = 1 + \frac{(6\pi)^{2/3} M^{4/3}}{8\delta^{2/3}} (T - T_c)^{2/3} + \frac{(6\pi^4)^{1/3} a_4}{960 M^{1/3} \delta^{7/3}} (T - T_c)^{4/3} + O\left(T - T_c\right)^{5/3},$$

$$P_{er} = \frac{2\pi}{\sqrt{M}} + \frac{\pi(M - m)\sqrt{M}}{\delta} (T - T_c) - \frac{6^{2/3}\pi^{5/3} M^{5/6} P_5}{20\delta^{8/3}} (T - T_c)^{5/3} + h.o.t.$$

and

$$\mu_r = -\frac{(48\pi)^{1/3} M^{7/6}\delta^{2/3}}{D^2+M^3}(T-T_c)^{1/3} + O(T-T_c)^{2/3},$$
$$\mu_a = \frac{2\pi D}{M^{3/2}} + \frac{(48\pi)^{1/3}}{M^{5/6}}\left(\frac{Mt-D}{\delta^{1/3}} + \frac{M^2\delta^{2/3}}{D^2+M^3}\right)(T-T_c)^{1/3} + O(T-T_c)^{2/3},$$

where

$$\begin{aligned} a_4 &= -120tM^5 + \left(120D + 2t^3 + 21mt + 72d\right)M^4 + \\ &\quad + \left[-\left(93m + 27t^2\right)D + \left(27m - 2t^2\right)d\right]M^3 + \left(2t^2m + 25dt - 27m^2\right)DM^2 \\ &\quad + \left[25D^3 + 23\left(mt - d\right)D^2\right]M - 25mD^3, \\ P_5 &= \left[M\left(M-m\right)^2 + \left(Mt-d\right)^2\right]\left(Mt-D\right). \end{aligned}$$

In particular, if $\delta > 0$ and $D < 0$, then the limit cycle bifurcates for $T > T_c$ and is orbitally asymptotically stable.

When the coefficient δ is not equal to zero, Theorem 4.1 gives a complete characterization of the bifurcation criticality. Such coefficient δ plays a similar role to the coefficient of cubic term in the Poincaré-Andronov-Hopf normal form. When $\delta = 0$ the bifurcation is of higher codimension, requiring a specific treatment, see [28].

Theorem 4.1 describes a codimension one bifurcation, similar to the Hopf bifurcation of differentiable dynamics, see [12], but it should be remarked the differences that introduces the PWL case. In particular, the expressions characterizing the bifurcation are in terms of the parameter to the power one third instead of the power one half, and, what is more important, the limit cycle amplitude's leading order is $O(1)$. Thus, the stability change of the origin is accompanied by the abrupt appearance of a limit cycle of significant size, as we have also seen in the planar case, see Chapter 3.

As a final remark for this section, we want to emphasize that a similar phenomenon without symmetry can appear in 2CPWL$_3$ systems, see [7].

In the next section, we advance in the theory by considering the case where not only we have an eigenvalue pair of the matrix A_C crossing the imaginary axis of the complex plane but also a real zero eigenvalue.

4.2 The PWL analogous of Hopf-pitchfork bifurcation

A specific bifurcation in 3D vector fields is the Hopf-pitchfork bifurcation, also called Hopf-zero or fold-Hopf bifurcation. This bifurcation is characterized by the simultaneous appearance of three eigenvalues at the imaginary axis of the complex plane, see Section 7.4 of [36]. In a recent paper [61], as a first step to study the possible occurrence of an analogous to the Hopf-pitchfork bifurcation in continuous piecewise linear systems with symmetry, authors assumed a linear part controlling the dynamics at the origin near a critical situation with a pure imaginary pair and a single zero eigenvalue. However, strong assumptions on the spectra for the external linear parts involved were required in the quoted paper. Here, we suppress such restrictive assumptions and consider much more general linear parts, maintaining the eigenvalue structure leading to the analogous of a Hopf-pitchfork bifurcation. Thus, we give information about the general unfolding of such bifurcation in the framework of piecewise linear systems.

Our goal is to study the phenomena associated to the fold-Hopf bifurcation at the origin. To do this, we introduce ε as the bifurcation parameter and impose that the three eigenvalues of matrix A_C be

$$-\varepsilon \quad \rho\varepsilon \pm \omega i,$$

where $\rho \in \mathbb{R}$ and $\omega \in \mathbb{R}^+$ are auxiliary fixed parameters. Thus for $\varepsilon = 0$ the three eigenvalues are 0 and $\pm\omega i$, which are located on the imaginary axis of the complex plane. Accordingly we choose

$$\begin{aligned} T(\varepsilon) &= (2\rho - 1)\varepsilon, \\ M(\varepsilon) &= \omega^2 + \rho\varepsilon^2(\rho - 2), \\ D(\varepsilon) &= -\varepsilon(\rho^2\varepsilon^2 + \omega^2), \end{aligned} \tag{4.4}$$

to be assumed hereafter.

We emphasize in the next result an invariant property of systems (4.1)-(4.2), whose proof is direct and will be omitted.

Proposition 4.1 *System* (4.1)-(4.2) *is invariant under the following transformation*

$$(x, y, z, \tau, t, m, d, \varepsilon) \longrightarrow (x, -y, z, -\tau, -t, m, -d, -\varepsilon).$$

This symmetry property is useful for simplifying the analysis of the family under consideration. Next, we summarize the main assertions about possible equilibrium of the family.

Proposition 4.2 *For system* (4.1)-(4.2) *with* $\rho \neq 0$ *and* $\omega > 0$ *the following statements hold.*

(a) *If* $d\varepsilon < 0$ *the unique equilibrium point is the origin.*

(b) *If* $d\varepsilon > 0$ *then the equilibria are the origin and the two points*

$$\mathbf{x}_\varepsilon^+ = \left(1 - \frac{D(\varepsilon)}{d},\, T(\varepsilon) - t\frac{D(\varepsilon)}{d},\, M(\varepsilon) - m\frac{D(\varepsilon)}{d} \right)^T, \quad \mathbf{x}_\varepsilon^- = -\mathbf{x}_\varepsilon^+.$$

(c) *If* $\varepsilon = 0$ *then all the points of the segment*

$$\{(x, y, z)^T \in \mathbb{R}^3 : (x, y, z)^T = \mu(1, 0, \omega^2)^T, |\mu| \leq 1\}$$

are equilibria for the system. If furthermore $d \neq 0$*, the above segment captures all the equilibrium points.*

(d) *The origin is stable when* $\varepsilon > 0$ *and* $\rho < 0$*. The stability of equilibrium points* $\mathbf{x}_\varepsilon^\pm$ *that appear for* $d\varepsilon > 0$ *requires* $t < 0$*,* $d < 0$ *and* $mt - d < 0$*.*

Proof From the definition of system (4.1)-(4.2) under conditions (4.4) in the central zone, it is direct to assure that the unique equilibrium point for $\varepsilon \neq 0$ and $|x| < 1$ is the origin.

From the third component of equations of system (4.1)-(4.2), in the zone $x > 1$, the x-coordinate of the equilibrium point for $\varepsilon \neq 0$ is equal to

$$x_\varepsilon^+ = 1 + \frac{\varepsilon}{d}(\rho^2\varepsilon^2 + \omega^2).$$

If $d\varepsilon < 0$ then $x_\varepsilon^+ < 1$ and the equilibrium point is not a real equilibrium but it is a virtual one. The same is true for the zone $x < -1$ and x_ε^-. If $d\varepsilon > 0$

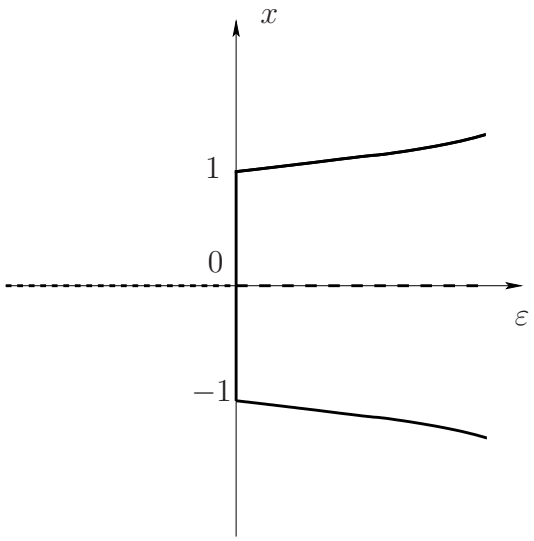

Figure 4.2: The bifurcation diagram for equilibria of system (4.1)-(4.2) when $d > 0$. We draw only the x-coordinate of equilibrium points.

then real symmetrical equilibrium points $\mathbf{x}_\varepsilon^+$ and $\mathbf{x}_\varepsilon^-$ are obtained, and the statements (a) and (b) hold.

For $\varepsilon = 0$ the computation of the segment of equilibrium points in statement (c) is straightforward.

Statement (d) comes from the classical Hurwitz conditions. ■

From statement (c) of Proposition 4.2 we see that at $\varepsilon = 0$ system (4.1)-(4.2) has a *degenerate pitchfork bifurcation*, see Figure 4.2. Note that for $d\varepsilon < 0$ the points $\mathbf{x}_\varepsilon^\pm$ are vanishing points for the vector field corresponding to $|x| > 1$ but they are out of their corresponding zones. They do not constitute real equilibria, although they still organize the dynamics of external regions. This type of equilibrium is usually called *virtual equilibrium point*.

In order to study the existence of periodic orbits in system (4.1)-(4.2), we start by considering the central zone of system (4.3) with $\varepsilon = 0$. In this case a direct computation shows that the solution of (4.3) starting from an arbitrary point $(x_0, y_0, z_0)^T$ for $\tau = 0$ is given by

$$\mathbf{x}(\tau) = e^{A_C \tau} \begin{pmatrix} x_0 \\ y_0 \\ z_0 \end{pmatrix} = \frac{1}{\omega^2} \begin{pmatrix} \omega^2 \cos\omega\tau & -\omega \sin\omega\tau & 1 - \cos\tau \\ \omega^3 \sin\omega\tau & \omega^2 \cos\omega\tau & -\omega \sin\omega\tau \\ 0 & 0 & \omega^2 \end{pmatrix} \begin{pmatrix} x_0 \\ y_0 \\ z_0 \end{pmatrix}. \tag{4.5}$$

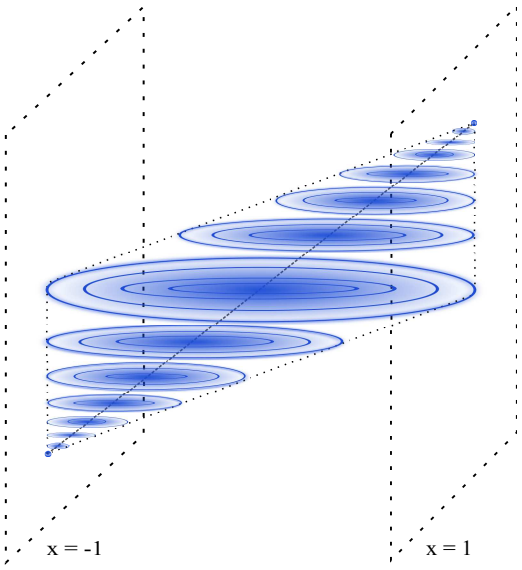

Figure 4.3: Structure of periodic orbits for $\varepsilon = 0$ in the central zone. The two solid cones are completely foliated by periodic orbits surrounding the segment of equilibrium points $\{(x, 0, x\omega^2)^T : |x| \leqslant 1\}$.

If $|x_0| < 1$ then the corresponding orbit is an arc of the ellipse

$$\left\{ (x,y,z)^T \in \mathbb{R}^3 : \frac{\left(x - \frac{z_0}{\omega^2}\right)^2}{\left(x_0 - \frac{z_0}{\omega^2}\right)^2 + \frac{y_0^2}{\omega^2}} + \frac{y^2}{\omega^2\left(x_0 - \frac{z_0}{\omega^2}\right)^2 + y_0^2} = 1,\ z = z_0 \right\}, \tag{4.6}$$

passing through the initial point. For some initial points we get complete ellipses in the region $|x| \leq 1$ and then we will have that $-\omega^2 < z_0 < \omega^2$.

Therefore, the orbits corresponding to solutions (4.5) of system (4.3) that are contained for all τ in the central zone are periodic orbits of system (4.1)-(4.2), and define a bounded set completely foliated by periodic orbits. This periodic bounded set has the shape of two solid cones sharing the elliptic disc $\omega^2 x^2 + y^2 \leqslant \omega^2$ in the plane $z = 0$ as their common basis, see Figure 4.3, each one being tangent to one of the planes $x = 1$ and $x = -1$.

The structure of periodic orbits of Figure 4.3 is independent on the values of t, m and d. For $\varepsilon \neq 0$ and small, most of these periodic orbits will disappear but some of them could give rise to limit cycles. In this chapter, we analyze

the possible appearance of limit cycles from the above set of periodic orbits for $\varepsilon \neq 0$ and small.

As it is well known, a linear system cannot have limit cycles. So that, limit cycles must cross the planar frontiers $x = 1$ or $x = -1$. If for some values of parameters there exits a limit cycle living in two zones it will be called bizonal limit cycle. Analogously, we speak of tri-zonal limit cycles when they cross the two separation planes. It should be noticed that, due to the symmetry of the vector field with respect to the origin, non-symmetric limit cycles should come in pairs, that is, when a non-symmetric limit cycle exists then there must be its symmetrical one. This is always the case for bizonal limit cycles.

We use in the sequel the ideas of Chapter 2. Let us consider a tri-zonal periodic orbit Γ, symmetric with respect the origin and living in the three zones of linearity. Therefore, there exists a point $\bar{P}_0 = (1, y_0, z_0)^T = (1, \bar{\mathbf{p}}_0)^T$ in Γ located in the plane $x = 1$, such that when time increases, the orbit will evolve in the zone $x > 1$, until it transversely crosses the plane $x = 1$ at the point $\bar{P}_1 = (1, y_1, z_1)^T = (1, \bar{\mathbf{p}}_1)^T$ after time $\bar{\tau}_R$. Next the orbit goes through the central zone until it hits the plane $x = -1$ after a time $\bar{\tau}_C$ at a point $\bar{P}_2$, which due to the symmetry is $-\bar{P}_0$. Then Γ goes through the zone $x < -1$ from the point $\bar{P}_2$ to the point $\bar{P}_3 = -\bar{P}_1$ during a time $\bar{\tau}_R$ and finally, after a time $\bar{\tau}_C$ it comes back to the point $\bar{P}_0$, see Figure 4.4.

Note that at the plane $x = 1$, the contact line $y = T(\varepsilon)$ splits the plane in two open half-planes, namely the regions where $\dot{x} > 0$ ($y < T(\varepsilon)$) and the one where $\dot{x} < 0$ ($y < T(\varepsilon)$). Consequently, we must have $y_0 < T(\varepsilon)$ and $y_1 > T(\varepsilon)$. The symmetry of the system (4.1)-(4.2) allows us to determine the periodic orbit Γ by using the half-orbit from $\bar{P}_0$ to $\bar{P}_2$ passing through $\bar{P}_1$.

By the continuity of the flow, it is possible to define in an adequate open set within the plane $x = 1$ the functions π_R and π_C, such that $\pi_R(\bar{\mathbf{p}}_0) = \bar{\mathbf{p}}_1$ and $\pi_C(\bar{\mathbf{p}}_1) = -\bar{\mathbf{p}}_0$ so that their composition $\pi_H = \pi_C \circ \pi_R$ is the half return map. We denote by $\tau_R(\mathbf{p}_0)$ the time spent by the orbit from P_0 to P_1, being $P_0 = (1, \mathbf{p}_0)$ and $P_1 = (1, \mathbf{p}_1)$ points with $x = 1$ in a neighborhood of $\bar{P}_0$ and $\bar{P}_1$ respectively. Let us call $\tau_C(\mathbf{p}_1)$ the time employed from P_1 to P_2. See Figure 4.5. We denote derivatives with respect to the restricted coordinates on the plane $x = 1$ as $D_{\mathbf{p}}(\cdot)$.

Then, if we denote by $\tau(\mathbf{p}_0)$ the total time spent by the orbit to pass from P_0 to P_2, we conclude that $D_{\mathbf{p}}\tau(\mathbf{p}_0) = D_{\mathbf{p}}\tau_R(\mathbf{p}_0) + D_{\mathbf{p}}\tau_C(\mathbf{p}_1)D_{\mathbf{p}}\pi_R(\mathbf{p}_0)$.

The eigenvalues of the derivative $D_{\mathbf{p}}\pi$ at the point $\mathbf{p}_0$ can be computed

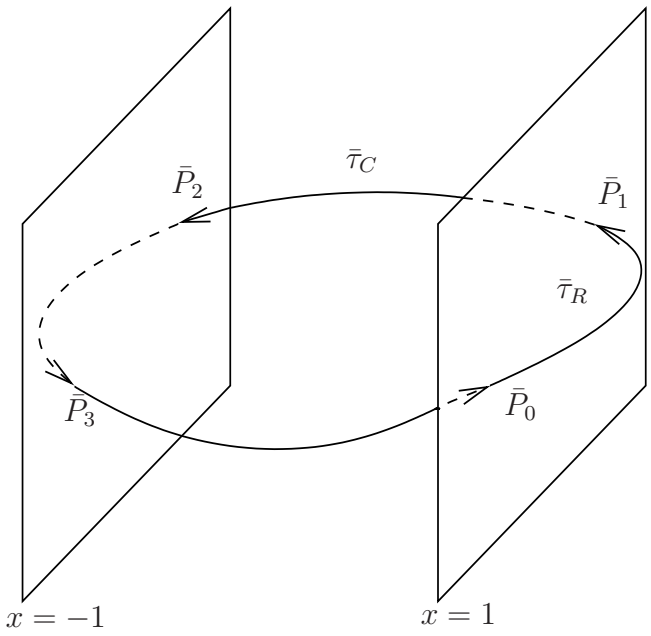

Figure 4.4: Tri-zonal periodic orbit of system (4.1)-(4.2) and the relevant points necessary to build the closing equations.

by using the next result which is a particularization of Proposition 2.13 for the 3D case and appeared in Proposition 3.2 of [27]. As usual, if a matrix Q is nonsingular, we say that the matrix QMQ^{-1} is similar to matrix M. Note that the complete return map Π can be obtained by composing π with another half-return map which, due to the symmetry, is identical to π, and so the eigenvalues of Π are the squares of the eigenvalues of π.

Proposition 4.3 *Consider a symmetrical tri-zonal periodic orbit of system* (4.1)-(4.2) *starting from* $(1, \bar{\boldsymbol{p}}_0)$ *and passing through* $(1, \bar{\boldsymbol{p}}_1)$ *with* $\bar{\boldsymbol{p}}_0$, $\bar{\boldsymbol{p}}_1 \in \mathbb{R}^2$. *Then the product of the two matrices*

$$\begin{pmatrix} 1 & D_{\boldsymbol{p}}\tau_C(\bar{\boldsymbol{p}}_1) \\ 0 & D_{\boldsymbol{p}}\pi_C(\bar{\boldsymbol{p}}_1) \end{pmatrix} \begin{pmatrix} -1 & D_{\boldsymbol{p}}\tau_R(\bar{\boldsymbol{p}}_0) \\ 0 & D_{\boldsymbol{p}}\pi_R(\bar{\boldsymbol{p}}_0) \end{pmatrix} = \begin{pmatrix} -1 & D_{\boldsymbol{p}}\tau(\bar{\boldsymbol{p}}_0) \\ 0 & D_{\boldsymbol{p}}\pi(\bar{\boldsymbol{p}}_0) \end{pmatrix}$$

is similar to the matrix

$$M = e^{A_C\tau_C(\bar{\boldsymbol{p}}_1)}e^{A_R\tau_R(\bar{\boldsymbol{p}}_0)} = e^{A_C\bar{\tau}_C}e^{A_R\bar{\tau}_R}. \tag{4.7}$$

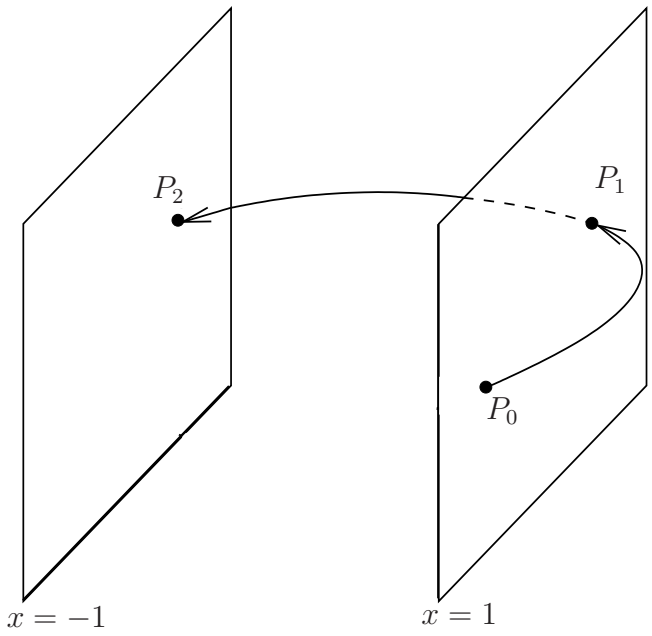

Figure 4.5: Half-return map of system (4.1)-(4.2) from section $x = 1$ to section $x = -1$.

Before the main results, we rewrite Lemma 3.7 that will be useful for the proofs.

Lemma 4.1 *Let $\eta = \xi^n \varrho(\xi)$ with n odd, where ϱ is a real analytic function in a neighborhood of the origin and such that $\varrho(0) \neq 0$. Then there exists a real analytic function χ in a neighborhood of the origin with $\chi(0) \neq 0$ such that $\xi = \eta^{1/n}\chi(\eta^{1/n})$.*

The next elementary result, which appeared in [73] as Lemma 5, is a straightforward criterion to assure that the two roots of a quadratic equation have modulus less than one.

Lemma 4.2 *The two solutions of the quadratic equation $x^2 - px + q = 0$ are inside the unit circle if and only if $|q| < 1$ and $|p| < 1 + q$.*

Using the above lemma, the following remark will be used to determine the stability of periodic orbits of system (4.1)-(4.2).

Remark 4.1 *We note that the matrix M in* (4.7) *has one eigenvalue equal to* -1*. We will denote by λ_1 and λ_2 the other two eigenvalues of M. Therefore, if we take $p = \lambda_1 + \lambda_2$ and $q = \lambda_1\lambda_2$, we have* $\operatorname{trace}(M) = -1 + p$ *and* $\det(M) = -q$*, and thus the characteristic equation of matrix M is* $(\lambda + 1)(\lambda^2 - p\lambda + q) = 0$*. Then λ_1 and λ_2 are the eigenvalues of the derivative $D_{\boldsymbol{p}}\pi$, and from Lemma 4.2 both eigenvalues λ_1 and λ_2 are inside the unit circle if and only if*

$$|\det(M)| < 1 \text{ and } |\operatorname{trace}(M) + 1| < 1 - \det(M). \tag{4.8}$$

Finally, the conditions (4.8) *are fulfilled if and only if the eigenvalues of the derivative of the complete Poincaré map Π, λ_1^2 and λ_2^2, are inside the unit circle.*

Our first result concerns the possible bifurcation of symmetrical periodic orbits using the three zones. We introduce a new parameter $\delta = d - t\omega^2$, which characterizes the criticality of the bifurcation, in a similar way to what happens in the cases considered in [7] and [27].

Theorem 4.2 *Let us consider system* (4.1)-(4.2) *under conditions* (4.4) *where it is assumed $\rho \neq 0$ and $\delta = d - t\omega^2 \neq 0$ and fixed. For $\varepsilon = 0$ the system* (4.1)-(4.2) *undergoes a tri-zonal limit cycle bifurcation, that is, from the configuration of periodic orbits that exists in the central zone for $\varepsilon = 0$, one limit cycle appears for $\rho\delta\varepsilon > 0$ and $|\varepsilon|$ sufficiently small. It is symmetric with respect to the origin and bifurcates from the ellipse $\{(x, y, z)^T \in \mathbb{R}^3 : \omega^2 x^2 + y^2 = \omega^2,\ z = 0\}$. This limit cycle has period*

$$P = \frac{2\pi}{\omega} + \frac{2\pi\rho(\omega^2 - m)}{\omega\delta}\varepsilon + \frac{(144\pi^5)^{1/3}\, t\rho^{5/3}[\delta^2 + \omega^2\,(m - \omega^2)^2]}{5\omega^{5/3}\delta^{8/3}}\varepsilon^{5/3} + O\left(\varepsilon^2\right),$$

its amplitude in x measured as $\max\{x\} - \min\{x\}$ *is*

$$A = \ 2 + \left(\frac{3\pi\rho\omega^2}{2\delta}\right)^{2/3}\varepsilon^{2/3} -$$

$$-\frac{(\pi^2\rho^2\omega)^{2/3}\,[\delta(21m + 2t^2 - 72\omega^2) + 48(t\omega^2 - dm)]}{40 \cdot 18^{1/3}\delta^{7/3}}\varepsilon^{4/3} + O\left(\varepsilon^{5/3}\right),$$

and it passes through the point $P_0 = (1, y_0, z_0)^T$, where

$$y_0 = \ -\left(\frac{3\pi\rho\omega^5}{2\delta}\right)^{1/3}\varepsilon^{1/3} + \frac{t}{3}\left(\frac{\pi\rho\omega^2}{2\delta}\right)^{2/3}\varepsilon^{2/3} + O(\varepsilon),$$

and

$$z_0 = -\frac{\pi d\rho\omega}{2\delta}\varepsilon + \left(\frac{3\pi\rho\omega^5}{2\delta}\right)^{1/3}\varepsilon^{4/3} + O(\varepsilon^{5/3}).$$

Furthermore, the bifurcating limit cycle is stable if and only if $t < 0$, $\delta > 0$ *and* $d < 0$.

Proof In order to determine symmetric tri-zonal limit cycles of system (4.1)-(4.2), our strategy will be the following. First, we integrate an orbit that starting from the point $P_0 = (1, y_0, z_0)^T$ stays in the zone $x > 1$, arriving to the point $P_1 = (1, y_1, z_1)^T$, after a time τ_R. If from P_0, we integrate the orbit backwards arriving at $-P_1$ after a time $-\tau_C$, then due to symmetry of the problem, we have completed the half of a periodic orbit. This approach allows the elimination of the coordinates y_1 and z_1 from the computation of the periodic orbit.

The solution of system (4.1)-(4.2) in the zone $x > 1$ passing through the point P_0 is determined by

$$\begin{pmatrix} x(\tau) \\ y(\tau) \\ z(\tau) \end{pmatrix} = e^{A_R\tau}\left[\begin{pmatrix} 1 \\ y_0 \\ z_0 \end{pmatrix} - \mathbf{x}_\varepsilon^+\right] + \mathbf{x}_\varepsilon^+, \tag{4.9}$$

where $\mathbf{x}_\varepsilon^+$ was defined in Proposition 4.2. Analogously, in the central zone, integrating backwards system (4.1)-(4.2) from P_0 one obtains the solution

$$\begin{pmatrix} x_b(\tau) \\ y_b(\tau) \\ z_b(\tau) \end{pmatrix} = e^{-A_C\tau}\begin{pmatrix} 1 \\ y_0 \\ z_0 \end{pmatrix}. \tag{4.10}$$

Obviously expressions (4.9) and (4.10) correspond with orbits of system (4.1)-(4.2) only if $x(\tau) \geqslant 1$ for all $0 \leq \tau \leq \tau_R$ and $|x_b(\tau)| \leqslant 1$ for all $0 \leq \tau \leq \tau_C$. By defining the variable $\mathbf{w} = (\tau_C, \varepsilon, y_0, z_0, \tau_R)$ and from equations (4.9) and (4.10) we obtain the closing equations $\widehat{\mathbf{G}}(\mathbf{w}) = \mathbf{0}$, where

$$\begin{aligned} \widehat{G}_1(\mathbf{w}) &= x(\tau_R) - 1, \\ \widehat{G}_2(\mathbf{w}) &= x_b(\tau_C) + 1, \\ \widehat{G}_3(\mathbf{w}) &= y(\tau_R) + y_b(\tau_C), \\ \widehat{G}_4(\mathbf{w}) &= z(\tau_R) + z_b(\tau_C). \end{aligned} \tag{4.11}$$

The system $\widehat{\mathbf{G}}(\mathbf{w}) = \mathbf{0}$ constitutes a nonlinear system with four equations and five unknowns, and its solutions with $\tau_C > 0, \tau_R > 0$ and $y_0 < T(\varepsilon)$

for $|\varepsilon|$ sufficiently small, correspond with periodic orbits symmetrical with respect to the origin. Of course, it has the solution $\bar{\mathbf{w}} = (\pi/\omega, 0, 0, 0, 0)$ which corresponds to the ellipse with $z_0 = 0$, $y_0 = 0$ and $x_0 = 1$ given in (4.6), namely $\omega^2 x^2 + y^2 = \omega^2$ and $z = 0$.

The closing equations defined by (4.11) have the spurious solution branch $\bar{\mathbf{w}}_s = (\pi/\omega, 0, \mu, 0, 0)$ for all $\mu \neq 0$, that does not correspond to periodic orbits of system (4.1)-(4.2) because taking $y_0 = \mu \neq 0$, it is easy to show that

$$\max_{0<\tau<\pi/\omega} |x_b(\tau)| = \max_{0<\tau<\pi/\omega} \left| \cos(\omega\tau) - \frac{\mu \sin(\omega\tau)}{\omega} \right| > 1.$$

This spurious solution branch can be removed by just dividing $\widehat{G}_1$ by a hidden factor τ_R and using modified closing equations, defined through the functions

$$G_1(\mathbf{w}) = \frac{1}{\tau_R} \widehat{G}_1(\mathbf{w}), \quad G_i(\mathbf{w}) = \widehat{G}_i(\mathbf{w}), \quad i = 2, 3, 4. \tag{4.12}$$

The modified closing equations $\mathbf{G}(\mathbf{w}) = \mathbf{0}$, have the same solution set of (4.11) without the spurious solution branch. Choosing τ_R as bifurcation parameter, we can write the closing equations as $\mathbf{G}(\mathbf{v}, \tau_R) = \mathbf{0}$, where $\mathbf{w} = (\mathbf{v}, \tau_R)$ and $\mathbf{v} = (\tau_C, \varepsilon, y_0, z_0)$, and we will parameterize their solutions for $\mathbf{v}$ in terms of τ_R. The corresponding Jacobian matrix is

$$J = D_{\mathbf{v}} \mathbf{G}(\bar{\mathbf{v}}, 0) = \begin{pmatrix} 0 & 2\rho - 1 & -1 & 0 \\ 0 & \pi\rho/\omega & 0 & 2/\omega^2 \\ \omega^2 & 0 & 0 & 0 \\ 0 & 0 & 0 & 2 \end{pmatrix}, \tag{4.13}$$

where $\bar{\mathbf{v}} = (\pi/\omega, 0, 0, 0)$. Since the determinant of (4.13) is equal to $2\pi\rho\omega \neq 0$, the matrix J has full rank and we can apply the Implicit Function Theorem for analytic functions [12], deducing the existence of a function

$$\mathbf{v}(\tau_R) = (\tau_C(\tau_R), \varepsilon(\tau_R), y_0(\tau_R), z_0(\tau_R))$$

in a neighborhood of $\tau_R = 0$. The corresponding series expansions, were

computed using Mathematica [88], as follows

$$\begin{aligned}
\tau_C &= \frac{\pi}{\omega} - \tau_R + \frac{\omega^2 - m}{12}\tau_R^3 + \\
&\quad + \frac{\omega^2(15m + 5t^2 - 9\omega^2) - 6(m^2 + dt) + mt^2}{720}\tau_R^5 + O\left(\tau_R^6\right), \\
\varepsilon &= \frac{\omega(d - t\omega^2)}{12\pi\rho}\tau_R^3 + \frac{\omega[d(9\omega^2 + t^2 - 6m) + t(12m\omega^2 - t^2\omega^2 - 15\omega^4)]}{720\pi\rho}\tau_R^5 + \\
&\quad + O\left(\tau_R^6\right), \\
y_0 &= -\frac{\omega^2}{2}\tau_R + \frac{t\omega^2}{12}\tau_R^2 + \frac{\omega[2(2\rho - 1)(t\omega^2 - d) + \pi m\rho\omega]}{24\pi\rho}\tau_R^3 + \\
&\quad + \frac{\omega^2(7mt - 6d - t^3)}{720}\tau_R^4 + O\left(\tau_R^5\right), \\
z_0 &= -\frac{d\omega^2}{24}\tau_R^3 + \frac{\omega^3(t\omega^2 - d)}{24\pi\rho}\tau_R^4 + O\left(\tau_R^5\right).
\end{aligned} \tag{4.14}$$

Defining the parameter $\delta = d - t\omega^2$, and assuming in what follows that $\delta \neq 0$, we can invert the series $\varepsilon(\tau_R)$ applying Lemma 4.1, and taking $n = 3$, $\xi = \tau_R$, $\eta = \varepsilon$. We obtain,

$$\tau_R(\varepsilon) = \left(\frac{12\pi\rho}{\omega\delta}\right)^{1/3}\varepsilon^{1/3} + \frac{\pi\rho(\delta(9\omega^2 - 6m + t^2) + 6t\omega^2(m - \omega^2))}{15\omega\delta^2}\varepsilon + O\left(\varepsilon^{4/3}\right). \tag{4.15}$$

The variable τ_R provides the time spent by the limit cycle in the zone $x > 1$. Since this time τ_R must be positive for $|\varepsilon|$ sufficiently small then the condition $\rho\delta\varepsilon > 0$ must hold.

Replacing $\tau_R(\varepsilon)$ in (4.14) we obtain the expressions of $P = 2\left(\tau_C(\varepsilon) + \tau_R(\varepsilon)\right)$, $y_0(\varepsilon)$ and $z_0(\varepsilon)$ given in the statement of Theorem 4.2.

The peak-to-peak amplitude of the limit cycle is measured by the difference between the maximum value reached by the x-coordinate along the periodic orbit and the minimum one. Let us denote by τ_{Rmax} the time for which $x(\tau)$ reaches its maximum value $x(\tau_{Rmax})$ in the zone with $x > 1$. Due to the symmetry of the system (4.1)-(4.2) the minimum value of x in

the periodic orbit is $-x(\tau_{Rmax})$. Therefore, the needed amplitude is equal to $2x(\tau_{Rmax})$.

In a similar way to what happens for the variables τ_C, ε, y_0 and z_0, the time τ_{Rmax} has a series expansion with respect to the variable τ_R. The variable x reaches its maximum value for $\tau_R = \tau_{Rmax}$, hence the following equality must hold

$$\dot{x} = tx(\tau_{Rmax}) - y(\tau_{Rmax}) + T(\varepsilon) - t = 0 \tag{4.16}$$

where

$$\begin{pmatrix} x(\tau_{Rmax}) \\ y(\tau_{Rmax}) \\ z(\tau_{Rmax}) \end{pmatrix} = \mathbf{x}_\varepsilon^+ + e^{\tau_{Rmax} A_R} \left[\begin{pmatrix} 1 \\ y_0(\tau_R) \\ z_0(\tau_R) \end{pmatrix} - \mathbf{x}_\varepsilon^+ \right]. \tag{4.17}$$

From equalities (4.14), (4.16) and (4.17), it is easy to compute the series expansion of τ_{Rmax}, namely

$$\tau_{Rmax} = \frac{\tau_R}{2} + \frac{t}{24}\tau_R^2 + \frac{-27d + 4mt - 2t^3}{5760}\tau_R^4 + \frac{\omega\delta}{288\pi\rho}\tau_R^5 + O(\tau_R^6). \tag{4.18}$$

Using (4.14) and (4.18) in (4.17) we obtain the following expansion,

$$x(\tau_{Rmax}) = 1 + \frac{\omega^2}{8}\tau_R^2 + \frac{\omega^2(15m - 2t^2)}{1152}\tau_R^4 + O(\tau_R^6),$$

where substituting τ_R by $\tau_R(\varepsilon)$ from (4.15), and multiplying by 2 due to the symmetry we obtain the expression of Theorem 4.2 for the amplitude.

In order to determine the stability of the periodic orbit, we follow Remark 4.1. We compute the determinant and trace of matrix M using (4.7), to obtain

$$\begin{aligned} \text{trace}(M) &= -1 + \left(\frac{2d}{\omega^2} - t\right)\tau_R + \left(\frac{dt}{\omega^2} - \frac{t^2}{2}\right)\tau_R^2 + \\ &\quad + \frac{2d\rho(\omega^2 + 2t^2 - 2m) + \omega^2(2t\rho(\omega^2 - t^2) - \delta)}{12\rho\omega^2}\tau_R^3 + O\left(\tau_R^4\right), \end{aligned}$$

and

$$\det(M) = 1 + t\tau_R + \frac{t^2}{2}\tau_R^2 + \frac{2\rho(t^3 - \delta) - \delta}{12\rho}\tau_R^3 + O\left(\tau_R^4\right).$$

For $|\varepsilon|$ sufficiently small, we have $\tau_R(\varepsilon)$ also small and positive, so that $|\det(M)| < 1$ if and only if $t < 0$, and $|\operatorname{trace}(M) + 1| < 1 - \det(M)$ if and only if $d < 0$ and $\delta > 0$. Therefore, using Remark 4.1, the eigenvalues of the derivative of the complete Poincaré map Π are inside the unit circle and then, the bifurcating limit cycle is stable if and only if $t < 0$, $d < 0$ and $\delta > 0$, and the theorem follows. ■

By using Proposition 4.1 we could add a new assertion saying that the bifurcating limit cycle is completely unstable (the two characteristic exponents have positive real part) if and only if $t > 0$, $\delta < 0$ and $d > 0$.

The case $\delta = 0$, that is, $d = t\omega^2$, when $d \neq 0$ can be shown with the same techniques but requires a special treatment.

Theorem 4.3 *Assume for system* (4.1)-(4.2) *under conditions* (4.4) *that* $\rho \neq 0$, $m \neq \omega^2$ *and* $d = t\omega^2 \neq 0$, *and fixed. For* $\varepsilon = 0$ *the system* (4.1)-(4.2) *undergoes a tri-zonal limit cycle bifurcation. For* $|\varepsilon|$ *sufficiently small and* $\rho\varepsilon t(\omega^2 - m) > 0$ *one limit cycle bifurcates from the ellipse* $\{(x, y, z)^T \in \mathbb{R}^3 : \omega^2 x^2 + y^2 = \omega^2,\ z = 0\}$.

This limit cycle is symmetric with respect to the origin and has period

$$P = \frac{2\pi}{\omega} + \left(\frac{2000\pi^3\rho^3(m-\omega^2)^2}{9t^3\omega^9}\right)^{1/5} \varepsilon^{3/5} + O(\varepsilon^{4/5}),$$

its amplitude in x *measured as* $\max\{x\} - \min\{x\}$, *is*

$$A = \ 2 + \left(\frac{15\pi\rho\omega^4}{4d(\omega^2-m)}\right)^{2/5} \varepsilon^{2/5} + \\ + \frac{(\pi^2\rho^2\omega^3)^{2/5}(39m - 2t^2 + 168\omega^2)}{56 \cdot 120^{1/5}\,[d(\omega^2-m)]^{4/5}} \varepsilon^{4/5} + O(\varepsilon),$$

and it passes through the point $P_0 = (1, y_0, z_0)^T$, *where*

$$y_0 = \ -\left(\frac{15\pi\rho\omega^7}{4(\omega^2-m)t}\right)^{1/5} \varepsilon^{1/5} + \left(\frac{25\pi^2t^3\rho^2\omega^4}{432(\omega^2-m)^2}\right)^{1/5} \varepsilon^{2/5} + O(\varepsilon^{3/5})$$

and

$$z_0 = -\left(\frac{125\pi^3t^2\rho^3\omega^{11}}{32 \cdot 18(\omega^2-m)^3}\right)^{1/5} \varepsilon^{3/5} + \frac{\pi\rho\omega(-9m + t^2 + 63\omega^2)}{84(m-\omega^2)}\varepsilon + O(\varepsilon^{6/5}).$$

Furthermore, the bifurcating limit cycle is stable if and only if $t < 0$ *and* $\rho\varepsilon > 0$.

Proof Since the bifurcation studied involves again the three linear zones, the procedure to detect and analyze these periodic orbits is the same as before and we can follow step by step the proof of Theorem 4.2. We arrive at the closing equations (4.12) for the case $\delta = 0$, with the same Jacobian matrix (4.13). After applying the Implicit Function Theorem for analytic functions [12], we can assure again the existence of a function $\mathbf{v}(\tau_R) = (\tau_C(\tau_R), \varepsilon(\tau_R), y_0(\tau_R), z_0(\tau_R))$ in the neighborhood of $\tau_R = 0$ with the following series expansions

$$\begin{aligned}
\tau_C &= \frac{\pi}{\omega} - \tau_R + \frac{\omega^2 - m}{12}\tau_R^3 + \frac{m(t^2 + 15\omega^2 - 6m) - t^2\omega^2 - 9\omega^4}{720}\tau_R^5 + O\left(\tau_R^6\right), \\
\varepsilon &= -\frac{t\omega^3(m - \omega^2)}{120\pi\rho}\tau_R^5 + O\left(\tau_R^6\right), \\
y_0 &= -\frac{\omega^2}{2}\tau_R + \frac{t\omega^2}{12}\tau_R^2 - \frac{m\omega^2}{24}\tau_R^3 + \frac{t\omega^2(7m - t^2 - 6\omega^2)}{720}\tau_R^4 + O\left(\tau_R^6\right), \\
z_0 &= -\frac{t\omega^4}{24}\tau_R^3 + \frac{t\omega^4(t^2 - 6m)}{1440}\tau_R^5 + O\left(\tau_R^6\right).
\end{aligned} \tag{4.19}$$

Since $m \neq \omega^2$, we can invert the series $\varepsilon(\tau_R)$ applying again Lemma 4.1, taking now $n = 5$, $\xi = \tau_R$ and $\eta = \varepsilon$, so that we obtain

$$\tau_R(\varepsilon) = \left(\frac{120\pi\rho}{t\omega^3(\omega^2 - m)}\right)^{1/5}\varepsilon^{1/5} + \frac{(\pi\rho)^{3/5}(-51m + 8t^2 + 63\omega^2)}{21 \cdot 450^{1/5}\left[t\omega^3(\omega^2 - m)\right]^{3/5}}\varepsilon^{3/5} + O\left(\varepsilon^{4/5}\right). \tag{4.20}$$

Since the time τ_R must be always positive, the condition $\rho\varepsilon t(\omega^2 - m) > 0$ must hold.

We obtain $\tau_C(\varepsilon)$, $y_0(\varepsilon)$ and $z_0(\varepsilon)$ replacing $\tau_R(\varepsilon)$ in their respective expressions of (4.19). Using that the period of the orbit is $P = 2(\tau_C + \tau_R)$ we get the corresponding series given in the Theorem 4.3.

Following the same reasoning and procedure employed in Theorem 4.2, we obtain the expression of the time τ_{Rmax}, where x reaches its maximum value $x(\tau_{Rmax})$,

$$\tau_{Rmax} = \frac{1}{2}\tau_R + \frac{t}{24}\tau_R^2 + \frac{t(4m - 27\omega^2 - 2t^2)}{5760}\tau_R^4 + O(\tau_R^6).$$

The computed expression of $x(\tau_{Rmax})$ is the same obtained in Theorem 4.2 up to fifth order in τ_R, where substituting τ_R by $\tau_R(\varepsilon)$ from (4.20), and multiplying by 2 due to the symmetry of the periodic orbit, we get the expression given for the amplitude.

In order to determine the stability of the periodic orbit, we follow Remark 4.1 again, now obtaining

$$\begin{aligned}\operatorname{trace}(M) &= -1 + t\tau_R + \frac{t^2}{2}\tau_R^2 + \frac{t(2\omega^2 + t^2 - 2m)}{6}\tau_R^3 + \\ &\quad + \frac{t^2(4\omega^2 + t^2 - 4m)}{24}\tau_R^4 + O\left(\tau_R^5\right),\end{aligned}$$

and

$$\det(M) = 1 + t\tau_R + \frac{t^2}{2}\tau_R^2 + \frac{t^3}{6}\tau_R^3 + \frac{t^4}{24}\tau_R^4 + O\left(\tau_R^5\right).$$

For $|\varepsilon|$ sufficiently small, we have $\tau_R(\varepsilon)$ also small and positive, so that $|\det(M)| < 1$ if and only if $t < 0$, and we claim that $|\operatorname{trace}(M) + 1| < 1 - \det(M)$ if and only if $m > \omega^2$. To show the claim, we write

$$\operatorname{trace}(M) = -1 + t\tau_R + \frac{t^2}{2}\tau_R^2 + \frac{t(t^2 + 2(\omega^2 - m))}{6}\tau_R^3 + O(\tau_R^4),$$

so that

$$\operatorname{trace}(M) + 1 = t\tau_R + \frac{t^2}{2}\tau_R^2 + \frac{t(t^2 + 2(\omega^2 - m))}{6}\tau_R^3 + O(\tau_R^4).$$

If τ_R is small enough the above expression is negative provided that $t < 0$, and the inequality $|\operatorname{trace}(M) + 1| < 1 - \det(M)$ is equivalent to

$$-t\tau_R - \frac{t^2}{2}\tau_R^2 - \frac{t(t^2 + 2(\omega^2 - m))}{6}\tau_R^3 + O(\tau_R^4) < -t\tau_R - \frac{t^2}{2}\tau_R^2 - \frac{t^3}{6}\tau_R^3 + O(\tau_R^4),$$

that is

$$-\frac{t(\omega^2 - m)}{3}\tau_R^3 + O(\tau_R^4) < 0,$$

and the claim is shown. Combining the conditions $t < 0$ and $m > \omega^2$ with $\rho\varepsilon t(\omega^2 - m) > 0$, we obtain the stability conditions given in Theorem 4.3 and the conclusions follows. ∎

We note that in the degenerate case of Theorem 4.3 the achieved expansions are analytical functions in the variable $\varepsilon^{1/5}$, while in the generic case of Theorem 4.2 the expansions were in the variable $\varepsilon^{1/3}$.

In order to analyze possible bizonal limit cycles of system (4.1)-(4.2),the present symmetry imposes that such bizonal limit cycles exist always in pairs, crossing each one the boundaries $x = 1$, and $x = -1$, respectively. So, in what follow, we are going to study the limit cycle which appears crossing the plane $x = 1$, by defining the auxiliary system,

$$\dot{\mathbf{x}} = \begin{cases} A_R\mathbf{x} + \mathbf{b}, & \text{if } x \geqslant 1, \\ A_C\mathbf{x}, & \text{if } x < 1, \end{cases} \tag{4.21}$$

with only two zones of linearity. Of course, only the limit cycles of system (4.21) that are contained in the region $x \in [-1, \infty)$ are also limit cycles of system (4.1)-(4.2), representing one of the two members of the pair.

The equilibria of system (4.21) are the origin in the zone with $x < 1$ and $\mathbf{x}_\varepsilon^+$ in the zone with $x \geq 1$ (see Proposition 4.2). In an analogous way to the analysis done for the tri-zonal periodic orbits, we consider system (4.21) with $\varepsilon = 0$. Then each solution in the zone with $x < 1$ starting from an arbitrary point $(x_0, y_0, z_0)^T$ for $\tau = 0$ is given by (4.5), and the corresponding orbit is an arc of a ellipse with the same expression given in (4.6). Now, if this ellipse is completely contained in the region $x < 1$ then we have $z_0 < \omega^2$. This family of ellipses completely contained in the region $x < 1$ generates an unbounded solid cone C foliated by periodic orbits.

Note that, this unbounded solid cone can be obtained by extending down to infinity the upper cone of Figure 4.3. In this case, only the periodic orbits of system (4.21) verifying $|x| \leq 1$ correspond to periodic orbits of system (4.1)-(4.2).

As we are going to see, a limit cycle of system (4.21) can appear for $\varepsilon \neq 0$ from a periodic orbit of the boundary of the cone C, that is from a horizontal ellipse with center at $(z/\omega^2, 0, z)^T$ and x-semiaxis $1 - z/\omega^2$. So when $|\varepsilon|$ is sufficiently small and $0 < z < \omega^2$, we can assure that the first coordinate of the points of the bifurcated limit cycle is in the range $x \in (-1, \infty)$ and consequently such limit cycle of system (4.21) is also a limit cycle for system (4.1)-(4.2). Furthermore, the symmetry of system (4.1)-(4.2) enforces the presence of a symmetrical limit cycle, now in the region $x \in (-\infty, 1)$. Thus the bifurcation to be shown involves the appearance of a couple of twin limit cycles for system (4.1)-(4.2), each one bifurcating from the boundary of one of the two cones of Figure 4.3.

First, we provide the auxiliary results which are related to periodic orbits that live in two linearity zones. In order to detect such orbits, we work with system (4.21), since every bizonal periodic orbit of system (4.1)-(4.2) not using the left zone, is also a periodic orbit of system (4.21).

Let us assume for system (4.21) that a periodic orbit Ω starts from a point $\bar{P}_0 = (1, y_0, z_0)^T = (1, \bar{\mathbf{p}}_0)^T$ at the plane $x = 1$, going into zone $x > 1$ and reaching a point $\bar{P}_1 = (1, y_1, z_1)^T = (1, \bar{\mathbf{p}}_1)^T$ after a time $\bar{\tau}_R$. The periodic orbit Ω continues from $\bar{P}_1$ and returns to the plane $x = 1$ at $\bar{P}_0$ employing a time $\bar{\tau}_C$. See Figure 4.6.

By the continuity of the flow, it is possible to define in an adequate open set within the plane $x = 1$ the functions π_R and π_C, such that $\pi_R(\bar{\mathbf{p}}_0) = \bar{\mathbf{p}}_1$ and $\pi_C(\bar{\mathbf{p}}_1) = \bar{\mathbf{p}}_0$ and their composition $\pi = \pi_C \circ \pi_R$ is the complete return map. We denote by $\tau_R(\mathbf{p}_0)$ the time spent by the orbit from P_0 to P_1, being $P_0 = (1, \mathbf{p}_0)$ and $P_1 = (1, \mathbf{p}_1)$ points with $x = 1$ in a neighborhood of $\bar{P}_0$ and $\bar{P}_1$ respectively. Let us call $\tau_C(\mathbf{p}_1)$ the time employed from P_1 to P_2. We denote derivatives with respect to the restricted coordinates on the plane $x = 1$ as $D_{\mathbf{p}}(\cdot)$. Then, if we denote by $\tau(\mathbf{p}_0)$ the total time spent by the orbit to pass from P_0 to P_2, we conclude that $D_{\mathbf{p}}\tau(\mathbf{p}_0) = D_{\mathbf{p}}\tau_R(\mathbf{p}_0) + D_{\mathbf{p}}\tau_C(\mathbf{p}_1)D_{\mathbf{p}}\pi_R(\mathbf{p}_0)$.

The eigenvalues of the derivative $D_{\mathbf{p}}\pi$ at the point $\bar{\mathbf{p}}_0$ can be computed by using the next result, which is a particularization of Proposition 2.12 for the 3D case and appeared in Proposition 3 of [7].

Proposition 4.4 *Assume that system* (4.21) *has a periodic orbit transversal to the plane* $x = 1$ *through the points* $(1, \bar{\boldsymbol{p}}_0)^T$ *and* $(1, \bar{\boldsymbol{p}}_1)^T$. *Then the product of the matrices*

$$\begin{pmatrix} 1 & D_{\boldsymbol{p}}\tau_C(\bar{\boldsymbol{p}}_1) \\ 0 & D_{\boldsymbol{p}}\pi_C(\bar{\boldsymbol{p}}_1) \end{pmatrix} \begin{pmatrix} 1 & D_{\boldsymbol{p}}\tau_R(\bar{\boldsymbol{p}}_0) \\ 0 & D_{\boldsymbol{p}}\pi_R(\bar{\boldsymbol{p}}_0) \end{pmatrix} = \begin{pmatrix} 1 & D_{\boldsymbol{p}}\tau(\bar{\boldsymbol{p}}_0) \\ 0 & D_{\boldsymbol{p}}\pi(\bar{\boldsymbol{p}}_0) \end{pmatrix}$$

is similar to the matrix

$$M = e^{A_C\tau_C(\bar{\boldsymbol{p}}_1)}e^{A_R\tau_R(\bar{\boldsymbol{p}}_0)} = e^{A_C\bar{\tau}_C}e^{A_R\bar{\tau}_R}. \tag{4.22}$$

The following remark, analogous to Remark 4.1, is used to determine the stability of periodic orbits.

Remark 4.2 *We note that the matrix* M *in* (4.22) *has one eigenvalue equal to* 1. *We call* λ_1 *and* λ_2 *the other two eigenvalues. Writing* $p = \lambda_1 + \lambda_2$ *and* $q = \lambda_1\lambda_2$ *we see that* $\mathrm{trace}(M) = 1 + p$, $\det(M) = q$ *and the characteristic*

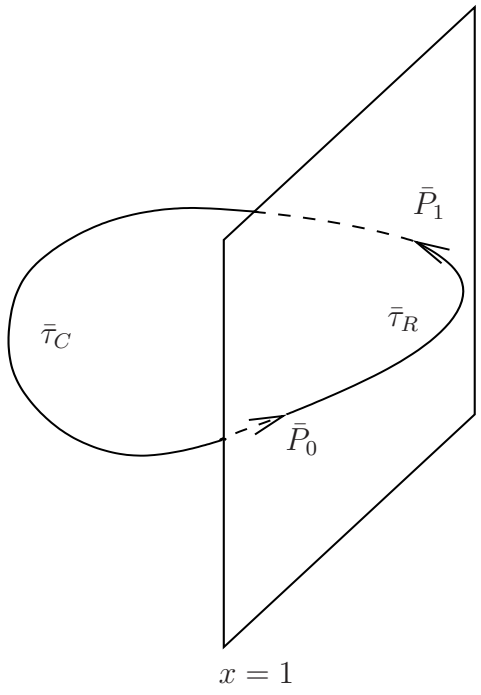

Figure 4.6: Bizonal periodic orbit of system (4.21) and the relevant points necessary to build the closing equations.

equation of matrix M is $(\lambda - 1)(\lambda^2 - p\lambda + q) = 0$. Thus λ_1 and λ_2 are the eigenvalues of the derivative $D_{\mathbf{p}}\pi$ and from Lemma 4.2 both eigenvalues λ_1 and λ_2 are inside the unit circle if and only if

$$|\det(M)| < 1 \quad \textit{and} \quad |\mathrm{trace}(M) - 1| < 1 + \det(M). \tag{4.23}$$

We summarize our results in the following theorem.

Theorem 4.4 *Assuming conditions* (4.4) *with $\rho \neq 0$, $\delta = d - t\omega^2 \neq 0$, $d\rho + \delta \neq 0$ and*

$$\hat{z} = \frac{d\rho\omega^2}{d\rho + \delta} < \omega^2,$$

and fixed, system (4.21) *undergoes a bizonal limit cycle bifurcation for the critical value $\varepsilon = 0$. Thus, a limit cycle exists when $\rho\delta\varepsilon > 0$ and $|\varepsilon|$ is sufficiently small.*

The limit cycle bifurcates from the ellipse

$$\frac{\left(x-\frac{\hat{z}}{\omega^2}\right)^2}{\left(1-\frac{\hat{z}}{\omega^2}\right)^2}+\frac{y^2}{\omega^2\left(1-\frac{\hat{z}}{\omega^2}\right)^2}=1, \quad z=\hat{z}, \tag{4.24}$$

its period is

$$P=\frac{2\pi}{\omega}-\frac{2\pi\rho\left(m-\omega^2\right)}{\delta\omega}\varepsilon+\frac{\left(576\pi^5\right)^{1/3}t\rho^2\left[\delta^2+\omega^2\left(m-\omega^2\right)^2\right]}{5(\delta^8\rho\omega^5)^{1/3}}\varepsilon^{5/3}+O\left(\varepsilon^{7/3}\right),$$

its amplitude in x measured as $\max\{x\}-\min\{x\}$ is

$$A=\frac{2\delta}{d\rho+\delta}+\frac{2d\rho^{5/3}(3\pi\omega^2)^{2/3}\left[2(d-mt)-5\delta\right]}{5\delta^{2/3}\left(d\rho+\delta\right)^2}\varepsilon^{2/3}+O\left(\varepsilon^{4/3}\right),$$

and it passes through the point $P_0=(1,y_0,z_0)^T$, where

$$y_0=\ -\frac{\left(3\pi\delta^2\rho\omega^5\right)^{1/3}}{d\rho+\delta}\varepsilon^{1/3}+\frac{\left(\pi^2\delta\rho^2\omega^4\right)^{1/3}t}{3^{1/3}(d\rho+\delta)}\varepsilon^{2/3}+O\left(\varepsilon^{4/3}\right),$$

and

$$z_0=\ \hat{z}+\frac{(9\pi^2\rho^5\omega^{10})^{1/3}d[3\delta+2t(m-\omega^2)]}{5\delta^{2/3}(d\rho+\delta)^2}\varepsilon^{2/3}+O\left(\varepsilon\right).$$

The limit cycle is stable if and only if $t<0$ and $\rho>0$, or $t=0$, $\rho>0$ and $d(2\rho-1)<0$.

Proof In order to determine limit cycles of system (4.21) that live in two linearity zones, we integrate the orbit that starts from a point $P_0=(1,y_0,z_0)^T$, staying in the zone $x>1$ arriving to the point $P_1=(1,y_1,z_1)^T$ after a time τ_R. If starting from P_0, we integrate backwards in the zone $x<1$ arriving at P_1 after a time $-\tau_C$ then we have completed a periodic orbit. The solution $(x(\tau),y(\tau),z(\tau))^T$ of system (4.21) in the zone $x>1$ passing through the point P_0 is again determined by (4.9).

In the same way, the backward solution $(x_b(\tau),y_b(\tau),z_b(\tau))^T$ of system (4.21) starting from P_0 is given again by (4.10). By defining the variable $\mathbf{w}=$

$(\tau_C, \varepsilon, y_0, z_0, \tau_R)$, we obtain the corresponding closing equations $\widehat{\mathbf{H}}(\mathbf{w}) = \mathbf{0}$, where

$$\begin{aligned}\widehat{H}_1(\mathbf{w}) &= x(\tau_R) - 1,\\ \widehat{H}_2(\mathbf{w}) &= x_b(\tau_C) - 1,\\ \widehat{H}_3(\mathbf{w}) &= y(\tau_R) - y_b(\tau_C),\\ \widehat{H}_4(\mathbf{w}) &= z(\tau_R) - z_b(\tau_C).\end{aligned}$$

System $\widehat{\mathbf{H}}(\omega) = \mathbf{0}$ constitutes a nonlinear system with four equations and five unknowns, and its solutions with $\tau_C > 0, \tau_R > 0$ and $y_0 < T(\varepsilon)$ for ε sufficiently small, correspond with periodic orbits of system (4.21), whenever $x(\tau) \geqslant 1$ for all $0 \leqslant \tau \leqslant \tau_R$ and $x_b(\tau) \leqslant 1$ for $0 \leqslant \tau \leqslant \tau_C$.

The above system has the solutions $\hat{\mathbf{w}} = (2\pi/\omega, 0, 0, z, 0)$ for all $z \leq \omega^2$, which correspond to ellipses with the same expressions (4.6) with $z_0 = z$, $y_0 = 0$ and $x_0 = 1$. From all this ellipses, which are tangent to the plane $x = 1$, we are going to study the possible bifurcation leading to the existence of limit cycles when $\varepsilon \neq 0$ and small. As we are going to show, such bifurcation appears from specific ellipse for a certain value $z = \hat{z}$, to be later determined.

Apart from the above solutions, for all $z \leq \omega^2$ the closing equations have the spurious solutions branch $\mathbf{w}_s = (2\pi/\omega, 0, \nu, z, 0)$ for all $z \leq \omega^2$ and for any $\nu \neq 0$, that does not correspond with periodic orbits of system (4.21) in a similar way to what happens in the proof of Theorem 4.2. This spurious solutions branch can be removed dividing $\widehat{H}_1$ by τ_R and defining the modified closing equations, through the functions

$$H_1(\mathbf{w}) = \frac{1}{\tau_R}\widehat{H}_1(\mathbf{w}), \quad H_i(\mathbf{w}) = \widehat{H}_i(\mathbf{w}), \quad i = 2, 3, 4.$$

Choosing τ_R as bifurcation parameter, we write the closing equations as $\mathbf{H}(\mathbf{v}, \tau_R) = \mathbf{0}$, where $\mathbf{v} = (\tau_C, \varepsilon, y_0, z_0)$ and we parameterize their solutions for $\mathbf{v}$ in terms of τ_R. The Jacobian matrix at the point $(\hat{\mathbf{v}}, 0)$ with $\hat{\mathbf{v}} = (2\pi/\omega, 0, 0, z)$, is

$$L = D_{\mathbf{v}}\mathbf{H}(\hat{\mathbf{v}}, 0) = \begin{pmatrix} 0 & 2\rho - 1 & -1 & 0\\ 0 & \dfrac{2\pi}{\omega}\left(\dfrac{\rho+1}{\omega^2}z - \rho\right) & 0 & 0\\ \omega^2 - z & 0 & 0 & 0\\ 0 & -\dfrac{2\pi}{\omega}z & 0 & 0 \end{pmatrix}.$$

Since the matrix L has not full rank, we can not apply the Implicit Function Theorem and we will use the Lyapunov Schmidt reduction procedure, see [33].

Assuming $z \neq \omega^2$ the rank of matrix L is equal to three and the image $\Im(L)$ of the corresponding linear map is generated by the vectors

$$\left\{(1,0,0,0)^T, (0,0,1,0)^T, \left(0, \rho - \frac{\rho+1}{\omega^2}z, 0, z\right)^T\right\},$$

while, $\ker(L)$, the kernel of L, is generated by the vector $(0,0,0,1)^T$. We decompose the space $\mathbb{R}^4$ as a direct sum of the subspace $\Im(L)$ and its orthogonal complement $\Im(L)^\perp$, which is generated by the vector $(0, \omega^2 z, 0, z(\rho+1) - \rho\omega^2)^T$.

The orthogonal projection matrix onto $\Im(L)^\perp$ is

$$Q_{\Im(L)^\perp} = \frac{1}{\sigma^2}\begin{pmatrix} 0 & 0 & 0 & 0 \\ 0 & z^2\omega^4 & 0 & z\omega^2(z(\rho+1)-\rho\omega^2) \\ 0 & 0 & 0 & 0 \\ 0 & z\omega^2(z(\rho+1)-\rho\omega^2) & 0 & (z(\rho+1)-\rho\omega^2)^2 \end{pmatrix},$$

where $\sigma = \sqrt{\omega^4 z^2 + (z(\rho+1)-\rho\omega^2)^2}$, and the orthogonal projection matrix onto $\Im(L)$ is obviously $Q_{\Im(L)} = I - Q_{\Im(L)^\perp}$.

Note that the vanishing of $\mathbf{H}(\mathbf{v}, \tau_R)$ implies the vanishing of its two projections onto $\Im(L)$ and $\Im(L)^\perp$. The condition $Q_{\Im(L)}\mathbf{H}(\mathbf{v}, \tau_R) = \mathbf{0}$ leads to

$$\begin{pmatrix} H_1 \\ (\sigma^2 - z^2\omega^4)\, H_2 - z\omega^2(z(\rho+1)-\rho\omega^2)H_4 \\ H_3 \\ -z\omega^2(z(\rho+1)-\rho\omega^2)H_2 + z^2\omega^4 H_4 \end{pmatrix} = \mathbf{0}, \tag{4.25}$$

while the condition $Q_{\Im(L)^\perp}\mathbf{H}(\mathbf{v}, \tau_R) = \mathbf{0}$ is

$$\begin{pmatrix} 0 \\ z^2\omega^4 H_2 + z\omega^2(z(\rho+1)-\rho\omega^2)H_4 \\ 0 \\ z\omega^2(z(\rho+1)-\rho\omega^2)H_2 + (z(\rho+1)-\rho\omega^2)^2 H_4 \end{pmatrix} = \mathbf{0},$$

and taking into account that the second row of this last expression is linearly dependent on the fourth row, we arrive after reducing non-vanishing factors at the reduced equation

$$g(z, \tau_R) = z\omega^2 H_2 + \left[z(\rho+1) - \rho\omega^2\right] H_4 = 0. \tag{4.26}$$

Analogously, the second row of expressions (4.25) is linearity dependent on the fourth row, so we can remove the such row and define after removing non-vanishing factor, the vectorial function $\mathbf{\Phi}(\mathbf{v}, \tau_R)$ such that

$$\begin{aligned}
&\Phi_1(\mathbf{v}, \tau_R) = H_1(\mathbf{v}, \tau_R),\\
&\Phi_2(\mathbf{v}, \tau_R) = (z(\rho+1) - \rho\omega^2)\, H_2 - z\omega^2 H_4,\\
&\Phi_3(\mathbf{v}, \tau_R) = H_3(\mathbf{v}, \tau_R),
\end{aligned}$$

so that system

$$\mathbf{\Phi}(\mathbf{v}, \tau_R) = \mathbf{0}, \tag{4.27}$$

is equivalent to (4.25).

The decomposition $\mathbb{R}^4 = \ker(L) \oplus \ker(L)^{\perp}$ leads to $\mathbf{v} = (\tau_C, \varepsilon, y_0, 0) + (0, 0, 0, z_0)$. We define the new variables $\tau_h = \tau_C - 2\pi/\omega$ and $z_h = z_0 - z$, so that $\mathbf{v} = (2\pi/\omega, 0, 0, z) + (\widetilde{\mathbf{v}}, z_h)$ where $\widetilde{\mathbf{v}} = (\tau_h, \varepsilon, y_0)$. In the new variables we can write the system (4.27) in the form $\mathbf{\Phi}(\widetilde{\mathbf{v}}, z_h, \tau_R) = \mathbf{0}$ with $\mathbf{\Phi}(\mathbf{0}, 0, 0) = \mathbf{0}$. The Jacobian matrix of Φ evaluated at $(\widetilde{\mathbf{v}}, z_h, \tau_R) = (\mathbf{0}, 0, 0)$ is equal to

$$D_{\widetilde{\mathbf{v}}}\mathbf{\Phi}(\mathbf{0}, 0, 0) = \begin{pmatrix} 0 & 2\rho - 1 & -1 \\ 0 & 2\pi\sigma^2/\omega^2 & 0 \\ \omega^2 - z & 0 & 0 \end{pmatrix},$$

and its determinant is different from zero if $z \neq \omega^2$.

Now, the Implicit Function Theorem for analytic functions, see [13], can be applied if $\hat{z} \neq \omega^2$, leading to the existence of the vectorial function $\widetilde{\mathbf{v}}(z_h, \tau_R) = (\tau_h(z_h, \tau_R), \varepsilon(z_h, \tau_R), y_0(z_h, \tau_R))$, such that equation $\mathbf{\Phi}(\widetilde{\mathbf{v}}(z_h, \tau_R), z_h, \tau_R) = \mathbf{0}$ is fulfilled. Once the existence of analytic function $\widetilde{\mathbf{v}}(z_h, \tau_R)$ has been assured we can determine the first terms of its series expansion.

These series can be computed assuming undetermined coefficients in the form

$$\begin{aligned}
\tau_C &= a_{10}\tau_R + a_{01}z_h + a_{11}\tau_R z_h + a_{20}\tau_R^2 + a_{02}z_h^2 + \cdots\\
\varepsilon &= b_{10}\tau_R + b_{01}z_h + b_{11}\tau_R z_h + b_{20}\tau_R^2 + b_{02}z_h^2 + \cdots\\
y_0 &= c_{10}\tau_R + c_{01}z_h + c_{11}\tau_R z_h + c_{20}\tau_R^2 + c_{02}z_h^2 + \cdots
\end{aligned}$$

Substituting these expressions in equation (4.27) and solving term by term

for each order in variables τ_R and z_h we obtain

$$\begin{aligned}
\tau_C(z_h,\tau_R) &= \frac{2\pi}{\omega}-\tau_R+\frac{1}{12}\tau_R^3\left(\omega^2-m\right)+\text{h.o.t.},\\
\varepsilon(z_h,\tau_R) &= \frac{\omega^3\left(\omega^2-z\right)\left[t\left((\rho+1)z-\rho\omega^2\right)+dz\omega^2\right]}{24\pi\sigma^2}\tau_R^3+\text{h.o.t.},\\
y_0(z_h,\tau_R) &= \frac{z-\omega^2}{2}\tau_R+\frac{\left(\omega^2-z\right)t}{12}\tau_R^2+\frac{z_h}{2}\tau_R+\text{h.o.t.}
\end{aligned} \tag{4.28}$$

We substitute these series in the reduced equation (4.26), obtaining

$$g(z_h,\tau_R)=\frac{1}{12}z\omega^2(z-\omega^2)(-dz-dz\rho+tz\omega^2+d\rho\omega^2)\tau_R^3+h.o.t.$$

Defining the parameter $\delta=d-t\omega^2$ and assuming in what follows that $\delta\neq 0$, the above equation only can have solution for $\tau_R\neq 0$ if we choose as the initial value for $\varepsilon=0$, the value $z=\hat{z}$, where

$$\hat{z}=\frac{d\rho\omega^2}{(\rho+1)d-t\omega^2}=\frac{d\rho\omega^2}{d\rho+\delta},$$

which is well defined and different from ω^2, from the hypotheses. Taking now $z=\hat{z}$ the new expression for $g(z_h,\tau_R)$ is

$$\begin{aligned}
g(z_h,\tau_R) &= \frac{\omega^2\delta}{12}\tau_R^3z_h-\frac{(t+d\omega^2)(d\rho+\delta)^2}{12(d^2+t^2)\rho\omega^2}\tau_R^3z_h^2-\\
&\quad-\frac{d\rho\delta\omega^6\left[5\delta+2(mt-d)\right]}{240(d\rho+\delta)^2}\tau_R^5+\text{h.o.t.},
\end{aligned} \tag{4.29}$$

and for $\tau_R\neq 0$ we can remove the factor τ_R^3. Now, since $\delta\neq 0$, a new application of the Implicit Function Theorem leads to the existence of a function $z_h=\zeta(\tau_R)$ such that $g(\zeta(\tau_R),\tau_R)=0$. The series expansion of such function $\zeta(\tau_R)$ has the form

$$\zeta(\tau_R)=d_1\tau_R+d_2\tau_R^2+O(\tau_R^3).$$

Introducing this series in (4.29) and solving for each order in τ_R, we obtain

$$\zeta(\tau_R)=\frac{d\rho\omega^4(3\delta+2mt-2t\omega^2)}{20(d\rho+\delta)^2}\tau_R^2+O(\tau_R^3).$$

Given that $\hat{z} = z_0 - z_h$, we substitute $z_h = \zeta(\tau_R)$ in (4.28) obtaining the following series expansions,

$$\begin{aligned}
\tau_C &= \frac{2\pi}{\omega} - \tau_R - \frac{m-\omega^2}{12}\tau_R^3 + \\
&\quad + \frac{t^2(m-\omega^2) - 6m^2 - 6\delta + 15m\omega^2 - 9\omega^4}{720}\tau_R^5 + O(\tau_R^6), \\
\varepsilon &= \frac{\omega\delta}{24\pi\rho}\tau_R^3 + \frac{\omega\left[6m(\delta - t\omega^2) - t^2\delta - 9\delta\omega^2 + 6t\omega^4)\right]}{1440\pi\rho}\tau_R^5 + O(\tau_R^6), \\
y_0 &= -\frac{\omega^2\delta}{2(d\rho+\delta)}\tau_R + \frac{t\omega^2\delta}{12(d\rho+\delta)}\tau_R^2 + O(\tau_R^3), \\
z_0 &= \hat{z} + \frac{d\rho\omega^4\left[3\delta + 2t(m-\omega^2)\right]}{20(d\rho+\delta)^2}\tau_R^2 + O(\tau_R^3).
\end{aligned} \tag{4.30}$$

Since $\delta \neq 0$, we can invert the series $\varepsilon(\tau_R)$ applying Lemma 4.1, by taking $n = 3$, $\xi = \tau_R$ and $\eta = \varepsilon$. We obtain,

$$\begin{aligned}
\tau_R(\varepsilon) &= 2(3\pi)^{1/3}\left(\frac{\rho}{\omega\delta}\right)^{1/3}\varepsilon^{1/3} + \\
&\quad + \frac{2\pi\rho\left[\delta(t^2 - 6m + 9\omega^2) + 6t\omega^2(m-1)\right]}{15\omega\delta^2}\varepsilon + O(\varepsilon^{4/3}).
\end{aligned} \tag{4.31}$$

Since the variable τ_R provides the time spent by the limit cycle in zone $x > 1$, this time τ_R must be positive and the condition $\rho\delta\varepsilon > 0$ must hold.

By replacing $\tau_R(\varepsilon)$ in expressions of (4.30) we obtain the expressions $\tau_C(\varepsilon)$, $y_0(\varepsilon)$ and $z_0(\varepsilon)$.

The peak-to-peak amplitude of the limit cycle is measured as before, but now we cannot exploit the symmetry. Let us denote by τ_{Rmax} the time for which $x(\tau)$ reaches its maximum value $x(\tau_{Rmax})$ in the zone with $x > 1$, and by τ_{Rmin} the time for which $x(\tau)$ reaches its minimum value $x(\tau_{Rmin})$ in the zone with $x < 1$, so that, the amplitude is equal to $x(\tau_{Rmax}) - x(\tau_{Rmin})$. Thus, equalities (4.16) and (4.17) apply to this case, and we can also compute a series expansion in the variable τ_R for τ_{Rmax}. We get

$$\tau_{Rmax} = \frac{\tau_R}{2} + \frac{t}{24}\tau_R^2 + O(\tau_R^3). \tag{4.32}$$

Using (4.30) and (4.32) in (4.17) we obtain the expansion

$$x(\tau_{Rmax}) = 1 + O(\tau_R^3).$$

Analogously, the time τ_{Rmin} has a series expansion in the variable τ_R. Since the variable x reaches its minimum value for $\tau_R = \tau_{Rmin}$, the following equality must hold

$$\dot{x} = T(\varepsilon)x(\tau_{Rmin}) - y(\tau_{Rmin}) = 0, \tag{4.33}$$

where

$$\begin{pmatrix} x(\tau_{Rmin}) \\ y(\tau_{Rmin}) \\ z(\tau_{Rmin}) \end{pmatrix} = \exp\left(-\tau_{Rmin} A_C\right) \begin{pmatrix} 1 \\ y_0(\tau_R) \\ z_0(\tau_R) \end{pmatrix}. \tag{4.34}$$

From equalities (4.30), (4.33) and (4.34), the series expansion of τ_{Rmin} is,

$$\tau_{Rmin} = \frac{\pi}{\omega} - \frac{\tau_R}{2} + \frac{t}{12}\tau_R^2 + O(\tau_R^3). \tag{4.35}$$

Using (4.30) and (4.35) in (4.34) we obtain the expansion,

$$x(\tau_{Rmin}) = \frac{d\rho - \delta}{d\rho + \delta} - \frac{d\rho\omega^2[2(d - mt) - 5\delta]}{10(d\rho + \delta)^2}\tau_R^2 + O(\tau_R^3).$$

Substituting τ_R by $\tau_R(\varepsilon)$ from (4.31) and computing $A = x(\tau_{Rmax}) - x(\tau_{Rmin})$, we arrive at the expression of Theorem 4.4 for the amplitude.

Using that the period of the orbit is $P = \tau_C + \tau_R$ and (4.30), we easily get its series.

In order to determine the stability of the periodic orbit, we follow Remark 4.2, and we compute the determinant and trace of matrix M using (4.22) to

obtain

$$\begin{aligned}
\text{trace}(M) &= 3 + t\tau_R + \frac{t^2}{2}\tau_R^2 + \frac{\delta(2\rho-1)+2t^3\rho}{12\rho}\tau_R^3 + \\
&\quad + \frac{2\pi d\,[\rho(2t\omega^2-\delta)-\delta] + d\omega^3(1-2\rho)}{24\pi\rho\omega^2}\tau_R^4 + \\
&\quad + \frac{t(\pi t\rho(t^2-4\omega^2)+(2\rho-1)\omega^3))}{24\pi\rho}\tau_R^4 + O(\tau_R^5) \qquad (4.36)\\
\det(M) &= 1 + t\tau_R + \frac{t^2}{2}\tau_R^2 + \frac{\delta(2\rho-1)+2t^3\rho}{12\rho}\tau_R^3 + \\
&\quad + \frac{\pi t(t^3\rho+4\rho\delta-2\delta)+\delta\omega(1-2\rho)}{24\pi\rho}\tau_R^4 + O(\tau_R^5).
\end{aligned}$$

We analyze first the case $t \neq 0$. For ε sufficiently small, we have $\tau_R(\varepsilon)$ also small and positive, so that $|\det(M)| < 1$ if and only if $t < 0$. Using (4.36) in the additional required condition to get stable limit cycles, that is, $|\text{trace}(M) - 1| < 1 + \det(M)$, we need the inequality

$$\frac{\delta(d\rho+\delta)}{\rho} > 0. \qquad (4.37)$$

The hypothesis $\hat{z} < \omega^2$ implies

$$\frac{d\rho}{d\rho+\delta} < 1.$$

Now, we distinguish two cases. Assume first that $d\rho+\delta < 0$. Then $d\rho > d\rho+\delta$ and so $\delta < 0$, and then (4.37) is equivalent to $\rho > 0$. If now we consider $d\rho + \delta > 0$ then we have $d\rho < d\rho + \delta$ and so $\delta > 0$. Again we get as before the equivalence of (4.37) and the condition $\rho > 0$.

Now, if we consider $t = 0$, then $\delta = d$ and from $\hat{z} < \omega^2$ we obtain

$$\frac{\rho}{\rho+1} < 1,$$

that is, we need $\rho > -1$. We analyzed first the inequality $|\text{trace}(M) - 1| < 1 + \det(M)$ what it is equivalent to $\rho(\rho+1) > 0$. Since we require $\rho > -1$,

we also need $\rho > 0$ for stability. If we consider now the condition for stability $|\det(M)| < 1$, we will require $d\rho(2\rho-1) < 0$, which gives rise to the inequality $d(2\rho - 1) < 0$ provided that $\rho > 0$.

After this reasoning, using Remark 4.2, we can conclude that the eigenvalues of the derivative $D_p\pi$ of the Poincaré map π are inside the unit circle, that is, the last assertion of this theorem holds. ■

As suggested before, this result about system (4.21) can be transferred to the original system (4.1)-(4.2) in the case $0 < \hat{z} < \omega^2$, as follows.

Theorem 4.5 *Assume for system* (4.1)-(4.2) *under conditions* (4.4) *that*

$$\rho \neq 0,\ \delta = d - t\omega^2 \neq 0,\ d\rho + \delta \neq 0 \text{ and } 0 < \hat{z} = \frac{d\rho\omega^2}{d\rho + \delta} < \omega^2,$$

and fixed. Under these hypotheses a bizonal limit cycle bifurcation takes place for the critical value $\varepsilon = 0$. Thus, a symmetrical pair of limit cycles appears when $\rho\delta\varepsilon > 0$ and $|\varepsilon|$ is sufficiently small. They are stable if and only if $t < 0$ and $\rho > 0$, or $t = 0$, $\rho > 0$ and $d(2\rho - 1) < 0$. Their periods and amplitudes are provided in Theorem 4.4. One limit cycle passes through $(1, y_0, z_0)^T$ and its symmetrical one passes through $(-1, -y_0, -z_0)^T$ with y_0, z_0 given in Theorem 4.4.

Proof Since $0 < \hat{z} < \omega^2$), the proof of Theorem 4.5 follows directly from the comments before the statement of Theorem 4.4. ■

The following result summarizes the information provided in Theorems 4.2 and 4.5 about the existence and stability of limit cycles when both theorems simultaneously apply.

Corollary 4.1 *Assume for system* (4.1)-(4.2) *under conditions* (4.4) *that*

$$\rho \neq 0,\ \delta = d - t\omega^2 \neq 0,\ d\rho + \delta \neq 0 \text{ and } 0 < \frac{d\rho}{d\rho + \delta} < 1,$$

and fixed. Then, for $\rho\delta\varepsilon > 0$ and for $|\varepsilon|$ sufficiently small, there exist one tri-zonal limit cycle and a symmetrical pair of bizonal limit cycles. Furthermore,

- **(i)** *if $t = 0$, $\rho > 0$ and $d(2\rho - 1) < 0$ the tri-zonal limit cycle is unstable and the bizonal ones are stable.*
- **(ii)** *if $t < 0$, $\rho < 0$, $d < 0$ and $\delta > 0$ the tri-zonal limit cycle is stable but the bizonal ones are unstable.*

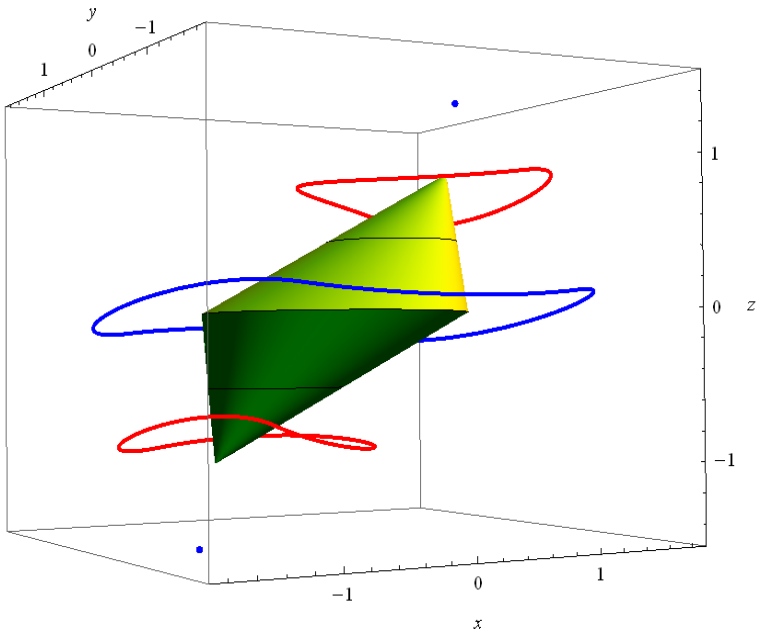

Figure 4.7: Limit cycles of system (4.1)-(4.2) under conditions (4.4) determined by Theorem 4.2 and Theorem 4.5 that exist for $\rho = -1$, $\varepsilon = -0.2$, $\omega = 1$, $t = -2$, $m = 2$ and $d = -1$. The tri-zonal limit cycle which appears in the center of the figure is stable, and the bizonal symmetrical ones are unstable. On the double cone, that exists only for $\varepsilon = 0$, there appear in thin line the ellipses where limit cycles have bifurcated from. The equilibria of external zones are stable.

(iii) *if $t < 0$, $\rho > 0$ but $d > 0$ or $\delta < 0$, the tri-zonal limit cycle is unstable and the bizonal ones are stable.*

(iv) *if $t > 0$ all the limit cycles are unstable.*

Just to illustrate the above results, we include some numerical examples. First, we consider system (4.1)-(4.2) and (4.4) with $\rho = -1$, $\varepsilon = -0.2$, $\omega = 1$, $t = -2$, $m = 2$ and $d = -1$. Here note that $\delta = d - t\omega^2 = 1 > 0$, and $\hat{z} = 1/2 < 1$. We show in Figure 4.7 the three different limit cycles predicted by our results, which have been obtained by direct computation and the double cone that existed for $\varepsilon = 0$. The tri-zonal limit cycle is the predicted by Theorem 4.2, being stable. As predicted by Theorem 4.5, other

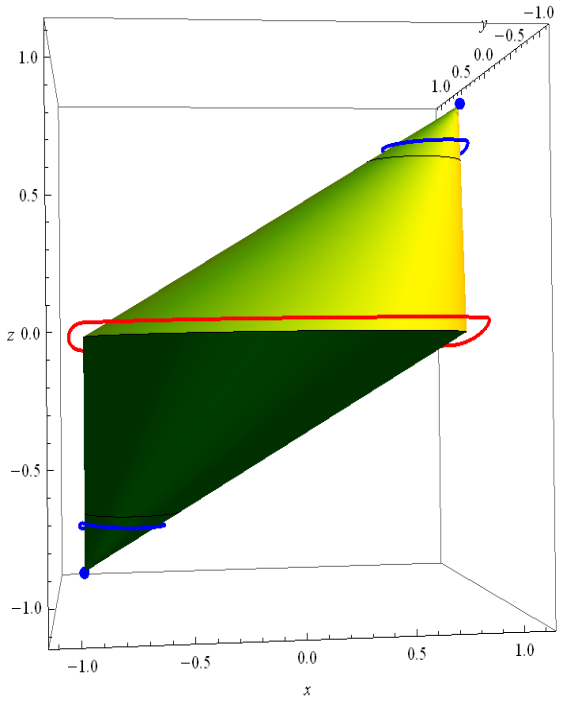

Figure 4.8: Limit cycles of system (4.1)-(4.2) under conditions (4.4) determined by Theorem 4.2 and Theorem 4.5 that exist for $\rho = 1$, $\varepsilon = -0.01$, $\omega = 1$, $t = -2$, $m = 2$ and $d = -3$. The tri-zonal limit cycle which appears in the center of the figure is unstable, and the bizonal symmetrical ones are stable. On the double cone, there appear in thin line the ellipses where limit cycles have bifurcated from. The equilibria of external zones are stable.

two limit cycles bifurcated from the marked ellipses on the double cone and they are unstable. From Proposition 4.2, apart from the origin we have two equilibrium near the vertices of the cones, which are stable.

Now, if we consider system (4.1)-(4.2) and (4.4) with $\rho = 1$, $\varepsilon = 0.1$, $\omega = 1$, $t = -2$, $m = 2$ and $d = 1$, three different limit cycles are also detected. Here $\delta = 3$. The tri-zonal one, predicted by Theorem 4.2, is unstable and the two bizonal limit cycles, predicted by Theorem 4.5, are stable. From Proposition 4.2, the positive sign of d implies the existence of two equilibria with $|x| > 1$, which are unstable.

Finally, as a third example, we consider system (4.1)-(4.2) and (4.4) with

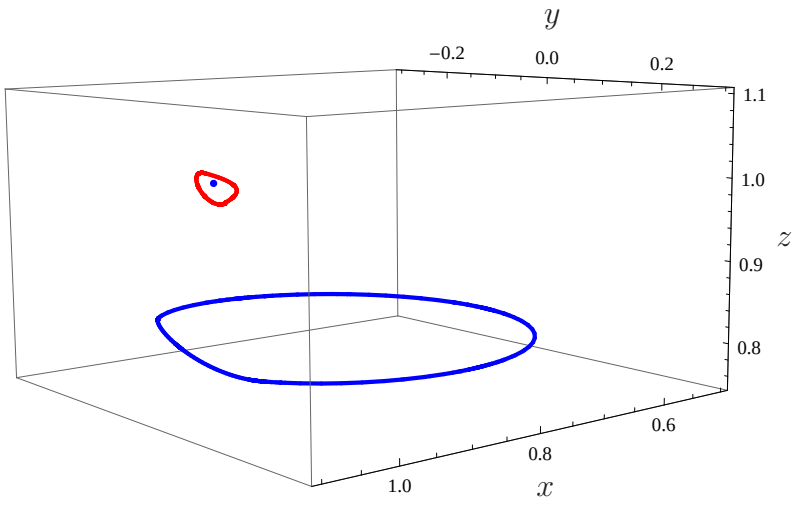

Figure 4.9: The periodic orbits in the vicinity of the upper equilibrium point for $\rho = 1$, $\varepsilon = -0.01$, $\omega = 1$, $t = -2$, $m = 2$ and $d = -3$, as in Figure 4.8. We show a new unstable periodic orbit, numerically detected which is between the stable equilibrium and the stable periodic orbit predicted by Theorem 4.5.

the values $\rho = 1$, $\varepsilon = -0.01$, $\omega = 1$, $t = -2$, $m = 2$ and $d = -3$. Now, $\delta = -1 < 0$ and $\hat{z} = 3/4 < 1$. From Theorem 4.2 and 4.5, for these parameter values three limit cycles also exist, appearing in Figure 4.8. The stability of the bifurcating limit cycles is the same that in the previous example, but now the equilibria of the external zones are stable because the Hurwitz conditions are fulfilled ($t < 0$, $d < 0$, $mt - d < 0$). Since we have that the bizonal limit cycles are stable and the isolated equilibria are also stable, it is natural to look for new invariant objects, between each nontrivial equilibrium and the nearest stable bizonal limit cycle. Thus, the invariant manifolds of these new objects should allow to organize the different attraction basins. In fact, after some numerical computations, we have detected a new pair of small unstable limit cycles, each one very near each nontrivial equilibrium point, see Figure 4.9. We conjecture that these new periodic orbits also bifurcate for $\varepsilon = 0$ and thus, the total number of periodic orbits related with the fold-Hopf bifurcation should be at least five. The analysis of this conjecture requires specific techniques and will be the aim of a future work.

4.3 A Hopf-pitchfork degeneration

In this section we tackle the degenerated case of the Hopf-pitchfork bifurcation (see [75]), analyzing what happens near $\delta = 0$, which requires $td > 0$. We use the parameters of the central zone to characterize this bifurcation, and since $\delta = d - t\omega^2$ we choose ω as the second bifurcation parameter, working in the parameter plane (ε, ω). In this plane, as we already know, the Hopf-pitchfork bifurcation takes place at the straight line $\varepsilon = 0$. On this line, δ vanishes at the point

$$(\varepsilon_*, \omega_*) = \left(0, \sqrt{d/t}\right). \tag{4.38}$$

We introduce the critical parameter deviations $\tilde{\varepsilon} = \varepsilon - \varepsilon_* = \varepsilon$ and $\tilde{\omega} = \omega - \omega_*$, to place the critical point $(\varepsilon_*, \omega_*)$ at the origin of the new parameter plane $(\tilde{\varepsilon}, \tilde{\omega})$. From the proof of Theorem 4.2, we know (see Section 4 of [77]) that there exists a symmetric periodic orbit using the three zones of linearity and with a flight time τ_R in the external zones, for the values of $\tilde{\varepsilon}$ satisfying

$$\begin{aligned}\tilde{\varepsilon} = \; & \frac{(\omega_* + \tilde{\omega})\left[d - t(\omega_* + \tilde{\omega})^2\right]}{12\pi\rho}\tau_R^3 + \\ & + \frac{(\omega_* + \tilde{\omega})\left[d(t^2 - 6m) + (\omega_* + \tilde{\omega})^2(9d + 12mt - t^3 - 15t(\omega_* + \tilde{\omega})^2)\right]}{720}\tau_R^5 + \\ & + O(\tau_R^6),\end{aligned}$$

which can be seen as the local definition of a surface in the space $(\tilde{\varepsilon}, \tilde{\omega}, \tau_R)$. In each point of the above surface we can assure the existence of a periodic orbit near the critical ellipse Γ that exists for $(\tilde{\varepsilon}, \tilde{\omega}) = (0,0)$. To analyze the above expression near the critical point $(\tilde{\varepsilon}, \tilde{\omega}) = (0, 0)$ we substitute $d = t\omega_*^2$ and write

$$\tilde{\varepsilon} = \left(-\frac{t\omega_*^2}{6\pi\rho}\tilde{\omega} + O(\tilde{\omega}^2)\right)\tau_R^3 + \left(\frac{(\omega_*^2 - m)t\omega_*^3}{120\pi\rho} + O(\tilde{\omega})\right)\tau_R^5 + O(\tau_R^6). \tag{4.39}$$

Disregarding higher order terms, we obtain the equality

$$\tilde{\varepsilon} + \frac{t\omega_*^2}{6\pi\rho}\tilde{\omega}\tau_R^3 + \frac{(m - \omega_*^2)t\omega_*^3}{120\pi\rho}\tau_R^5 = 0. \tag{4.40}$$

To determine the number of positive solutions in τ_R of (4.40), we enunciate the following auxiliary result.

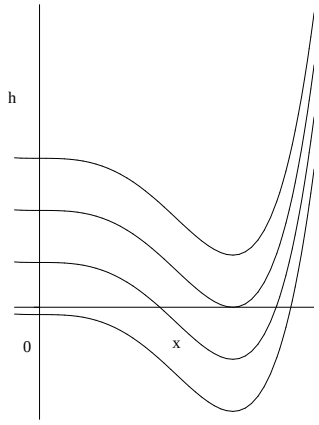

Figure 4.10: The graph of function h for statements (d) and (e) of Proposition 4.5 with different values of b_0.

Proposition 4.5 *Consider the function* $h(x) = b_0 + b_3x^3 + b_5x^5$, *and assume* $b_5 \neq 0$. *Then, the number of non-negative solutions of equation*

$$h(x) = 0, \tag{4.41}$$

behaves as follows.

(a) *For* $b_0 = 0$, *the equation always has the zero solution, it has no positive solution if* $b_3b_5 > 0$ *and it has the solution* $x = \sqrt{-b_3/b_5} > 0$ *when* $b_3b_5 < 0$.

(b) *For* $b_3 = 0$, *the equation has no positive solution if* $b_0b_5 > 0$, *having one positive solution for* $b_0b_5 < 0$.

(c) *If* $b_0b_5 > 0$ *and* $b_0b_3 > 0$, *there are no positive solutions.*

(d) *If* $b_0b_5 < 0$, *there is only one positive solution.*

(e) *When* $b_0b_5 > 0$ *and* $b_0b_3 < 0$, *the following cases arise after defining in the parameter plane* (b_0, b_3) *the expression*

$$h_*(b_0, b_3) = b_0 + \frac{2}{5}b_3\left(\frac{-3b_3}{5b_5}\right)^{3/2}. \tag{4.42}$$

(i) *If* $b_0h_*(b_0, b_3) < 0$, *then equation* (4.41) *has two positive solutions.*

(ii) *If $h_*(b_0, b_3) = 0$, then equation* (4.41) *has only one positive solution, namely $x = \sqrt{-3b_3/5b_5}$.*

(iii) *If $b_0 h_*(b_0, b_3) > 0$, then equation* (4.41) *has no positive solutions.*

Proof Statements (a) (b) and (c) are trivial.

Under hypotheses of statement (d), as there is one sign variation in the coefficients of $h(x)$, there exists only one positive solution from Descartes Rule of signs.

In statement (e), it is easy to check that $b_3 b_5 < 0$ and function $h(x)$ has only one local extremum for $x_* = \sqrt{-3b_3/5b_5} > 0$, where h takes the value given in (4.42). Since $h''(x_*) = -6b_3 x_*$, the extremum is a minimum point for $b_3 < 0$, and a maximum point for $b_3 > 0$. Furthermore, for $b_3 < 0$, $h(x)$ is monotonically decreasing in $[0, x_*)$ (increasing for $b_3 > 0$) and monotonically increasing (decreasing for $b_3 > 0$) in $(x_*, +\infty)$ since $h'(x) = x^2(3b_3 + 5b_5 x^2)$ has constant sign in these intervals.

Hereinafter we assume $b_0 > 0$, being the case $b_0 < 0$ completely analogous. Thus, in statement (e)-(i) we have $h_*(b_0, b_3) < 0$, so if $b_3 < 0$ then $h(x)$ has a global minimum point in $[0, +\infty)$ for $x = x_*$, with $h(x_*) = h_*(b_0, b_3) < 0$. It is easy to deduce that there are exactly two solutions with $x > 0$ for equation (4.41).

In the case (e)-(ii), the condition $h_*(b_0, b_3) = 0$ implies $h(x_*) = 0$, and this point is unique due to the monotony of $h(x)$ in $[0, x_*)$ and $(x_*, +\infty)$.

In statement (e)-(iii), as $b_0 > 0$, $b_5 > 0$ and $b_3 < 0$, $h(x)$ has a global minimum in $[0, +\infty)$ for $x = x_*$, being $h(x_*) = h_*(b_0, b_3) > 0$, so $h(x)$ has no zero with $x > 0$. ■

In Figure 4.10 we show the graph of function $h(x)$ according to different situations of statements (d) and (e) of the above proposition by moving the parameter b_0. In Figure 4.11, the number of positive solutions of (4.41) for different regions of the parameter plane (b_0, b_3) is represented for the case $b_5 > 0$, where the change from two positive roots to none happens at the curve

$$b_0 = -\frac{2}{5} b_3 \left(\frac{-3b_3}{5b_5} \right)^{3/2},$$

with $b_3 < 0$.

The following theorem is the main result of this section.

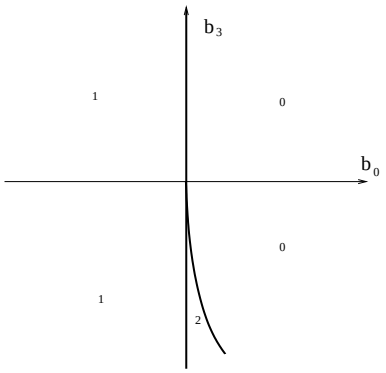

Figure 4.11: Number of positive solutions of (4.41) in the parameter plane (b_0, b_3) for $b_5 > 0$.

Theorem 4.6 *Assume $\rho \neq 0$, $td > 0$ and $m \neq \omega_*^2$ for system (4.1)-(4.2) under conditions (4.4). Consider in the parameter plane $(\tilde{\varepsilon}, \tilde{\omega})$ a sufficiently small neighborhood of the origin. This neighborhood is crossed by the straight line $\tilde{\varepsilon} = 0$, where the PWL Hopf-pitchfork bifurcation takes place. For parameter values in such neighborhood, and regarding the number of periodic orbits within a tubular neighborhood of the critical ellipse Γ, the following statements hold.*

(a) *In the region of the $(\tilde{\varepsilon}, \tilde{\omega})$ plane where condition $\rho t(m - \omega_*^2)\tilde{\varepsilon} < 0$ holds, there exists only one limit cycle born from the PWL Hopf-pitchfork bifurcation.*

(b) *In the region of the $(\tilde{\varepsilon}, \tilde{\omega})$ plane where condition $\rho t(m - \omega_*^2)\tilde{\varepsilon} > 0$ and within the zone where $\rho t\tilde{\varepsilon}\tilde{\omega} > 0$, there are no periodic solutions.*

(c) *In the region of the $(\tilde{\varepsilon}, \tilde{\omega})$ plane where condition $\rho t(m - \omega_*^2)\tilde{\varepsilon} > 0$ and within the zone where $\rho t\tilde{\varepsilon}\tilde{\omega} < 0$, there is a curve in the plane $(\tilde{\varepsilon}, \tilde{\omega})$ with local expression*

$$\tilde{\varepsilon}_{SN} = \frac{-1}{15\pi} \frac{t\omega_*^2 \tilde{\omega}}{\rho} \left(\frac{12\tilde{\omega}}{\omega_*(\omega_*^2 - m)} \right)^{3/2} + O(\tilde{\omega}^3), \tag{4.43}$$

so that there are two periodic orbits when $\tilde{\varepsilon}$ is between $\tilde{\varepsilon}_{SN}$ and zero, only one if $\tilde{\varepsilon} = \tilde{\varepsilon}_{SN}$, and no periodic orbits otherwise.

Proof To prove this theorem, we consider equation (4.40). We study this equation in a neighborhood of $(\tilde{\varepsilon}, \tilde{\omega}, \tau_R) = (0, 0, 0)$ small enough. We can assure that the number of solutions of equation (4.40) with $\tau_R > 0$ is equal, when $m \neq \omega_*^2$, to the number of periodic orbits of system (4.1) that bifurcate from the critical ellipse Γ in a neighborhood of $(\tilde{\varepsilon}, \tilde{\omega}) = (0, 0)$, see [77].

If we denote the coefficients of equation (4.40)

$$b_0 = \tilde{\varepsilon},\ b_3 = \frac{t\omega_*^2\tilde{\omega}}{6\pi\rho} \text{ and } b_5 = \frac{(m-\omega_*^2)t\omega_*^3}{120\pi\rho},$$

given that $\omega_* > 0$, by its definition, we can observe that

$$\begin{array}{rcl} \operatorname{sgn}(b_0) & = & \operatorname{sgn}(\tilde{\varepsilon}), \\ \operatorname{sgn}(b_3) & = & \operatorname{sgn}(t\rho\tilde{\omega}), \\ \operatorname{sgn}(b_5) & = & \operatorname{sgn}(t\rho(m-\omega_*^2)). \end{array} \tag{4.44}$$

Since from our hypotheses we have $b_5 \neq 0$, we can neglect higher order terms in determining the local number of solutions of (4.40) and apply Proposition 4.5 using the above expressions for b_0, b_3 and b_5. The statement (d) of this proposition implies that equation (4.40) has only one positive solution when $b_5\tilde{\varepsilon} < 0$. Taking into account the equalities (4.44), this condition is equivalent to $\rho t(m-\omega_*^2)\tilde{\varepsilon} < 0$, so that under this hypothesis and for points of the plane $(\tilde{\varepsilon}, \tilde{\omega})$ sufficiently near the origin, equation (4.39) also has a unique positive solution. Then the statement (a) of Theorem 4.6 is proved.

Using equalities (4.44), the conditions $b_5\tilde{\varepsilon} > 0$ and $b_3\tilde{\varepsilon} > 0$ are equivalent to $\rho t(m-\omega_*^2)\tilde{\varepsilon}$ and $\rho t\tilde{\varepsilon}\tilde{\omega} > 0$, so that from statement (c) of Proposition 4.5, equation (4.40) has no positive solutions and statement (b) of Theorem 4.6 is proved.

If $b_5\tilde{\varepsilon} > 0$ and $b_3\tilde{\varepsilon} < 0$, statement (e) of Proposition 4.5 assures the existence of a curve $h^*(b_0, b_3) = 0$, where the number of solutions changes by two. From (4.42), a first order approximation of such curve, in a neighborhood of $(b_0, b_3) = (0, 0)$, is

$$b_0 = -\frac{2}{5}b_3\left(\frac{-3b_3}{5b_5}\right)^{3/2}. \tag{4.45}$$

Thus, using (4.44) and assuming $\rho t(m-\omega_*^2)\tilde{\varepsilon} > 0$ and $\rho t\tilde{\varepsilon}\tilde{\omega} < 0$, we can deduce the existence of a curve in the plane $(\tilde{\varepsilon}, \tilde{\omega})$ where the number of positive solutions of (4.39) is equal to one, establishing the transition from two solutions to none. Substituting the values of b_0, b_3 and b_5 in (4.45), such

curve is given locally by the expression

$$\tilde{\varepsilon}_{\rm SN} = \frac{-1}{15\pi}\frac{t\omega_*^2\tilde{\omega}}{\rho}\left(\frac{-12\tilde{\omega}}{\omega_*(m-\omega_*^2)}\right)^{3/2} + O(\tilde{\omega}^3). \tag{4.46}$$

The condition $b_0 h^*(b_0, b_3) < 0$ of Proposition 4.5 $(e.i)$ written in the variables $\tilde{\varepsilon}$ and $\tilde{\omega}$ near the origin translates to

$$\tilde{\varepsilon}\,(\tilde{\varepsilon} - \tilde{\varepsilon}_{\rm SN}) < 0.$$

Then, for $\tilde{\varepsilon}$ between zero and the value $\tilde{\varepsilon}_{\rm SN}$ given in (4.46), in a neighborhood of $(\tilde{\varepsilon}, \tilde{\omega}) = (0, 0)$, equation (4.39) has two positive solutions corresponding to periodic orbits. The remaining cases of statement (c) follow in a analogous way. Theorem 4.6 is proved. ■

We emphasize that around the origin, in the parameter plane $(\tilde{\varepsilon}, \tilde{\omega})$, the unfolding is very similar to the one appearing in the generalized Hopf bifurcation of differentiable dynamics. The analysis of this section, which will appear in [75], advances the analysis made in [77]. Future work should be directed to complete this analysis by considering the excluded case $m = \omega_*^2$, which corresponds to a higher degeneracy.

4.4 Examples for PWL Hopf-pitchfork

In this section we take some electronic oscillator as a benchmark in looking for practical devices where the PWL Hopf-pitchfork bifurcation can appear.

4.4.1 Realization in a generalized Chua's circuit

Here, we consider the generalized version of Chua's circuit that appears in Figure 4.12 (a), where a negative resistance device R_N has been introduced with respect to the standard model (see for example [45]). To obtain more information about negative resistance devices, see [13].

The state equations of the circuit of Figure 4.12 are (see [14])

$$\begin{aligned}
\frac{dv_1}{d\tau} &= \frac{1}{C_1}[G(v_2 - v_1) - f(v_1)], \\
\frac{dv_2}{d\tau} &= \frac{1}{C_2}[G(v_1 - v_2) + i_3], \\
\frac{di_3}{d\tau} &= -\frac{1}{L}\,(v_2 + R_N i_3)\,,
\end{aligned} \tag{4.47}$$

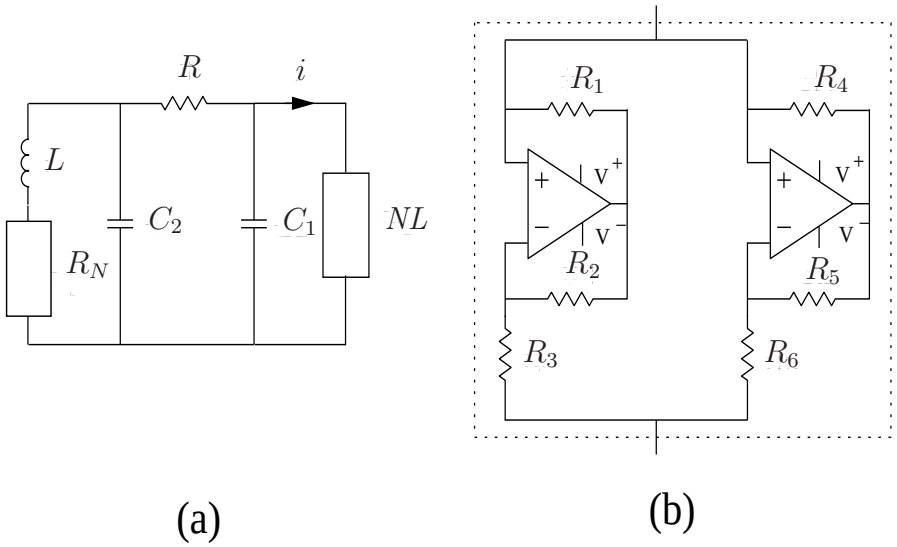

Figure 4.12: (a) Generalized version of Chua's circuit, including an extra negative resistance device R_N apart from the nonlinear resistance device NL. (b) Detailed circuit of the NL device.

where v_1 and v_2 are the voltages across the capacitors C_1 and C_2, i_3 is the current through the inductance L, the main conductance is $G = 1/R$, and the function

$$f(v_1) = G_b v_1 + \frac{1}{2}\left(G_a - G_b\right)\left\{|v_1 + E| - |v_1 - E|\right\}, \tag{4.48}$$

models the relevant part of the $v - i$ characteristics of the nonlinear resistor NL. The symbol E stands for the saturation voltage of the operational amplifiers in the implementation of the non-linear conductance NL, see Figure 4.12 (b). This characteristics is responsible for the appearance of multiple equilibria. In fact, after some algebraic manipulation, the existence of non-trivial equilibrium points is equivalent to the existence of solutions for the equation

$$-\frac{G}{1 + GR_N} v_1 = f(v_1).$$

The slopes

$$G_a = -\frac{1}{R_6} - \frac{1}{R_3}, \quad G_b = \frac{1}{R_4} - \frac{1}{R_3},$$

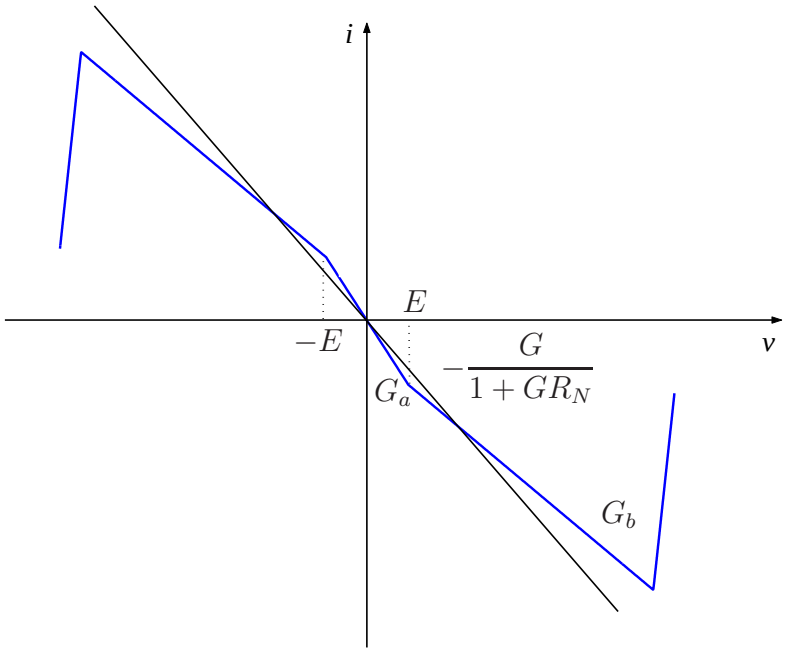

Figure 4.13: Current-voltage characteristic of the nonlinear resistance NL and the graph of the straight line $i = -(Gv)/(1 + GR_N)$.

characterize the inner regions where the circuit works, see Figure 4.13. It must be emphasized that there exist other two more external passive zones represented which are not used at all. In fact, it is usual to represent only the three innermost pieces of the characteristic of Figure 4.13.

Note that the dynamics in the circuit is governed by three linear systems which globally define a continuous piecewise linear vector field with three linear regions.

As suggested in [45], we may write Chua's circuit equations (4.47) in normalized dimensionless form by making the following change of variables

$$x = \frac{v_1}{E}, \quad y = \frac{v_2}{E}, \quad z = \frac{i_3}{EG}, \quad \bar{\tau} = \frac{\tau G}{C_2}.$$

Thus, we get

$$\begin{array}{rcl} \dfrac{dx}{d\bar{\tau}} & = & \begin{cases} \alpha\left[y - bx - (b-a)\right], & x < -1, \\ \alpha\left[y - ax\right], & |x| \leq 1, \\ \alpha\left[y - bx + (b-a)\right], & x > 1, \end{cases} \\ \dfrac{dy}{d\bar{\tau}} & = & x - y + z, \\ \dfrac{dz}{d\bar{\tau}} & = & -\beta y - \gamma z, \end{array} \tag{4.49}$$

where

$$a = 1 + \frac{G_a}{G}, \quad b = 1 + \frac{G_b}{G}, \quad \alpha = \frac{C_2}{C_1} > 0, \quad \beta = \frac{C_2}{LG^2} > 0, \quad \gamma = \frac{R_N C_2}{LG} < 0.$$

In this way, each set of circuit parameters has an equivalent set of five normalized dimensionless parameters $\{a, b, \alpha, \beta, \gamma\}$.

The linear matrix governing the dynamics n the central zone is

$$A_C = \begin{pmatrix} -\alpha a & \alpha & 0 \\ 1 & -1 & -1 \\ 0 & -\beta & -\gamma \end{pmatrix},$$

and the coefficients of the characteristic polynomials in each linear zone are expressed as follows

$$\begin{array}{rcl} T & = & -\alpha a - \gamma - 1, \\ M & = & \alpha(\gamma+1)a - \alpha + \beta + \gamma, \\ D & = & \alpha[\gamma - (\beta+\gamma)a], \\ t & = & -\alpha b - \gamma - 1, \\ m & = & \alpha(\gamma+1)b - \alpha + \beta + \gamma, \\ d & = & \alpha[\gamma - (\beta+\gamma)b], \end{array} \tag{4.50}$$

where capital letters correspond to the region with $|x| < 1$.

The observability matrix turns out to be

$$\mathcal{O} = \begin{pmatrix} 1 & 0 & 0 \\ -\alpha b & \alpha & 0 \\ \alpha^2 b^2 & -\alpha^2 b - \alpha & \alpha \end{pmatrix},$$

so that for $\alpha \neq 0$ the observability condition holds, see Chapter 2. Thus, there exists a linear change of variables putting the system in the canonical form (4.1)-(4.2).

In looking for the Hopf-pitchfork bifurcation, we need to check, apart from the hypotheses of different theorems, the feasibility of conditions (4.4), or in other words that it is possible to move parameters of the circuit in such a way that for ε in a neighborhood of 0 the desired eigenvalue transition occurs. Therefore, for all ε in a neighborhood of 0 the mentioned conditions must be satisfied, namely

$$\begin{array}{rcl} E_1 & := & (2\rho-1)\varepsilon+\alpha a+\gamma+1=0, \\ E_2 & := & \omega^2+\rho\varepsilon^2(\rho-2)-\alpha(\gamma+1)a+\alpha-\beta-\gamma=0, \\ E_3 & := & \varepsilon(\rho^2\varepsilon^2+\omega^2)+\alpha[\gamma-(\beta+\gamma)a]=0. \end{array} \tag{4.51}$$

In what follows we assume $b \neq a$, otherwise the model becomes linear, and we write $\alpha(\varepsilon)$, $\beta(\varepsilon)$ and $\gamma(\varepsilon)$ for the functions satisfying (4.51).

To avoid square roots, we introduce a new auxiliary parameter $\nu > 0$, such that

$$\nu^2 = 1-a-a^2\omega^2 = 1-a(1+a\omega^2), \tag{4.52}$$

and taking $\varepsilon = 0$ in the three equations of (4.51) and looking for positive values of α, we get

$$\begin{array}{rcl} \alpha_0=\alpha(0) & = & \dfrac{\nu-1}{a^2}, \\ \beta_0=\beta(0) & = & \dfrac{(1-a)(1-a-\nu)}{a^2}, \\ \gamma_0=\gamma(0) & = & \dfrac{1-a-\nu}{a}. \end{array} \tag{4.53}$$

We see that $\alpha_0 > 0$ requires $\nu > 1$, and from (4.52) we need $a(1+a\omega^2) < 0$, finally arriving at the condition

$$-\frac{1}{\omega^2} < a < 0.$$

Under this condition, we have

$$1 < \nu = \sqrt{1-a-a^2\omega^2} < \sqrt{1-a},$$

along with

$$1-a-\nu > 1-a-\sqrt{1-a} > 0,$$

sp that it is easy to see that $\beta_0 > 0$ and $\gamma_0 < 0$ always. Using now(4.53) it is easy to check that the condition

$$\det\left(\frac{\partial(E_1,E_2,E_3)}{\partial(\alpha,\beta,\gamma)}\right)_{\varepsilon=0} = \gamma_0 - a(2\alpha_0+\beta_0+\gamma_0) + a^2\alpha_0(1+\gamma_0) - a^3\alpha_0^2 = \\ = 2\nu\frac{1-\nu}{a} \neq 0$$

is fulfilled, so that the Implicit Function Theorem assures the existence of a branch of solutions of (4.51) starting from the point $(\alpha_0, \beta_0, \gamma_0)$, with $\alpha(\varepsilon) > 0$, $\beta(\varepsilon) > 0$ and $\gamma(\varepsilon) < 0$ for $|\varepsilon|$ sufficiently small. It is possible therefore to reproduce the Hopf-pitchfork bifurcation in this circuit, by moving ε in an neighborhood of 0 and taking such functions as reference for the values of parameters. We must notice that the linear invariant of the external zones would be not constant, however, contrarily to what was assumed in the proof of our previous results. This is not really problematic whenever we are far from a possible degeneration. In particular, we see that, from the last three equations of (4.50) for $\varepsilon = 0$, we obtain

$$\begin{aligned} t &= \frac{(b-a)(1-\nu)}{a^2}, \\ m &= \frac{(a-b)(\nu-1)^2 + a(1-a-\nu^2)}{a^3} = \omega^2 - \frac{(b-a)(\nu-1)^2}{a^3}, \\ d &= \frac{(b-a)(1-\nu)(1-a-\nu)}{a^4}. \end{aligned}$$

For this set of parameters corresponding to $\varepsilon = 0$, it is easy to check that the non-degeneracy condition

$$\delta = d - t\omega^2 = -\frac{(b-a)\nu(1-\nu)^2}{a^4} \neq 0, \tag{4.54}$$

holds. Then, the appearance of our non-smooth Hopf-pitchfork bifurcation in system (4.49) for $\varepsilon = 0$ and $\rho \neq 0$ is guaranteed by Theorem 4.2.

The bifurcating tri-zonal limit cycle is always unstable since $\mathrm{Sgn}(\delta) = \mathrm{Sgn}(t) = \mathrm{Sgn}(d)$. If we select $\rho > 0$ all the hypotheses of Theorem 4.5 are automatically fulfilled and we obtain that two bizonal limit cycles bifurcate and they are stable when $a < b$. In such case, the three limit cycles appear for $\varepsilon < 0$. From Proposition 4.2, there also appear two isolated equilibrium points and they turn out to be unstable, as an easy computation shows.

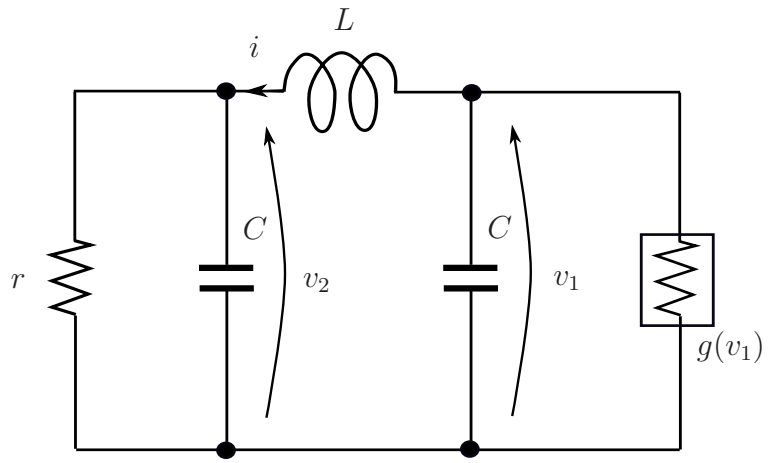

Figure 4.14: The extended BPV oscillator proposed in [71].

On the other hand, note that for the degenerated Hopf-pitchfork bifurcation studied in Section 4.3 exists in system (4.49), the degeneracy condition $\delta = 0$ must be fulfilled. Obviously, this condition holds if and only if $a = b$, $\nu = 0$ or $\nu = 1$. The case $a = b$ should be discarded because otherwise the model becomes linear, and the physical constraint $\alpha > 0$, which implies $\nu > 1$, excludes the other two possibilities. In conclusion, in this system, we cannot reproduce such a degenerated case for the Hopf-pitchfork bifurcation.

4.4.2 Realization in a extended BPV oscillator

Another physically and biologically interesting oscillator system is the Bonhoeffer-van der Pol (BVP for short) oscillator, which can be considered as a generalization of both the Duffing oscillator and the well-known van der Pol oscillator, see [54]. It is pointed out that apart from the familiar period-doubling bifurcations leading to chaotic motions, the system also exhibits resonance or *phase-locking* phenomena when external constant and periodic forces are applied. In this section we consider an extended BVP oscillator, which is consisted of two capacitors, an inductor and a linear resistor as shown in Figure 4.14. To obtain more information about this circuit, see [71], where a smooth nonlinearity is assumed and a rich variety of dynamical behaviors

is found. The circuit equation is described as follows:

$$\begin{cases} C\dfrac{dv_1}{dt} = & -i - g(v_1), \\ C\dfrac{dv_2}{dt} = & i - \dfrac{v_2}{r}, \\ L\dfrac{di}{dt} = & v_1 - v_2, \end{cases}$$

where v_1 and v_2 are the voltages across the capacitor C, i is the current through the inductance L, and the $v - i$ characteristics of the nonlinear resitor is written as $g(v) = -av - b\,\mathrm{sat}(cv)$. Note that here we adopt a PWL version of the nonlinearity considered in [71].

The normalized equation of the extended BVP oscillator is described as follows

$$\begin{cases} \dot{x} = & -z + \alpha x + \mathrm{sat}(\beta x), \\ \dot{y} = & z - \gamma y, \\ \dot{z} = & x - y, \end{cases}$$

where the dot represents derivative with respect to the time τ, and

$$\tau = \frac{1}{\sqrt{LC}}t, \quad \alpha = a\sqrt{\frac{L}{C}}, \quad \beta = bc\sqrt{\frac{L}{C}}, \quad \gamma = \frac{1}{r}\sqrt{\frac{L}{C}},$$

$$x = \frac{v_1}{b}\sqrt{\frac{C}{L}}, \quad y = \frac{v_2}{b}\sqrt{\frac{C}{L}}, \quad z = \frac{i}{b}.$$

Making the change of variables $X = \beta x$, we obtain the following system

$$\begin{cases} \dot{x} = & \alpha x - \beta z + \beta\,\mathrm{sat}(x), \\ \dot{y} = & -\gamma y + z, \\ \dot{z} = & \dfrac{1}{\beta}x - y, \end{cases} \tag{4.55}$$

where we have renamed X as x for convenience. This system is in its Luré form,

$$\dot{\mathbf{x}} = \begin{pmatrix} \alpha & 0 & -\beta \\ 0 & -\gamma & 1 \\ 1/\beta & -1 & 0 \end{pmatrix}\mathbf{x} + \begin{pmatrix} \beta \\ 0 \\ 0 \end{pmatrix}\mathrm{sat}(\mathbf{e}_1^T\mathbf{x}),$$

so applying Proposition 2.3, system (4.55) is observable if and only if the observability matrix $\mathcal{O}$ has rank 3, where

$$\mathcal{O} = \begin{pmatrix} 1 & 0 & 0 \\ \alpha & 0 & -\beta \\ \alpha^2 - 1 & \beta & -\alpha\beta \end{pmatrix}.$$

It is immediate to see that $\mathcal{O}$ has full rank is equivalent to $\beta \neq 0$.

Now, assuming $\beta \neq 0$, according to Proposition 2.4, there exists a linear change of variables putting the system (4.55) in the canonical form (4.1)-(4.2). Such linear change is given by the matrix

$$P = \frac{1}{\beta} \begin{pmatrix} \beta & 0 & 0 \\ \gamma^2 - 1 & \gamma & 1 \\ \gamma & 1 & 0 \end{pmatrix},$$

which has been built as shown in the proof of Proposition 2.4. Then, we can write system (4.55) in its Liénard form as

$$\dot{\mathbf{x}} = \begin{pmatrix} \alpha - \gamma & -1 & 0 \\ 2 - \alpha\gamma & 0 & -1 \\ \alpha - \gamma & 0 & 0 \end{pmatrix} \mathbf{x} + \begin{pmatrix} \beta \\ -\beta\gamma \\ \beta \end{pmatrix} \mathrm{sat}(x). \tag{4.56}$$

Therefore, the trace, the sum pf second order principal minors and the determinant in the central and external zones respectively, are

$$\begin{array}{ll} T = & \alpha + \beta - \gamma, \\ M = & 2 - \gamma(\alpha + \beta), \\ D = & \alpha + \beta - \gamma, \\ t = & \alpha - \gamma, \\ m = & 2 - \alpha\gamma, \\ d = & \alpha - \gamma. \end{array} \tag{4.57}$$

Similarly to what was done for the Chua's circuit, for the Hopf-pitchfork bifurcation to appear in this model we need to check, apart from the hypotheses of different theorems of this chapter, the feasibility of conditions (4.4), that is we need

$$\begin{array}{lll} E_1 & := & (2\rho - 1)\varepsilon - \alpha - \beta + \gamma = 0, \\ E_2 & := & \omega^2 + \rho\varepsilon^2(\rho - 2) - 2 + \gamma(\alpha + \beta) = 0, \\ E_3 & := & -\varepsilon(\rho^2\varepsilon^2 + \omega^2) - \alpha - \beta + \gamma = 0. \end{array} \tag{4.58}$$

Note that as $T = D$ always, we cannot move at will the position of eigenvalues. More precisely, from (4.58) by subtractiong E_3 from E_1 we have

$$\varepsilon(\rho^2\varepsilon^2 + \omega^2) + (2\rho - 1)\varepsilon = 0,$$

leading for $\varepsilon \neq 0$ to the condition

$$\varepsilon^2\rho^2 + 2\rho + \omega^2 - 1 = 0. \tag{4.59}$$

and therefore the value of ρ cannot be arbitrarily chosen, nor constant (as we supposed before). Indeed we have

$$\rho = \rho(\varepsilon) = \frac{1 - \omega^2}{1 + \sqrt{1 - \varepsilon^2(\omega^2 - 1)}},$$

with

$$\rho(0) = \frac{1 - \omega^2}{2},$$

and consequently we have the condition $2\rho(0) < 1$. We assume in the sequel the above choice for $\rho(\varepsilon)$ and neglect the third equation, to be automatically fulfilled. We also rewrite the second equation by using the above relation, namely

$$\begin{array}{rcl} E_1 & := & (2\rho(\varepsilon) - 1)\varepsilon - \alpha - \beta + \gamma = 0, \\ E_2 & := & -1 - 2\rho(\varepsilon)(1 + \varepsilon^2) + \gamma(\alpha + \beta) = 0. \end{array} \tag{4.60}$$

In looking for the Hopf-pitchfork bifurcation to take place at $\varepsilon = 0$, we need

$$\begin{array}{rcl} E_1^0 & := & -\alpha - \beta + \gamma = 0, \\ E_2^0 & := & \omega^2 - 2 + \gamma(\alpha + \beta) = 0. \end{array} \tag{4.61}$$

In what follows, we assume that β is a fixed parameter and we move only α and γ, and we write $\alpha(\varepsilon)$ and $\gamma(\varepsilon)$ for the functions satisfying (4.60). From equations (4.61) we obtain the following equalities,

$$\begin{array}{l} \alpha_0 = \alpha(0) = -\beta + \sqrt{2 - \omega^2}, \\ \gamma_0 = \gamma(0) = \sqrt{2 - \omega^2}. \end{array} \tag{4.62}$$

Note that, these equations require $\omega < \sqrt{2}$ and so $-1 < 2\rho(0) < 1$.

From (4.58) and using the equalities of (4.62), it is easy to check that the required condition to reproduce the eigenvalues transition is

$$\det\left(\frac{\partial(E_1, E_2)}{\partial(\alpha, \gamma)}\right)_{\varepsilon=0} = -2(\alpha_0 + \beta) = \gamma_0 \neq 0.$$

Under this last condition, the Implicit Function Theorem assures, for $|\varepsilon|$ sufficiently small, the existence of a branch of solutions $(\rho(\varepsilon), \alpha(\varepsilon), \gamma(\varepsilon))$ of (4.58), with β a fixed parameter, which assures the eigenvalue transition corresponding to the Hopf-pitchfork bifurcation.

From the last three equations of (4.57), when ε vanishes, we obtain

$$\begin{aligned} &t = d = -\beta, \\ &m = \omega^2 + \beta\sqrt{2-\omega^2}. \end{aligned}$$

For this set of parameters, it is easy to check for $\varepsilon = 0$ that the non-degeneracy condition

$$\delta = d - t\omega^2 = -\beta\left(1-\omega^2\right) \neq 0, \tag{4.63}$$

holds, if and only if $\omega \neq 1$, and then we have necessarily $\rho(0) \neq 0$.

Then, the appearance of our non-smooth Hopf-pitchfork bifurcation in system (4.56) for $\varepsilon = 0$ is guaranteed by Theorem 4.2 in two cases: (a) $0 < \omega < 1$, which leads to $\rho(0) > 0$, and (b) $1 < \omega < \sqrt{2}$, with $\rho(0) < 0$.

We know that the bifurcating tri-zonal limit cycle appears for $\rho\delta\varepsilon > 0$, that is, for

$$-\beta\frac{(1-\omega^2)^2}{2}\varepsilon > 0,$$

or equivalently for $\varepsilon < 0$. It is stable if and only if $t < 0$, $d < 0$ and $\delta > 0$, that is, if $\beta > 0$ and $\omega > 1$. Thus we have a tri-zonal unstable limit cycle in case (a) and a stable limit cycle in the case (b), appearing for $\varepsilon < 0$ in both cases.

We compute now the value of $d\rho(0) + \delta$, obtaining

$$-\beta\frac{1-\omega^2}{2} - \beta\left(1-\omega^2\right) = -3\beta\frac{1-\omega^2}{2},$$

and the value of

$$\frac{d\rho(0)}{d\rho(0)+\delta} = \frac{1}{3}.$$

Thus, the hypotheses of Theorem 4.5 are fulfilled both in case (a) and (b). We obtain that two bizonal limit cycles bifurcate for $\rho\delta\varepsilon > 0$, that is, for $\varepsilon < 0$. These bizonal limit cycles are stable for $t < 0$ and $\rho > 0$ so that they are stable in case (a) and unstable in case (b).

From Proposition 4.2, if $\beta\varepsilon < 0$, there also appear two isolated equilibrium points and they are stable if $t, d < 0$, that is $\beta > 0$, and $mt - d < 0$, which leads to $m - 1 > 0$. This last inequality is equivalent to

$$\beta > \frac{1 - \omega^2}{\sqrt{2 - \omega^2}},$$

which gives a positive lower bound in the case (a) and a negative lower bound in the case (b). Thus, this inequality is required for stability in the former case, being stable the equilibrium points for all $\beta > 0$ in the latter.

We observe that $\omega = 1$ is a critical value that separates two different types of Hopf-pitchfork bifurcations, so that we must suspect at such a value a degeneration. In fact, we see that then the condition (4.63) fails. Unfortunately, in such case we also have $\rho(0) = 0$ leading to a more degenerate situation than the one stated in Section 4.3. We loose the transversality at $\varepsilon = 0$, since the complex eigenvalues cross the imaginary axis of the complex plane with zero velocity, and so a new, specific analysis is required to deal with this situation. Looking for simple, real examples in order to illustrate our theoretical results, we have found in a serendipitous way an exciting problem for future work!

CHAPTER 5

Conclusions

It is time now to add some conclusions and suggestions for future work. As usual, a research like ours, in a field where there is not at our disposal a sound general theory, has to be partial and not totally definitive. Evidently, it remains much to be done, and here we only emphasize the points more connected with the contributions included in this thesis that deserve to be investigated further, probably after recruiting other techniques of analysis.

Some advances in the analysis of continuous planar systems have been achieved. The two zone case has been revisited and simplified proofs have been proposed. New results have been obtained for the three zone case with no symmetries. In this last case, a future line of research is the study of degenerate cases, for instance the situation when the central determinant vanishes and we move the parameter that determines the equilibrium position. This problem is of interest in the context of Petri nets, see [68].

The analysis of electronic Wien bridge oscillators has achieved an excellent degree of maturity and is a good paradigm of the usefulness and power of piecewise linear models. We propose such analysis as an obligated subject in any course on PWL systems, gathering richness of behavior and a simple setting, being also very easy to obtain quantitative predictions to be later tested in the laboratory, as done in [26].

We are very proud for the discovering of algebraically computable nodal oscillators. It is also remarkable to have found real devices belonging to

the studied family of oscillators. It is clear that the idea could be extended by considering other eigenvalue proportions but we honestly think that it should be not very productive to follow that way. More interestingly, we could use such idea of choosing some easy eigenvalue proportions to analyze other nonlinear phenomena. In fact we know for instance some preliminary analysis of Teixeira points, where the idea is also useful.

In discontinuous, planar PWL systems with two zones there exists nowadays a very intense line of research, mainly oriented to the determination of the maximum number of limit cycles these systems can exhibit. Examples with three limit cycles have been recently reported, but it is still an open question if three is the upper bound looked for. Our interest, more focused to bifurcations and its quantitative characterization, allowed to obtain information about the focus-center-limit cycle bifurcation in the first possible step to pass from continuous to discontinuous cases. Thus, our contribution here can be qualified as incidental, but we strongly think that it is a good starting point for extending the unfolding of such a focus-center-limit cycle bifurcation to co-dimension two cases, in particular by allowing the parameter b to be different from zero.

After the Hopf bifurcation analysis included in [7, 27], our study of the Hopf-pitchfork bifurcation in 3D PWL systems with symmetry was a pending problem now partially solved. Obviously, the dynamics to be found near such a non-hyperbolic set of periodic orbits is far from being completely understood. Our next goal in this direction is to get some analytical proof of our conjecture on the possible simultaneous bifurcation of five limit cycles; in particular, the bifurcation of small periodic orbits that seem to emerge along with the near non-trivial equilibrium points.

No doubt, the 3D electronic oscillators partially analyzed will constitute the subject of future research; the very degenerate situations we have found ask for new, more powerful techniques of approaching the Hopf-pitchfork singularity in PWL systems.

MELIOR EST FINIS QVAM PRINCIPIVM

Bibliography

[1] V. N. Afanas'ev, V. B. Kolmanovskii, and V. R. Nosov. *Mathematical theory of control systems design*. Mathematics and its applications. Kluwer Academic, Dordrecht, Boston, London, 1996. Translated from the Russian.

[2] A. A. Andronov, A. A. Vitt, and S. E. Khaikin. *Theory of oscillators*. Pergamon Press, Oxford, 1966.

[3] S. Barnett and R. Cameron. *Introduction to mathematical control theory*. Oxford applied mathematics and computing science series. Clarendon Press, 1985.

[4] L. Bernardin, P. Chin, P. DeMarco, K. O. Geddes, D. E. G. Hare, K. M. Heal, G. Labahn, J. P. May, J. McCarron, M. B. Monagan, D. Ohashi, and S. M. Vorkoetter. *Maple 16 Maple Programming Guide*. Maplesoft, Waterloo ON, Canada, 2012.

[5] V. Carmona. *Bifurcaciones en sistemas dinámicos lineales a trozos*. PhD thesis, Universidad de Sevilla, 2002.

[6] V. Carmona, S. Fernández-García, E. Freire, and F. Torres. Melnikov theory for a class of planar hybrid systems. *Physica D: Nonlinear Phenomena*, 248:44–54, 2013.

[7] V. Carmona, E. Freire, E. Ponce, J. Ros, and F. Torres. Limit cycle bifurcation in 3D continuous piecewise linear systems with two zones. Application to Chua's circuit. *International Journal Bifurcation and Chaos*, 15:2469–2484, 2005.

[8] V. Carmona, E. Freire, E. Ponce, and F. Torres. On simplifying and classifying piecewise-linear systems. *IEEE Transactions in Circuits and Systems*, 49:609–620, 2002.

[9] V. Carmona, E. Freire, E. Ponce, and F. Torres. Invariant manifolds of periodic orbits for piecewise linear three-dimensional systems. *Ima Journal of Applied Mathematics*, 69:71–91, 2004.

[10] V. Carmona, E. Freire, E. Ponce, and F. Torres. Bifurcation of invariant cones in piecewise linear homogeneous systems. *International Journal of Bifurcation and Chaos*, 15:2469–2484, 2005.

[11] V. Carmona, E. Freire, E. Ponce, and F. Torres. The continuous matching of two stable linear systems can be unstable. *Discrete and Continuous Dynamical Systems*, 16:689–703, 2006.

[12] S. Chow and J. Hale. *Methods of bifurcation theory*. Grundlehren der mathematischen Wissenschaften. Springer-Verlag, 1982.

[13] L. Chua, J. Yu, and Y. Yu. Negative resistance devices. *International Journal of Circuit Theory and Applications*, 11:161–186, 1983.

[14] L. O. Chua, C. W. Wu, A. Huang, and G.-Q. Zhong. A universal system for studying and generating chaos - Part I: Routes to chaos. *IEEE Trans. Circuits Systems I Fund. Theory Appl.*, 40(10):732–744, 1993.

[15] B. Coll, A. Gasull, and R. Prohens. Degenerated hopf bifurcations in discontinuous planar systems. *J. Math. Analysis and Applications*, 253:671–690, 2001.

[16] S. Coombes. Neuronal networks with gap junctions: A study of piecewise linear planar neuron models. *SIAM Applied Dynamical Systems*, 7:1101–1129, 2008.

[17] M. Desroches, E. Freire, S. J. Hogan, E. Ponce, and P. Thota. Canards in piecewise-linear systems: explosions and super-explosions. *Proceedings of the Royal Society A*, 2013.

[18] M. Di Bernardo, C. Budd, A. R. Champneys, and P. Kowalczyk. *Piecewise-smooth dynamical systems: theory and applications*, volume 163 of *Appl. Math. Sci.* Springer-Verlag, 2007.

[19] M. Di Bernardo, A. Nordmark, and G. Olivar. Discontinuity-induced bifurcations of equilibria in piecewise-smooth and impacting dynamical systems. *Physica D*, 237:119–136, 2008.

[20] M. Di Bernardo, D. Pagano, and E. Ponce. Nonhyperbolic boundary equilibrium bifurcations in planar filippov systems: a case study approach. *International Journal of Bifurcation and Chaos in Applied Sciences and Engineering*, 18:1377–1392, 2008.

[21] F. Dumortier, J. Llibre, and J. Artés. *Qualitative Theory of Planar Differential Systems*. Universitext - Springer-Verlag. Springer London, Limited, 2006.

[22] S. Fernández García. *Bifurcaciones de Órbitas Periódicas y Conjuntos Invariantes en Sistemas Dinámicos Lineales a Trozos*. PhD thesis, Universidad de Sevilla, 2012.

[23] E. Freire, E. Ponce, F. Rodrigo, and F. Torres. Bifurcation sets of continuous piecewise linear systems with two zones. *Int. J. Bifurcation and Chaos*, 8:2073–2097, 1998.

[24] E. Freire, E. Ponce, F. Rodrigo, and F. Torres. Bifurcation sets of continuous piecewise linear systems with three zones. *Int. J. Bifurcation and Chaos*, 12:1675–1702, 2002.

[25] E. Freire, E. Ponce, F. Rodrigo, and F. Torres. A piecewise linear electronic circuit with a multiplicity of bifurcations. *International Journal of Bifurcation and Chaos Appl. Sci. Engrg.*, 14(11):3871–3881, 2004.

[26] E. Freire, E. Ponce, and J. Ros. Limit cycle bifurcation from center in symmetric piecewise-linear systems. *International Journal of Bifurcation and Chaos*, 9:895–907, 1999.

[27] E. Freire, E. Ponce, and J. Ros. The focus-center-limit cycle bifurcation in symmetric 3D piecewise linear systems. *SIAM Journal of Applied Mathematics*, 65:1933–1951, 2005.

[28] E. Freire, E. Ponce, and J. Ros. Bistability and hysteresis in symmetric 3d piecewise linear oscillators with three zones. *International Journal of Bifurcation and Chaos*, 18:3633–3645, 2008.

[29] E. Freire, E. Ponce, and F. Torres. Transformaciones de Filippov en sistemas lineales a trozos. In *Actas XV CEDYA-V CMA VIgo 23-26 IX Tomo 1*, 1997.

[30] E. Freire, E. Ponce, and F. Torres. Canonical discontinuous planar piecewise linear systems. *SIAM Journal Applied Dynamical Systems*, 11:181–211, 2012.

[31] E. Freire, E. Ponce, and F. Torres. On the critical crossing cycle bifurcation in planar Filippov systems. *Preprint*, 2013.

[32] E. García Medina. *Conexiones Globales y Comportamientos Periódicos en Sistemas Dinámicos Lineales a Trozos*. PhD thesis, Universidad de Sevilla, 2011.

[33] M. Golubitsky and D. G. Schaeffer. *Singularities and groups in bifurcation theory.*, volume 69 of *Applied Mathematical Sciences*. Springer-Verlag, New York, 1988.

[34] M. Götz, U. Feldmann, and W. Schwarz. Synthesis of higuer dimensional Chua circuits. *IEEE Trans. Circuits Syst.*, 40:854–860, 1993.

[35] M. Guardia, T. Seara, and M. Teixeira. Generic bifurcations of low codimension of planar Filippov systems. *J. Differential Equations*, 250:1967–2023, 2011.

[36] J. Guckenheimer and P. Holmes. *Nonlinear Oscillations, Dynamical Systems and Bifurcations of Vector Fields.*, volume 42 of *Applied Mathematical Sciences*. Springer-Verlag, New York, 1983.

[37] P. Hartman. *Ordinary Differential Equations*. Birkhäuser, Boston, 1982.

[38] A. Hodgkin and A. Huxley. A qualitative description of membrane current and its application to conduction and excitation in nerve. *J.Phys.s*, 177:500–544, 1952.

[39] S. Hogan. Relaxation oscillations in a system with a piecewise smooth drag coefficient. *Journal of Sound and Vibration*, 263(2):467–471, 2003.

[40] D. Jordan and P. Smith. *Nonlinear ordinary differential equations*. Oxford University Press, Oxford, fourth edition, 2007.

[41] P. Julian, A. Desages, and O. Agamennoni. High-level canonical piecewise representation using a symplicial partition. *IEEE Trans. Circuits Syst.*, 46:463–480, 1999.

[42] C. Kahlert and L. O. Chua. A generalized canonical piecewise-linear representation. *IEEE Trans. Circuits Syst.*, 37:373–383, 1990.

[43] C. Kahlert and L. O. Chua. The complete canonical piecewise-linear representation: I geometry of the domain space. *IEEE Trans. Circuits Syst.*, 39:226–236, 1992.

[44] J. Keener. Analog circuitry for the Van der Pol and Fitzhugh-Nagumo equations. *IEEE Trans. Syst. Man Cybern.*, 13:1010–1014, 1983.

[45] M. P. Kennedy. Three steps to chaos Part II: A Chua's circuit premier. *IEEE Transactions on Circuits and Systems I: Fundamental Theory and Applications*, 40:657–674, 1993.

[46] T. A. M. Kevenaar and D. M. W. Lenaerts. A comparison of piecewise-linear model descriptions. *IEEE Trans. Circuits Syst.*, 39:996–1004, 1992.

[47] H. Khalil. *Nonlinear Systems*. Prentice Hall, third edition, 2000.

[48] G. Kovatch. A method for the computation of self-sustained oscillations in systems with piecewise linear elements. *IEEE Transactions on Automatics Control*, 8:358–365, 1963.

[49] G. A. Kriegsmann. The rapid bifurcation of the Wien bridge oscillator. *IEEE Trans. Circuits Syst.*, 34:1093–1096, 1987.

[50] T. Kuepper. Invariant cones for non-smooth dynamical systems. *Mathematics and Computers in Simulation*, 79:1396–1408, 2008.

[51] T. Kuepper and S. Moritz. Generalized Hopf bifurcation for non-smooth planar systems. *Philosophical Transactions of the Royal Society A*, 359:2483–2496, 2001.

[52] Y. A. Kuznetsov. *Elements of Applied Bifurcation Theory.*, volume 112 of *Applied Mathematical Sciences*. Springer-Verlag, New York, third edition, 2004.

[53] Y. A. Kuznetsov, S. Rinaldi, and A. Gragnani. One-parameter bifurcations in planar filippov systems. *I. J. Bifurcation and Chaos*, 13(8):2157–2188, 2003.

[54] M. Lakshmanan and K. Murali. *Chaos in Nonlinear Oscillators: Controlling and Synchronization*, volume 13 of *Series on Nonlinear Science*. World Scientific Publishing Company, Incorporated, 1996.

[55] J. Lin and R. Unbehauen. Canonical piecewise-linear networks. *Neural Netw.*, 6:42–50, 1995.

[56] J. Lin, H. Xu, and R. Unbehauen. A generalization of canonical piecewise-linear functions. *IEEE Trans. Circuits Syst.*, 41:345–347, 1994.

[57] J. Lipton and K. Dabke. Softening the nonlinearity in Chua's circuit. *International Journal of Bifurcation and Chaos*, 6(1):179–183, 1996.

[58] J. Llibre, E. Núñez, and A. Teruel. Limit cycles for planar piecewise linear differential systems via first integrals. *Qualitative Theory of Dynamical Systems*, 3:29–50, 2002.

[59] J. Llibre, M. Ordoñez, and E. Ponce. On the existence and uniqueness of limit cycles in planar continuous piecewise linear systems without symmetry. *Nonlinear Analysis: Real World Applications*, 2013.

[60] J. Llibre, E. Ponce, and J. Ros. Algebraic determination of limit cycles in a family of 3-dimensional piecewise linear differential systems. *Nonlinear Analysis*, 74:6712–6727, 2011.

[61] J. Llibre, E. Ponce, J. Ros, and F. Torres. On the fold-Hopf bifurcation for continuous piecewise linear differential systems with symmetry. *Chaos*, 20:033119–1–033119–13, 2010.

[62] J. Llibre and J. Sotomayor. Phase portraits of planar control systems. *Nonlinear Analysis, Theory, Methods & Applications*, 27(10):1177–1197, 1996.

[63] R. Lum and L. Chua. *The Identification of Pseudo-gradient Vector Fields*. Memorandum (University of California, Berkeley, Electronics Research Laboratory). Electronics Research Laboratory, College of Engineering, University of California, 1990.

[64] R. N. Madan. *Chua's circuit : a paradigm for chaos*. World scientific series on nonlinear science. World scientific, Singapore, London, Hong-Kong, 1993.

[65] J. Massera. Sur un théorème de g. sansone sur l'equation de liénard,. *Boll. Un. Mat. Ital.*, 9:367–369, 1954.

[66] T. Matsumoto, M. Komuro, H. Kokubu, and R. Tokunegra. *Bifurcations*. Springer-Verlag, 1993.

[67] A. Mees and L. Chua. The Hopf bifurcation theorem and its applications to nonlinear oscillations in circuits and systems. *IEEE Trans. Circuits Syst.*, 26:235–254, 1979.

[68] A. Meyer, M. Dellnitz, and M. Hessel-von Molo. Symmetries in timed continuous petri nets. *Nonlinear Analysis: Hybrid Systems*, 5:125–135, 2011.

[69] N. Minorsky. *Nonlinear oscillations*. R. E. Krieger Pub. Co., 1974.

[70] J. Nagumo, S. Arimoto, and S. Yoshizawa. An active pulse transmission line simulating nerve axon. *Proc. IRE*, 50:2061–2070, 1962.

[71] Y. Nishiuchi, T. Ueta, and H. Kawakami. Stable torus and its bifurcation phenomena in a simple three-dimensional autonomous circuit. *Chaos, Solutions and Fractals*, 27:941–951, 2006.

[72] D. Pagano, E. Ponce, and F. Torres. On double boundary equilibrium bifurcations in piecewise smooth planar systems. *Qualitative Theory of Dynamical Systems*, 10:277–301, 2011.

[73] E. Ponce and J. Ros. On periodic orbits of 3D symmetric piecewise linear systems with real triple eigenvalues. *International Journal Bifurcation and Chaos*, 19:2391–2399, 2009.

[74] E. Ponce, J. Ros, and E. Vela. Algebraically computable piecewise linear nodal oscillators. *Applied Mathematics and Computation*, 219:41944207, 2013.

[75] E. Ponce, J. Ros, and E. Vela. *Dynamical systems: 100 years after Poincaré*, chapter A Hopf-zero degenerated case in symmetric piecewise linear systems. Springer, 2013.

[76] E. Ponce, J. Ros, and E. Vela. *Dynamical systems: 100 years after Poincaré*, chapter The focus-center-limit cycle bifurcation in discontinuous planar piecewise linear systems without sliding. Springer, 2013.

[77] E. Ponce, J. Ros, and E. Vela. Unfolding the fold-Hopf bifurcation in piecewise linear continuous differential systems with symmetry. *Physica D: Nonlinear Phenomena*, 250:34–46, 2013.

[78] J. Pospíšil and J. Brzobohatý. Elementary canonical state models of Chuass circuit family. *IEEE Trans. Circuits Syst.*, 43:702–705, 1996.

[79] J. Pospíšil, Z. Kolja, J. Horská, and J. Brzobohatý. Simplest ODE equivalents of Chuass equations. *Int. J. Bifurcation Chaos*, 10:1–23, 2000.

[80] F. Rodrigo. *Comportamiento dinámico de osciladores electr?nicos del tipo Van Der Pol-Duffing*. PhD thesis, Universidad de Sevilla, 1997.

[81] J. Ros. *Estudio del comportamiento dinámico de sistemas autónomos tridimensionales lineales a trozos*. PhD thesis, Universidad de Sevilla, 2003.

[82] M. Sabatini and G. Villari. On the uniqueness of limit cycles for liénard equations: the legacy of g. sansone. *Le Matematiche*, 65:201–214, 2010.

[83] A. Teruel. *Clasificación topológica de una familia de campos vectoriales lineales a trozos simétricos en el plano*. PhD thesis, Universitat Autònoma de Barcelona, 2000.

[84] R. Thul and S. Coombes. Understanding cardiac alternans: A piecewise linear modeling framework. *Chaos*, 20:045102–1–045102–13, 2010.

[85] A. Tonnelier. The McKean's caricature of the Fitzhugh-Nagumo model I. The space-clamped system. *SIAM Journal of Applied Mathematics*, 63(2):459–484, 2003.

[86] A. Tonnelier and W. Gerstner. Piecewise linear differential equations and integrate-and-fire neurons: insights from two-dimensional membrane models. *Phys. Rev. E*, 67:21908, 2003.

[87] H. Wolf, J. Kodvanj, and S. Bjelovučić-Kopilović. Effect of smoothing piecewise-linear oscillators on their stability predictions. *Journal of Sound and Vibration*, 270:917–932, 2004.

[88] I. Wolfram Research. *Mathematica Edition: Version 8.0.* Inc. Wolfram Research, 2010.

[89] Y. Yan-Qian. *Theory of limit cycles.* American Mathematical Society, 1986.

[90] Z. Zhang, T. Ding, W. Huang, and Z. Dong. *Qualitative theory of differential equations.* AMS Translations of Math. Mon., Providence, 1992.

[91] Y. Zou, T. Kupper, and W. J. Beyn. Generalized Hopf bifurcations for planar filippov systems continuous at the origin. *Journal of Nonlinear Science*, 16:159–177, 2006.